

**Role of the Hedgehog pathway in
the pancreatic
tumour microenvironment**

FRANCESCA SAINI

**Thesis submitted to the University of Nottingham
for the degree of Doctor of Philosophy**

December 2014

Abstract

Pancreatic cancer is a solid tumour with poor prognosis and ineffective therapeutic approaches. Pancreatic tumour progression is characterised by a strong desmoplastic reaction and the role of the tumour microenvironment in supporting tumour growth and metastasis has been demonstrated. In particular, a new concept of the stem cell niche as a mixed population of mesenchymal stem cells and niche cells (myofibroblast cells) involved in promoting these processes is emerging. Paracrine transmission of the Hedgehog (Hh) pathway in the tumour microenvironment of pancreatic cancer has previously been reported.

Based on these studies, this project aimed to identify and characterise the stromal pancreatic cancer cells able to respond to Hh pathway exogenous stimuli and to investigate their relationship to tumour progression, in order to define new targets for pancreatic cancer therapies.

Screening of pancreatic primary tumours by gene and protein expression analysis demonstrated overexpression of Shh ligand not only at the epithelial but also at the stromal level in advanced stages of pancreatic cancer. *In vitro* modelling of the mesenchymal stem cell niche (mSCN) using human bone marrow-derived mesenchymal stem cells (MSCs) co-cultured with cancer-associated fibroblasts (CAFs) or myofibroblast-like cells (MF-like, obtained by treating MSC with TGF β) showed up-regulation of Shh gene and protein expression in comparison to single stromal cell populations (MSCs; CAFs and MF-like cells). The investigation of Hh paracrine signalling in pancreatic tumour

microenvironment using different 2D *in vitro* assays (transwell and direct co-cultures, NShh treatments and tumour condition media cultures) demonstrated the inability of cancer associated fibroblasts (CAFs) and mesenchymal stem cells (MSCs), when grown in culture conditions that prevent their activation (increase of α SMA), to respond to Hh exogenous stimuli and suggested the mSCN as the stromal context in which paracrine induction of the Hh pathway takes place.

Taken together, these results suggest a new concept, that Shh expression is an indicator of the mSCN in the pancreatic cancer microenvironment and that its role as a possible target for chemotherapy should be explored.

Acknowledgements

I would like to thank my supervisors: Professor Sue Watson who has been and will be an example to follow, Dr Anna Grabowska for her constant availability humanity and professionalism which impassioned me and made me fond of my project and of my work and Dr Argent Richard for his advice in many aspects of this PhD. I would also like to thank Andrea Greener for her administrative support.

I would really like to thank everyone in the Division of Pre-Clinical Oncology who helped me every day with their encouragements and their precious advice. In particular, I would like to thank Dr David Onion, Dr Nektaria Papadopoulou and Dr Madeleine Craze who with their knowledge, passion and availability strongly supported and excited me. I would like to extend my gratitude to Dr Phil Clarke, for his guidance and patience in teaching me immunohistochemistry and data analysis, Narinder Mann for her friendship and support in tissue culture and Tara Claringburn, Cannon Donna and Bramley Beverly for their administrative support. Great thanks to Luana Sasso, Musah-Eroje Ahmed, Pamela Collier, Maria Estévez Cebrero, Niovi Nicolaou Dr Alexander Reece Smith, Suzy Underwood, Dr Simon Jiang, Dr Eve Lee and Dr Cerys Mayne for making my time in the department a pleasure and encourage me in my work.

Finally, I would like to thank my parents, my grandmother my brother, my sister for being always supportive, helpful and for loving me in the way they do. Thanks to my second family in particular to Ezia who really helped me in any possible way. A huge thank to Marco, who

became my husband during this PhD, for his incredible patience and support, which pulled me through the hardest moments.

Finally, I would like to dedicate my thesis and these years of work to my grandfather “nonno Sandro” who is always in my thoughts and my baby Dario who I can consider, with no doubt, my best “result”.

Table of Contents

Chapter 1 - Introduction.....	18
1.1 Cancer underlying causes	19
1.1.1 Cancer and prevention.....	19
1.1.2 Pancreatic cancer	22
1.1.2.1 The Stroma component of pancreatic cancer	25
1.1.2.2 In vivo models of pancreatic cancer.....	26
1.2 The role of stroma in tumour development	29
1.2.1 Interplay between epithelial and stromal cells	30
1.2.2 Tumour microenvironment, cancer stem cells and resistance to chemotherapeutic treatment.	33
1.3 Hedgehog signalling in development and homeostasis	38
1.3.1 The Hedgehog Pathway	38
1.3.2 Hh ligand expression regulation.....	42
1.3.3 The Gli Transcription Factors.....	44
1.4 Hedgehog Signalling and Cancer	51
1.4.1 Paracrine transmission of Hedgehog signalling	54
1.4.1.1 In vivo and in vitro evidence supporting Hh paracrine signalling in tumour microenvironment	55
1.4.2 Paracrine signalling vs autocrine signalling.....	60
1.4.3 Hh signalling in pancreatic cancer	61
1.4.4 Antagonists of Hh signalling and effect of Hh pathway inhibition on cancer	65
1.5 The stem cell niche	73
1.5.1 Mesenchymal stem cell niche and its role in cancer.....	76
1.5.2 Stem cell niche markers.....	78
1.5.3 Hedgehog pathway and the stem cell niche.....	79
1.6 Hypothesis and aims	85
1.6.1 Summary of the main concepts.....	85
1.6.2 Hypothesis.....	86
1.6.3 Aims	87
Chapter 2 - Materials and Methods	88
2.1 Human Primary tissues	89
2.2 Cell culture	94
2.2.1 Cell culture conditions.....	94
2.2.1.1 Epithelial cancer cell line culture conditions.....	94

2.2.1.2 Primary cell and MSC cell culture	95
2.2.2 Sub-culturing of cells	96
2.2.2.1 Cell counting	97
2.2.2.2 Freezing cells	97
2.2.2.3 Cell recovery	98
2.2.3 <i>In vitro</i> cell treatments.....	98
2.2.3.1 NShh treatment	98
2.2.3.2 TGF β treatment.....	99
2.2.3.3 Cell harvesting from in vitro cell treatment assays for RNA extraction and immunofluorescence (IF).....	100
2.2.4 Transwell co-culture.....	100
2.2.5 Direct co-culture.....	102
2.2.5.1 Cell harvesting from direct co-culture for RNA extraction.....	103
2.2.6 Optimisation of <i>in vitro</i> mesenchymal stem cell niche models	103
2.2.6.1 Transwell co-culture between in vitro mSCN models and epithelial cancer cells	105
2.2.7 Tumour conditioned media (TCM) assay	107
2.3 Molecular Techniques	109
2.3.1 RNA extraction from cells	109
2.3.2 RNA extraction from tissues.....	109
2.3.3 cDNA synthesis.	111
2.3.4 Quantitative Real-time Polymerase chain reaction (qPCR).	111
2.3.4.1 RT-PCR data analysis.	118
2.4 Protein expression analysis.....	119
2.4.1 Immunohistochemistry	119
2.4.1.1 IHC staining of Shh and Ptch1 Hh proteins in pancreatic tumour and normal tissues	120
2.4.1.2 IHC staining of Vimentin in pancreatic tumour and normal tissues.....	122
2.4.1.3 Data analysis of IHC.....	124
2.4.2 Immunofluorescence (IF)	125
2.4.2.1 Data Analysis of IF staining	129
2.5 Statistics.....	131

Chapter 3 - Results: Analysis of Hh signalling in primary tissues132

3.1 Introduction	133
3.2 Screening of Hh pathway gene expression in pancreatic and lung tumour tissues	134
3.2.1 Investigation of Hh pathway signalling in pancreatic samples	134
3.2.2 Hh pathway expression in normal and NSCLC tumour lung primary tissues	141
3.2.3 Protein expression analysis of Hh pathway in primary pancreatic tumour tissues.	144

3.2.4 Hh ligand protein expression analysis in pancreatic tissues	144
3.2.5 Investigation of the activity of the Hh pathway in pancreatic tissues	153
3.4 Summary of results	161
Chapter 4 - Results: Characterisation of Hh pathway in epithelial and stromal cells.....	163
4.1 Introduction	164
4.2 Screening of pancreatic epithelial and fibroblast cells.....	165
4.2.1 Hh pathway expression in pancreatic cancer epithelial and primary-derived fibroblasts cells	165
4.2.2 Protein expression analysis of Hh ligand expression in cancer epithelial cells	170
4.3 Investigation of pancreatic CAF responsiveness to exogenous Hh stimuli	174
4.3.1 Investigation of the mesenchymal-like phenotype in CAFs stroma cells	174
4.3.2 Investigation of responsiveness of CAFs to NShh treatment.....	176
4.4 Investigation of the CAF responsiveness to paracrine signals in 2D co-culture and using tumour-conditioned medium (TCM).....	179
4.4.1 TCM effect of Hh signalling pathway paracrine induction in CAFs.....	179
4.4.2 Investigation of Hh pathway paracrine induction in stromal-like cells by 2D <i>in vitro</i> co-culture assays	182
4.4.2.1 The pancreatic CAFs responsiveness in a trans-well system.....	182
4.4.2.2 The responsiveness of pancreatic CAFs in a direct co-culture system.....	188
4.5 Summary of chapter	190
Chapter 5 - Results: The Stem Cell Niche	191
5.1 Introduction	192
5.2 Investigation of the responsiveness of MSCs to Hh paracrine stimuli	193
5.2.1 NShh treatment of MSCs	193
5.2.2 Effect of TCM on Hh paracrine activation in MSCs	195
5.2.3 Effect of 2D transwell co-culture on Hh paracrine activation in MSCs	200
5.3 Investigation of the effect of different media on MSC activation and Hh pathway activation	203
5.3.1 <i>In vitro</i> investigation of Hh pathway in MSCs cultured in “free differentiation” medium.....	208
5.4 Investigation of the effect of TGF- β on the differentiation of MSCs and Hh pathway expression.....	213
5.4.1 TGF- β effect on MSC activation.....	213
5.4.2 TGF- β Effect on the Hh pathway.....	217

5.5 The mesenchymal stem cell niche and the establishment of an <i>in vitro</i> model.....	223
5.5.1 Investigation of Shh as marker of the stem cell niche	224
5.5.2 Investigation of Shh expression in the mesenchymal stem cell niche	244
5.6 Investigation of paracrine responsiveness to Hh pathway stimuli in the stem cell niche model	250
5.6.1 Investigation of the effect of pancreatic TCM and NShh on Hh pathway activation in the mSCN <i>in vitro</i> model	250
5.6.2 Comparison between the responsiveness of MSC single population and mSCN model to Hh paracrine stimuli	254
5.6.3 Comparison between responsiveness of different mSCN models to Hh paracrine stimuli.....	257
5.7 Summary of results	262
Chapter 6 - Discussion.....	264
6.1 Results overview	265
6.2 Shh is over-expressed in primary tumour pancreatic tissues at the epithelial and stromal level.....	267
6.2.1 <i>SHH</i> ligand is over express in pancreatic primary tissue in comparison to lung tissues	267
6.2.2 Shh is over-expressed in pancreatic cancer not only at the epithelial level but also at the stromal level.....	269
6.2.3 Hh downstream pathway expression suggests the existence of both paracrine and stromal autocrine signal in PDAC.....	275
6.3 Hh pathway expression in epithelial and stromal pancreatic tumour cells	278
6.3.1 Pancreatic CAF or MSCs alone are not able to respond to Hh paracrine stimuli in 2D <i>in vitro</i> assays.....	280
6.4 A myofibroblast-like cell population originates from MSCs and expresses Shh ligand.....	288
6.4.1 TGF- β treatment of MSCs triggers an increase in α SMA expression and is likely to be responsible for GLI1 gene expression regulation	292
6.5 The mesenchymal stem cell niche.....	296
6.5.1 A mesenchymal stem cell niche (mSCN) model can be reproduced <i>in vitro</i> and results in up regulation of the Shh ligand.....	297
6.5.2 The mSCN is the best tumour stromal context able to respond to Hh paracrine stimuli	309
6.5.2.1 Shh paracrine responsiveness comparison between different mesenchymal mSCN <i>in vitro</i> models	312
6.5.2.2 Next step in the paracrine induction of Hh signalling in a <i>in vitro</i> mSCN model.....	313
6.6 Applicability of the data presented in this thesis for development of novel therapeutic approaches	315

6.7 Conclusions	319
6.8 Future work	321
6.9 Final Conclusions.....	328
Chapter 7 - References	329
Appendix: Software Programmes	350

Table of figure

Figure 1.1 Therapeutic Targeting of the Hallmarks of Cancer.....	21
Figure 1.2 Origin of stroma cells in tumour microenvironment. ...	30
Figure 1.3 Tumour microenvironment regulates drug sensitivity.	34
Figure 1.4 Tumour microenvironment regulates drug sensitivity.	35
Figure 1.5 Activation of Hh signaling.	39
Figure 1.6 Gli2 and Gli3 proteins can act both as repressor and activators.	46
Figure 1.7 Hh pathway expression during development.	48
Figure 1.8 Example of Hh paracrine signaling.	59
Figure 1.9 Distribution of stem cell niches in a adult human body	74
Figure 1.10 Intestinal stem cell niche regulation.	80
Figure 1.11 Mesenchymal Stem Cell Niche formation and recruitment in pancreatic tumour microenvironment.	84
Figure 3.1 Screening of the gene expression Hh ligands in normal and tumour pancreatic tissues.	136
Figure 3.2 Hh ligand expressions in different tumour stage of primary pancreatic tissues.	138
Figure 3.3 Hh pathway activity in primary pancreatic tissues.	140
Figure 3.4 Screening of <i>SHH</i> gene expression in normal and tumour lung tissues.	142
Figure 3.5 Screening of <i>GLI1</i> gene expression in normal and tumour lung tissues.	143
Figure 3.6 Shh protein expression in primary pancreatic normal and tumour tissues.	146
Figure 3.7 Quantification of Shh protein expression in primary pancreatic normal and tumour tissues.	147
Figure 3.8 Vimentin expression in normal and pancreatic tumour tissues.	149
Figure 3.9 Shh epithelial and stromal expression correlates with % stromal component.	150
Figure 3.10 Shh expression in the stromal component increases in proportion to the level of staining in the epithelial component.	151
Figure 3.11 Shh was expressed at the stroma level and increased with tumour aggressiveness.	152

Figure 3.12 Ptch1 protein expression analyses in normal and tumour pancreatic tissues.....	154
Figure 3.13 Ptch1 expression at the stromal level does not correlate with its expression in the epithelial component.....	156
Figure 3.14 Expression of Ptch1 within the epithelial and stroma compartments do not correlate.....	157
Figure 3.15 Ptch1 is highly expressed in the epithelial component of normal and tumour pancreatic tissues	158
Figure 3.16 Correlation analysis between Shh and Ptch1 protein expressions in pancreatic normal and tumour tissues.	160
Figure 4.1 Screening of epithelial cells, CAFs and MSCs for the main genes associated with the Hh pathway and epithelial/ myofibroblast markers	167
Figure 4.2 Shh and Dhh protein expression analyses by IF in epithelial pancreatic cancer cells	171
Figure 4.3 Gli1 expression in pancreatic epithelial cancer cells .	172
Figure 4.4 CAF cells express α SMA cell activation marker.	175
Figure 4.5 Investigation of the responsiveness of CAFs to NShh.	177
Figure 4.6 <i>GLI1</i> and <i>ACTA2</i> gene expression induction in pancreatic CAFs treated with NShh.....	178
Figure 4.7 Pancreatic TCM effect on Hh pathway expression in CAFs.....	181
Figure 4.8 Investigation of paracrine interaction between P5T pancreatic fibroblast and P308T primary epithelial cancer cells.....	183
Figure 4.9 Time-course of Hh pathway paracrine induction in pancreatic CAFs.....	185
Figure 4.10 Investigation of pancreatic CAFs dose-dependent responsiveness to Hh ligands paracrine induction.	187
Figure 4.11 Epithelial pancreatic primary fibroblast direct co-cultures..	189
Figure 5.1 MSC responsiveness to NShh treatment.....	194
Figure 5.2 <i>GLI1</i> expression correlated with <i>ACTA2</i> gene expression.	195
Figure 5.3 Effect of pancreatic tumour conditioned medium (CM) on Hh pathway expression in MSCs.....	197

Figure 5.4 MSCs passage effects on Hh pathway paracrine responsiveness to TCM stimuli.....	199
Figure 5.5 MSCs passage effects on paracrine responsiveness to Hh pathway stimuli in 2D co-culture.....	201
Figure 5.6 Gene and protein expression analysis of α SMA in MSCs cultured in free differentiation medium.....	204
Figure 5.7 MSCM prevented the activation of MSCs over time. ..	207
Figure 5.8 Hh pathway expression in MSCs cultured in free differentiation medium.....	210
Figure 5.9 Media effect on Shh signalling pathway expression in MSCs.	212
Figure 5.10 Effect of TGF- β on MSCs activation in PCA free differentiation media.	214
Figure 5.11 Different media effect on TGF- β treatment of MSCs.	216
Figure 5.12 Effect of TGF- β treatment on Hh pathway expression in MSCs cultured in PCA free differentiation media.....	218
Figure 5.13 TGF- β treatment effect on Hh pathway gene expression in MSCs grown in different media.....	219
Figure 5.14 Effect of TGF- β treatment on Hh pathway expression in MSCs grown in different media.....	221
Figure 5.15 Correlation analyses between <i>GLI1</i> and <i>ACTA2</i> gene expression after TGF- β treatment.....	222
Figure 5.16 Investigation of <i>SHH</i> gene expression in a stem cell niche <i>in vitro</i> model.	226
Figure 5.17 Investigation of stem cell niche marker gene expression in a stem cell niche <i>in vitro</i> model.	229
Figure 5.18 Investigation of α SMA protein expression in a stem cell niche <i>in vitro</i> model.	231
Figure 5.19 Investigation of <i>SHH</i> gene expression in different ratios of MSCs and MF-like cells in the mSCN <i>in vitro</i> model.....	234
Figure 5.20 Investigation of mSCN marker gene expression in different mSCN model co-culture ratios.....	236
Figure 5.21 Investigation of the effect of CAFs on mSCN <i>in vitro</i> model and <i>SHH</i> gene and protein expression	238
Figure 5.22 Investigation of the effect of CAFs on mSCN marker expression in an <i>in vitro</i> model.....	240
Figure 5.23 Investigation of the effect of CAFs on Postn protein expression in a mSCN <i>in vitro</i> model.....	241

Figure 5.24 Investigation of the effect of CAFs on the α SMA protein expression in a mSCN <i>in vitro</i> model.....	242
Figure 5.25 Investigation of Shh as marker of stem cell niche....	246
Figure 5.26 Comparison between Postn marker in the mSCN model and single populations	248
Figure 5.27 Comparison between α SMA marker in the mSCN model and single populations	249
Figure 5.28 TCM effect on mSCN <i>in vitro</i> model.....	251
Figure 5.29 Effect of NShh and FBS concentration on the paracrine responsiveness of the Hh pathway in a mSCN <i>in vitro</i> model.....	253
Figure 5.30 Comparison between MSC single population and mSCN model responsiveness to Hh paracrine stimuli in a transwell (TW) system	255
Figure 5.31 Comparison between MSC single population and mSCN model responsiveness to NShh stimuli.....	256
Figure 5.32 Comparison between different mSCN models in their responsiveness to Hh paracrine signalling:	260
Figure 5.33 Ptch1 protein expression induction by Hh paracrine signalling in different mSCN models:.....	261
Figure 6.1 MSCs in culture are able to differentiate into MF-like cells	302
Figure 6.2 Schematic diagram that depicts the conclusions, hypothesis and future aims (red writing) defined in this project.	320

List of Tables

Table 1.1 Hh pathway inhibitors and their phase I clinical trial.....	69
Table 1.2 Hh inhibitors under preclinical research investigation. 71	71
Table 2.1 Clinical Data of Lung Primary Tissues. SCC: Squamous Cell Carcinoma of Lung; NSCLC: Non Small cells Lung Carcinoma.....	90
Table 2.2 Clinical Data of Pancreatic Primary Tissues.....	91
Table 2.3 Type of cells, origin and culture media included in this study.....	96
Table 2.4 Primers utilised for qPCR.....	117
Table 2.5 Material chosen in the IF staining.....	128

List of Abbreviations:

BCC: Basal Cell Carcinoma

BSA: Bovine Serum Albumin

CAFs: Cancer Associated Fibroblasts

CML: Chronic Myeloid Leukaemia

DAB: 3,3'-Diaminobenzidine

DHH: Desert Hedgehog

DMEM: Dulbecco's Modified Eagle Medium

EACC: European Collection of Cell Cultures

ECM: Extracellular Matrix

EDTA: ethylenediaminetetraacetic acid

EMT: Epithelial Mesenchymal Transition

FBS: Fetal Bovine Serum

FDM: Free Differentiation Media

GFP: Green Fluorescence Protein

GLI1: Glioma-associated oncogene 1

GLI2: Glioma-associated oncogene 2

GLI3: Glioma-associated oncogene 3

HPI : Hedgehog Pathway Inhibitor

HPRT: Hypoxanthine–Guanine Phosphoribosyltransferase gene

HRP: Horse Radish Peroxidase

HGF/SF: /hepatocyte growth factor/ scatter factor

IF: Immunofluorescence

IHC: Immunohistochemistry

IHH: Indian Hedgehog

IPMN: Intraductal Pancreatic Mucinous Neoplasm

MCN: Mucinous Cystic Neoplasm

MDT: Moderate Differentiate Tumour

MF: Myofibroblast

MSCs: Mesenchymal Stem cells

MSCM: Mesenchymal Stem Cell Media

MSCGS: Mesenchymal Stem Cell Growth Supplement

NSCLC: Non Small Cell Lung Carcinoma

NT: Normal tissue

PanIN: Intraepithelial Pancreatic Lesion

PBS: Phosphate Buffered Saline

PDAC: Pancreatic Ductal Adenocarcinoma

PDT: Poorly Differentiated Tumour

PSC: Pancreatic Stellate Cells

PTCH1: patched homolog1

PTCH2: patched homolog2

RFP: Red Fluorescence Protein

SCLC: Small Cell Lung Carcinoma

SCN: Stem Cell Niche

SHH: Sonic Hedgehog

SMO: Smoothened

TGF β : Tumour Growth Factor β

TME: Tumour Condition Media

Chapter 1 - Introduction

1.1 Cancer underlying causes

1.1.1 Cancer and prevention

Cancer is a consequence of the alteration of normal cell proliferation and can start from one or few cells of a tissue and then spread in all directions via the circulation. It can be considered a genetic disease as it arises from modifications in the normal expression of genes implicated in important processes during the lifetime of a cell, such as division, differentiation, apoptosis and DNA repair. The contribution of inherited factors to cancer development has been estimated around 5-10% of cases, highlighting the high impact of environmental factors that play a role in 90-95% of tumours [Anand *et al.* 2008]. Environmental and inherited factors should not, however, be considered as independent factors that play an autonomous role in cancer formation but as interdependent causes of it [Mucci *et al.* 2001]. The development of cancer can be in fact considered a multistep process characterised by progressive evolution from a normal cell phenotype to a cell with aggressive and invasive behaviour. Cancer cells acquire six biological characteristics that accumulate in a multistep process: uncontrolled cell proliferation, reduced ability to undergo apoptosis, evasion of growth suppression, support of angiogenesis, self sufficiency in growth signals, and capacity for invasiveness and metastasis [Hanahan and Weinberg 2011]. The proliferative phenotype can be triggered by mutations affecting functionality in genes classified in two main groups: oncogenes and tumour suppressor genes. These two kinds of genes

encode proteins that maintain and regulate the balance of cell proliferation by respectively triggering and inhibiting it in normal tissue. Modification in genes implicated in the regulation of cell apoptosis and DNA repair are also a major cause of cancer development [Hanahan and Weinberg 2011].

An important influence on cancer development is also exerted by the tumour micro-environment. The interplay between cancer cells and cells constituting the microenvironment (stromal cells) seems to strongly affect the survival of both cell types and contribute to the progression of the tumour [Tysnes and Bjerkvig, 2007].

There are more than 200 types of cancer, each with different causes, symptoms and treatments. Each year in the UK there are 289,000 new cases diagnosed, and the latest statistics show that 324,579 people were diagnosed with cancer in 2010 (www.cancerresearchuk.org). These data suggest that prevention would be the most appropriate approach. Prevention is based mainly on the avoidance of cancer-producing agents that range from the well characterised ones, such as smoking tobacco, to environmental hazards and the effect of diet. Moreover, screening programmes to identify tumours before they produce symptoms have been carried out for several types of cancer. However, identification of cancer in the first stages of its development is still a major challenge. For this reason it is important to define the right therapeutic approach, in order to treat cancer once it is already at an advanced stage. Cancer can be treated by using different therapies like chemotherapy (the use of drugs to kill cancer cells) radiotherapy (use of

X-ray to kill cancer cells); hormone therapy (stops hormones from reaching hormone-sensitive cancer cells) and biological therapy (that include immunotherapy, cancer vaccination and gene therapy). Chemotherapy is the therapy most commonly used and investigated. One of the basic concepts of therapy is to inhibit cancer hallmarks in order to inhibit their acquired capability of uncontrolled proliferation, growth and invasiveness (Figure 1). Cancer cells are, however, often able to become resistant to treatment by compensating via signalling through alternative pathways. For this reason, combined drugs with different hallmarks target could be more effective and reduce the probability of developing resistance.

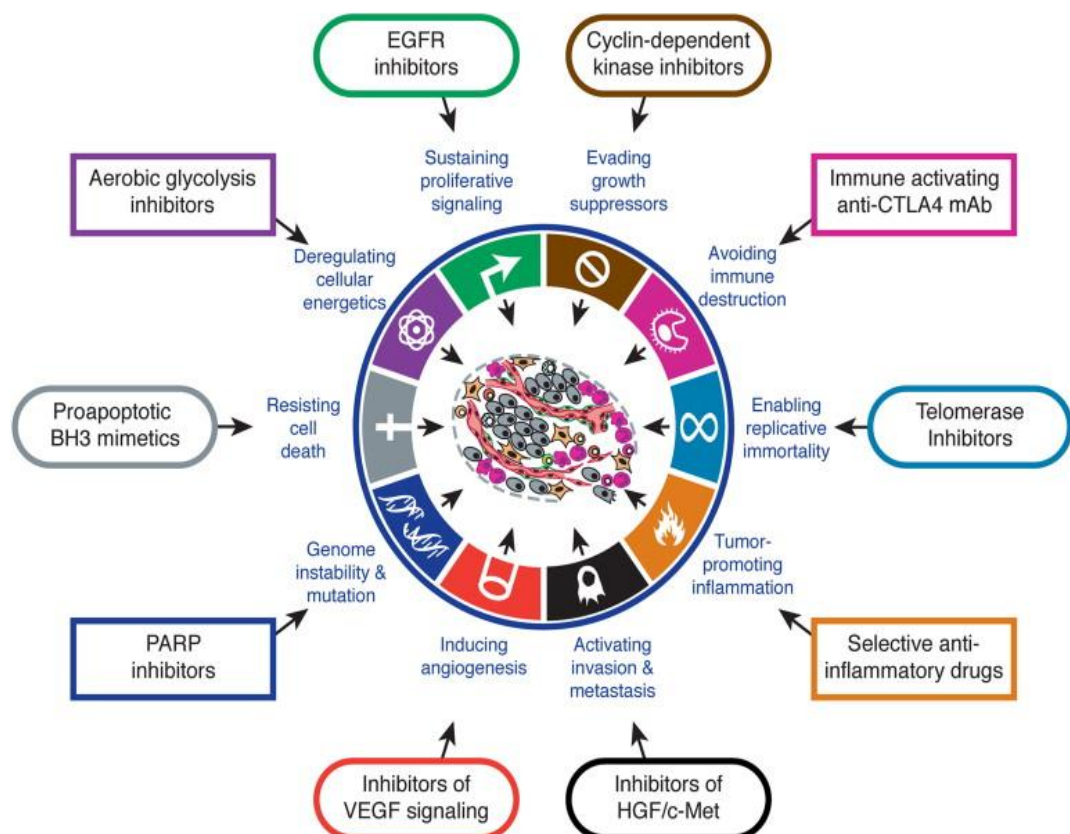


Figure 1.1 Therapeutic Targeting of the Hallmarks of Cancer. Picture taken from Hanahan and Weinberg 2011 article in *Cell*, Volume 144, Issue 5, Pages 646-674 [Hanahan and Weinberg 2011] Copyright licence obtained from Elsevier.

1.1.2 Pancreatic cancer

Pancreatic cancer is one of the most dangerous solid tumours with a 5 year survival rate around 6 %. In the United States, in 2012, it was estimated there would be 43,920 new cases, of which 37,390 were predicted to die within 5 years [Siegel 2012].

Therapeutic approaches in pancreatic cancer are still not good enough to overcome it, especially if discovered at a late stage. The most used chemotherapeutic agents at the moment to fight the progression of pancreatic cancer are fluorouracil (5FU) (an anti-metabolite that affects the DNA-repair process resulting in cell death) and gemcitabine (a nucleoside analogue that blocks DNA replication after its incorporation) [Barone *et al* 2003; Oliani *et al* 2004; Hidalgo *et al.* 2010]. Of these two drugs gemcitabine seems to have fewer side effects and so it is more widely used (www.cancerresearchuk.org). Different combinations of gemcitabine with drugs targeting other pathways involved in cancer progression are also under trial but still not really applied in patients [Oliani *et al* 2004; Hidalgo *et al.* 2010]. In advanced tumours chemotherapy is just a palliative to increase survival by only a few weeks, or months, but is not very effective [Oliani *et al* 2004; Hidalgo *et al.* 2010]. Moreover 5% of the epithelial pancreatic cancer cells seems to be formed from cancer stem cells (identified for their expression of CD44, CD24, and epithelial specific antigen ESA stem cell markers) known to be able to exert an important role on chemotherapy resistance [Ischenko *et al.* 2010] clearly suggesting the need for new drugs able to

overcome this resistance and to be more effective than those currently used.

Pancreatic cancer often starts with pre-malignant lesions that then progress to malignant tumour by accumulating mutations in key genes involved in cell proliferation control, like K-ras, p16/CDKN2A, TP53 and SMAD4 [Feldmann *et al* 2007].

There are three types of pancreatic precursor lesions: intraepithelial pancreatic lesion (Pan IN), intraductal mucinous neoplasm (IPMNs) and mucinous cystic neoplasm (MCN). The precursor lesions that normally develop into invasive pancreatic ductal adenocarcinoma (PDAC), the most common form of pancreatic tumours, are the PanIN. These lesions are divided in three groups (PanIN1; PanIN2, PanIN3) based on a gradual acquisition of a papillary architecture and cytological degenerative criteria [Hruban *et al.* 2001]. PanIN1 lesion presents with K-ras mutation, whereas PanIN2 and PanIN3 acquire also respectively p16/CDKN2A and TP53, SMAD4 tumour suppressor gene mutations that drive the degenerative progression towards PDAC. In fact, PDACs show the expression of more than one of these mutations and their effect synergise in a final uncontrolled cell proliferation and invasive phenotype [Feldmann 2007].

K-ras protein is a proto-oncogene involved in cell growth and differentiation. Its mutated form in codon 12 is very common in pancreatic cancer (95% of pancreatic cancers) [Almouguera *et al.* 1988] and is able to trigger uncontrolled proliferation of pancreatic epithelial cells in engineered mice conditionally expressing it (K-rasG12D).

However to fully develop PDAC, synergistic effects of the other suppressor gene mutations are needed [Tuveson *et al.* 2004].

It was also observed that 48 of 50 samples (98%) of pancreatic cancer analysed presented an alteration in the Rb/P16 (also called INK4a) pathway. This signalling is implicated in the regulation of cell cycle phase G1, and the alteration of the P16 tumour suppressor activity triggers an uncontrolled cell proliferation and then neoplasia [Schutte *et al.* 1997].

Finally the role of SMAD4 was demonstrated to have differential tumour stage-dependent roles in pancreatic tumours. SMAD4 is a transcription factor triggered during the activation of the tumour growth factor β (TGF β) pathway. A study in a genetically engineered mouse model showed a double effect of this pathway in PDAC. Deletion of SMAD4 in mouse with Kras^{G12D} mutation and inhibition of INK4a resulted in an increase in PDAC formation into a moderately or well differentiated tumour stage, indicating its role as a tumour suppressor protein. However, expression of wild-type SMAD4 can increase, in the same engineered mouse (Kras^{G12D}-INK4a null), the progression to poorly differentiated tumour by promoting epithelial mesenchymal transition (EMT), a mechanism that induces the trans-differentiation of epithelial cell into mesenchymal cells increasing their motility and the property of tumour cells invasiveness. This process shows its double role in the determination of tumour grade, differentiation and aggressiveness in PDAC [Bardeesy *et al.* 2006].

Pancreatic cancer is also characterised by the alteration of pathways normally involved in development like Hedgehog, Wnt and Notch pathways. All these signalling pathways play a role in regulation of cell proliferation, survival and differentiation and their alteration seems to synergise with Kras mutation in PDAC [Maitra *et al.* 2008; Morris *et al.* 2010].

1.1.2.1 The Stroma component of pancreatic cancer

A very important role in pancreatic tumour progression is exerted by the stromal component. PDAC is characterised by a strong desmoplastic reaction associated with tumour progression. The origin of this stromal component is a consequence of proliferation of *in situ* fibroblasts, pericytes and pancreatic stellate cells (PSCs) [Feig *et al.* 2012].

PSCs are cells normally inactivated that, under stimuli from epithelial cells, express α -smooth muscle protein (α SMA), collagen type I and III, laminin, fibronectin and extracellular matrix (ECM) protein. All these proteins contribute to increased stromal volume, cell contractility and invasion [Omary *et al.* 2007]. Study of the origin of fibrosis showed a clear role for activated PSC in the increase in connective tissue in the pancreas [Haber *et al.* 1999].

Another important stromal cell observed in pancreatic cancer is myofibroblast cells recruited from bone marrow that constitutes approximately 25% of cancer-associated fibroblast (CAFs) [Chu *et al.* 2007]. Other components of tumour stroma are endothelial cell

precursors and cells of the inflammatory/ immune system [Scarlett *et al.* 2011].

1.1.2.2 *In vivo models of pancreatic cancer*

Xenograft models have been performed for pancreatic cancer in order to investigate the main pathways involved in this type of tumour and to identify targets for new therapies. These models successfully showed the reconstitution of PDAC and its desmoplastic effect (Feldmann *et al* 2008; Bailey *et al* 2008; Berman *et al* 2003). However, the growth of tumour cells *in vitro* before mouse implantation has been demonstrated to alter the molecular characteristics of the cells (Daniel *et al* 2009) and, moreover, these models seem unable to represent the tumour stroma in all its complexity. Studies focused on patient-derived xenografts (PDX), models obtained by tumour fragment engraftment into immunocompromised mice, support the idea that *in vitro* growth reduces, by clonal selection, the variety of cellular type and subtype normally present in the pancreatic tumour (Kopetz *et al* 2012), including cancer stem cells (CSC) responsible for resistance to chemotherapy (Li *et al* 2007; Jimeno *et al* 2009). PDX have been used in the investigation of new therapeutic drugs directed against the main pathways involved in the development of pancreatic cancer (e.g. K-RAS, HER2 and Hh) with the aim of reducing the pancreatic tumour mass and blocking metastasis [Mattie *et al* 2013; Siolas *et al* 2013; Walters *et al* 2013]. The molecular characterisation (gene expression and microRNA microarrays, mutation analysis, short tandem repeat (STR) profiling,

and immunohistochemistry) of 8 human patient tumours was compared to the corresponding xenograft models and showed a high correlation [Mattie *et al* 2013]. PDX models for pancreatic tumour showed the ability to metastasise and develop the desmoplastic reaction typical of this type of cancer [Fu *et al* 1992; Suetsugu *et al* 2012]. These models have been largely used for the investigation of the stromal reaction in this tumour. Considering the tendency of the mouse stromal cells to substitute the original human stroma, the implantation of primary tumour in transgenic mice expressing fluorescent protein like GFP (green fluorescent protein) allowed the investigation and characterisation of the stromal cells involved in the pancreatic cancer [Suetsugu *et al* 2012]. Moreover an interesting method to image the progression of tumour stroma has also been used: the human tumour was initially established as a xenograft in a mouse and then orthotopically transplanted into a sequence of transgenic mice expressing different fluorescent markers (e.g. RFP, GFP). In this way, progression in the tumour stroma was observed [Suetsugu^{article 2} *et al* 2012]. Nevertheless, the PDX models have shown some limitations: the necessity to implant the human tumour in immunodeficient mice completely eliminates the possibility of testing immunotherapies. Moreover, problems associated with storage of tumour specimens and the need to re-establish after freezing can alter the tumour. Furthermore, in PDX as well as in xenograft models, the human stroma is still being replaced by mouse stroma. Finally, primary tumour resected and transplanted before the therapeutic treatment exclude the investigation of refractory cancers.

Other important models for the investigation of pancreatic cancer and chemotherapeutic approaches able to maintain an intact immune-system are the engineered mice, such as that described in the literature [Bardeesy *et al.* 2006]. A very interesting and representative engineered model was obtained by constitutively expressing the Kras-P53 mutation in the, so called, KPC mice. This model was successfully used to investigate the role of gemcitabine and Hh pathway inhibitors on drug delivery and pancreatic volume mass reduction, highlighting the importance of the Hh pathway in this tumour [Olive *et al.* 2009]. However, in a recent study focused on the investigation of the genomic alterations in pancreatic cancer, 12 pathways were showed to be involved in this tumour and all these pathways were showed to be important for its development. In view of this study transgenic mice expressing only 2 or 3 mutation could fail to reproduce the human PDAC [Jones *et al* 2008].

1.2 The role of stroma in tumour development

The microenvironment of a tumour plays a fundamental role in the process of development, growth and metastasis. This microenvironment comprises tumour epithelial cells and the surrounding stroma which is made up of fibroblasts, vascular and lymph endothelial cells, extracellular matrix, and a range of immune and inflammatory cells [De Wever *et al.* 2008]. Stromal cells can be classified into a number of subtypes including myofibroblasts, CAFs, fibrocytes, and pericytes. An important role for myofibroblasts in the modulation of the stroma physiology and pathology in the cancer setting has been demonstrated [Spaeth *et al.* 2009]. The myofibroblasts are the main components of the stroma and in normal tissue act in the process of wound healing, but also in tissue morphogenesis at an embryonic level. In the tumour setting, through the secretion of chemokines, cytokines, matrix metalloproteinases (MMPs) and extracellular matrix (ECM) components, they are able to modify the structure of stroma and to induce the invasion and migration of tumour cells to other tissues (metastasis). A number of positive and negative markers have been used to identify myofibroblasts. All myofibroblasts express α -smooth muscle actin (α -SMA), as well as vimentin, desmin, cadherin11 and Collagen Type 1. However, it is impossible to find a profile of markers to define perfectly a sub-population due to the diversity of the origins of CAFs present in a tumour [De Wever *et al.* 2008 ; Anderberg C, Pietras K 2009]. In fact, as shown in Figure 2, the source of myofibroblasts and CAFs can be a

consequence of trans-differentiation of several kinds of cells resident in the tumour (adipocyte, epithelial and endothelial cells) or differentiation of circulating mesenchymal stem cells (MSCs) [De Wever *et al.* 2008].

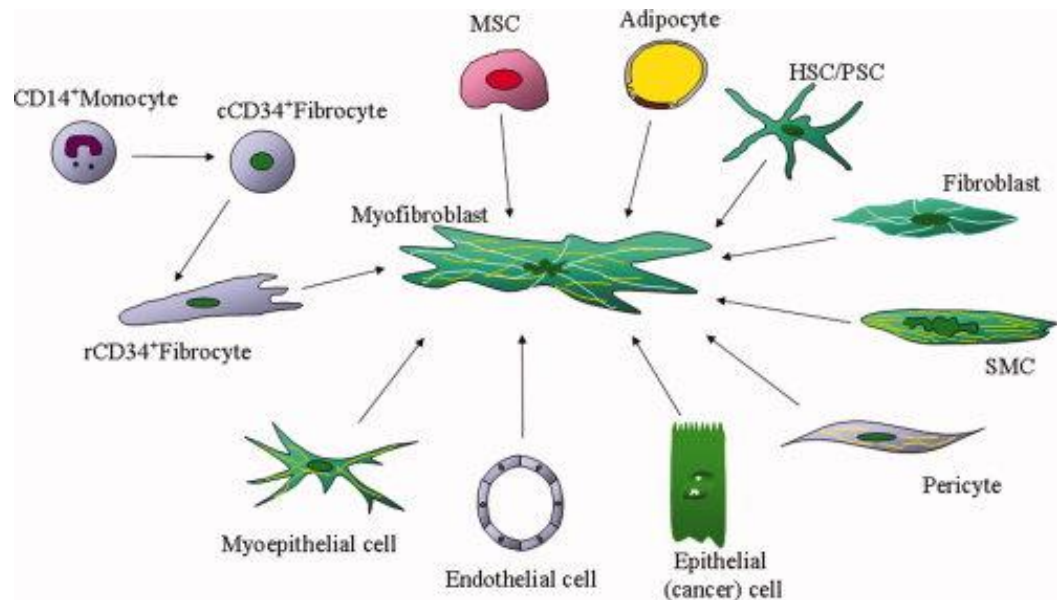


Figure 1.2 Origin of stroma cells in tumour microenvironment. Stroma cells can derive from transdifferentiation of different types of cell lines resident in the tumour microenvironment or from circulating and recruited MSC from bone marrow. Image taken from De Wever *et al.* International Journal of Cancer Volume 123, Issue 10, pages 2229-2238, 5 SEP 2008
Copyright licence obtained from John Wiley and Sons.

1.2.1 Interplay between epithelial and stromal cells

A role for these fibroblasts in the signalling network between stroma and tumour-derived epithelial cells and in overall growth, vascularisation and invasion of the tumour, has been confirmed *in vivo* and *in vitro* studies.

Co-culture *in vitro* shows the reciprocal paracrine communication between CAFs and epithelial tumour cells. A mixed population of cancer cells and CAFs showed a synergistic effect on the expression of

cytokines and growth factors that sustain tumour growth, like VEGF (vascular endothelial growth factor) and G-CSF (granulocyte colony formation factor) [Kurcenova *et al* 2010]. Furthermore, co-cultures between CAFs and human melanoma cells showed a supportive role of CAFs in the cancer cell proliferation process. It seems, in fact, that CAFs release paracrine factors that protect tumour cells from serum deprivation-induced apoptosis and cytotoxicity and stimulate their colony formation ability [Kucerova *et al.* 2010]. The effect of stroma on tumour invasiveness has been demonstrated *in vitro* with co-cultures of myofibroblast and cancer cells isolated from colon cancer. After 48h it was possible to see migration of cancer cells on a collagen gel only when myofibroblasts were present. Cancer cell pro-invasive activity was stimulated by two factors secreted from myofibroblasts: the scatter factor/hepatocyte growth factor (SF/HGF) and TGF- β up-regulated extracellular matrix tenascin C (TNC) [De Wever *et al.* 2004]. Finally normal fibroblasts co-cultured with pancreatic tumour cells expressing K-ras, express Palladin protein which in turn stimulates their activation (detected as increase of α SMA and vimentin expression). Activated fibroblasts are then able to increase tumour cell invasion and create a tunnel structure that allows the migration of cancer cells [Brentnall *et al.* 2012].

As well as *in vitro* experiments the interplay between stroma and epithelial cancer cells has been thoroughly demonstrated by *in vivo* experiments. Pancreatic stellate cells when co-transplanted with pancreatic cancer cells in orthotopic mice were able to induce tumour

growth, angiogenesis and cancer cell metastasis. Tracking of the movement of cancer cells through use of mixed female pancreatic cancer cells transplanted with or without male PSC, which could be monitored using a Cy3-labeled fluorescent probe able to detect the Y chromosome, showed how human PSC migrate with cancer cells to the secondary site of the tumour, directly participating in the metastatic process [Xu *et al.* 2010].

In the tumour microenvironment, 20% of cancer-associated fibroblasts originate from MSCs [Spaeth *et al.* 2009]. This differentiation is induced by paracrine factors released from epithelial cancer cells [Mishra *et al.* 2008]. A recent study identified GRP78 factor the responsible to induce the α SMA expression (a marker of CAFs) in MSCs via TGF β /Smad pathway activation [Peng *et al.* 2013]. *In vivo* experiments have confirmed the effect of MSCs on the growth and proliferation of a tumour. For example xenograft tumour formed from a 1:1 mix of the ovarian tumour cell line Skov3 and MSCs grew significantly more than the Skov3 cells implanted alone. Moreover, in the mixed tumour the secretion of growth factors by both kinds of cells was observed: epithelial cancer cells grown in MSC-conditioned media secreted an increased amount of IL-6, HGF, TGF- β , VEGF, and the same effect could be obtained stimulating the MSC cells with Skov3-conditioned media [Spaeth *et al.* 2009].

Moreover, MSCs have been observed to have an angiogenic effect through the release of VEGF and desmin in xenografts formed from

Skov3 cells and MSCs compared to a xenograft tumour alone [Spaeth *et al.* 2009].

Finally, subcutaneous injection of MSCs and breast cancer cells into mice, in order to form xenografts, triggers the expression of the chemokine CCL5 in mesenchymal stem cells which in turn enhances the motility and metastasis of breast cancer cells (by paracrine activation) [Karnoub *et al.* 2007].

1.2.2 Tumour microenvironment, cancer stem cells and resistance to chemotherapeutic treatment

Recent evidence showed a very important role of the tumour microenvironment in promoting chemotherapeutic drug resistance observed in cancer cells of different tumours.

The basic mechanism consists of mutational changes due to DNA damage caused from drug treatment on mesenchymal stroma cells. Chemotherapeutic activation of transcription factor NF- κ B in mesenchymal stroma cells was demonstrated [Sun *et al* 2012], which in turn is able to stimulate the transcription of the Wnt family member WNT16B. This factor was then demonstrated by *in vitro* and *in vivo* experiments to trigger the Wnt pathway in prostate, breast and ovarian cancer cells and increase their resistance to drug treatment via paracrine mechanism (Figure 1.3) [Sun *et al.* 2012].

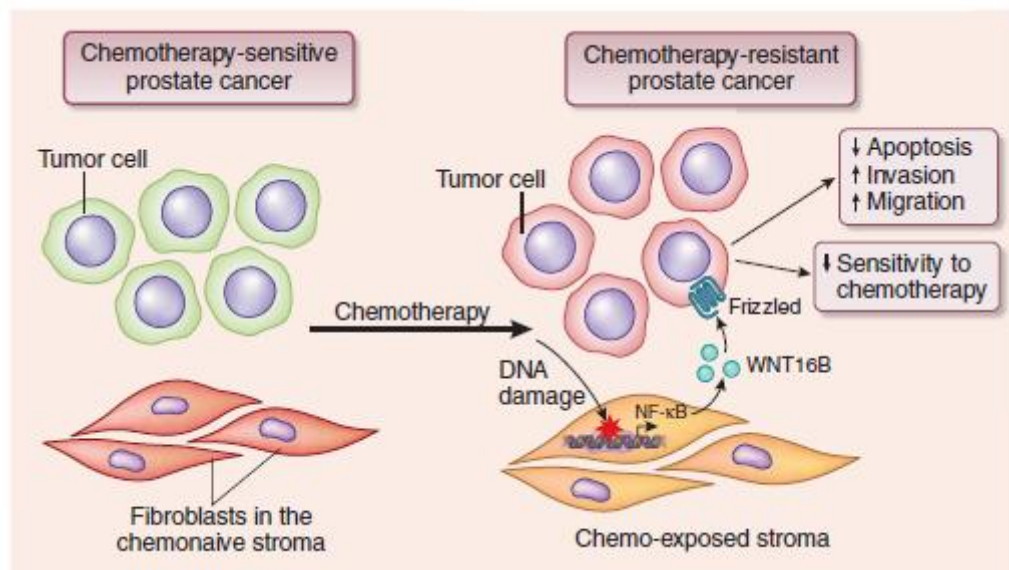


Figure 1.3 Tumour microenvironment regulates drug sensitivity. Drug responses of cancer epithelial cells are not exclusively determined by their intrinsic characteristics, but are also controlled by signals derived from the TME. (Figure taken from Arne Östman volume 18 | number 9 | September 2012 nature medicine). Copyright licence obtained from Nature Publishing Group.

Stromal cell response to chemotherapy and radiation treatment also result in the up-regulation of HGF which enhances paracrine activation of the c-Met receptor in breast cancer cells leading to resistance to RAS inhibitors (often used in the chemotherapeutic treatment of breast cancer). Chemotherapeutic resistance is also increased via the same mechanism in colorectal cancers with BRAF mutations and HER2 positive breast cancer (two markers of drug sensitivity already known and used to identify the molecular mechanism of treatment resistance) (Figure 1.4) [Wilson *et al.* 2012; Straussman *et al.* 2012].

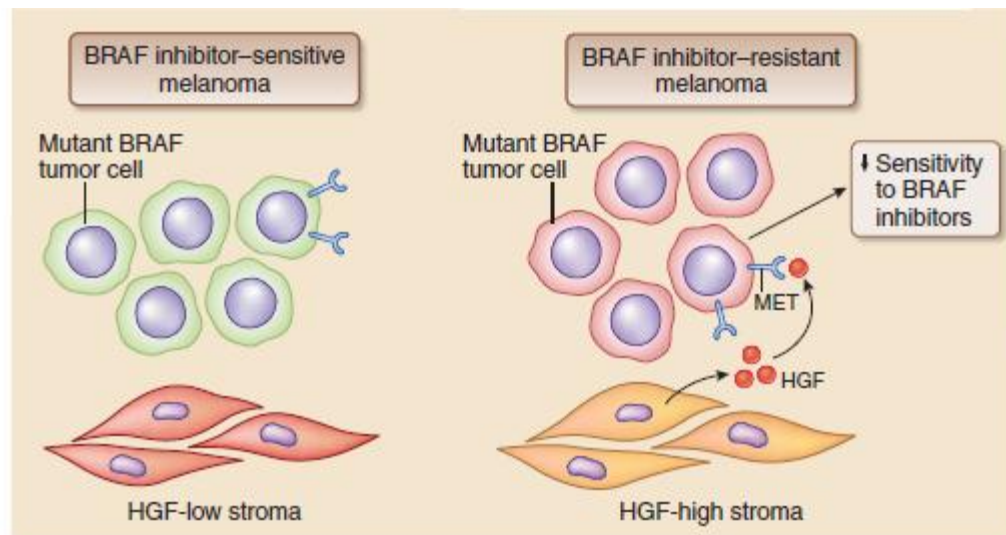


Figure 1.4 Tumour microenvironment regulates drug sensitivity. Figure taken from Arne Östman volume 18 | number 9 | September 2012 nature medicine . Copyright licence obtained from Nature Publishing Group.

Stromal cells exert chemotherapeutic resistance also in a more indirect way, by supporting the survival of cancer stem cells (CSC). These cells constitute a small percentage of the entire tumour but are able to trigger tumour formation and growth when implanted in mice [Al-Hajj *et al.* 2003]. CSC have been in fact observed to be involved in the origin of leukemia [Lapidot *et al.* 1994], breast [Alhajj *et al.* 2003], and pancreas tumour [Li *et al.* 2007]. Although CSC are a minority of the cells in the context of pancreatic cancer, when transplanted in NOD/SCID mice they are able to trigger significant tumour growth [Li *et al.* 2007]. CSC are defined based on three main biological properties: capacity of self-renew, ability to differentiate into different cell types and, as said, ability to induce *in vivo* formation of a new tumour after implantation in a mouse model. Currently, these are many controversial theories about their origin including that they derive from:

- Stem cells resident in the tissue where the tumour is formed
- Mutated mesenchymal stem cells recruited following inflammation and wound healing
- Fusion of bone marrow stem cells with resident cells resulting transformed cancer stem cells
- Progenitor cells that acquire a capacity for self-renewal through deregulation of self-renewal pathways like Hedgehog, Wnt, Notch [Tysnes and Bjerkvig 2007].

CSC are demonstrated to be resistant to chemotherapy and to be capable of causing tumour relapse in different type of tumour highlighting the importance of their role in the tumour microenvironment (TME) [Rajan *et al.* 2008].

Recent studies showed the important role of myofibroblast cells within the TME in cancer stem cell survival, introducing the concept of a cancer stem cell niche and its role in promoting tumour progression and metastasis [Malanchi *et al.* 2012, Lonardo *et al.* 2012]. It has been shown that myofibroblast cells secreting factors like Periostin protein (POSTN), a component of extracellular matrix, help the survival of cancer stem cells by recruiting Wnt pathway that is able to maintain the cancer stem cell survival and self-renew. The re-programming of cancer stem cell niche in the metastatic secondary site seems to be fundamental in triggering the tumour to begin metastasis [Malanchi *et al.* 2012].

Thus, this study highlights the importance of a deeper understanding of the mechanisms that regulate the interplay between tumour and stroma

that can give important information for future combinatorial clinical treatments designed to block this interaction which is a fundamental step in cancer progression.

1.3 Hedgehog signalling in development and homeostasis

1.3.1 The Hedgehog Pathway

Hedgehog (Hh) signalling was identified for the first time in the fruit fly *Drosophila melanogaster* as one of the signalling molecules implicated in development. Subsequently Hh proteins have been characterised in a multitude of species, including humans. The Hh pathway is now implicated in many important processes such as development, adult tissue homeostasis, tissue repair in chronic inflammation, carcinogenesis and stem cell maintenance [Ingham PW 2008; Katoh y Katoh 2006].

Three homologous Hh ligands are secreted from different tissues at various stages of development: Shh (Sonic Hedgehog); Ihh (Indian Hedgehog) and Dhh (desert Hedgehog) [Ingham and Mc Mahon 2001]. The Hh ligands bind to a 12-pass transmembrane protein, Patched-1 (Ptch-1), relieving the repression exerted on a seven-pass transmembrane GPCR-like (G protein coupled receptor) protein, Smoothened (SMO), and triggers the Hh signalling cascade. SMO de-repression activates the serine/threonine kinase STK36 which in turn phosphorylates the negative regulator of the Hh pathway SUFU that becomes inactivated and subsequently promotes the nuclear accumulation of full-length GLI transcription factors (Gli1, Gli2 and Gli3) (Figure 1.5) [Ingham PW 2008; Katoh y Katoh 2006].

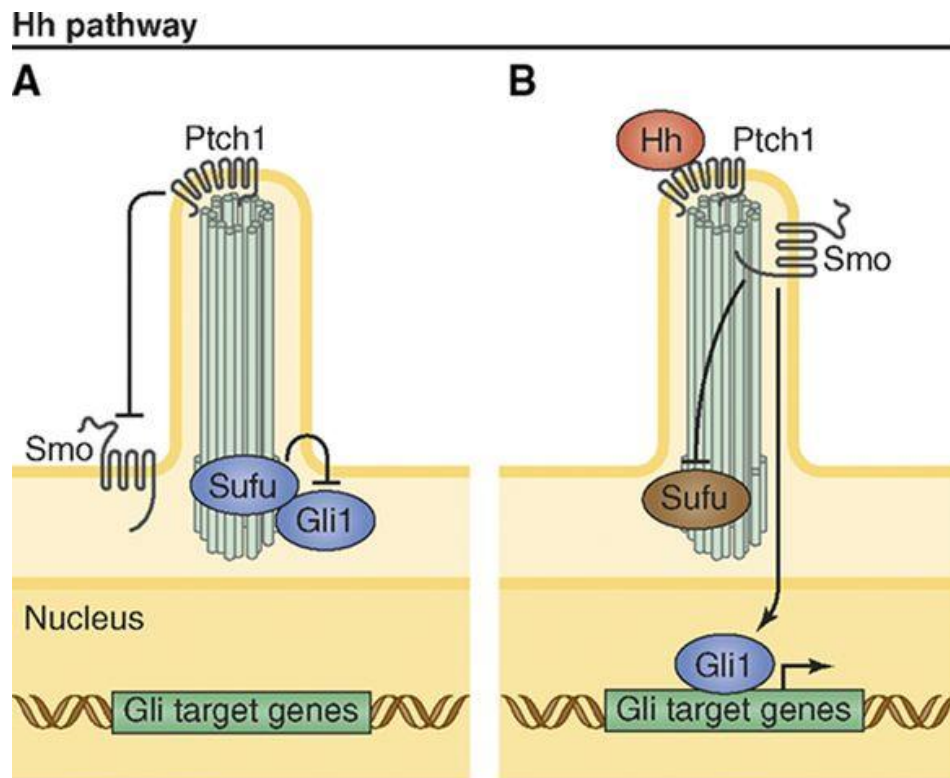


Figure 1.5 Activation of Hh signaling. A) Inactivated Hedgehog signaling. B) The Hh ligand, binding to transmembrane protein receptor Patch, relieves from repression the transmembrane protein SMO that becomes activate. Once activated SMO trigger a signal cascade during which the inhibition of the Hh pathway inhibitor Suppressor of Fused (SuFu) allows the activation of Gli transcription factors and the Hh gene target transcription [Image taken from Atwood *et al.* 2012, original published in JCell Biol.; 199:193-197 doi: 10.1083]. No Copyright permission license was requested for non commercial reuse.

The regulation of Hh pathway expression is quite complex and can occur at many different levels. For instance, Gli1 and Ptch1 are also target genes of the Hh pathway and they are normally used as indicators of Hh pathway activity [Lee *et al* 1997; Hidalgo and Ingham 1990]. Gli1 and Ptch1 respectively exert a positive and negative feedback on the Hh pathway in order to balance the expression of the pathway gene targets. Ptch1 negative feedback prevents its own overexpression which would otherwise result in inhibition of the Hh

pathway with severe consequences during development [Goodrich *et al.* 1999]. Moreover, both isoforms of Ptch, Ptch1 and Ptch2, can be activated by Shh but a stronger correlation was seen between Ptch2 and Dhh. The Dhh-Ptch2 complex has been observed mainly to act in specific organs and tissues like prostate, ovary, testis, skin and cerebellum suggesting a different localisation of action of these two receptor forms [Carpenter *et al.* 1998; Rahn timer *et al.* 2004; Bajestan *et al.* 2006]. Due to the Ptch1 negative feedback induction, analysis of Hh pathway activity by detection of Ptch1 expression, even if recognised and used in many papers, could be more difficult.

Gli1 expression regulation is also intricate, with recent evidence from literature showing that Ptch1 is able to inhibit Gli1 expression, not just through SMO inhibition relief, but also via an alternative non-canonical (independent from Smo and SuFu) mechanism. Two distinct domains in Ptch1 were identified as responsible for this new mechanism of Gli1 inhibition and they are distinct and independent from the C-terminal region responsible for the canonical Hh pathway inhibition thorough Smo [Rahn timer *et al.* 2006]. Moreover, other studies have shown activation of Gli1 via different non-canonical pathways including KRas and TGF β [Nolan-Steva timer *et al.* 2009] making the picture more complex and complicating the analysis of this pathway.

Hh signalling transduction also depends on its localisation on the primary cilium of cells. There is still little known about regulation of this process but SMO localisation and activation in the cilium as a fundamental requirement for triggering of Hh signalling have been

suggested [Corbit *et al.* 2005; Rohatgi *et al.* 2009]. Moreover, mutation in the intraflagellar transport (IFT) proteins inhibited Hh signalling in the development of the murine limb bud [Haycraft *et al.* 2005]. It seems, in fact, that a very important role in the localisation of an Hh pathway complex of activators and repressors that acts downstream of SMO but before the GLI transcription factor is exerted by the IFT122 protein [Qin *et al.* 2011]. Further investigations on the relationship between cilium localisation and Hh pathway activity showed that Shh ligand or mutations that constitutively activates SMO are both able to induce SMO localisation to the cilium [Corbit *et al.* 2005] confirming a role of cilium in Hh pathway signalling regulation. However, constitutive localisation of SMO in the cilium, by overexpression of SMO in the cell, is not enough to reach the maximum Hh pathway activation, suggesting that localisation in the cilium and SMO activation are two independent steps both necessary to signal transduction [Rohatgi *et al.* 2009].

Further regulation of the pathway involves the localisation of GLI2 /GLI3 transcription factors and the inhibitor SuFu in the apical part of the cilium where, in the absence of Hh signalling they are in a repressive form that does not translate the signal [Haycraft *et al.* 2005]. Recent evidence seems to implicate PKA (a protein involved in the machinery of Hh signalling transduction) in this localisation. PKA is a protein kinase, which in the context of cilium localisation, does not act by phosphorylation of Gli2 and Gli3 but in a more indirect way [Zeng *et al.* 2010].

In conclusion the Hh pathway is characterised by different levels of regulation showing the complexity of this signalling.

1.3.2 Hh ligand expression regulation

The Hh ligands, responsible for triggering the pathway, are found in mammals as three different genes *SHH*, *DHH* and *IHH* which probably originated via a duplication event. Dhh is the most similar ligand to the single homologous ligand in *Drosophila*, whereas Shh and Ihh developed later on in vertebrates [Ingham and McMahon 2001].

SHH/Shh act during vertebrate development at many different levels and in almost all organ and tissue formation (neural tube, limb, heart, gut, eye, bone and cartilage, muscle and others) by regulating cell fate differentiation, proliferation and survival. In this entire development process, Shh mainly acts in a paracrine manner inducing the downstream Hh pathway via short range action or in more distant cells (long range action) [Ingham and McMahon 2001].

The secretion of Shh requires modification and organisation of the ligand. Full length Shh has a lipid modification that results in cholesterol and palmitic acid moieties at the C-terminus and N-terminus of the protein respectively [Porter *et al.* 1996; Pepinsky *et al.* 1998]. Cholesterol modification is very important for the anchorage to the cellular membrane and both lipid modifications regulate the ligand concentration and the potency of long range signalling [Grover *et al.* 2011].

To be secreted Shh needs to be organised in oligomers. Interestingly the structural organisation of these oligomers can influence the Shh mechanism of action. Small oligomers formed by electrostatic interaction and multimeric structures (consequence of a covalent binding with heparan sulphate proteoglycans (HSPG)) are in fact able to respectively trigger short and long range pathway activation [Vyas *et al.* 2008] . Another regulator of Hh pathway long and short range activity is the intracellular localisation and secretion of the ligand. Hh ligand is distributed both basally and apically in the epithelial cells. Association between long range activity mediated by extracellular matrix proteins (ECM) (Dally and Dally-like glypicans) and apical secretion has been demonstrated [Ayers *et al.* 2010]. Consistently short range action correlated with basal secretion and did not seem to be affected by alteration of apical secretion [Ayers *et al.* 2010].

The secretion of Shh from the cells is mediated by a protein called Dispatched (Disp). As proof of the role of Dispatched in Shh secretion, Disp-null mice showed a very similar phenotype to Smoothed-null mice, with no Hh signalling. Moreover, the loss of Hh signalling in these null-mice was not a consequence of unsynthesised Hh molecules but of the inability to transport the Hh ligand across long distances to allow the long range paracrine activation, typical of developmental processes [Kawakami *et al.* 2002].

Other different methods of Shh transportation have also been suggested (e.g. extracellular vesicular particles, exosomes or for short

range communication cellular protrusion or nanotubes) [Therond *et al.* 2012].

The complexity of Hh ligand organisation and the regulation of its secretion is an important aspect of the Hh signalling since it is probably responsible for its ability to exert so many functions not just in development but also, as explained later on, in cancer development and formation.

1.3.3 The Gli Transcription Factors.

The net effect of Hh stimuli in vertebrates is the activation of three zinc-finger transcription factors: Gli1, Gli2 and Gli3. [Ruiz I Altaba *et al.* 2007]. These proteins encode both activator and repressor functions and act in a combinatorial and cooperative fashion [Aza-Blanc 2000; Park *et al.* 2000; Buttitta *et al.* 2003, Bai *et al.* 2004]. In *Drosophila* this transcriptional role is carried out by the homologous transcription factor Cubitus interruptus (Ci). Much of the information that we have so far, comes from studies on *Drosophila* which have revealed an intricate network of several factors during Hh signal transduction.

Gli1, Gli2 and Gli3 proteins all have a C-terminal transactivation domain but only Gli2 and Gli3 have an N-terminal repressor domain [Sasaki *et al.* 1999]. When the Hh signal is absent, Gli2 and Gli3 in vertebrates, and Ci in *Drosophila*, are present in a latent transcriptional repressor form, binding to a multiple protein complex in the cytoplasm. This complex contains the kinesin-related protein Costal-2 (Cos2), the Fused kinase (Fu) and Suppressor of Fused (SuFu) [Ingham and McMahon

2001; Kasper *et al.* 2006]. The Gli2/3 proteins, as shown by studies in *Drosophila* focused on the homologous Ci, blocked in the cytoplasm by the Cos2 complex, are phosphorylated by PKA, GSK3 β and CK1 proteins and cleaved by the proteasome Slimb (supernumerary limb) within the C-terminal transactivation domain conferring on them repressor activity [Wang *et al.* 1999; Price and Kalderon 2002]. After cleavage the proteins retain the N-terminal repressor domain, allowing them to bind to promoters and inhibit transcription of Hh target genes (Figure 1.6).

When the Hh signalling is activated the Gli2/3 proteins are not bound but are released as full-length transcription factors. During this process, the Cos2 complex undergoes several changes including the recruitment of Cos2 protein by the cytoplasmic tail of Smo, the activation of Fu and the phosphorylation of SuFu. All these modifications lead to the release and stabilisation of Gli proteins as transcriptional factors that activate the gene target of Hh signalling (Figure 1.6) [Ingham and Mc Mahon 2001; Kasper *et al.* 2006].

The regulation of Gli1 activity differs from that of Gli2 and Gli3 because this takes place at the transcriptional level and the mRNA expression of Gli1 can be considered a direct indicator of Hh signalling activity [Lee *et al.* 1997]. Evidence shows that the regulation of Gli1 activity is dependent on the presence of functional Gli2 and Gli3. In fact Gli2 and Gli3 can directly activate Gli1 at the DNA level by binding to its promoter [Ding *et al.* 1998; Dai *et al.* 1999; Buttitta *et al.* 2003, Bai *et al.* 2004].

The activation or inhibition of a target gene by Gli proteins can be enhanced by others factors that act during Hh signalling. For example SuFu, through the activation of histone deacetylase (Sap18 and Sin3), can enhance the inhibition of gene targets when the Hh signal is absent. On the other hand, proteins like Missing in Metastasis (MiM) and Yak1 related kinase (Dyrk) can enhance the transcriptional activity of Gli1 and Gli2 (Figure 1.6)[Kasper *et al.* 2006].

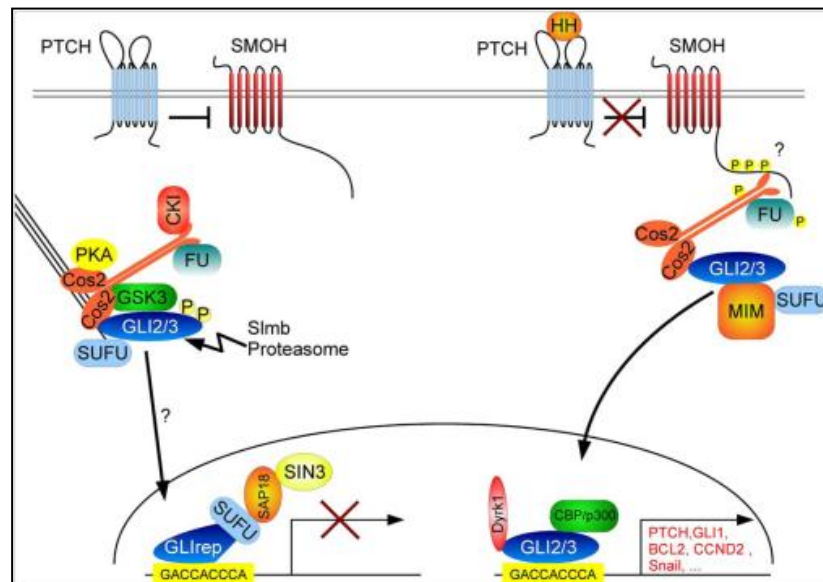


Figure 1.6 Gli2 and Gli3 proteins can act both as repressor and activators. When there is no signaling the multi-protein complex Cos2 blocks the Gli2/3 proteins in the cytoplasm. Here Gli2/3 proteins are phosphorylated by PKA, GSK3 β and CK1 proteins and cleaved by the proteasome Slimb within the C-terminal transactivation domain conferring on them repressor activity. When the Hh signaling is activated the Gli2/3 proteins are not tied but are released as full-length transcription factors. The activation or inhibition of a target gene by Gli proteins can be enhanced by others factors that act during Hh signalling such as SUFU (inhibitor of the pathway), MIM and Dyrk (activators of the pathway). Images taken from Kasper *et al.* 2006. Copyright licence obtained from Elsevier.

The ability of Hh signalling to regulate so many different processes including development, proliferation and homeostasis is a consequence

of an interplay between the Gli proteins that act in an age-context and species-specific way, and the ability of each Gli protein to activate a distinct set of gene targets preferentially [Ruiz I Altaba *et al.* 2007; Buttitta *et al.* 2003; Ding *et al.* 1998].

Several studies show how Gli proteins act in a species-specific way having different effects depending on their context. For example in the mouse, loss of the function of any single or all Gli proteins does not completely abolish neural tube neurogenesis [Bai *et al.* 2004], in contrast with the results obtained in frog where there is a critical involvement of Gli function in the patterning of the neural plate and a important requirement for each Gli protein in the induction of all primary neurons [Nguyen *et al.* 2005]. The ability of these proteins to act in a context-dependent manner could be explained by their combinatorial activity [Bai *et al.* 2004, Buttitta *et al.* 2003, Park *et al.* 2000], their capability, in the case of Gli2 and Gli3, to act both as repressor and activator [Aza-Blanc 2000; Park *et al.* 2000; Buttitta *et al.* 2003, Bai *et al.* 2004] and by the interaction of the Gli proteins with the other, above-mentioned, proteins involved in the Gli network.

A good example of the interplay between the Gli proteins is the development of vertebrates' neural plate and neural tube and sclerotome induction. In the ventral neural plate a double Gli gradient with an opposite distribution of repressor and activator is responsible for tissue patterning (Figure 1.7). These double gradients regulate the differentiation of stem cells during development, and it is possible to observe an increase in Gli1 and Gli2 activator expression during the

undifferentiated and proliferating phases which gradually decreases during the differentiated stages, giving rise to high expression of the repressor forms of Gli3 and Gli2 (Figure 1.7) [Ruiz I Altaba *et al.* 2007].

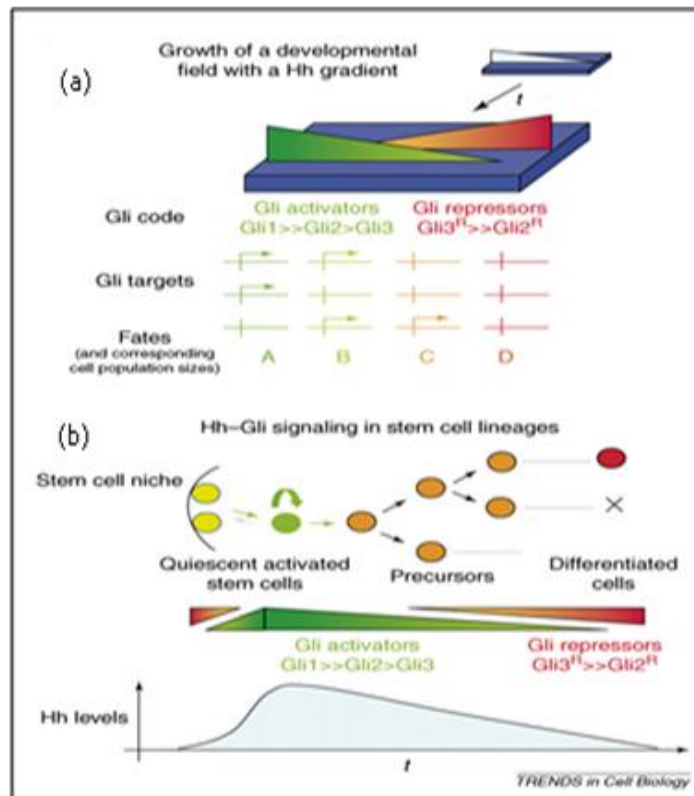


Figure 1.7 Hh pathway expression during development. a) Gli repressors and activators are differentially distributed in vertebral neural plate leading to a differential expression of Hh gene target in time and space determining in this way the fate and the proliferation/survival rate of cells. b) Hh pathway in stem cell differentiation. Gli activators are highly expressed in undifferentiated and proliferating phases, and low expressed in differentiated cells, giving rise to increased expression of the repressor forms of Gli3 and Gli2 [Image taken from Altaba *et al.* 2007]. Copyright licence obtained from Elsevier.

A study of the role of Shh in sclerotome induction confirmed the importance of Gli2 and Gli3 in development but it also showed how they can act both as repressors then as activators. In sclerotome induction, in fact, it is possible to observe repressor activity of Gli2 and activator

activity of Gli3 that are normally difficult to detect. Indeed regulation of Gli1 and Ptch1 in cultured cells by Gli3 activity has been observed. Moreover Gli2^{-/-}Gli3^{+/-} transgenic mice express the Shh target genes in contrast with Gli2^{-/-}Gli3^{-/-}. In the same study a role for Gli2 in the inhibition of Shh gene targets was confirmed by the observation that a Gli2^{-/+}Gli3^{-/-} mouse does not exhibit the same level of Shh target derepression as a Gli2^{-/-}Gli3^{-/-} mouse. An explanation for the difficulty in detecting Gli3 activator and Gli2 repressor activity could be that in normal conditions Gli2 is a stronger activator than Gli3 and Gli3 is a stronger repressor than Gli2. Therefore when Gli2 is expressed this would usually mask the activator activity of Gli3 and vice-versa [Buttitta *et al.* 2003].

The complexity of Gli regulation and function and their capacity to influence each other's activity, as observed in neural plate development and sclerotome induction, can be explained by the existence of protein complexes. The zinc finger structure of the Gli proteins supports this hypothesis, which may provide a possible binding site for other Gli proteins leading to the formation of homo- and/or heterodimers. Other observations support this hypothesis. For example in amphibians, when all but one Gli is removed it is possible to observe a loss of the neurogenic activity of Gli1 [Nguyen *et al.* 2005]. In mouse mesoderm the induction of Hh gene targets by Gli1 depends on the presence of Gli2 and Gli3 [Buttitta *et al.* 2003], and co-immunoprecipitation assays showed physical interaction of Gli proteins [Nguyen *et al.* 2005].

However, there is currently too little data available to confirm this hypothesis with any certainty.

In conclusion, this complex interplay of Gli proteins, even if still not well understood, may explain the numerous functions of the Hedgehog pathway and, as will be explained in the next paragraphs, their functional alterations are tightly involved in the development of cancer.

1.4 Hedgehog Signalling and Cancer

The target genes of the individual GLI transcription factors are numerous and have a variety of roles. Genes include cell-specific targets and their up-regulation can induce premalignant events including inhibition of apoptosis (via BCL2) [Bigelow *et al.* 2004], enhanced proliferation (via CCND2) [Duman-Scheel *et al.* 2002], angiogenesis (via VEGF) [Coultas *et al.* 2010], epithelial-mesenchymal transition (via SNAIL) [Li *et al.* 2006], and stem cell clonogenicity [Peacock *et al.* 2007]. For these reasons, deregulation of Hh signalling has been associated with several different cancers.

Different types of tumours such as oesophageal [Berman *et al.* 2003], gastric [El Zaatary 2007; Yan *et al.* 2013], pancreatic [Feldmann *et al.* 2008; Xu *et al.* 2009], multiple myeloma [Peacock *et al.* 2007] and ovarian [Bhattacharya *et al.* 2008; Liao *et al.* 2008] show reactivation and overexpression of the Hh pathway. Recently deregulation of Hh pathway was seen also in breast [Tao *et al.* 2011], colon adenocarcinoma [Bian *et al.* 2007]; prostate [Chen *et al.* 2009] and lung [Yuan *et al.* 2007]. Moreover, the role of Hh pathway in these cancers seems to be involved in different stages of the carcinogenesis process. For example, an effect of Hh pathway in tumour development and in metastasis has been observed in pancreatic and gastric cancer [Thayer *et al.* 2003; Bailey *et al.* 2009; Yoo *et al.* 2011; Yan *et al.* 2013], while in other tumours like prostate [Show *et al.* 2009], breast [Tao *et al.* 2011], and ovarian [Liao *et al.* 2009] it has been shown that there is an

important role for the Hh pathway in progression, tumour growth and proliferation [Yang *et al.* 2010]

Other tumours associated with the Gorlin syndrome like basal cell carcinoma (BCC), medulloblastoma and rhabdomyosarcoma have been found to be associated with a loss of function of *PTCH1* or *SuFu* genes [Unden *et al.* 1996; Lee *et al.* 2007; Goddich *et al.* 1997; Tostar *et al.* 2006]. The treatment of these tumours with Hh pathway inhibitors blocks tumour progression indicating a role for this pathway in these kinds of tumour.

Screening of BCC samples and medulloblastoma has also shown an important association with two mutations (SMO^{M1} and SMO^{M2}) consequence of two nucleobase transitions in two different exons of the SMO protein [Xie *et al.* 1998; Lam *et al.* 1999; Reifenberger *et al.* 1998]. Transgenic mice with SMO^{M2} expression driven from a keratin 5 promoter showed an overexpression of SMO^{M2} and a skin phenotype typical of BCC. The same transgenic mice with SMO^{WT} expression did not show any particular skin phenotype [Xie *et al.* 1998]. Finally the Smo^{M2} mutation was found to be associated with 3 BCCs of 31 analysed but also with 1 PNET (Primitive Neuroectodermal Tumours of the Central Nervous System) tumour. The level of SMO expression in these tumours was higher compared to the control and was associated with increased expression of *Gli1* and *Ptch1*. These results demonstrate that SMO mutations results in ligand-independent activation of SMO and consequently activation of the Hh pathway [Reifenberger *et al.* 1998]

Evidence from the literature suggests a link between the Hh pathway and cancer stem cell frequency in breast cancer [Liu *et al.* 2006], multiple myeloma [Peacock *et al.* 2007] and chronic myelogenous leukemia [Zhao *et al.* 2009]. In all these tumours Hh induced self-renewal and expansion of cancer stem cells. Hh pathway expression was also identified in pancreatic cancer stem cells (recognized as CD44+CD24+ESA+ cells) and its role in self-renewal and formation of new tumours in immunodeficient mice was confirmed. Gene expression analysis of SHH was compared between CD44+CD24+ESA+, CD44-CD24-ESA- (considered non stem cells), pancreatic tumour cells and normal pancreatic cells. The expression of Shh was up-regulated around 43 times in pancreatic cancer stem cells in comparison to normal cells and only 4 times in CD44-CD24-ESA- and bulk pancreatic tumour cells [Li *et al.* 2007]. Consistent with Hh expression in cancer stem cells, stem cells cultured from glioblastoma multiforme (GBM) (gliomaspheres) when treated with cyclopamine, showed dose-dependent decreased proliferation, suggesting the presence of the Hh pathway signalling in these cells. In support of this, shRNA targeting SMO affected cell survival and induced apoptosis of gliomaspheres, suggesting the decreasing stem cell proliferation observed after cyclopamine treatment occurs not as a consequence of toxicity but as a direct consequence of Hh pathway inhibition [Clement *et al.* 2007].

Since stem cells are known to be resistant to chemotherapy and radiotherapy, a better understanding of the role of Hh in these cells

could be important for future clinical application of new anti-cancer drugs.

1.4.1 Paracrine transmission of Hedgehog signalling

The mechanisms of Hh pathways activation in different cancer types are currently a topic of great interest. Recent studies [Yauch *et al.* 2008; Tian *et al.* 2009; Nakamura *et al.* 2010] suggest a paracrine model for Hh signalling in certain cancers in contrast with the previous finding of tumour epithelial cells responding to Hh ligand overexpression in an autocrine manner [Thayer *et al.* 2003; Berman *et al.* 2003; Stecca *et al.* 2007]. So far in the literature, four different types of Hh signalling in cancer have been proposed [Scales-De Sauvage 2009]. Type I tumour involves ligand-independent, mutation-driven signalling, i.e. medulloblastoma, and basal cell carcinoma, that are often a consequence of Gorlin's Syndrome in which mutation of PTCH1 and SuFu lead to constitutive activation of Hh signalling [Xie *et al.* 1998, Lam *et al.* 1999]. Type II is a ligand-dependent cancer, in which tumour cells respond to Hh ligand overexpression, triggering signalling in an autocrine manner. The type III tumour is tumour ligand-dependent and involves paracrine interactions in which tumour cells secrete Hh-ligands which trigger the signalling cascade of Hh pathway in the stromal component of the tumour microenvironment. Finally the type IV tumour follows a "reverse paracrine model" in which Hh ligands are secreted by the supporting stromal cells which act on malignant cells. So far this last

kind of signalling has only been observed in a hematologic model and a more thorough analysis is needed [Scales-De Sauvage 2009].

More recent articles show some weaknesses in the proposed autocrine model and propose that a paracrine model is more relevant for all cancer [Yauch *et al.* 2008; Tian *et al.* 2009; Olive *et al.* 2009; O'Tool *et al.* 2011].

1.4.1.1 *In vivo and in vitro evidence supporting Hh paracrine signalling in tumour microenvironment*

The role of the stromal microenvironment in human tumour growth is supported by evidence that Hh ligands failed to activate signalling in tumour epithelial cells [Yauch *et al.* 2008].

To verify the existence of Hh signalling in tumour epithelial cells, the sensitivity of these cells (measured by cell viability) to a small molecule SMO-acting antagonist and cyclopamine (also a SMO antagonist) has been correlated with the expression of Hh pathway activity in these cells. As predicted, no correlation was found in epithelial cells, but the half maximal inhibitory concentration (IC₅₀) of the SMO antagonist required to inhibit the cell growth in an Hh-responsive mesenchymal cell line (HEPM) was found to be 400 times lower than that necessary to obtain the same effect in cancer cell lines. Moreover, co-culture of an epithelial cancer cell line and 10T1/2 mouse embryo cell line transfected with a Gli reporter construct showed a correlation between the induction of Gli activity in fibroblasts and the levels of Hh ligands expressed by tumour

cells, demonstrating the capacity of the epithelial cells to induce paracrine signalling in fibroblast cells [Yauch *et al.* 2008].

Furthermore, separation of epithelial cells and stromal cells by using FACS sorting for CD24 (a marker expression of epithelial cells) from human breast tumour, showed high immunofluorescence (IF) staining of Shh and hedgehog interacting protein Hhip (gene target of Hh pathway) respectively in epithelial and stroma like cells (co-stained with vimentin to confirm their fibroblasts nature). These results support the idea of the paracrine signalling between tumour cells and stromal fibroblast cells [O'Toole *et al.* 2011].

Tests *in vivo* have been carried out using mouse xenograft models established with surgical biopsies from cancer patients. The mouse stroma substitutes for the human stroma, and then, by using species-specific probes it is possible to distinguish the human tumour vs. mouse stroma. The expression of Hh ligands in the human tumour cells correlated with the expression of Gli1 in mouse stroma confirming a paracrine-type induction [Yauch *et al.* 2008]. Finally, in order to test the effect of Hh signalling on tumour growth, mouse embryonic fibroblasts (MEFs) engineered to have conditional removal of SMO were implanted with colon epithelial cell lines expressing luciferase and compared with a mouse control in which there was a normal expression of SMO. The mouse with the SMO knockout in MEF cells showed a reduction in tumour size as assessed by reduced luciferase activity [Yauch *et al.* 2008].

An additional recent publication from the same group also showed paracrine Hh signalling. The expression of an oncogenic allele of Smoothed (Smo^{M2}) was induced in epithelial pancreatic cells in a mouse model. Surprisingly, no impact on pancreatic development and neoplasia was observed, showing the absence of Hh signalling in cells possessing the mutant SMO [Tian *et al.* 2009]. Mice obtained by crossing PdxCre/Smo^{M2} mice (in which SMO^{M2} is expressed only in epithelial pancreatic cells) with Ptch-LacZ mice did not show β -galactosidase expression (detected by Ptch-LacZ reporter immunostaining) in ductal epithelial cells but only in mesenchymal pancreatic cells, demonstrating that the pancreatic epithelium is not competent to transduce autocrine Hh signalling. Finally the PdxCre;Kras mice with Kras-driven pancreatic tumours after treatment of pancreatic ductal epithelial cell (PDEC) line with recombinant Shh or molecule agonist of SMO, induced strong activation of the Hh pathway (determined by Gli1 mRNA expression) only in fibroblasts and not in epithelial cells [Tian *et al.* 2009].

A recent study of Nolan-Stevaux's group confirms the observation in pancreatic ductal adenocarcinoma (PDAC), demonstrating that genetic deletion of SMO in KrasG12D-driven PDAC has no effect on tumour progression and development and so indicating a possible absence of the pathway in these cells [Nolan-Stevaux *et al.* 2009].

Moreover, experiments on prostate cancer support the paracrine Hh signalling model, and the fundamental role of myofibroblasts in this process [Shaw *et al.* 2009]. It was observed that biclonal xenograft

tumours obtained from a 1:1 mix of prostatic cancer cells (LNCaP) and immortalized urogenital mesenchymal cells (UGSM-2), showed significantly lower tumour growth in comparison to a bclonal xenograft in which the prostatic cancer cells over-expressed Shh (LNShh+UGSM-2) [Shaw *et al.* 2009]. There was also a strong association between increased tumour proliferation and the amount of myofibroblasts present in the stroma, confirming the fundamental role of the stroma in cancer progression [Shaw *et al.* 2009]. In order to better understand this role a microarray analysis of target genes expression in these myofibroblasts was performed. As result of this analysis a correlation between the expression of the main genes of the Hh pathway (Shh, Gli1, Gli2 and Patch) and nine gene targets that are normally expressed in the stroma of the prostate during embryonic development was observed. There is growing evidence for a stromal phenotype in prostate cancer that responds to Hh ligands by exerting growth-promoting activities that stimulate tumour cell proliferation [Shaw *et al.* 2009].

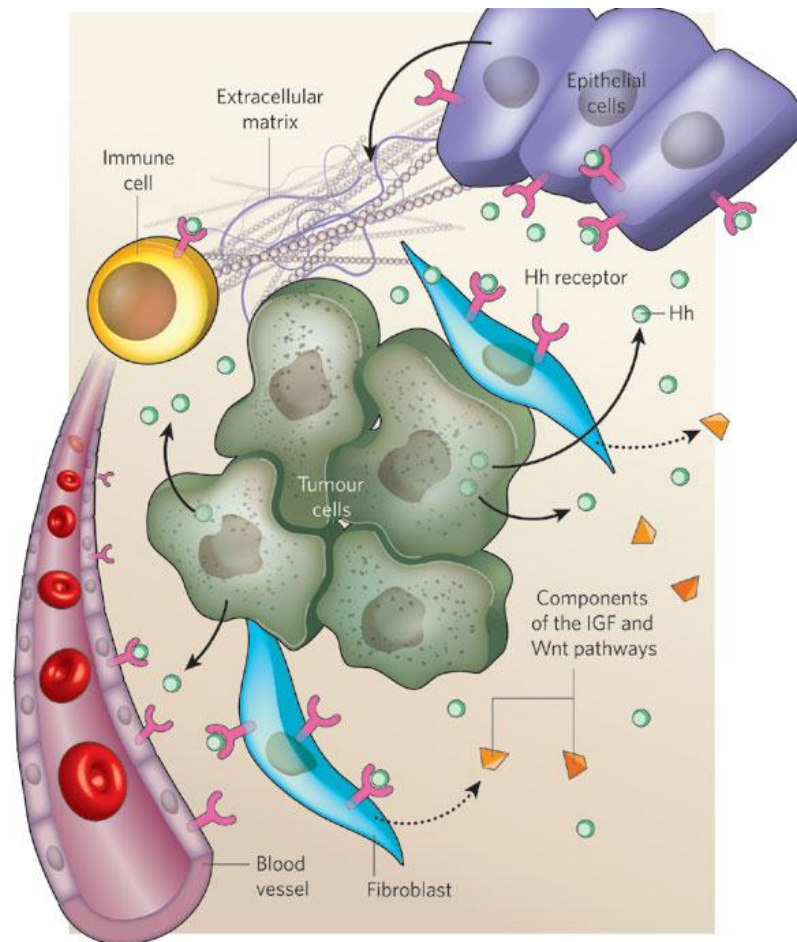


Figure 1.8 Example of Hh paracrine signaling. Epithelial tumor cells produce Hh ligands which activate the Hh pathway in stroma cells of the surrounding tumour microenvironment (including fibroblast cells, epithelial cells, endothelial cells, and immune cells). As reply to this induction the stroma cells produce growth factors and matrix proteins that promote tumor growth. Image taken from Curran and Ng, volume 455 (7211) 2008 Nature. Copyright licence obtained from Nature Publishing Group.

The paracrine transmission of Hh signalling is important for future clinical applications as demonstrated by a recent work that showed an effect of Hh pathway inhibition in stromal cells in enhancing the delivery of chemotherapeutic agents. Mouse models for pancreatic tumour obtained by conditional expression of mutant p53 and Kras proteins in cancer cells, showed a reduction of metastasis and increased tumour cell apoptosis when treated with the Hh pathway inhibitor IPI-926 and with the chemotherapeutic agent gemcitabine. IPI-926 is a drug which

targets SMO and blocks its activity. It was demonstrated that blocking SMO activity led to a depletion of the pancreatic stroma and increased vascularisation of the tumour allowing the delivery of gemcitabine and consequently a significant reduction of the tumour volume [Olive *et al.* 2009].

1.4.2 Paracrine signalling vs autocrine signalling

The results described so far seem to confirm paracrine transmission of the Hh pathway in cancer; however, other works continue to show contrasting results. In more than one study, epithelial cancer cells treated with cyclopamine in the absence of the stroma cells *in vitro*, induced apoptosis [Qualtrough *et al.* 2004; Sanchez *et al.* 2004; Mukherjee, *et al.* 2006]. Moreover, the same pancreatic cell lines as those used in Yauch's work, have, in other experiments, shown a dose-dependent decrease in cell proliferation after cyclopamine treatment and Gli1 knock-down by Gli1 siRNA transfection [Xu *et al.* 2009]. These results could be explained by a non-specific effect of cyclopamine or drug toxicity; however, competition of cyclopamine binding using purmorphamine (an Hh agonist that bind to SMO) [Xu *et al.* 2009] or reproduction of its effect by using siRNA targeting Gli1 and SMO [Sanchez *et al.* 2004; Mukherjee, *et al.* 2006; Xu *et al.* 2009] seems to support its specific role in Hh pathway inhibition and so, autocrine Hh signalling in cancer epithelial cells. In addition, a number of studies have shown Hh pathway overexpression in epithelial cancer cells including pancreatic [Thayer *et al.* 2003; Xu *et al.* 2009], prostate

[Sanchez *et al.* 2004], ovarian [Liao *et al.* 2009], gastrointestinal [Berman *et al.* 2003], breast [Mukherjee, *et al.* 2006] and melanoma [Stecca *et al.* 2007].

Many of these discrepancies could be explained by different methods used to define Hh signalling. Another possible explanation is that the involvement of Hh pathway could be cell type-dependent (i.e. stromal cells could have different response kinetics in comparison to epithelial cells) [Ruiz I Altaba *et al.* 2008]. Recently the existence of a non-canonical pathway has been described, in which the Gli proteins are regulated from different pathways like p53 [Abe *et al.* 2008; Stecca and Ruiz I Altaba 2008]; TGF- β , Kras [Nolan-Stevaux *et al.* 2009] and Wnt [Yang *et al.* 2008] and could explain the expression of Gli1 mRNA in epithelial tumour cells.

1.4.3 Hh signalling in pancreatic cancer

Pancreatic cancer is characterised by a very high desmoplastic response during the tumour development. At the advanced tumour stage, the stromal component is very high and is able to increase tumour cell proliferation and metastasis [Merika *et al.* 2012].

The Hh pathway has been investigated in this cancer for its role in promoting the increase of desmoplasia. It was shown how pancreatic cancer cells constitutively expressing or over-expressing Shh ligand and orthotopically implanted into mice were able to significantly augment the stromal mass and induce the activation of stromal cells into a more aggressive phenotype, marked by the increased expression

of α SMA, Collagen I and fibronectin [Bailey *et al.* 2008]. In the same work, *in vitro* assays showed how myofibroblast cells increase GLI1 gene and protein expression after treatment with ectopic Shh, indicating an active Hh signalling in these cells. Moreover rhShh (10 μ g/ml) treatment increased the *in vitro* invasion capability of myofibroblasts cells. Finally, modulation of Shh expression affected the α SMA expression in murine stroma cells and induced the differentiation of pancreatic stellate cells into myofibroblast cells suggesting a role for Shh in driving stromal cell activation [Bailey *et al.* 2008].

Therefore, mainly paracrine induction of Hh pathway in this tumour seems to be likely. Other work strongly confirms and supports this observation. Hh-antagonist treatment does not affect GLI1 gene expression and cell growth in pancreatic tumour cells indicating no pathway activity in them [Yauch *et al.* 2008]. Moreover, co-culture of pancreatic cancer cells, expressing different level of Hh ligands, with fibroblast cells increased GLI1 gene expression in the fibroblast cells proportionally to the level of ligands detected. Finally implantation of pancreatic cancer cells with different levels of ligands in xenograft mice Ptch1-lacZ;Rag2^{-/-} confirmed the same ligand-dependent paracrine activation in stromal cells observed *in vitro* [Yauch *et al.* 2008]. Ptc-LacZ reporter mouse, as already discussed, were also used in the work of Tian *et al.* and confirmed the downstream activation of Hh pathway in the stromal microenvironment and its absence in cancer epithelial cells [Tian *et al.* 2009]. Finally comparison between fibroblasts from pancreatic ductal adenocarcinoma (PDAC) and normal pancreas

showed 100 times greater expression of SMO in CAFs. The modulation of SMO by siRNA in these cells also reduced GLI1 expression and blocked the ability of these cells to respond to ectopic NShh treatment, confirming the activity of Hh pathway in these stromal cells [Walter *et al.* 2010].

The role of Hh pathway in development of pancreatic cancer was investigated in mice with overexpression of Shh at an early stage of pancreatic development, and showed abnormal pancreas with characteristics very similar to PanIN lesions; the mice were not able to survive [Thayer *et al.* 2003]. Further studies on xenograft mice supported the formation of a histologically undifferentiated pancreatic tumour. However, this tumour developed without following the progression via PanIN lesions typical of the PDAC. It did not follow the pattern formation typical of PDAC in which a gradual progression of still differentiated epithelial tumour cyokeratine (CK19) positive cells is common. However, this does not exclude a role of the pathway in the early stage of the tumour [Pasca di Magliano *et al.* 2006]. In the same work, simultaneous activation of Shh and K-Ras synergistically increase the formation of human PDAC in comparison to K-Ras mutated mice [Pasca di Magliano *et al.* 2006]. Moreover the co-expression of Shh at epithelial level and K-Ras significantly increased the tumour growth and cancer cell proliferation and survival [Morton *et al.* 2007]. The relationship between K-Ras and the Hh pathway is, however, still unclear. A synergistic effect was observed in this study but the inhibition of Shh in K-Ras mutated mouse did not alter cell proliferation; however,

simultaneous inhibition of Shh and PI3 Kinase blocked cancer cell proliferation. These data indicate that K-Ras and the Hh pathway act independently but they are both very important for PDAC cancer development and progression [Morton *et al.* 2007]. It was also shown that autocrine Hh pathway transmission seems optional especially during the first stage of tumour development, suggesting that different kinds of signals may be involved at different steps of this tumour [Morton *et al.* 2007]. In contrast to this idea, in another study, p48-Cre;LSL-KrasG12D;Smoflox/flox mice with no expression of SMO in pancreatic cancer cells, and so unable to respond to Hh ligand autocrine stimuli, did not show any difference in the formation of PDAC and PanIN lesion in comparison to mice wild type for SMO expression, suggesting again a role for Hh in PDAC but the inability of cancer cells to trigger it via autocrine signals [Nolan-Stevaux *et al.* 2009].

These evidences support the role of Hh pathway in pancreatic cancer development and progression and they highlight the importance of Hh inhibition in the treatment of this cancer. Paracrine activation of Hh pathway in this type of cancer seems very likely but it is not yet possible to exclude also the existence of an autocrine signal in cancer cells. This overview of Hh pathway in PDAC shows the difficulty in the fully understanding the behaviour of this pathway in cancer and the necessity of further studies.

Inhibition of Hh pathway for PDAC treatment, as well as for other types of cancer, is already under investigation and important results have been observed as described in the next section.

1.4.4 Antagonists of Hh signalling and effect of Hh pathway inhibition on cancer

The compounds screened for Hh pathway inhibition can be divided into three main groups based on the target protein: inhibitors that target the binding between Shh and Ptch1, such as the antibody 5E1 and robotnikinin; inhibitors of SMO protein (Cyclopamine, IPI-926 GDC-0449, Cur6141, SANT-1, SANT-4) and Gli inhibitors (GANT-56, GANT-61, HPI-1) [Yang *et al.* 2010].

The first Hh pathway inhibitor (HPI) used for the treatment of cancer (i.e. basal cell carcinoma) was cyclopamine, a natural compound extracted from corn lilies that binds SMO protein, blocking its activity [Taipale *et al.* 2000; Chen *et al.* 2002]. The treatment of orthotopic xenograft models for pancreatic cancer with cyclopamine showed reduced tumour development, and *in vitro* studies resulted in a reduced proliferation and invasiveness of cancer cells [Feldmann *et al.* 2008]. However, in some studies cyclopamine showed high toxic effects, teratogenic properties and poor bioavailability [Lipinsky *et al.* 2008, Yauch *et al.* 2008]. This led to the testing of a similar natural compound, IPI-926, and to the synthesis of other novel inhibitors directed against the SMO protein, such as Hh-antag, SANT-1, SANT-4 [Chen *et al.* 2002] Cur-61414 [Williams *et al.* 2003] and GDC-0449 [Lo Russo *et al.* 2011].

GDC-0449 (Vismodegib) is one of the most efficient chemotherapeutic agents against the Hh pathway and has recently been tested on patients with locally advanced solid tumour (33 patients with BCC; 8 patients with pancreatic cancer; 1 patient with medulloblastoma; and 17

patients with other types of tumours). Fifty-seven percent of the patients affected by BCC showed tumour regression and significant results have been obtained in the treatment of medulloblastoma. However, no tumour regression was observed in the 8 patients affected by pancreatic cancer [Lo Russo *et al* 2011]. Recently, the emergence of a SMO mutation that confers resistance to the treatment has been demonstrated [Yauch *et al.* 2009] in medulloblastoma cancer cells treated with GDC-0449.

A number of research projects are currently focused on inhibition of the Hh pathway in the treatment of pancreatic cancer. Considering the strong desmoplastic effect characteristic of this cancer and its poor prognosis (Chu *et al* 2007), a treatment combining a drug targeting the stroma component and an agent able to block the epithelial tumour cell proliferation is now becoming the main approach used in new trials.

Phase II clinical trial studies on pancreatic cancer have been performed for either IPI-969209 or GDC-0449 in combination with gemcitabine [Madden 2012; Catenacci *et al* 2013]. The patients treated with IPI-969209 (also known as Sarigedib) or GDC-0449 and gemcitabine were compared with patients treated with a placebo combined with gemcitabine. None of the combined treatments (Hh antagonist and gemcitabine) show a regression of the tumour or an improvement in the survival rate, in comparison to gemcitabine alone [Madden 2012; Catenacci *et al* 2013].

Variable and contrasting results have been obtained in the investigation in pancreatic cancer of co-treatment with IPI-969209 and gemcitabine.

The treatment of mice with an orthotopic tumour with IPI-969209 and gemcitabine resulted in inhibition of pancreatic cancer stem cell migration and a significant reduction of the metastasis [Feldmann *et al.* 2008]. Consistent with these results, in transgenic mice with pancreatic tumours the same combined treatment resulted in a strong reduction in the desmoplastic reaction typical of this type of tumour [Olive *et al.* 2009]. However, a more recent study from the same group showed that in an engineered mouse model capable of developing PDAC, histologically very similar to the human type, the prolonged (more than 3 months) inhibition of Hh pathway (by treatment with IPI-969209 or by knocking down Shh in the cancer cells) reduced the survival rate of mice with tumour and was associated with an undifferentiated aggressive tumour phenotype. Although, consistent with the Olive *et al* work, the tumour mass was reduced in these mice and the stroma mass was comparable to that found in normal pancreas, the combination of IPI-969209 and gemcitabine failed to obtain tumour regression. The reason for these results seems to be increased formation of vasculature. The main hypothesis formulated in this work suggests that myofibroblast cells have the tendency to inhibit endothelial cell proliferation. This would explain the poor vasculature in the stroma of pancreatic cancer. In agreement with this hypothesis, the inhibition of the Hh pathway in the tumour microenvironment and, as consequence, the depletion of the stroma mass, led to an increase of the vasculature, which indirectly induced an undifferentiated phenotype by supporting cancer cell proliferation [Rhim *et al* 2014]; treatment with antiangiogenic

drugs (showed to be effective [Rhim *et al* 2014]) combined with inhibition of Hh pathway could be an interesting strategy to investigate. The IPI-969209 trial has been suspended; however, other five trials are ongoing for the use of GDC-0449 in pancreatic cancer [Kim and Rudin 2014].

A suggested explanation for the failures observed in phase II clinical trials, was that pancreatic stellate cells are able to support the survival of cancer stem cells in pancreatic tumour by constituting a cancer stem cell niche [Lonardo *et al* 2012.]. Additionally, targeting pancreatic stellate cells, with Hh inhibitor CUR199691, as well as a combination of gemcitabine and an inhibitor of cancer stem cells SB431542, did result in tumor growth. This could have a very important impact on tumour relapse in which cancer stem cells are known to have a major role [Lonardo *et al.* 2012].

At present, other SMO inhibitors BMS-833923 (Bristol-Myers Squibb), PF04449913 (Pfizer) and LY2940680 (Eli Lilly), are under investigation in clinical trials of a range of advanced cancers (<http://www.clinicaltrials.gov/>).

Moreover, other more recent drugs (MS-0022 and AZD8542) targeting SMO in the pancreatic tumour microenvironment showed interesting *in vitro* and *in vivo* effects on the reduction of tumour mass and progression [Strand *et al* 2011; Hwang *et al* 2012]. However, both of these new drugs are still in a preclinical phase. in their investigation as chemotherapeutic drugs.

The table below shows the main Hh pathway inhibitors currently used in clinical phase trials:

Table 1.1 Hh pathway inhibitors and their phase I clinical trial.

Modified from Amakye et al Nature Medicine 19(11): 1410-1422 (2013). Copyright obtained from Nature Publishing Group.

Agent	Mechanism of Action	Phase(s)	Cancer(s)
GDC-0449	SMO Inhibitor	1, 2	BCC, medulloblastoma, pancreatic, breast, SCLC, ovarian, gastric, glioblastoma, , multiple myeloma
BMS-833923 (XL139)	SMO Inhibitor	1, 2	CML, BCC, gastric, multiple myeloma
LY2940680	SMO Inhibitor	1	SCLC, advanced solid tumours
IPI-926	SMO Inhibitor	1, 2	Pancreatic cancer
LDE225 (Sonidegib)	SMO Inhibitor	1, 2,3	Pancreatic cancer, Breast cancer SCLC, BCC, medulloblastoma, CML, advanced solid tumours
LEQ506	SMO Inhibitor	1	BCC, medulloblastoma
PF-04449913	SMO Inhibitor	1	CML

BCC: basal cell carcinoma, CML: Chronic Myeloid Leukaemia; SCLC Small cell lung cancer.

As illustrated so far, the main approach currently for targeting Hh pathway in cancer is by binding SMO and inhibiting its activation. However, as explained before, some types of cancer can be a consequence of overexpression of Gli proteins triggered by alternative pathways. In these cases, and also in cancer arising from a SMO mutation, which may compromise the binding of chemotherapeutic agents, it may be important to develop new drugs targeting Gli1 or Gli2 proteins directly. So far, new therapeutic agents against Gli proteins, like GANT58 and GANT61 have been tested but they still need further investigation [Lauth *et al.* 2007]. Moreover, other key steps of the Hh signalling, like the binding of the Shh ligand to its receptor, the translocation of the transmembrane protein SMO in the cilium and the fosforilation of key intracellular proteins, are also under investigation but still at the preclinical phase.

The following table summarise the Hh antagonist currently under preclinical investigation [Amakye et al 2013].

Table 1.2 Hh inhibitors under preclinical research investigation

Modified from Amakye et al Nature Medicine 19(11): 1410-1422 (2013).

Copyright obtained from Nature Publishing Group.

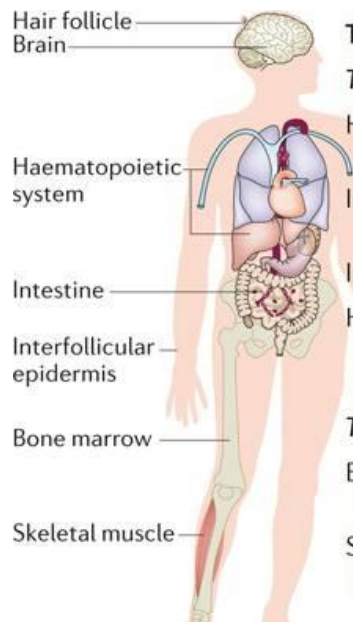
Hh pathway inhibitor	Mechanism of Action	Phase of investigation
Cyclopamine	SMO Inhibitor	Research
SANT 1,2,3	SMO Inhibitor	Research
CA1 and CA2	Inhibit cilia biogenesis, do not bind SMO	Research
SMANT	Inhibits cilia accumulation, distinct binding mode on SMO	Research
Glucocorticoids, class I (FA and TA)	Induce SMO accumulation in cilia	Research
Glucocorticoids , class II (Bud and Cic)	Inhibit cilia accumulation of SMO	Research
ALLO1 and ALLO2	Distinct binding mode to SMO	Research
Compound 5	Binds SMO and inhibits cilia translocation	Research
Robotnikinin	Binds to SHH and blocks pathway activity	Research
RU-SKI	Inhibits Hh acyltransferase	Research
Hh-specific monoclonal antibody 5E1	Blocks binding of Hh ligands to PTCH1	Research
GANT58 and GANT61	Block GLI1- and GLI2-mediated reporter activity; GANT61 interferes with DNA binding of GLI1	Research
HPI 1–4	Act at or downstream of SUFU; modulate GLI1 processing, activation and or trafficking	Research
Arsenics	Act at level of GLIs	Research
Myristoylated aPKC peptide inhibitor (PSI)	Inhibits the phosphorylation and activation of GLI1 by PKC	Research
Rapamycin	Inhibits TNF- α -induced and mTOR-S6K-mediated phosphorylation and activation of GLI1	Research

Considering the new evidence reporting paracrine transmission of Hh signalling in cancer, further inhibitors need to be tested in order to check their efficiency in the types of tumour showing paracrine mechanisms of Hh signalling.

1.5 The stem cell niche

The concept of the stem cell niche consists in the interaction between human stem cells and support cells (niche cells) which are responsible for maintaining, by direct cell contact or paracrine signalling, the proliferation, survival and self-renewal capacity of stem cells [Schofield *et al.* 1978]. The stem cell niche is not just present during embryonic development but also in adult tissues. In the human adult body there are different stem cell niches divided to low and high turnover niches based on the frequency of self-renewing and differentiating stem cells activity (Figure 1.9) [Hsu and Fuchs 2012].

Niche cells can directly derive from stem cell differentiation, and their interplay with stem cells through regulatory positive and negative feedback is mediated by important pathways involved in development like Wnt, BMP (Bone morphogenetic protein), Notch and Hedgehog [Hsu and Fuchs 2012 ; Yeung *et al.* 2011]. For example in the intestinal stem cell niche, myofibroblast cells keep the stem cells undifferentiated and maintain their survival by secreting factors like Wnt gene targets and BMP antagonists that regulate the stem cell activity (Gremlin1) [Yeung *et al.* 2011].



Tissue type	Stem cell location	Niche components
<i>Tissues with constant turnover</i>		
Haematopoietic system	Bone marrow	Macrophages*, T _{Reg} cells*, osteoblasts, adipocytes, nestin ⁺ MSCs, CAR cells, glia
Intestine	Fast-cycling: base of crypt Slow-cycling: '+4 position'	Paneth cells*, mesenchymal cells
Interfollicular epidermis	Basal layer of epidermis	Dermal fibroblasts
Hair follicle	Bulge	K6 ⁺ bulge*, dermal papilla, adipocyte precursor cells, subcutaneous fat, dermal fibroblasts
<i>Tissues with low or no turnover</i>		
Brain	Subventricular zone, subgranular zone	Ependymal cells, vasculature
Skeletal muscle	Between the basement membrane and the muscle fibres	Myofibres* (?)

Figure 1.9 Distribution of stem cell niches in a adult human body .Picture taken from Hsu and Fuchs 2012, Nat Rev Mol Cell Biol. 2012 January 23; 13(2): 103–114. Copyright licence obtained from Nature Publishing Group.

One of the most important adult niches is present in human bone marrow and is made up of mesenchymal stem cells (MSCs) and fibroblast cells (niche cells). MSCs are multipotent but not pluripotent cells characterised by their ability to self-renew and differentiate into different cell lineages such as chondrocytes, adipocytes and osteocytes [Pittenger *et al.* 1999]. MSCs do not originate exclusively from mesoderm but also from the endodermic and ectodermic layer during development. In these locations, MSCs are in their quiescent state which can be reactivated under particular conditions, such as wound healing and inflammation but also cancer [Khun *et al.* 2010].

There are three main criteria to identify MSCs: 1) the ability to adhere to plastic as a monolayer when in standard *in vitro* culture, 2) multipotency i.e. the ability to differentiate into the three cell lineages described above and 3) the expression of specific surface markers. So far there is no one marker that allows identification of MSCs but rather a combination of different expressed and unexpressed superficial markers. Expression of CD105, CD73 and CD90, and lack of expression of CD45, CD34, CD14 or CD11b, CD79alpha or CD19 and HLA-DR surface molecules appear to be the best criteria to distinguish these cells from other stem or non-stem cells [Dominici *et al.* 2006].

Interestingly, the bone marrow mesenchymal stem cell niche (mSCN) is often located very near to another niche, the haematopoietic one, and so near to blood vessels. However, even if these niches tend to strictly interact they are separate. This proximity of bone marrow to blood

vessels could however clarify how MSCs are easily able to migrate to different parts of the body [Mendez-Ferrer *et al.* 2010].

1.5.1 Mesenchymal stem cell niche and its role in cancer

The mSCN has been investigated for its role in tumour microenvironment using α SMA-RFP+ transgenic mice (in which expression of RFP was regulated by α SMA promoter) to investigate the stromal changes that characterise tumour progression [Quante *et al.* 2011]. Generation of chronic gastritis, metaplasia and dysplasia was induced by *Helicobacter felis* infection or constitutive expression of IL-1 β in the stomach. Increase of α SMA positive cells (myofibroblast cells) was observed in both mouse models at the late stage of dysplasia in comparison to control samples. These cells were then investigated for their growing and survival property in culture and for their vimentin expression to confirm their myofibroblast (MF) nature. Interestingly, the myofibroblasts originated in the infected mice showed a natural tendency to survive in culture in comparison to myofibroblasts from healthy donors. Moreover, in culture, these cells were often surrounded by RFP^{-ve} cells (undifferentiated MSCs) suggesting the existence of an *in vitro* niche. It was demonstrated that the 20 % of α SMA-positive CAFs in the tumour microenvironment were bone marrow-derived and that their source was MSCs. Furthermore bone marrow-derived CAFs were longer-lived and promoted tumour growth significantly more than other stromal cells. Finally, the mSCN (MSCs and MF cells) was observed to be recruited in a SDF-1/CXCR4 dependent manner into the

gastric cancer stroma [Quante *et al.* 2011]. In agreement with this work, the tail vein injection of bone marrow MSCs in mice with partial pancreatectomy, resulted in recruitment of these cells to the pancreas and their differentiation as PSC (that as explain have features of myofibroblast cells). Moreover, a significant reconstitution of pancreas in comparison to mice controls (mice not injected and mice with no pancreatectomy) was observed [Han *et al.* 2012].

Finally a mutual role of MSCs and myofibroblast niche cells in maintaining their reciprocal survival was observed introducing the new concept that both cell types need each other to survive and that they secrete different factor, and behave differently in the niche context than alone [Quante *et al.* 2011].

The origin of myofibroblast niche cells directly from MSC activation is probably a consequence of an asymmetrical division of stem cells. In agreement with this, quiescent intestinal stellate cells and MSC cells grown *in vitro* were able to arise and be activated into myofibroblast cells. This activation was measured as increased α SMA, Collagen I and mesenchymal associated transcription factor Lhx2 and Msx2 [Quante *et al.* 2011; Choi *et al.* 2009]. Moreover, in agreement with the niche concept, in the *in vitro* context, after long culturing far from the niche or after isolation by FACS sorting, MSCs become senescent and die [Quante *et al.* 2011; Pevsner-Fischer *et al.* 2011].

1.5.2 Stem cell niche markers

The presence of an *in situ* stem cell niche at the stromal level in primary tumour has been shown not just as a factor which promotes tumour progression but as a requisite to promote tumour metastasis [Malanchi *et al.* 2011]. However, this study was more focused on the investigation of a cancer stem cell niche in which cancer stem cells could derive from genetic changes of normal stem cells and on how a tumour in order to colonise a second tissue needs to recreate a cancer stem cell niche. The role of periostin (POSTN) was highlighted as a protein in the cancer stem cell niche context that seems very important for the survival and the maintenance of cancer stem cells. Periostin was in fact shown to be mainly expressed in fibroblasts within the cancer stem cell niche in comparison to fibroblasts alone. Periostin is a cell adhesion molecule for pre-osteoblasts and act in bone, teeth and limb development and in osteoblast recruitment and spreading [Erkan *et al.* 2007; Malanchi *et al.* 2012]. In wound repair, it is able to induce myofibroblast differentiation and contraction [Elliott *et al.* 2012]. Its expression was observed in the stroma of pancreatic ductal adenocarcinoma (PDAC) from α SMA and vimentin positive cells (myofibroblast like cells) in response to interaction with cancer cells. Moreover, once secreted, Postn seems to be able to induce a positive feed-back that maintains its expression in fibroblast cells and also induces the expression of α SMA collagen-1, fibronectin, and transforming growth factor 1 in PSC [Malanchi *et al.* 2012; Erkan *et al.*

2007]. Speculation based on these results could suggest periostin as a good candidate for a marker of MF cells in the mSCN.

A marker of MSCs in the niche context could instead be Nestin. Nestin expression was used and observed at the stromal level in gastric dysplasia together with myofibroblast-like cells [Quante *et al.* 2011]. Moreover, the investigation of the interaction between haematopoietic and bone marrow mSCN showed the expression of Nestin from a subpopulation of bone marrow mesenchymal stem cells [Mendez-Ferrer *et al* 2010]. Positive Nestin cells were shown to localise in the proximity of the hematopoietic stem cell niche. Moreover, Nestin positive cells were shown to respond in a paracrine manner to astrocyte cells by a process of self-renewal suggesting their stem cell nature [Becher *et al.* 2008].

1.5.3 Hedgehog pathway and the stem cell niche

Hh pathway is known to be one of the main pathways involved in the interplay between stem and niche cells. However, contrasting theories describe its role in the niche suggesting an effect on cell differentiation into myofibroblast cells [Yeung *et al.* 2011; Shaw *et al.* 2009; Bailey *et al.* 2008] or in contrast in the self-renewal and proliferation of stem cell [Zhou *et al.* 2006; Becher *et al.* 2008; Zhao *et al.* 2009]. Mouse models with reduced expression of SMO showed a defect in long term function of hematopoietic stem cells (HSC) in comparison to mice with functional SMO suggesting a role in stem cell self renewal. This was also shown to be involved in BCR-ABL1-induced chronic myelogenous leukaemia

(CML). $SMO^{-/-}$ mice transplanted with BCR-ABL1 cells showed a 50% reduction in CML. Finally constitutive expression of SMO in transgenic mice induced an increase in stem cells and development of CML [Zhao *et al.* 2009].

The same effect of Hh pathway on stem cell proliferation was observed in human fetal epidermis. Hh pathway main component (like Shh, Smo, GLI1 and Ptch1) were expressed in human putative epidermal stem cells (HPESCs) and modulation of the pathway with NShh (Hh pathway agonist) and Cyclopamine (Hh pathway antagonist) respectively increased and decreased the stem cell proliferation [Zhou *et al.* 2006].

In contrast with these observations, in the Yeung *et al.* review it was hypothesized that the Hh pathway is activated in myofibroblast cells of the intestinal stem cell niche. Accordingly to their theory, epithelial cells secrete Shh ligand that by paracrine induction induces myofibroblast cells to secrete BMP and Wnt pathway antagonist inducing in this way MSCs differentiation (Figure 1.10).

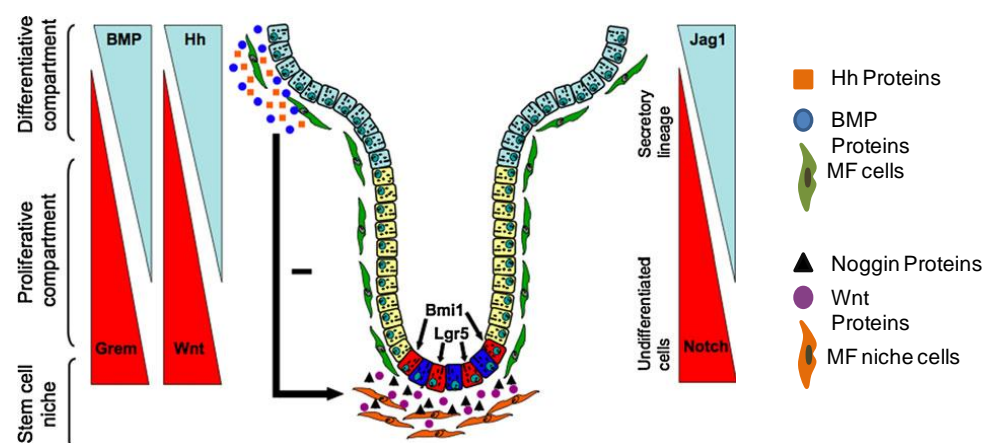


Figure 1.10 Intestinal stem cell niche regulation. Image taken from Yeung TM, Chia LA, Kosinski CM, Kuo CJ. *Cell Mol Life Sci.* 2011 Aug;68(15):2513-23. Epub 2011 Apr. Copyright licence obtained from Springer.

The effect of Shh ligand on myofibroblast activation (detected as α SMA expression increase) has also been demonstrated in other studies. Shh expression in epithelial cancer cells promoted desmoplasia and increase of myofibroblast-like cells [Bailey *et al* 2008], whereas in prostate tumours a correlation between Hh pathway expression and reactive stroma (classified by its abundance of myofibroblast cells) was observed following microarray analysis of normal and tumour prostate samples [Show *et al.* 2009].

Other studies also observed the relationship between α SMA and Hh pathway expression in non-tumorigenic tissue. For example, the effect of Hh modulation was investigated in the adult gut [Zacharias *et al.* 2011]. Transgenic mice with under-regulation of *Ihh* and *Shh* presented mislocalization of intestinal sub epithelial myofibroblasts, loss of smooth muscle in villus cores and muscularis mucosa and crypt hyperplasia. Moreover, chronic over-expression of *Ihh* in the intestinal epithelium of transgenic mice led to progressive expansion of villus smooth muscle cells. These *in vivo* data support the promotion of Hh ligand-induced myofibroblast phenotype acquisition and are supported by *in vitro* assays in which treatment of mesenchymal cells extracted from mouse with ectopic *Shh* and *Ihh* showed an increase of α SMA positive cells. The analysis of these mesenchymal cells for their expression of desmin (used as marker of undifferentiated precursor cells) and α SMA (used as marker of myofibroblast differentiated cells), revealed a mixed population consisting of progenitor cells (expressing desmin), differentiated cells (expressing only α SMA) and cells derived from

progenitor cells (expressing desmin and α SMA). So speculating, the response observed could be interpreted as the effect of Hh ligands on a mixed population that mimics the concept of the stem cell niche. Finally, rat hepatic stellate cells (HSC) (the analogue of pancreatic stellate cells in liver) induced increased Shh expression and myofibroblast markers expression in CCL4-cirrhosis *in vivo* models and in *in vitro* cell culture with serum. Interestingly, when in a quiescent state these cells expressed Hh pathway inhibitor Hhip which then decreased during the activation process (proved observing the increase of α SMA expression, Collagen1 β , and mesenchymal-associated transcription factors Lhx2 and Msx2) induced by serum-rich cultures or in presence of inflammation. Moreover, in this activated stage, expression of Shh ligand and Gli2 transcription factor was increased. Consistently, the mesenchymal phenotype acquisition was inhibited by treatment with cyclopamine [Choi *et al* 2009.] This strongly links the Hh pathway with the myofibroblast cell phenotype but moreover it makes the myofibroblast phenotype acquisition a reversible process, suggesting that α SMA and other markers used, are more an indicator of an activated state than an irreversible differentiated state. Finally, the expression of Shh in mesenchymal cells is an interesting observation that needs to be investigated. In agreement with the observation by Choi *et al.*, *SHH* gene expression was increased during MSC differentiation into a myofibroblast-like cell (detected as α SMA protein and gene expression increase) without the presence of epithelial cells. Moreover, the expression was shown specifically in a mixed population

consisting of bone marrow MSCs and myofibroblast cells in comparison to single cell populations [Quante *et al* 2011]. These data locate the expression of Shh ligand not just at the epithelial level but at the stromal level too and suggest a new interpretation of Shh expression as a marker of the mSCN. In support of this observation, expression of Shh at stromal level was confirmed, and interestingly was observed to increase with tumour grade. Moreover, its localisation in the context of the hematopoietic stem cell niche and its role in promoting, by paracrine induction, stem cell self-renew has been shown [Becher *et al.* 2008].

These data support the idea of a role for Hh in the mSCN but its role in promoting self-renewal or myofibroblast cell activation needs further investigation. Moreover, the investigation of Shh ligand expression and function in the stromal context is a new aspect that could have great impact in cancer treatment.

Figure 1.11 shows the role of the Hh pathway in pancreatic cancer. The Hh pathway paracrine signalling activation in the main stroma cells that constitute the pancreatic cancer microenvironment and its expression in the mSCN were also shown.

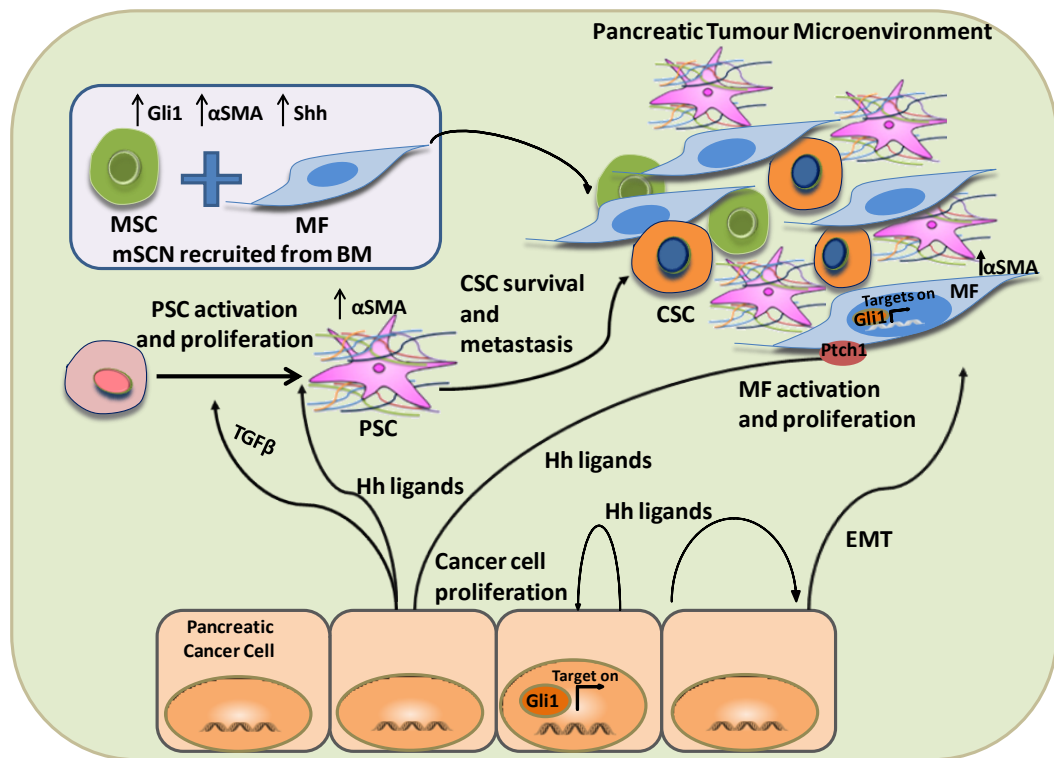


Figure 1.11 Mesenchymal Stem Cell Niche formation and recruitment in pancreatic tumour microenvironment. Pancreatic epithelial cells secrete Hh ligands that are able to paracrinally activate the Hh pathway in myofibroblast (MF) cells in the paracrine stroma. The Hh pathway activation in these cells induce their activation (Increase of αSma) and increase their proliferation. Hh ligands also induce the activation (Increase of αSma) of pancreatic stellate cells (PSC), which, once activated, strongly contribute to the desmoplastic reaction observed in pancreatic tumour. Hh ligands finally are able to autocrinally activate the Hh pathway in cancer cells, to induce the EMT (Epithelial Mesenchymal Transition) process in them and to increase their proliferation. Recent evidence suggest the recruitment of a mesenchymal Stem Cell Niche (mSCN) in the tumour microenvironment. The mSCN likely express Shh ligand. It is believed (still not proved) that PSCs and the mSCN constitute the microenvironment that support CSC (Cancer Stem Cell) survival and metastasis.

1.6 Hypothesis and aims

1.6.1 Summary of the main concepts

Pancreatic tumour is a cancer with poor prognosis: there are very few chemotherapeutic agents available to treat it and those available are not effective. It is characterised by a high stromal content and stromal components are thought to have an important role in tumour progression and induction of metastasis. Several studies have confirmed the importance of the Hh pathway in this cancer at different stages of the carcinogenesis process and the suitability of Hh inhibition as a chemotherapeutic approach. However, the mechanism of action of the Hh signalling in tumour progression is not clear yet, with many discrepancies emerging from the literature.

Thus, there is a need for further investigation in order to better comprehend the role of Hh pathway in tumour development, progression and metastasis. Based on new evidence demonstrating paracrine signalling between epithelial cells and fibroblasts, a more accurate analysis of the stromal feedback to the tumour is required, and new Hh pathway targets in the stroma should be further investigated to enhance the efficiency and reduce the collateral effect of drugs used as chemotherapeutic agents.

The recruitment of MSCs in tumour microenvironment and their differentiation into activated (expressing α SMA) cancer-associated fibroblasts is confirmed in numerous works as well as their role in tumour growth. Recently, the role of mesenchymal stem cell niche

(mSCN), constituted from mesenchymal stem cells and myofibroblast cells, has been investigated. The reciprocal dependence of both cell types to survive and form a niche is required to support activation and formation of the 20% of myofibroblasts in the tumour microenvironment. The investigation of the mSCN in tumour has shown the expression of Shh ligand when is present in a mixed population. However, no further studies have been performed on the role of Shh in the mSCN. Evidence from the literature described Hh both as promoter of stem cell activation into myofibroblast cells and in stem cell self-renewal.

1.6.2 Hypothesis

Considering the evidence from literature, in this project it was hypothesised that the expression of Shh ligand at the stromal level is a marker of a mesenchymal stem cell niche in the late stage of pancreatic tumour progression. Moreover, as Hh paracrine transmission has been shown to occur between cancer epithelial cells and the pancreatic tumour microenvironment [Yauch *et al* 2008], the mSCN, as part of the cancer stroma, was hypothesised to be able to respond to Shh paracrine stimuli during pancreatic cancer progression in a more efficient way than in cancer-associated fibroblasts or mesenchymal stem cells, also known to be part of the tumour stroma in different types of cancer [Spaeth *et al* 2009].

1.6.3 Aims

The aims of this project were as follows:

- 1) Investigation of Shh ligand expression at the stromal level and its correlation with late stage of PDAC progression (Chapter 3)
- 2) Confirmation, investigation and characterisation of stroma-like cells able to respond to Hh paracrine stimulation by pancreatic cancer cells (Chapter 4 and 5).
- 3) Characterisation of an *in vitro* model of the mSCN and of the expression and role of Shh in its maintenance/formation (Chapter 5).
- 4) Investigation of the mSCN as the best microenvironment context able to respond to Hh paracrine stimuli from epithelial pancreatic cancer cells (Chapter 5).

Chapter 2 - Materials and Methods

2.1 Human Primary tissues

The primary pancreatic and lung tissues used in this project were collected from Queen's Medical Centre (Nottingham, UK) with informed patient consent and with full ethical approval (MREC reference H0403/37). Primary normal and tumour tissue samples were cut and collected by a consultant histopathologist from the same primary pancreatic or lung tissue of the same patient, in order to allow a direct comparison and nullify the inter-patient variability. Clinical information about the TNM tumour malignant classification [A staging system to classify tumours based on their size and /or extent (T) on their spread in lymph nodes (N) and whether they metastasised (M)], the level of tumour differentiation and the tumour histology were obtained from the histopathologist's report and are summarised in the following tables (Table 2.1 and Table 2.2):

Table 2.1 Clinical Data of Lung Primary Tissues. SCC: Squamous Cell Carcinoma of Lung; NSCLC: Non Small cells Lung Carcinoma

Lung Samples	Hystology	Tumour Differentiation	T	N	M	Lung Samples	Hystology	Tumour Differentiation	T	N	M
LU22N	Adenocarcinoma		1B	0	X	LU46T	SCC	Moderate	1B	0	X
LU22T						LU47T	Adenocarcinoma		2	0	X
LU23N	Adenocarcinoma	Moderate	2	X	X	LU48T	SCC		2B	1	X
LU23T						LU50T	Adenocarcinoma	Moderate	3	1	X
LU27T	Adenosquamous	Poor	2	0	X	LU51T	Adenocarcinoma		2A	0	0
LU28N	SCC	Poor	2A	0	X	LU52T	Adenosquamous	Moderate	2A	0	X
LU28T						LU53T	Adenosquamous		2A	0	X
LU29N	Adenocarcinoma		1A	0	X	LU54T	Adenocarcinoma		2	0	X
LU29T						LU55N	SCC	Moderate	2B	1	0
LU30N	Adenocarcinoma		2A	0	X	LU55T					
LU30T						LU56T	Adenocarcinoma		3	0	X
LU31N	Pleomorphic Type NSCLC		2A	0	0	LU57T	SCC		2B	0	X
LU31T						LU58T	Mucinous Adenocarcinoma		1B	X	X
LU32N	Mixed; SCC+ Neuroendocrine		1A	0	X	LU59T	Adenocarcinoma		2	2	X
LU32T						LU60T	Adenocarcinoma		2A	1	X
LU33N	SCC		1B	0	X	LU61T	SCC		2B	2	X
LU33T							Large cCell Neuroendocrine		2A	0	X
LU34N	SCC	Poor	1B	X	X	LU63T	Renal Metastasis				
LU34T						LU64T	Mixed: SCC +Neuroendocrine		2A	1	0
LU35N	Adenocarcinoma		2A	0	X	LU66T	SCC		2B	0	X
LU35T						LU67T	Adenocarcinoma		1A	0	X
LU42T	SCC		3	1	0	LU68T	SCC		2A	1	0
LU44T	Adenocarcinoma		3	0	X	LU87N	Large Cell Neuroendocrine		3	0	X
LU45T	Adenocarcinoma		1A	0	X	LU87T					

Table 2.2 Clinical Data of Pancreatic Primary Tissues.

Pancreatic Samples	Histology of Tumour	Level of differentiation	Pancreatic Samples	Histology of Tumour	Level of differentiation
P4N		Poorly	P27N	Adenocarcinoma	Moderate
P4T			P27T		
P5N	Adenocarcinoma	Moderate	P28N	Adenocarcinoma	Poorly
P5T			P28T		
P6N	Adenocarcinoma	moderate	P30N	Adenocarcinoma	
P6T			P30T		
P9N	Adenocarcinoma	moderate	P31N	Adenocarcinoma	Moderate
P9T			P31T		
P10N	Adenocarcinoma	Poorly	P32N	Adenocarcinoma	Moderate
P10T			P32T		
P12N	Adenocarcinoma	Moderate	P33N	Adenocarcinoma	Moderate
P12T			P33T		
P18N		unknown	P35N	Adenocarcinoma	Moderate
P18T			P35T		
P20N	Adenocarcinoma	Moderate	P40N	Adenocarcinoma	unknown
P20T			P40T		
P23N	Adenocarcinoma and Pancreatitis	Poorly	P41N	Adenocarcinoma	Poorly
P23T			P41T		
P26N	Adenocarcinoma	moderate	P42T	Adenocarcinoma	unknown
P26T					

The samples were cut and then immediately stored in RNA*later* (Ambion) or fixed in at least 20 volumes of formal calcium (0.9% (w/v) calcium chloride in 3.7% (v/v) formaldehyde). Tissues in RNA*later* were held at 4°C overnight before long-term storage at -80°C, and were used for extraction of genomic DNA and total RNA (see Section 2.3.2 below). Samples in formal calcium were processed as follows:

- The pieces of tissues were left to fix for at least 24 h (penetrating the tissue at 1 mm per hour) before processing and paraffin embedding.
- Tissue cassettes were labelled appropriately in pencil, including specimen details and block numbers. Fixed tissues were then placed in the corresponding cassette. Tissues too big to fit in the cassette were trimmed and divided into additional cassettes. Once closed into the cassettes, tissues were stored in 70% (v/v) methanol until processing.
- Cassettes were loaded into a Leica TP1020 tissue processor and automatically dehydrated through one bath of 70% (v/v) methanol, one bath of 90% (v/v) methanol, five baths of 100% methanol, then cleared through three baths of xylene, for 1 h each, and then passed through two baths of molten paraffin wax at 65°C. After the processing cycle, the cassettes were removed from the tissue processor and placed into the paraffin wax reservoir, pre-warmed to 65°C, of a Leica E61160 embedding station. Tissues were removed from the cassettes and placed

into moulds containing molten paraffin wax, and then the labelled portion of the cassettes placed on top.

- The cassettes were placed on a cooling plate to solidify.
- Once the paraffin had solidified the tissue blocks were removed from the moulds and excess paraffin was removed using a Thermo Scientific Shandon Para Trimmer.

2.2 Cell culture

2.2.1 Cell culture conditions

Different types of cell lines were included in this study: 3 human epithelial pancreatic cancer cell lines (PANC1; BXPC3; PAN1); a human primary pancreatic tumour-derived epithelial cell line (P308T); 10 human primary-derived pancreatic cancer-associated fibroblasts (CAFs) (P1T, P3T, P4T, P5T, P6T, P9T, P10T, P14T, P30T, P35T) and human bone marrow-derived mesenchymal stem cells (MSCs). Each type of cell line was cultured under specific growing conditions.

2.2.1.1 Epithelial cancer cell line culture conditions

PANC1 and BXPC3 pancreatic cancer epithelial cell lines were obtained from the European Collection of Cell Cultures (ECACC); the PAN1 cell line was previously derived in the Academic Unit of Cancer Studies (Division of Pre-Clinical Oncology), University of Nottingham. All these cell lines were cultured in Dulbecco's Modified Eagle Medium (DMEM) (Sigma-Aldrich, Dorset, UK) containing 1% (w/v) glutamine (Sigma-Aldrich), 10% (v/v) FBS (Sigma-Aldrich) 100 U/ml penicillin, and 100 U/ml streptomycin (Invitrogen, Paisley, UK) at 37°C in a 5% CO₂ air-humidified atmosphere.

2.2.1.2 Primary cell and MSC cell culture

The isolation of primary epithelial (P308T) and fibroblast cells from primary tissues was performed by post-doc researchers of the Pre-clinical Oncology Division by using the following protocol: primary tissues were disaggregated with 2.4 U/ml dispase (Invitrogen) and 100 U/ml collagenase type II (Invitrogen) at 37°C. The cells derived from tissue disaggregation were then cultured on collagen-coated plates and then expanded into T75 flasks in PCA medium (DMEM medium supplemented with 7.2 µg/ml insulin (Sigma-Aldrich), 1 µg/ml hydrocortisone (Sigma-Aldrich), 100 U/ml penicillin, 100 U/ml streptomycin, 0.25 µg/ml amphotericin B, 2 mM L-glutamine, and 20% (v/v) FBS).

Primary cells were frozen in labelled tumour bank tubes in liquid nitrogen (-150°C) in order to maintain a stock of cells to be use in the experiments. At this stage cells were available to be used in this project. Once defrosted different culture conditions, were used depending the experimental purpose CAFs were grown in mesenchymal stem cell media (MSCM) (Sciencell, Buckingham United Kingdom UK) with mesenchymal stem cell growth supplement (MSCGS) (Sciencell, Buckingham United Kingdom UK) and 5% (v/v) FBS (Sciencell, Buckingham United Kingdom UK) at 37°C in a 5% CO₂ air-humidified atmosphere.

The human MSCs were obtained from TCS Cellworks (Buckingham UK) and grown in the same culture condition as CAFs (MSCM plus

MSCGS added and 5% (v/v) FBS) at 37°C in a 5% CO₂ air-humidified atmosphere.

Table 2.3 Type of cells, origin and culture media included in this study.

Cell lines	Type of Cell line	Tissue of Origin	Growth of Media
PANC1	Epithelial cancer cells	Pancreas	DMEM + 10% FBS (1% of Glutamine)
PAN1	Epithelial cancer cells	Pancreas	DMEM + 10% FBS (1% of Glutamine)
BXPC3	Epithelial cancer cells	Pancreas	DMEM + 10% FBS (1% of Glutamine)
P308T	Primary epithelial cancer cells	Pancreas	DMEM + 10% FBS (1% of Glutamine)
CAFs	Primary cancer associated Fibroblast	Pancreas	MSCM + 5% FBS+ MSCGS
MSCs	Mesenchymal Stem Cells	Bone marrow	MSCM + 5% FBS+ MSCGS

2.2.2 Sub-culturing of cells

Cells were expanded in two or more flasks after reaching 80-90% confluence. 5ml Ethylenediaminetetraacetic acid (EDTA) (SIGMA-Aldrich, Dorset, UK) was then added in a 75cm² flask in order to detach the cell lines from the flask. For the same purpose, MSCs and pancreatic CAFs were instead treated with trypsin (SIGMA-Aldrich, Dorset, UK) (5ml/75cm²). EDTA and trypsin are a chelating agent and a serine protease, respectively, that are used in cell culture in order to disrupt cellular interactions, enabling the detachment from the flask. Both agents have maximal efficiency at 37°C. For this reason, cells treated with EDTA and trypsin were incubated for 5 min at 37°C and

then transferred into a universal tube and centrifuged at 200g for 5 min. The EDTA/trypsin was then aspirated and the cell pellet was resuspended in an appropriate volume of medium depending on the size of the pellet.

2.2.2.1 Cell counting

In order to quantify the number of cells in a flask or a plate, the cell pellet was re-suspended in a small amount of media defined by the pellet volume (typically 1-2 ml). 50 µl of the cell suspension was mixed 1:1 with 0.4% (w/v) trypan blue (SIGMA-Aldrich, Dorset, UK) in phosphate buffered saline (PBS) (Thermo scientific, Basingstoke Hampshire, UK) used to stain the dead cells. The cells that excluded trypan blue were then counted using a haemocytometer.

2.2.2.2 Freezing cells

In order to create a stock, cells were frozen at the lowest cell passage possible. Cells were harvested from the flasks at a confluence of 80% and the cell pellet was re-suspended in a freezing solution [10% (v/v) dimethylsulphoxide (DMSO) (Sigma-Aldrich) in the appropriate medium] at a concentration of 2×10^6 cells/ml. Cells were then transferred in labelled tumour bank tubes and rapidly frozen at -80°C over-night, before long-term storage in liquid nitrogen.

2.2.2.3 Cell recovery

Frozen cells were resuscitated from frozen stocks when necessary. The bank tubes containing the cells were rapidly transferred from the storage bank to a small volume of nitrogen liquid. Media (15 ml) was placed into a T75 flask and pre-warmed for 30 min at 37°C in a 5% CO₂ air-humidified atmosphere. The frozen cells were placed into a bath at 37°C. When 90% of the cell suspension was defrosted, cells were carefully transferred under a Class II biosafety hood into the pre-warmed media and incubated at 37°C in a 5% CO₂ air-humidified atmosphere over night. The day after, the media in the flask was changed in order to eliminate the residual DMSO and to re-feed the cells.

2.2.3 *In vitro* cell treatments

2.2.3.1 NShh treatment

CAFs and MSCs were plated in 24 or 6 well plates depending on the experimental plan: 8×10^4 cells were plated into each well of 24-well plates, and 2×10^5 cells were plated into each well of 6-well plates, and incubated under standard culture conditions overnight. The media used include MSCM with 5% FBS, PCA or DMEM with 5% FBS. The day after, the media were aspirated and the cells treated with 5 nM and 10 nM human sonic hedgehog N-terminal (NShh) (R&D System, Abingdon, UK) for 2, 3 and 6 days. These concentrations were chosen for being successfully used in the literature [Taipale *et al* 2000]. Moreover, cells

were also treated with much higher concentration of NShh (50 nM) for 48 h as found in the literature [Bailey *et al* 2008]. In each experiment a control sample (i.e. untreated cells) was run in parallel. Two replicates were plated for each treatment performed. After each experiment, cells were harvested for RNA extraction as described below. Data analysis was performed by comparing each variable to the control sample (single culture of stromal-like cells).

2.2.3.2 TGF β treatment

Based on the literature [Hu *et al* 2003; Bardeesy *et al* 2006], TGF β treatment was used in this study in order to investigate its effect on MSCs activation (α SMA expression) and its interaction with the Hh pathway in these cells.

Cells were harvested and plated in a T25 or a T75 flask depending on the experimental plan: 10^5 cells were plated in a T25 flask and re-suspended in 5 ml of growing media, 10^6 cells were plated in a T75 flask and re-suspended in 15ml of growing media. The day after, the growing medium was aspirated and substituted with a 10 ng/ml (concentration suggested by the manufacturer) solution of TGF β 1 (Humanzyme, Chicago USA) in the medium required for the experimental purpose. The following media were tested for this treatment: DMEM with 0.5% FBS; PCA; MSCM 5% FBS with no GF (growth factors) added and MSCM 5% FBS). Cells were incubated for 3 or 7 days under standard culture conditions. The TGF β was replaced every 2 days. Control samples (i.e. untreated cells) were run in parallel.

Data analysis was performed by comparing treated and untreated samples grown under the same experimental conditions.

2.2.3.3 Cell harvesting from in vitro cell treatment assays for RNA extraction and immunofluorescence (IF)

Assays performed in 24 well plates were used exclusively for gene expression analysis. For this purpose the medium was aspirated and then replaced with 500 µl of TRI-reagent (Sigma-Aldrich) and incubated for 5 min in order to lyse the cells. The lysate was then transferred into 1.5 ml Eppendorf tubes then used immediately for RNA extraction or was frozen at -80°C for future analysis.

The experiments performed in 6 well-plates or inT25 flasks were plated for analysis of gene expression by q-RT-PCR and protein expression by IF (using half of the cells for each analysis). For this purpose the media were aspirated and then the wells/flasks washed with PBS in order to remove the residual medium and any dead cells, before harvesting. The cells for RNA extraction were re-suspended in 1 ml of TRI-reagent and stored at -80°C. Cells harvested for IF staining were fixed with 500 µl of 4% (v/v) paraformaldehyde (PFA in PBS) for 10 min, before centrifugation and re-suspension in 600 µl 70% (v/v) EtOH and storage at 4°C for less than one week.

2.2.4 Transwell co-culture

The transwell assay performed in this study was used to co-culture different types of cells by separating them with a permeable membrane.

This system establishes paracrine signalling processes between the two cell populations, and allows analysis of the separated cell types. In this study 12-well and 6-well transwell plates were used (12 mm and 24 mm of membrane diameter, respectively) (Corning Life Sciences, Amsterdam, The Netherlands) in order to have enough cells for subsequent gene and protein expression analysis. The transwell membranes had pores of 0.4 μm that permitted the migration of drugs and molecules but not of cells. The material used for the permeable support was polyester (PET) in the optimisation phase of the experiments then polycarbonate (PC). PET membranes are transparent and allowed the visibility of the cells plated in the inserts. At the start of the experiment the number of cells and their growing conditions were important factors to check. Once the experimental conditions of co-culture (number, time and media) were optimised, the PET membranes were substituted with PC membranes which are less visible but contain a higher number of pores and so should permit improved communication between the two cell types.

In the 12- and 6-well transwell plates the total number of cells plated (epithelial cells and CAFs or MSC) was 7×10^4 and 1.8×10^5 cells/well, respectively, in epithelial cells: CAF or epithelial cells: MSC ratios of 3:1. Epithelial cell were plated in the well plate and CAFs/MSCs were plated in the insert of the trans-wells, and cells were cultured in MSCM 5%. For each assay performed, control trans-wells were prepared by plating a single cell population (epithelial cells or MSCs/CAF) either in the well plates or in the inserts. In the control well/insert units the same final

number of cells as in the co-culture well/insert units was plated. Both controls and co-cultures were cultured for 3 days in MSCM 5% (v/v) FBS without changing the media.

At the end of the experiment, cells were harvested for RNA and IF analysis following the protocol described in section 2.2.3.3

Statistical analysis was performed by comparing the gene and protein expression in the co-cultured stroma like cells with the gene and protein expression detected in the control samples (single culture of CAFs or MSCs).

2.2.5 Direct co-culture

2D direct co-culture is an *in vitro* assay that allows direct cell-cell contact and communication.

CAFs were co-cultured by using this assay with pancreatic tumour epithelial cells in epithelial cells: CAFs ratio of 3:1. 8×10^4 total cells were plated in each well of a 24 well plate. Control wells containing 8×10^4 of unmixed CAFs were plated in parallel and grown in the same media and culture conditions. Mixed and unmixed cells were plated in replicates in order to confirm the results achieved. The co-cultures and the control wells were cultured for 3 days without changing the media. Data analysis was performed by comparing each variable to the control sample (single culture of CAFs cells).

2.2.5.1 Cell harvesting from direct co-culture for RNA extraction

At the end of the culture, the medium was aspirated and the cells washed with PBS. Once detached, cells were re-suspended in 1 ml of PBS containing 0.1% (w/v) bovine serum albumin (BSA) in a sterile Eppendorf tube. 25 μ l of magnetic beads (Dynal, Norway) pre-coated with an anti-EpCAM (epithelial cell adhesion molecule) antibody were then added to the cell suspension in order to bind the epithelial cells. The cells were then tumbled 20 min at 4°C, before EpCAM-positive epithelial cells were harvested using a magnet. The remaining supernatant containing the fibroblast cells was carefully aspirated and transferred to other eppendorf tubes. In order to isolate a pure fibroblast population the suspension was then incubated with magnetic beads coated with an anti-CD90 antibody (a specific marker for mesenchymal cells). As for the epithelial cells, the fibroblasts cells, bound to the CD90 antibody-beads complex were isolated using a magnet. Both cell types were then washed 3 times with 500 μ l PBS/0.1% BSA. After washing, both cell lines were lysed with TRI-reagent prior to RNA extraction.

2.2.6 Optimisation of *in vitro* mesenchymal stem cell niche models

In order to optimise an *in vitro* mesenchymal stem cell niche model, different cell ratios, times of culture, culture media, and type of stromal cells were co-cultured by using a 2D direct co-culture assay.

MSCs at low passage (P3-P4), and maintained in MSCM to keep them in an undifferentiated state, were co-cultured with MF-like cells in 1:1,

1:3 and 3:1 ratios or with CAFs in a 1:1 ratio. MF-like cells were obtained by culturing MSCs in MSCM without adding the supplement of GF, and by treating them with TGF β for 1 week as indicated in Section 2.2.3.2. CAFs were cultured in MSCM 5%FBS (demonstrated to be the best growing condition for these cells) until the start of the co-culture. Once calculated, the concentration of cells, the correct volume (defined by the dilutions to perform) was taken from the cell suspensions (performed in DMEM 10%) of MSCs and transferred into a T25 flask. MF-like cells or CAFs, as for the MSCs, were counted and the appropriate volume (performed in DMEM 10%) (defined by the ratios to perform) was transferred into the same flask as the MSCs. Finally, up to 5 ml of the culture medium (DMEM 10%) was added and the flask rocked in order to well mix the cells well and distribute the cells in the flask. The total number of cells per T25 flask was 1.8×10^5 cells.

All four mSCN models (MSCs:MF-like cells ratios of 1:1, 3:1; and 1:3, and MSCs:CAFs ratio of 1:1) were cultured in DMEM 10% media and harvested after 3, 12 and 21 days. In parallel, MSCs alone and MF-like cells alone or CAFs alone were cultured and harvested under the same conditions as the mSCN models.

Due to the high number of cells required in each experiment, each assay was performed once; however, as explained in the results, the same experimental conditions were repeated two or three times in the context of different experimental design, in order to confirm the results obtained. At the end of the experiment, cells were harvested and used

for RNA extraction and IF analysis by following the protocol illustrated in paragraph 2.2.3.3.

2.2.6.1 Transwell co-culture between *in vitro* mSCN models and epithelial cancer cells

Different mSCN *in vitro* models were prepared by mixing MSCs and MF-like cells and/or by changing the growing condition of these two populations in order to co-culture them in a transwell assay with the pancreatic epithelial cell line PANC1. PANC1: mSCN models were plated using a 1:3 ratio. The final cell number in each insert/well unit was 1.8×10^5 cells. Therefore, all mSCN models were plated in the insert with a final number of 4.5×10^4 cells. The transwell assay was run for 3 days and then the cells were harvested following the methods described in section 2.2.4.2.

Five mSCN *in vitro* models were performed in this assay:

- MSCs single population (MSCs S.P): As negative control of the experiment, MSCs maintained at low passage were plated in the insert. The cells were defrosted and left to recover for 3 days in MSCM 5% before being harvested, counted and re-suspended as described in Section 2.2.2. Once counted, the equivalent volume of cell suspension to 4.5×10^4 cells was transferred in MSCM 5% into the insert of a 6-well transwell plate. These cells, named MSCs single population (MSCs S.P.), were then co-cultured with PANC1 cells (plated in the well plate) in MSCM 5% for 72h.

- mSCN model 1: This model was obtained by culturing MSCs in DMEM 10% for 1 week before plating them in the insert of the transwell. These cells were harvested and 4.5×10^5 cells added to the insert of a 6-well transwell plate, then co-cultured with PANC1 cells in DMEM 10% media for 72 h.
- mSCN model 2: MSCs S.P. with a low passage number (P4) after a short recovery (around 3 days from being defrosted) were harvested, and 2.25×10^5 cells added to the insert of a 6-well trans-well plate. In parallel MF-like cells (obtained by treating MSCs with TGF- β for 1 week as described in Section 2.2.3.2) were harvested and 2.25×10^5 cells were mixed with MSCs S.P. and added to the insert of the transwell in MSCM 5%. Hence, in this model MSCs and MF-like cells were plated in a 1:1 ratio and the final number of cells plated in the insert was 4.5×10^5 . Once plated, mSCN model 2 was co-cultured with PANC1 cells (plated in the well plate) in MSCM for 72 h.
- mSCN model 3: The set-up and the cells used in this model (MSCs S.P. mixed in a 1:1 ratio with MF-like cells) were the same as the previous mSCN model 2, but after being plated in the insert, mSCN model 3 was co-cultured with PANC1 cells in DMEM 10% medium for 72 h.
- mSCN model 4: MSCs were cultured for 1 week in DMEM 10%. The cells were then harvested, counted and re-suspended in 2 ml MSCM 5%. In parallel MSCs with low passage number (P4) were defrosted (MSCs S.P.). After a short recovery, MSCs S.P.

were then harvested, counted and re-suspended in MSCM 5%.

The correct volume of MSCs and MSCs S.P. (equivalent to 2.25×10^5 cells each) were mixed and re-suspended in MSCM 5% in the insert in order to co-culture them in a 1:1 ratio. Once plated, the mSCN model was co-cultured with PANC1 cells in MSCM 5% for 72 h.

- mSCN model 5: The set up and the cells used (MSCs cultured for 1 week in DMEM 10% mixed with MSC S.P in a 1:1 ratio) in this model was the same as the previous model (mSCN model 4), except that the mSCN model 5 was co-culture with PANC1 cells in DMEM 10% medium for 72 h.

For each mSCN model a control sample comprising the equivalent mSCN model in the absence of PANC1 cells, plated both in the insert and in the plate, was run in parallel.

2.2.7 Tumour conditioned media (TCM) assay

In order to prepare the TCM, tumour epithelial cells (10^6 cells) were cultured in a T75 flask with 20 ml of MSCM 5% (v/v) FBS for 3 days before the medium was harvested and filtered. Control CM was prepared by growing the CAFs or MSCs in the same conditions of epithelial cells. The conditioned medium (50% CM, 50% MSCM) was used to culture stromal-like cells (CAF or MSCs) for 72 h or 14 days, with the medium replaced twice a week.

The CAFs and MSCs were plated in T25 flasks. The number of cells plated was optimised taking into account the growth profile of each cell

line (10^5 cells for P5T CAFs and MSCs and 3×10^5 cells for P3T CAFs). The cells were harvested, re-suspended and counted as indicated in Section 2.2.2. Control samples were cultured in parallel in each experiment and were obtained by culturing CAFs or MSCs in the control CM for the same amount of time as the other experimental conditions. Due to the high number of cells required for this experiment no replicates were plated. Data analysis was performed by comparing gene and protein expression detected in the conditioned sample to the gene and protein expression detected in the samples grown in the control CM. At the end of the experiment, cells were harvested and used for RNA extraction and IF analysis by following the protocol illustrated in paragraph 2.2.3.3.

2.3 Molecular Techniques

2.3.1 RNA extraction from cells

Total RNA was extracted from cells lines TRI reagent, a monophasic solution for RNA extraction (Sigma-Aldrich).

5-10 x 10⁶ cells were lysed in 1 ml TRI-reagent, prior to the addition of 200 µl chloroform, vigorous mixing, and centrifugation at 13,000 rpm for 15 min at 4°C. The upper aqueous phase was mixed with 500 µl propan-2-ol, and the RNA allowed precipitating for 10 min at room temperature, prior to centrifugation at 13,000 rpm for 10 min at 4°C. The RNA pellet was washed with 1 ml 70% (v/v) ethanol, centrifuged at 13,000rpm for 10 min, air dried, re-suspended in 50 µl RNase-free water and stored at -80°C.

2.3.2 RNA extraction from tissues

Human pancreatic tissues for RNA extraction were kept in bank tubes with 10 µl of RNA*later* per mg of tissue at -80°C. RNA*later* is a reagent able to stabilise the RNA in the tissues.

Total RNA, along with genomic DNA, was isolated from tissue samples using the AllPrep DNA/RNA Micro kit (Qiagen, Crawley, UK). Once defrosted at room temperature, tissue was removed from the RNA*later* and transferred to a plastic petri dish and a piece roughly 1.5 mm cubed (approximately 5 mg tissue) was removed. The piece was then snap frozen in liquid nitrogen and ground to a powder using a pestle and

mortar. When the nitrogen had evaporated the tissue was covered with 350 μ l RTL Plus containing 10 μ l/ml 2-mercaptoethanol, and the lysate transferred to a QIAshredder spin column (Qiagen) and centrifuged at maximum speed for 2 min. The supernatant was transferred to an All-prep DNA spin column placed in a 2ml collection tube and centrifuged for 30 s at 15,000 x *g*. During this step the genomic DNA bound to the filter of the spin column, whereas the RNA remained in solution. The DNA spin columns were transferred to an empty 2 ml collection tube and stored at 4°C for subsequent genomic DNA extractions.

To the flow-through containing the RNA was added 350 μ l 70% (v/v) ethanol to precipitate the RNA, and the mixture transferred onto a RNA MinElute spin column to bind the total RNA, placed in a 2 ml collection tube and centrifuged for 15 s at 15,000 x *g*. The flow-through was discarded and the column washed with 700 μ l Buffer RW1 then 500 μ l Buffer RPE for 15 s each at 15,000 x *g*. A final wash was performed using 80% (v/v) ethanol 2 min at 15,000 x *g*. The column was dried by centrifugation for 5 min at full speed. RNA was eluted from the column by the addition of 10 μ l RNase-free water to the RNA Min-Elute spin column placed in a 1.5 ml Eppendorf tube and centrifugation for 1 min at full speed.

2.3.3 cDNA synthesis.

For each RNA extraction, one positive cDNA sample and one cDNA negative control (no primers and no superscript enzyme) were prepared. The RNA samples were reverse transcribed into cDNA using Superscript II Reverse Transcriptase enzyme (Invitrogen).

10µl RNA was mixed with 1 µl of random hexamers (Invitrogen) (1 µl of water for the negative control) and incubated for 10 min at 70°C followed by rapid cooling on ice in order to remove tertiary structures from the RNA. To each tube was added 4 µl 5x First Strand Buffer, 2 µl 0.1 M dithiothreitol, 0.6 µl 10 mM dNTPs (Sigma-Aldrich), 3 µl nuclease-free water, and 0.4 µl SuperScript II enzyme (Invitrogen) (or water instead of enzyme for the negative controls). The mixtures were incubated at 25°C for 10 min, 42°C for 60 min, and 95°C for 5min in an Applied Biosystems GeneAmp PCR System 9700 thermal cycler, prior to the addition of 80 µl nuclease-free water. The cDNA was stored at -20°C.

2.3.4 Quantitative Real-time Polymerase chain reaction (qPCR).

The qPCR is a powerful method commonly used in research for the investigation of gene expression. It is based on a polymerase chain reaction in which double-stranded DNA (dsDNA) is amplified and the product are detected in real-time. The gene expression analysis by qPCR start with the RNA extraction from cells or tissue and its conversion in cDNA (paragraph 2.3.3) in order to amplify a sequence

corresponding to a segment (In this study design to be 150bp long) of the gene under investigation. This amplification is possible using forward and reverse primers with sequences that perfectly match respectively to the extremities 3' to 5' and 5'to 3' of the segment to be amplified. The DNA amplification is characterised by an exponential phase that terminates with a plateau determined by the complete consumption of the reagents included in the reaction [“Real-Time PCR: from theory to practice”; 2008; “Real Time PCR Handbook” n.d.].

Currently, there are two common qPCR techniques defined by the use of non-specific fluorescent dye or sequence-specific DNA probes [“Real-Time PCR: from theory to practice”; 2008].

The sequence-specific DNA method is based on the use of an oligonucleotide probe with a specific sequence that hybridises with a segment of the gene investigated and on the activity of the Taq DNA polymerase (a 5' endonuclease enzyme). Briefly, the oligonucleotide sequence is labelled with a fluorescent reporter and a quencher that inhibits the fluorescent signal. During the cDNA template amplification, the TaqMan polymerase cleaves the oligonucleotide sequence causing the detachment of the quencher from the probe, which enables the reporter to emit a detectable signal. The specificity of this amplification is conferred by the reverse and forward primers and by the oligonucleotide probe [http://www.ncbi.nlm.nih.gov/genome/probe/doc/TechQPCR.shtml].

The PCR non-specific probe method is based on the use of a fluorescent probe (Sybr Green) able to bind exclusively to DNA double

strand sequences. During the process of amplification guided by the forward and reverse primers and the DNA polymerase the cDNA template is exponentially duplicated over a number of PCR cycles. The Sybr Green probe binds to every new amplicon (dsDNA amplified) allowing the quantification of the new product generated. The specificity of this reaction is guaranteed by the primer design [Ponchel *et al* 2003; “Real-Time PCR: from theory to practice”; 2008; “Real Time PCR Handbook” n.d.]. A disadvantage of the use of a non-specific dye is the risk of false positive signal generation as a consequence of the binding of the dye to non-specific double strand DNA sequence. For this reason, in this context, the qPCR system generates a melt curve at the end of the reaction in order to check the purity of the amplification. The melting curve (or dissociation curve) represents the dsDNA dissociation into single strand DNA (ssDNA) as a consequence of the rise of the temperature. The melting curve then shows the relationship between the Sybr green fluorescence signalling and the melting temperature and is plotted as $\Delta F/\Delta t$ (change in fluorescence/change in temperature) against the temperature. The melting point (T_m) represents the temperature at which all dsDNA is dissociated and coincides with the pick of the melting curve. Non-specific double strand construct (like primer dimerisation) show different melting points than that for the specific cDNA of interest and so only a single dissociation curve with a single peak will guarantee the purity of the product amplified [“Real Time PCR Handbook” n.d.]

In this studies both qPCR methods described above were applied, however, the Sybr Green method was predominantly used.

In general, each PCR reaction is characterised by a baseline value represented by the number of PCR cycles in which the signalling emitted by the probe is still not detectable by the machine, which means that the amount of DNA amplified is still too low to be quantified. The baseline also influences the threshold value, considered an arbitrary level of fluorescence that lies within the exponential phase of amplification of the cDNA and is higher than the base line. Every signal detected above the threshold is considered a real signal. In line with this, an important parameter for the gene expression quantification is the threshold cycle value (C_t) value. It represents the minimal number of cycles necessary to detect a value of fluorescence higher than the threshold. The higher the C_t value, the lower the gene expression level. [Ponchel *et al* 2003 ;“Real-Time PCR: from theory to practice”; 2008] In order to reduce the quantitation variability caused by differences in the DNA amount added to each reaction, and to distinguish for differences in efficiency of RNA extraction and cDNA synthesis between test and control samples, the expression of the gene investigated is normalised to the gene expression of an endogenous control (a gene constitutively expressed in all experimental sample: reference gene) [“Real-Time PCR: from theory to practice”; 2008“; Real Time PCR Handbook” n.d.]. The final gene expression is expressed as $2^{-\Delta C_t}$ in which $\Delta C_t = C_t \text{ target gene} - C_t \text{ reference gene}$ [Livak *et al* 2001].

In this study, the qPCR reactions were carried out in 96 well plates (Applied Biosystems, Warrington, UK) containing 5 µl of cDNA and 20 µl of a reaction mixture. The reaction mixture was prepared with 10 µl 2x SYBR Green Master Mix (Applied Biosystems), plus 4 µl nuclease-free water and 1 µl primers (forward and reverse primers combined 5 µM each).

The reactions were performed in a StepOnePlus Real Time PCR machine (Applied Biosystems) using the following conditions: denaturation at 95°C for 10 min, followed by 40 cycles of 95°C for 15 sec and 60°C for 60 sec), and a final melt curve stage of 95°C for 15 sec, 60°C for 1 min and 95°C for 15 min).

IHH gene was amplified using a different qPCR method that, instead of using the SYBR green dye, used TaqMan reagents. The reason of this choice was the difficulty found in designing primers highly specific for this gene. The sequence-specific qPCR method (TaqMan polymerase system), by adding a new level of specificity (the oligonucleotide probe) to that conferred by the primers, was considered more appropriate in this context. Gene detection was performed by using 10 µl of 2x Taq-man real time PCR master mix (Applied Biosystems), 1 µl of a specific solution of *IHH* Taq-man probe and *IHH* primers (Applied Biosystems) and 4 µl nuclease-free water. This final solution was then mixed with 5 µl of cDNA obtained from the cells under investigation.

For every sample analysed, a negative cDNA control was run to detect any potential contamination, such as genomic contamination or primer dimerisation.

Primers were designed by using the primer design centre (i.e. www.ncbi.nlm.nih.gov/tools/primer-blast) by following strict criteria to achieve the maximal efficiency and specificity in the gene amplification. The PCR product size had to be between 50 and 150 bp and the melting temperature was around 58°C. Finally, primers had at least two mismatches with unintended targets and were separated by introns >1000 bp in order to prevent amplification from any contaminating genomic DNA. All primers, once designed, were tested on positive cell controls and their efficiency checked by comparing the slope of the expression curve of the gene amplified in serial cDNA dilutions with the slope of the same curve obtained for hypoxanthine-guanine phosphoribosyltransferase (*HPRT*) housekeeping gene expression [Livak *et al* 2001]. Good primers efficiency was obtained when the difference between the gradient of the two slopes was < 0.1. The following table shows the primers used for the amplification of the genes analysed in this study.

Table 2.4 Primers utilised for qPCR

Gene	Forward Primer (5'-3')	Reverse Primer (5'-3')
<i>HPRT</i>	ATTATGCTGAGGATTTGGAAAGGG	GCCTCCCATCTCCTTCATCAC
<i>SHH</i>	CGACCGCAGCAAGTACGGCA	CGATTTGGCCGCCACCGAGT
<i>DHH</i>	GCAACAAGTATGGGTTGCTG	CGGACCGCCAGTGAGTTA
<i>IHH</i>	Hs01081801_m1	
<i>GLI1</i>	ATCAGGGAGGAAAGCAGACTGA	AGTCATTTCCACACCACTGTCTGTA
<i>SMO</i>	CCTGACCGCTTCCCTGAA	TCCGAACCAAGGGCACTTC
<i>PTCH1</i>	CCGCGTTAATCCAATTCC	CATGGCAAATTGAACACCACTA
<i>PTCH2</i>	TGGAACAGCTCTGGGTAGAAG	CCCAGCTTCTCCTTGGTGTA
<i>ACTA2</i>	AACATGGCATCATCACCAACTG	GCAACACGAAGCTCATTGTAGAA
<i>CDH1</i>	GAACAGCACGTACACAGCCCT	GCAGAAGTGTCCCTGTTCCAG
<i>VIM</i>	AAAACACCCTGCAATCTTTCAGA	CACTTTGCGTTCAAGGTCAAGAC
<i>HGF</i>	TGTTTCACAAGCAATCCAGAGGTA	CTCCCCATTGCAGGTCATG
<i>POSTN</i>	ACACACCCGTGAGGAAGTTGC	TGAGAACGACCTTCCCTTAATCGTC
<i>NES</i>	AAC-AGA-GGT-TGG-AGG-GCC-GC	TGCTGCCGACCTTCCAGGAC

2.3.4.1 RT-PCR data analysis.

The data obtained from qPCR was determined from the cycling threshold (Ct) value detected, considered, as explained, the minimum number of cycles necessary for detecting SYBR green fluorescence incorporated into the new DNA synthesised.

All samples were analysed in triplicate and each Ct value was normalised to the triplicate Ct values obtained for expression of the housekeeping gene *HPRT* in the same cDNA sample.

Gene expression was expressed as $2^{-\Delta C_t}$ in which $\Delta C_t = C_t \text{ target gene} - C_t \text{ reference gene (HPRT)}$ [Livak *et al* 2001].

2.4 Protein expression analysis

The expression of the main proteins of the Hh pathway was analysed by the following two staining methods: immunohistochemistry (IHC) and IF.

IHC was used in order to investigate the expression of Shh and Ptch1 in human pancreatic tissues and to determine their localisation within the stroma or within the epithelium. Moreover, quantification of the stromal component was performed by IHC staining of Vimentin.

Finally IF was chosen to analyse the expression of Shh and Ptch1 and expression of stem cell niche markers α SMA and Postn within epithelial and stromal-like cells used for *in vitro* studies.

2.4.1 Immunohistochemistry

Immunohistochemistry is a technique frequently used in the literature, including for Hh pathway investigation [Yan *et al* 2013; Hinterseher *et al* 2013; Thayer *et al* 2013].

In order to prepare the slides with the tissues to stain using IHC, the paraffin blocks, obtained following the embedding process illustrated in paragraph 2.1, were cooled on ice and then cut using a Leica RM2135 microtome at a standard thickness of 4 μ m. The sliced tissue sections were then carefully floated onto the surface of warm water in a bath (R. A. Lamb E65), then transferred onto labelled poly-lysine coated slides (Thermo Scientific, Braunschweig, Germany). Finally, the tissues were left to dry over-night before staining.

In this study, IHC staining was performed for Shh (Abcam, Cambridge UK), Ptch1 (United States Biological, Newmarket UK) and Vimentin protein expression following a process of optimisation: different antigen retrieval methods, primary and secondary antibody concentrations and negative controls were all tested to find the best protocol to be applied.

2.4.1.1 IHC staining of Shh and Ptch1 Hh proteins in pancreatic tumour and normal tissues

The final protocol obtained from the optimisation process was similar for both Shh and Ptch1 proteins.

Sections of paraffin embedded tissue on poly-lysine coated slides were de-waxed in two xylene baths for 5 min each, washed in two 100% methanol baths for 1 min each, then rinsed in running tap water for 1 min.

Tissues were then blocked for endogenous peroxidase using 1% hydrogen peroxide in 100% methanol for 15 min. Tissue sections were rinsed twice in 100% methanol baths then under running tap water.

In order to increase the staining efficiency, antigen retrieval was performed by microwaving slides in 10 mM citric acid pH 6.0 at 98°C for 20 min. This treatment was used to expose the antigens to the primary antibody, normally hidden by methylene bridges with proteins as a consequence of the fixation process.

After this, the sections were quenched immediately in running tap water and then washed in PBS for 5min.

The tissue sections were then incubated for 15 min in a blocking serum from the same species as the secondary antibody (swine serum for both Shh and Ptch1) diluted 1/5 in 1% (w/v) bovine serum albumin (BSA) in PBS to reduce non specific binding due to hydrophobic reactions. This process is a common step in immunohistochemistry to reduce the cross reaction of secondary antibody with endogenous immunoglobulines.

Tissue sections were then incubated for 60 min with primary antibody diluted in PBS (1/100 dilution for Shh antibody and 1/300 dilution for Ptch1 antibody).

Each section was also stained using a negative control. The goal of using a negative control was to test and guarantee that the eventual stain observed was a consequence of real expression of the proteins investigated and not due to nonspecific background staining. The negative controls used (rabbit serum) came from the same species and were diluted in a PBS-BSA1% solution at the same concentration as Shh and Ptch1 primary antibody.

After this incubation the sections were rinsed in PBS and then incubated with a biotinylated swine anti-rabbit secondary antibody at 1/300 in PBS for 30min.

After this, the secondary antibody was rinsed off by washing the tissues with PBS (3 times 5min), and then incubated for 20 minutes with avidin-biotin complex (ABC) (Vector Laboratories, Peterborough, UK) containing avidin bound to biotinylated horseradish peroxidase. The binding of this complex to the biotinylated secondary antibody results in

amplification of the signal and the conjugation of the primary-secondary antibodies with the HRP enzyme. The HRP enzyme is a 40 KDa protein that catalyses the conversion of hydrogen peroxide into water and atomic oxygen. In order for this reaction to proceed electron donors (polyphenols or nitrates) that drive the reaction and become oxidated, are needed. In IHC the electron donors are usually chromogens that once oxidated become coloured. Based on this, in order to stain the primary-secondary antibody complex, the tissues were washed in PBS and then incubated with 3'-Diaminobenzidine liquid chromogenic substrate kit (DAB Liquid system, Dako). DAB is a chemical agent that acts like electron donor in presence of HRP, and produces a brown colour at the site of protein expression. Sections were then rinsed with water and counter stained with Haemalum (Mayers' aqueous) (Fisher Scientific, Loughborough, Uk). Tissue were then dehydrated by using 100% alcohol bath and then cleared in Xylene prior to mounting with DPX (Sigma).

2.4.1.2 IHC staining of Vimentin in pancreatic tumour and normal tissues

As for the Hh protein staining, the primary tissues were subjected to the de-waxing process in xylene and washed in 100% methanol baths (2 times for 1 min)

In order to eliminate the methanol, the slides were then washed under running tap water for 1min and in PBS 3 times for 3 min.

The antigen retrieval was performed by microwaving the slides in citric acid buffer (10mM pH6.0) at 98°C for 20 min. At the end of this incubation, the tissues were quenched in running tap water.

The tissues were then incubated for 10 min in a solution of 3% hydrogen peroxide and distilled water. Tissue sections were then rinsed twice in water baths (5 min each) and washed in PBS 3 times for 5 min. The blocking step was performed by using PBS 5% rabbit serum for 30 min.

At the end of the blocking process, the tissues were incubated for 30 min at RT with Mouse IgG1 anti-human vimentin clone V9 (Dako) at 1/50 dilution in PBS 5% rabbit serum. The negative controls were, in parallel, incubated for 30 min with mouse IgG1 control (1/24 dilution) in PBS 5% rabbit serum.

After the primary antibody incubation, tissues were rinsed in PBS (3x 5 min) and then incubated 30min with a biotinylated rabbit anti-mouse 1/300 diluted in PBS 5% rabbit serum.

The secondary antibody was then rinsed off by washing the slides 3x 5 min with PBS and incubated with the ABC complex for 30 min.

After this incubation, the tissues were washed 3 times for 3 min in PBS and then incubated with the DAB.

Finally, sections were rinsed with water and incubated with Haemalum for 1 min. The tissues were then dehydrated by using 100% alcohol bath and then cleared in Xylene.

2.4.1.3 Data analysis of IHC

19 paired normal and tumour primary pancreatic tissues plus 1 unpaired tumour tissues (39 total samples) were analysed for Shh and Ptch1 protein expression. Considering the extent of tumour differentiation, tissue organisation and type of cells, tissue sections were classified as normal, or moderately and poorly differentiated tumours, as obtained from the histopathologist's report.

The IHC protein expression quantification was performed by using different methods dictated from the experimental purpose. The methods used were the H-score quantification, the DAB quantification and the stromal and epithelial staining quantification by eye.

The overall protein expression in each tissue was the result of the average of the H-score of 6 images at 20x objective from the same section. The H-score was calculated by taking into consideration three levels of staining intensity: low, medium and high [H score= (3x percentage of high intensity value) + (2x percentage of medium intensity value) + (1x percentage of low intensity value)], giving a range from 0 to 300.

Vimentin staining was performed by measuring the DAB staining in 6 area of each section. The final staining was the average of the staining of the 6 areas. This quantification method was chosen in order to measure the overall vimentin staining. In this context, taking into account the contribution of the different staining intensity levels, as in

the H-score, was considered not relevant to the final goal of the assay: stromal quantification.

For both these analyses a semi-automated system was implemented using either the H score or the DAB quips routine written in Qwin standard (leica microsystem). Both the H score and DAB programme software, used in this thesis, are illustrated in details in the Software Programmes Appendix.

Shh and Ptch1 protein expressions were also assessed in the stroma and epithelial separately. For this analysis the staining was quantified by eye in 6 different images of the same tissue and the final result was the average of the 6 estimated percentages. The quantification was confirmed by a second blinded observer. Data was then analysed for its normal distribution and statistical comparison was performed between the Shh and Ptch1 protein expression in the different tumour classifications and between stroma and epithelial compartments.

2.4.2 Immunofluorescence (IF)

Protein expression analyses for the *in vitro* cell experiments were performed in this study using IF staining. As for IHC, a strict process of optimisation was initially performed to optimise the protocol to be used. Each optimisation process was performed by using positive controls (cells known to highly express the protein to be stained).The aspects that were investigated, in order to obtain the efficient protocol, were: types of negative control (normally an isotype control was preferred to the use of general serum); types of primary antibody; concentrations of

the primary and secondary antibodies; times of primary antibody incubation; concentrations of the blocking solution. This optimisation process was carried out for the following proteins: Shh, Ptch1, Postn and α SMA.

Cells for IF were harvested from flasks or plates and processed as described in Section 2.2.2 above. Approximately 4×10^4 cells (80 μ l from a total volume of 700 μ l of fixed cells) were cytopspun onto poly-lysine coated slides using a Thermo Scientific Shandon Cytospin.

In order to reduce the risk of cross-reaction of the secondary antibody with non-specific immunoglobulines and permeabilise the cells to help the primary antibody intake, the cells were incubated in a solution of PBS containing 0.1% (v/v) Tween-20, 1% (w/v) BSA, 10% (v/v) normal serum, and 0.3M glycine for 1 h.

The cells were then incubated for 16 h at 4°C with 100 μ l of the primary antibody diluted in a BSA-PBS 1% solution (w/v).

In order to ascertain the reliability of the staining, negative controls were carried out in parallel, by substituting the primary antibody with an Isotype control at the same concentration of the primary antibody.

The slides were then washed in PBS 3 times for 5 min each and then incubated for 60 min with a secondary antibody conjugated with a fluorescent dye (AlexaFluor488) diluted in a BSA-PBS 1% (w/v) solution. The secondary antibody was then washed away by soaking the slides in PBS 3 times for 5 min.

A drop of ProLong® Gold antifade reagent with DAPI (Invitrogen) was then added on the cell ring and then covered with a cover-slip. The

slides were then left to dry at room temperature in the dark. When dried the slides were stored at 4°C in order to avoid the fading of the fluorescence and finally analysed by microscopy.

The following table 2.3 show the material used for the staining of the protein investigated in this project.

:

Table 2.5 Material chosen in the IF staining				
Protein Investigated	Primary Antibody	Secondary Antibody	Blocking Serum	Negative CTRL
Shh	Rat monoclonal to Sonic Hedgehog (Abcam) (1/25 dilution)	Alexa fluor® 488 chicken polyclonal to rat Ig (Molecular Probes, Paisley, Uk) (1/1000 dilution)	Chicken serum	Rat IgG isotype CTRL
Ptch1	Rabbit Anti- Human Patched Polyclonal Antibody (USBiological) (1/70 dilution)	Alexa Fluor® 488 goat anti-rabbit IgG (H+L) (Molecular Probes) (1/1000 dilution)	Goat Serum	Rabbit Serum
αSMA	Alpha-SMA mouse IgG antibody Clone 1A4 (Sigma Aldrich) (1/100 dilution)	Alexa Fluor® 488 rabbit anti-mouse IgG (H+L) (Molecular Probes) (1/1000 dilution)	Rabbit Serum	Mouse IgG isotype CTRL
Postn	Rabbit polyclonal anti periostin (Abcam) (1/100 dilution)	Alexa Fluor® 488 goat anti-rabbit IgG (H+L) (Molecular Probes) (1/1000 dilution)	Goat Serum	Rabbit serum

2.4.2.1 Data Analysis of IF staining

IF quantification was performed in triplicate by manual observation, taking into account the average of the staining intensity and of the number of cells stained in each replicate. The success of the IF was assured from the staining of positive and negative controls. Each experiment was stained at the same time in order to have the same staining efficiency and the time of exposure during image capture from the fluorescence microscope was always kept strictly constant.

The changes in fluorescence intensity observed under different experimental conditions will be properly quantified, as a next step of this project, by using a semi-quantitative ranking system.

Figure 5.30 and 5.31 of chapter 5 show an example of this IF quantification. Each IF staining was quantified by analysing 3 images for each slide at 20x magnification.

Each image was then splitted in 4 equal sized regions of interest (ROI's) in order to increase the power of the analysis by improving counting accuracy and increasing the sample size. The number of cells with strong, medium and weak staining was assessed by manual observation in each ROI and a final H score (one for each ROI, 4 for each image) was calculated by using the following formula: $H\ score = (3 \times \text{percentage of high intensity value for the ROI}) + (2 \times \text{percentage of medium intensity value for the ROI}) + (1 \times \text{percentage of low intensity value for the ROI})$, giving a range from 0 to 300. The H-score values

was then ranked (e.g. values between 0 and 100 = 1, 100-200=2; 200-300=3).

The threshold to quantify the high, low and medium level of intensity was decided considering the level of expression detected in a positive CTRL (i.e. cells known to highly express the protein analysed).

A version of the thesis in PDF format is available at the back of the thesis to allow more detailed review of the IF images.

2.5 Statistics

Data in each experiment was tested for normal distribution using the D'Agostino & Pearson omnibus test. The analysis of the differences between groups of data was then performed by using one or two-way ANOVAs (considering the number of variables included in the experiment) for normally distributed data, or the Kruskal & Wallis test for non-parametric data distribution. In the case of comparison between only two groups a T-test for paired or unpaired data were considered.

Correlation analysis was performed by using Spearman and Pearson for non-parametric and parametric data distribution respectively.

In the case of two replicates for each data Kruskal & Wallis non-parametric assay was performed between the ($2^{-\Delta C_t}$) control and the treated samples.

Chapter 3 - Results: Analysis of Hh signalling in primary tissues

3.1 Introduction

Evidence from the literature shows Hh pathway over-expression in non-small cell lung cancer and its role in epithelial to mesenchymal transition (EMT) promotion in lung tumour cells [Yuan *et al.* 2007; Maitah *et al* 2011]. Moreover, treatment with SMO inhibitors results in reduced cell viability in lung tumour cells reinforcing the idea of a role of the Hh pathway in this cancer [Singh *et al* 2011]. Interestingly all these studies suggest autocrine transmission of the Hh pathway in this kind of tumour [Yuan *et al* 2007; Maitah *et al* 2011; Singh *et al* 2011].

On the other hand, pancreatic cancer is one of the main tumour types in which paracrine transmission of this pathway between epithelial cells and stroma cells that constitute the tumour microenvironment, has been observed [Bailey *et al* 2008; Tian *et al* 2009; Olive *et al* 2009].

Taking into consideration such evidence, lung and pancreatic primary tumours were analysed in this study as representative of two types of cancer in which Hh signalling, through different routes of transmission, contributes to tumour development and progression.

3.2 Screening of Hh pathway gene expression in pancreatic and lung tumour tissues

3.2.1 Investigation of Hh pathway signalling in pancreatic samples

Initially, overexpression of the Hh pathway in pancreatic primary tumour samples was examined and compared to normal samples in order to verify and confirm what had been observed in the literature. In order to achieve this aim, 14 paired pancreatic normal and tumour tissues (Figure 3.1) were screened for Hh pathway ligand gene expression by qRT-PCR.

Gene expression of *SHH* and *IHH* ligands was significantly higher (non-parametric paired T test) in pancreatic tumours in comparison to the equivalent normal tissues (Figure 3.1 A; C) suggesting a role of the Hh pathway in this type of cancer. Only two patients (P6 and P9) showed a higher *SHH* expression in tumour tissues than in normal tissues. Interestingly, in one of these two patients (P9) also *IHH* expression resulted to be higher in the tissue section (Figure 3.1 A; C). No significant difference between the 2 groups analysed (normal and tumour) was observed in *DHH* expression and 5 different patients showed a higher expression of *DHH* in the normal tissue in comparison to the tumour tissue (Figure 3.1 B). Moreover, a number of normal and tumour samples showed no expression of either *IHH* or *DHH* (Figure 3.1 B and C). Moreover, the comparison of median values in tumour samples for all 3 ligands showed a 8.6 and 3 times higher levels of *SHH* than *DHH* and *IHH* ($p < 0.05$ for both comparisons, Figure 3.1 A,B,C),

indicating that this ligand was the main one expressed in pancreatic cancer at gene level.

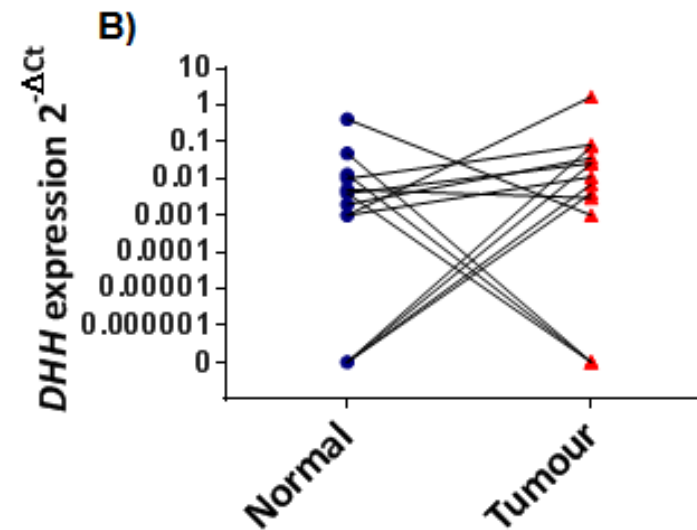
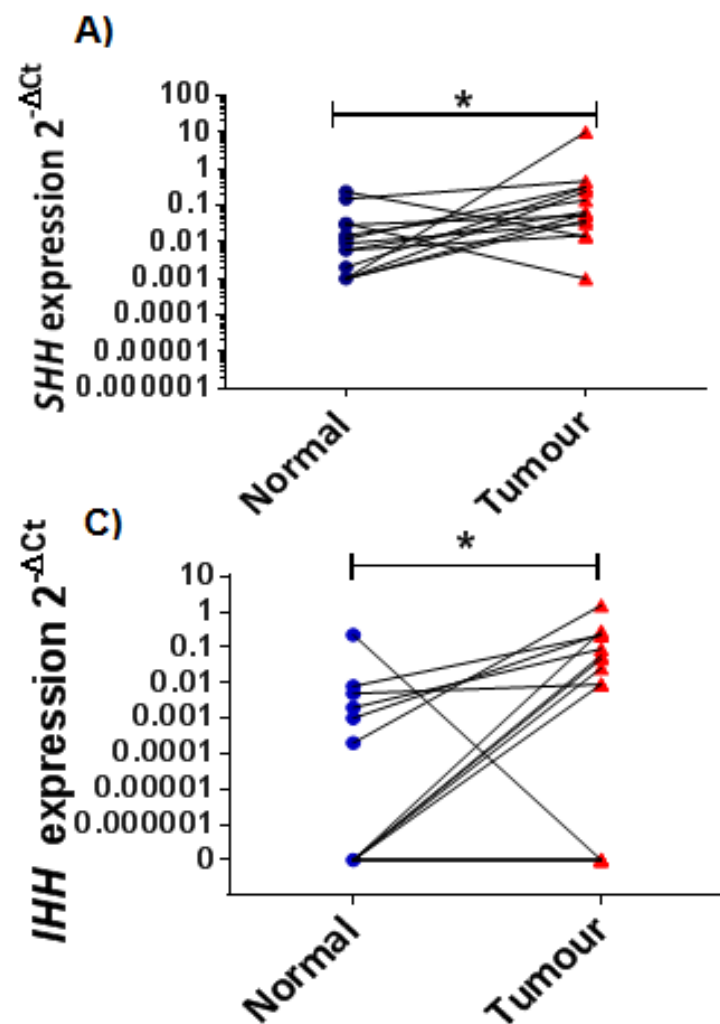


Figure 3.1 Screening of the gene expression Hh ligands in normal and tumour pancreatic tissues. A) *SHH* expression in 14 normal (blue circles) and 14 tumour (red triangles) primary pancreatic tissues selected from the same patients. B) and C) *DHH* and *IHH* ligands were analysed in the same 28 primary pancreatic tissues. Significant difference between normal and tumour samples was observed (non parametric paired t-test) for *SHH* (* $p < 0.05$) and *IHH* (* $p < 0.05$) expression. The horizontal line represents the median of the *SHH* (A), *DHH* (B), *IHH* (C) gene expressions either in normal or tumour samples. Statistical analysis for *DHH* expression ($p = 0.22$) did not show any significance.

Hh pathway expression was then investigated for its correlation with tumour differentiation in order to see if it was possible to co-localise this signalling in a particular phase of tumour development or progression. In order to achieve this goal, Hh ligand expression was compared between moderately (MDT) and poorly differentiated (PDT) pancreatic tumours (as defined by assessment carried out by a histopathologist) (Figure 3.2 A;B;C). No significant difference between MDT and PDT was observed for any of the ligands. However, the lack of significance in this comparison could be a consequence of a too low number of PD samples.

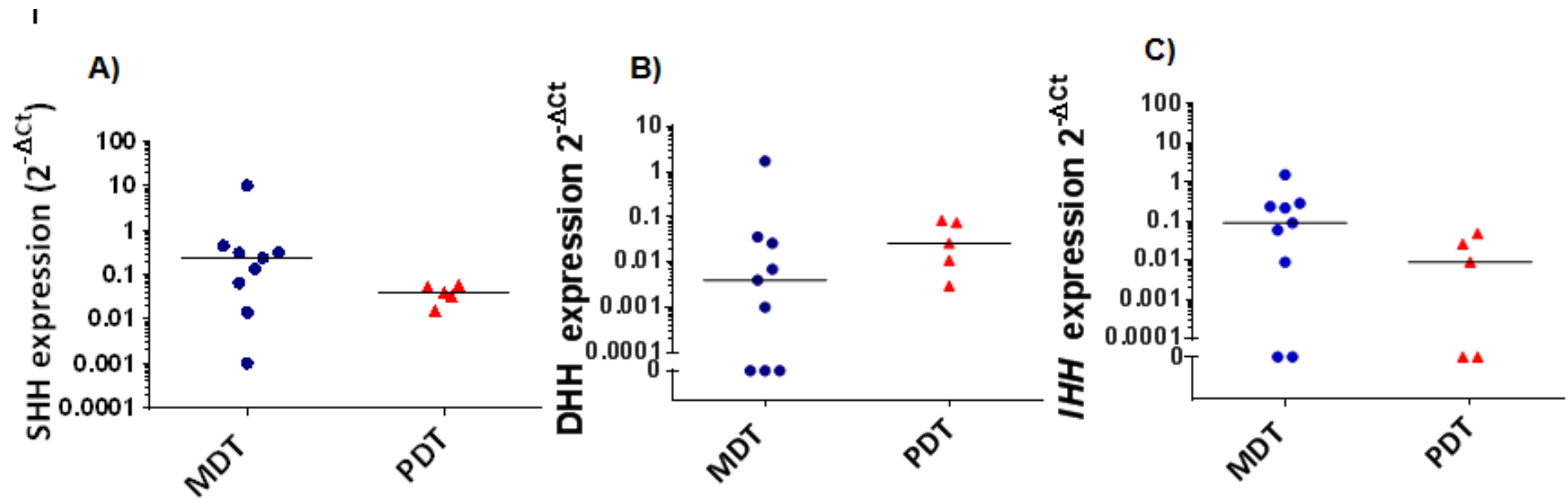


Figure 3.2 Hh ligand expressions in different tumour stage of primary pancreatic tissues. A) Comparison of *SHH* expression between moderately differentiated tumour (MDT) (blue circles) and poorly differentiated (PDT) pancreatic tumour (red triangles). B) and C) *DHH* and *IHH* respectively expression in MDT (blue squares) and PDT (red triangles). Non parametric t-test was used to analyse the difference between MDT and PDT. No significance was observed for any of the ligands.

In the same pancreatic samples, investigation of *GLI1*, *PTCH1* and *PTCH2* gene expression (Figure 3.3) as indicators of Hh pathway activity was also performed. In agreement with the observation for *SHH*, *GLI1* (Figure 3.3A) was slightly higher ($p < 0.05$, non-parametric T test for paired samples) in pancreatic tumour samples. The expression of *PTCH1* (Figure 3.3B) and *PTCH2* (Figure 3.3C) was very similar between the normal and matched tumour samples and the difference was not significant.

These data do not prove, but are suggestive, of overexpression of the Hh pathway in pancreatic cancer.

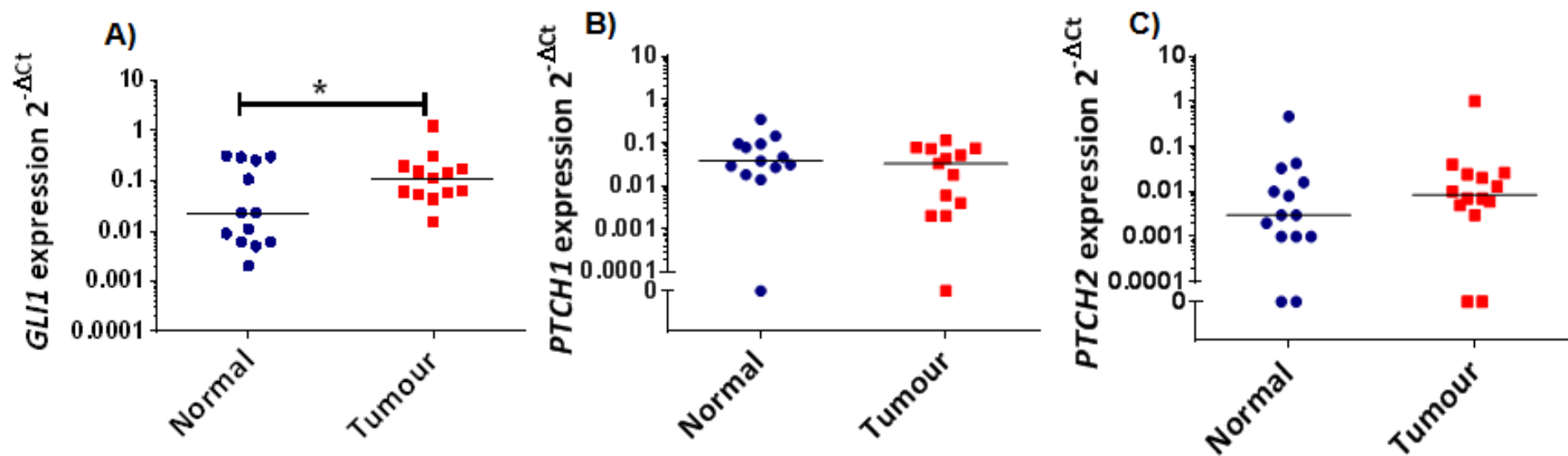


Figure 3.3 Hh pathway activity in primary pancreatic tissues. A) *GLI1* gene expression in normal (blue circles) and tumour samples (red squares). B) *PTCH1* gene expression comparison between 15 normal and tumour samples obtained from the same original patients. C) Same analysis in same samples was performed for the other potential Hh pathway receptor and gene target *PTCH2*. Statistical analysis between normal and tumour samples was performed by using non parametric paired t-test. *GLI1* expression was significantly (* p<0.05) upregulated in tumour samples. No significant over-expression was detected for *PTCH1* and *PTCH2* expression.

3.2.2 Hh pathway expression in normal and NSCLC tumour lung primary tissues

SHH gene expression was also investigated by qRT-PCR in 47 primary lung normal and tumour samples and the comparison between normal and tumour tissues was performed to study its role in this kind of cancer. Lung samples were also analysed for *SHH* expression according to tumour stage (T1, T2 and T3) in order to investigate a possible association between tumour aggressiveness and Hh ligand expression (Figure 3.4). The *SHH* screening in lung tissues (Figure 3.4 A) indicated very low expression of this ligand in tumour tissues with significantly lower expression ($p < 0.01$, non-parametric paired T test) than in normal samples and a high percentage (24%) of tumour samples completely lacking expression. Finally, no difference between classification groups was observed in lung tumour tissues (Figure 3.4B).

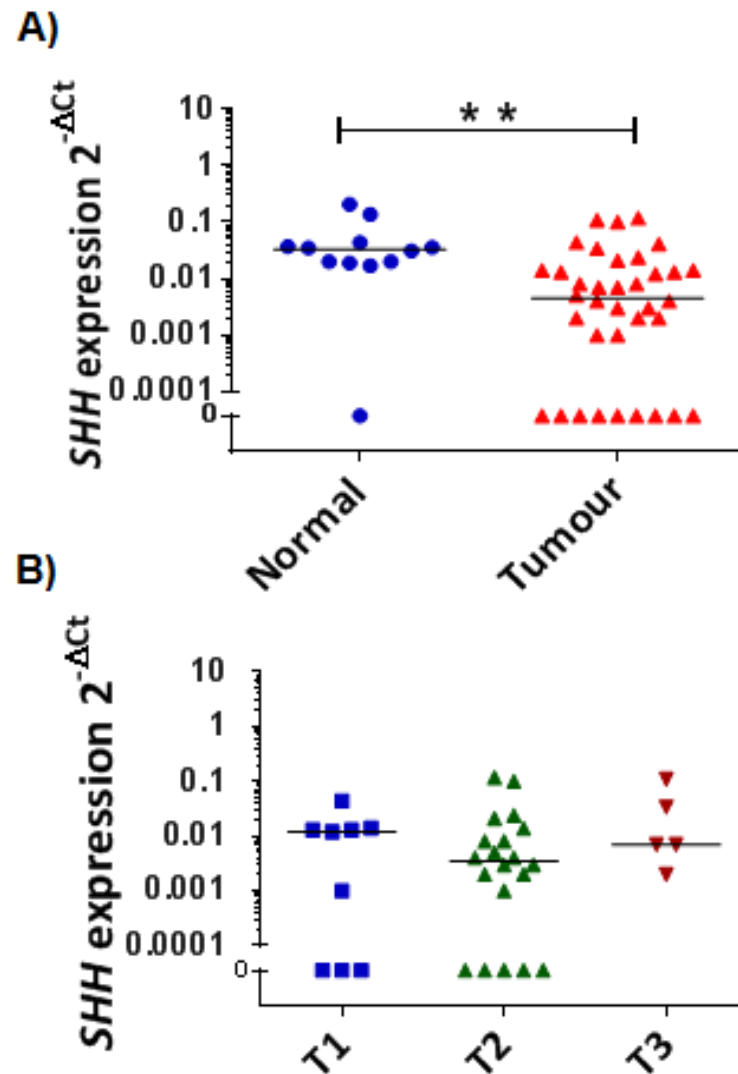


Figure 3.4 Screening of *SHH* gene expression in normal and tumour lung tissues. A) *SHH* expression analysis performed in 12 normal (blue circle) and 35 tumour (red triangles) lung tissues. Normal and tumour samples were obtained from the same 12 patients. B) Comparison of *SHH* gene expression between different lung tumour stages (the level of tumour aggressiveness increase with the numbers): T1 (blue squares); T2 (green triangles); T3 (red triangles). Statistical analysis (non parametric t-test) showed significant higher *SHH* expression (** $p < 0.01$) in normal samples in comparison to tumour samples. No significant difference for *SHH* expression was observed between tumour stages.

As carried out for pancreatic primary tissues, lung normal and tumour tissues were then studied for their expression of Hh pathway activity through analysis of *GLI1* gene expression. *PTCH1* and *PTCH2* gene expression, which when included in the previous examination of

pancreatic tissues did not show any differences between normal and tumour samples (suggesting lower sensitivity for Hh pathway activity detection) were not included in this analysis. There was no significant difference in *GLI1* expression between normal and tumour samples.

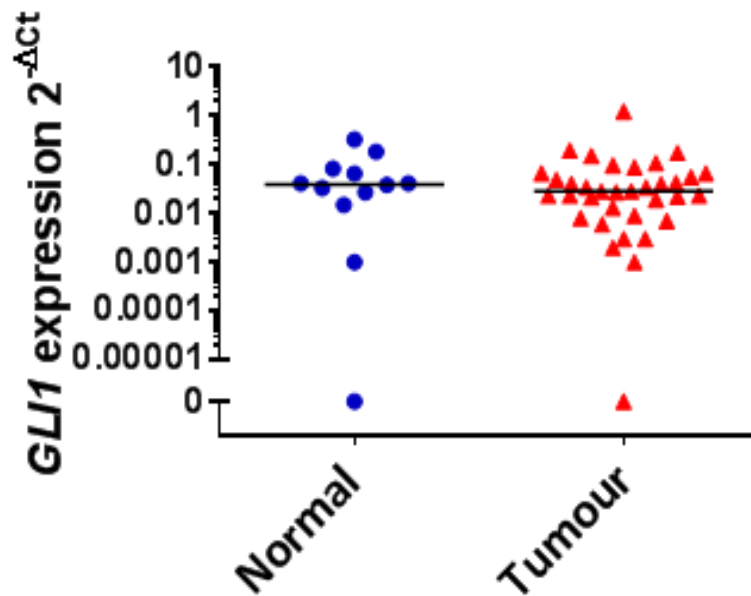


Figure 3.5 Screening of *GLI1* gene expression in normal and tumour lung tissues. *GLI1* gene expression performed in 12 normal (blue circles) and 34 tumour (red triangles) lung tissues. Normal and tumour samples were obtained from the same 12 patients, two (one normal and one tumour) primary tissues showed no expression of *GLI1* gene. No significance difference (no-parametric paired t-test) between normal and tumour samples was observed.

Considering the higher expression of *SHH* in normal lung samples (Figure 3.4) and the similar expression of Hh pathway activity between normal and tumour samples (Figure 3.5), pancreatic, rather than lung tumour was focused on as a model for investigation of the Hh pathway in cancer.

3.2.3 Protein expression analysis of Hh pathway in primary pancreatic tumour tissues

Since gene expression analysis may not be sensitive enough to detect the Hh pathway expression and activity in primary tissues (because RNA is an unstable molecule and expression may be localised to individual populations of cells within each sample), protein expression was also analysed.

Shh and Ptch1 protein expression were investigated by immunohistochemistry (IHC). Quantification of protein expression was performed by considering the general intensity of Shh and Ptch1 staining and their relative levels of expression in the epithelial and stromal areas.

3.2.4 Hh ligand protein expression analysis in pancreatic tissues

IHC analysis of Shh was performed in a panel of 19 paired primary normal and tumour tissues plus 1 unpaired tumour tissue (39 total samples). Negative controls, obtained by substitution of the primary antibody with a serum from the same species, were performed for each sample.

Initially, Shh staining intensity was analysed based on the average H-score detected in 6 different images of each section (Figure 3.6 and 3.7). In order to investigate the role of Shh in pancreatic ductal adenocarcinoma (PDAC) and its correlation with the level of tumour

differentiation, normal pancreatic tissues were compared to moderately and poorly differentiated PDAC tumours (Figure 3.6 and 3.7).

An increase in Shh expression was observed in increasingly aggressive (poorly differentiated) tumours. Moreover, the difference between poorly differentiated tumour (PDT) and normal tissues was significant ($p < 0.05$; 1 way ANOVA test) (Figure 3.7) highlighting a role for Shh in pancreatic cancer especially in the late stage of tumour development. In this analysis one normal sample was eliminated, as it was histologically poorly-differentiated with tumour characteristics, as well as two tumour tissues, since their histological classification was unknown. The presence of tumour characteristics in a normal tissue could be due to the fact that normal tissues were taken from near tumour and so may not really be normal.

Shh Staining

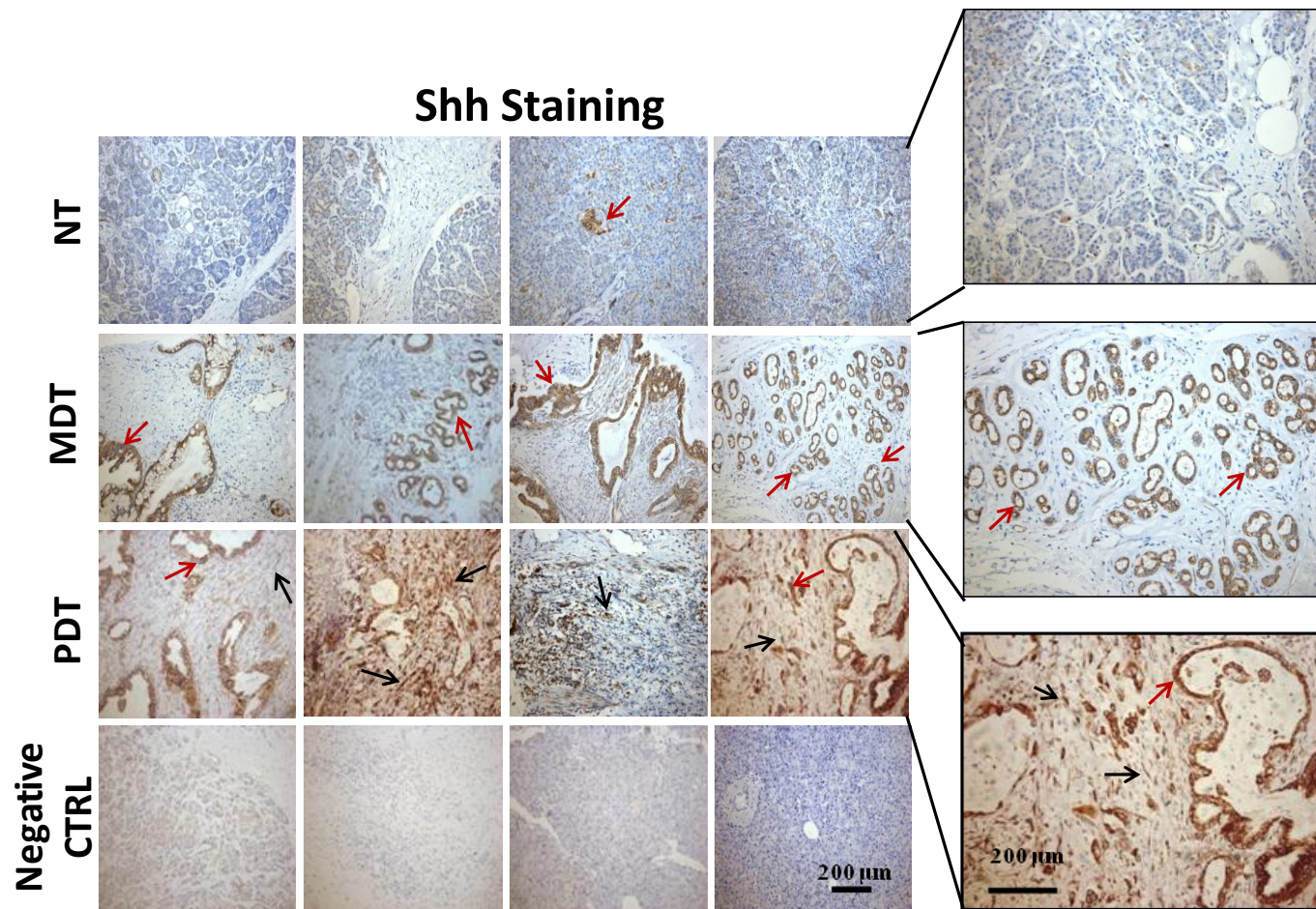


Figure 3.6 Shh protein expression in primary pancreatic normal and tumour tissues. Examples of IHC for Shh staining in normal tissue NT; moderately differentiated tumour MDT and poorly differentiated tumour PDT. The level of staining increased in more aggressive tumours (PDT). Red arrows indicate the Shh expression in epithelial cells in pancreatic ducts. Black arrows indicate Shh expression in stromal cells. In PDT samples the expression was present at both the stromal and epithelial level. On the bottom row: negative control (rabbit serum).

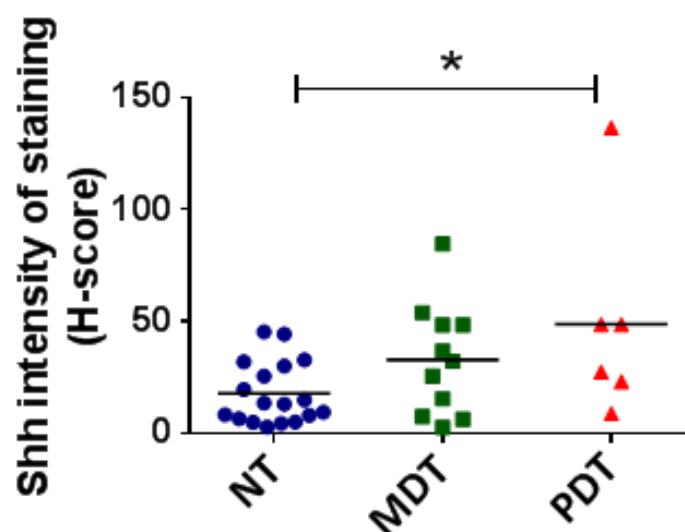


Figure 3.7 Quantification of Shh protein expression in primary pancreatic normal and tumour tissues.. Shh staining intensity was quantified by using H-score. A significant (* $p < 0.05$) Shh expression increase was observed in PDT in comparison to NT (1 way ANOVA test).

Vimentin has been used as a valuable marker of stromal-like cells [Shaw *et al* 2008; Mishra *et al* 2008; Brentnall *et al* 2012]; therefore, in order to identify the stromal component in tumour and normal tissues, vimentin staining by IHC was performed in this study. The quantification of vimentin staining was quantified as the average area stained, measured in 6 different images of the same section and for each sample a negative control was performed (in which the primary antibody was substituted by a serum from the same species of the primary antibody) to check the reliability of the staining.

In the same set of 19 normal and 20 pancreatic tumour samples (39 total samples), analysed for Shh protein expression, there was an increase of stroma in moderately and poorly differentiated tumour in

comparison to normal samples, but the difference between these groups was not statistically significant (Kruskal-Wallis non-parametric test) (Figure 3.8 A, B).

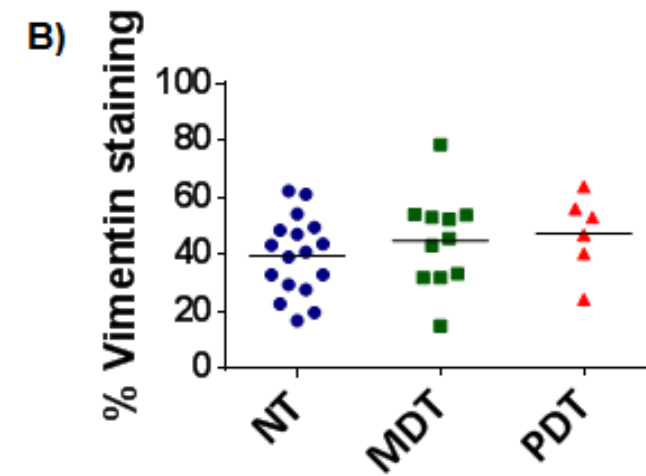
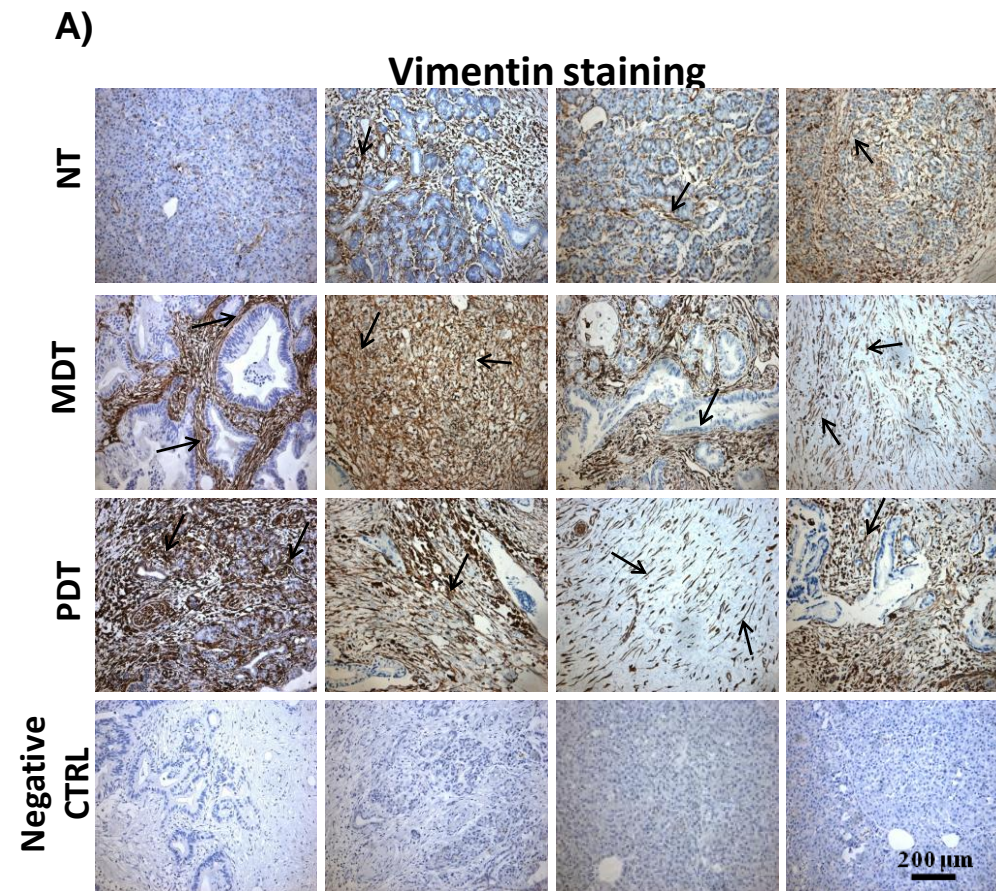


Figure 3.8 Vimentin expression in normal and pancreatic tumour tissues .A) Example of vimentin staining in normal tissue (NT); moderately differentiated tumour (MDT); poorly differentiated tumour (PDT). The black arrows indicate the localisation of staining in stroma like cells. On the bottom: Negative Control of the same tissue sections. **B)** Vimentin staining quantification was compared between normal NT (blue circle); moderately differentiated tumour MDT (green squares) and poorly differentiated tumour PDT (red triangle). No significant difference (Kruskal-Wallis non parametric test) was observed between these three groups.

In parallel, quantification of the percentage of Shh staining in stroma and epithelium separately showed a significant correlation of both with the amount of stroma (Figure 3.9 A, B) suggesting an effect of Shh expression on the induction of desmoplasia.

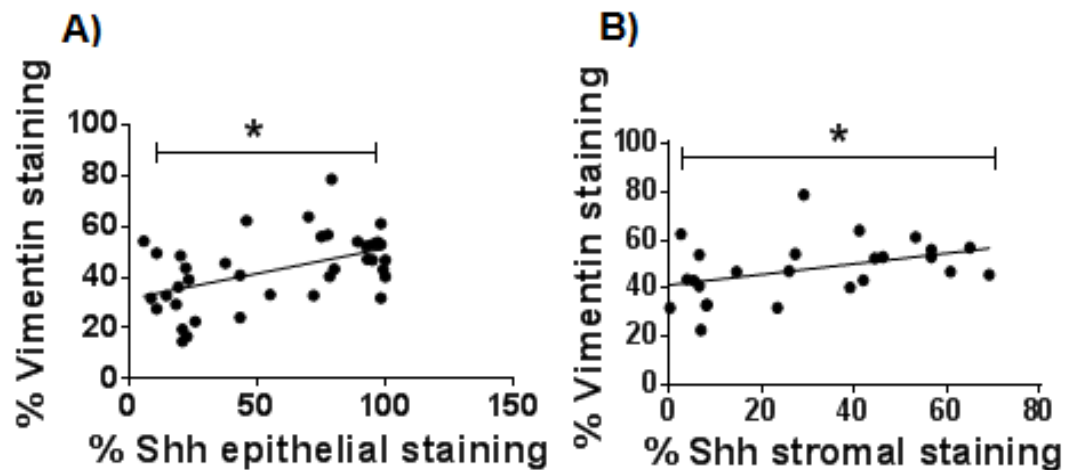


Figure 3.9 Shh epithelial and stromal expression correlates with % stromal component. .Percentage of Shh staining at epithelial (A) and stromal (B) level was investigated for correlation with vimentin protein expression in the same tissue sections. Significant correlation (Spearman rank test) was observed between the % of vimentin staining and either the % of Shh at epithelial ($p < 0.05$) or at stromal level (* $p < 0.05$).

The analysis of Shh staining separately in the epithelial and stromal component showed that Shh protein expression in the stroma paralleled staining in epithelial cells (Figure 3.10, $p = 0.028$, Spearman rank correlation). These data indicate the expression of Shh not just at epithelial level but at the stromal level too.

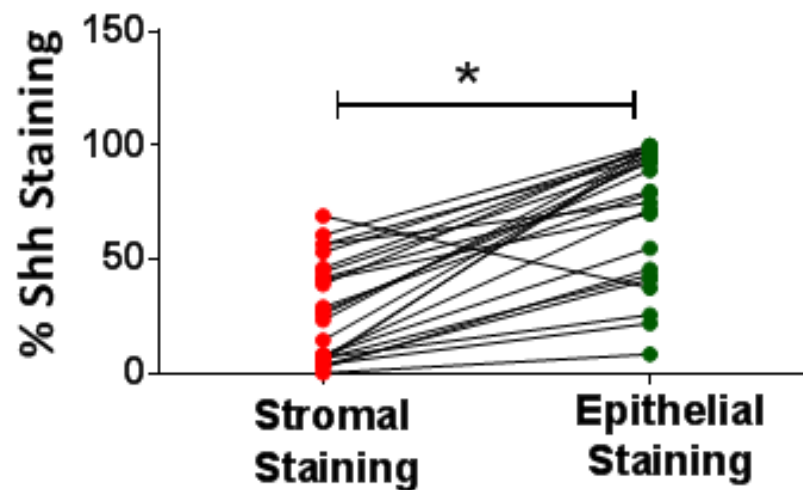


Figure 3.10 Shh expression in the stromal component increases in proportion to the level of staining in the epithelial component.. Shh staining was quantified as an average of 6 different images from the same sample both in the stromal and in the epithelial components of the same section. Samples with higher Shh expression in the stroma showed the highest expression at the epithelial level. Statistical analysis showed a significant (* $p < 0.05$) correlation (Spearman test) between the epithelial and the stromal staining.

Moreover, there was a significant increase (Kruskal-Wallis non-parametric test) in Shh protein staining at the stromal level in more aggressive tumors (Figure 3.11). In this analysis only samples in which stroma were present were included.

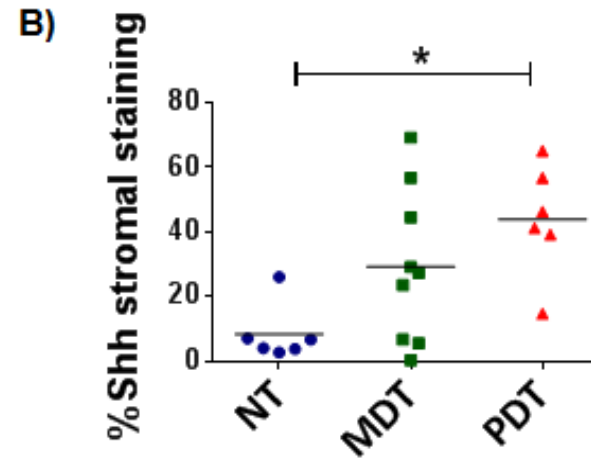
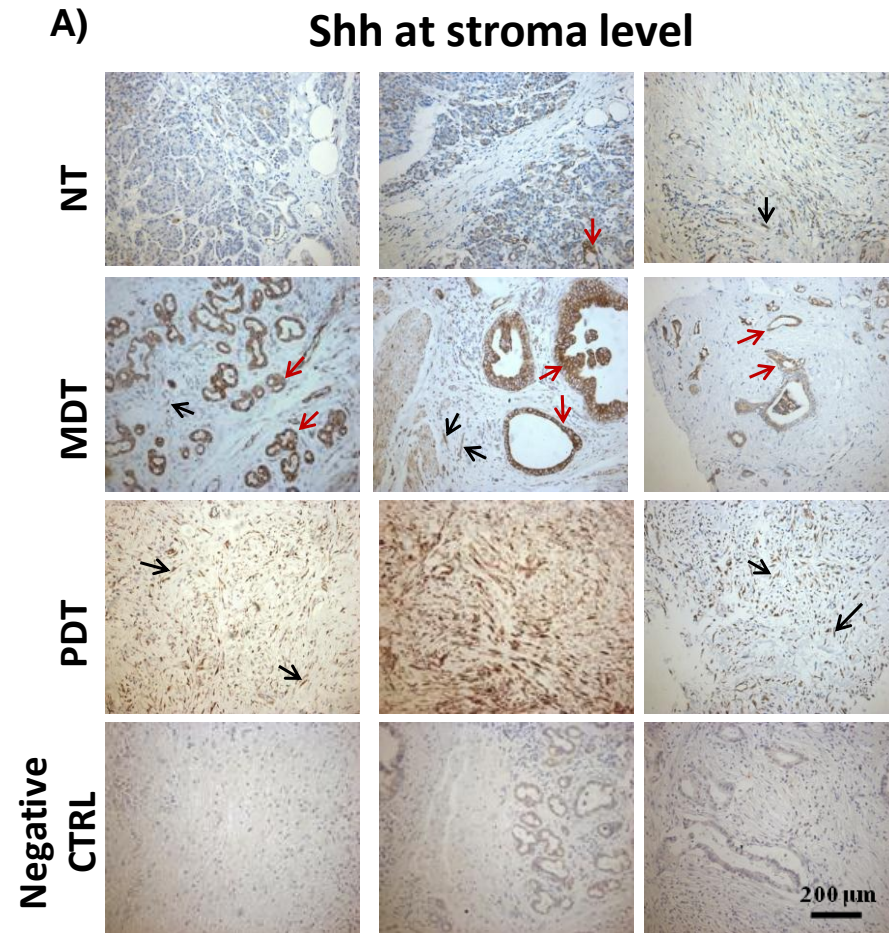


Figure 3.11 Shh was expressed at the stroma level and increased with tumour aggressiveness.. A) Example of Shh staining by IHC in different grades of tumour differentiation (PDT and MDT). Red arrows indicate Shh expression in ductal epithelial cells. Black arrows in samples show Shh expression in stroma like cells. Bottom Row: negative controls of the same tissue sections. B) Comparison between Shh at stroma level in normal NT (blue circle); Moderate differentiated tumour MDT (green square); Poorly differentiated tumour PDT (red triangle). Protein expression of Shh significantly (Kruskal-Wallis non-parametric test) increased (* $p < 0.05$) in more aggressive tumours in comparison to normal samples.

In order to investigate the activity of the Hh pathway in pancreatic tissues at the stromal and epithelial levels and to better understand the type of transmission (autocrine or paracrine) occurring in this pathway in the tumour microenvironment, in the next section the protein expression of Hh target Ptch1 was analysed.

3.2.5 Investigation of the activity of the Hh pathway in pancreatic tissues

In this section, Ptch1 was used as an indicator of the Hh activity by paracrine or autocrine activation. In the absence of autocrine signaling at the epithelial level, Ptch1 should be mainly expressed in stroma [Tian *et al* 2009], and no expression should be detected in epithelial cells.

Initially in order to compare Ptch1 expression between normal and tumour samples, Ptch1 staining, was quantified for its overall expression in the pancreatic tissues (19 normal paired and 20 tumour pancreatic tissues, 39 samples in total) included in the Shh screening of paragraph 3.3.1 and 3.3.2. This quantification, as for Shh (Figure 3.7) was based on the average of the H-score detected in 6 different images of the same tumour or normal pancreatic tissue sections. Negative controls obtained by substitution of the primary antibody with a serum from the same species of the primary antibody were performed for each sample. Quantification of Ptch1 staining intensity showed the same level of expression in normal tissue, and in moderately and poorly differentiated tumours (Figure 3.12 A and B).

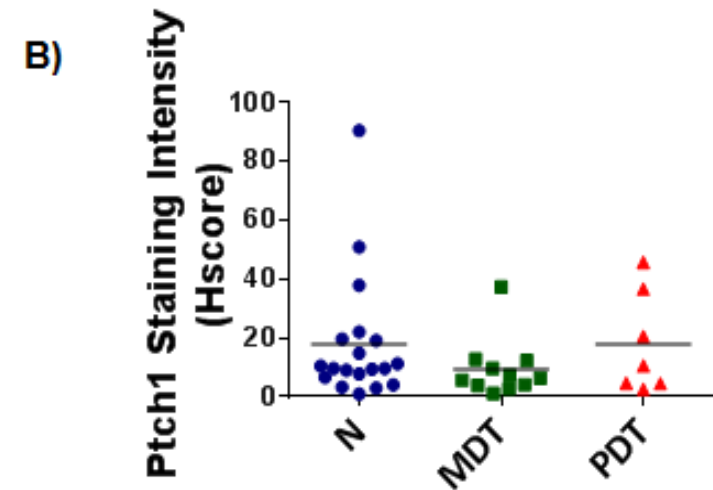
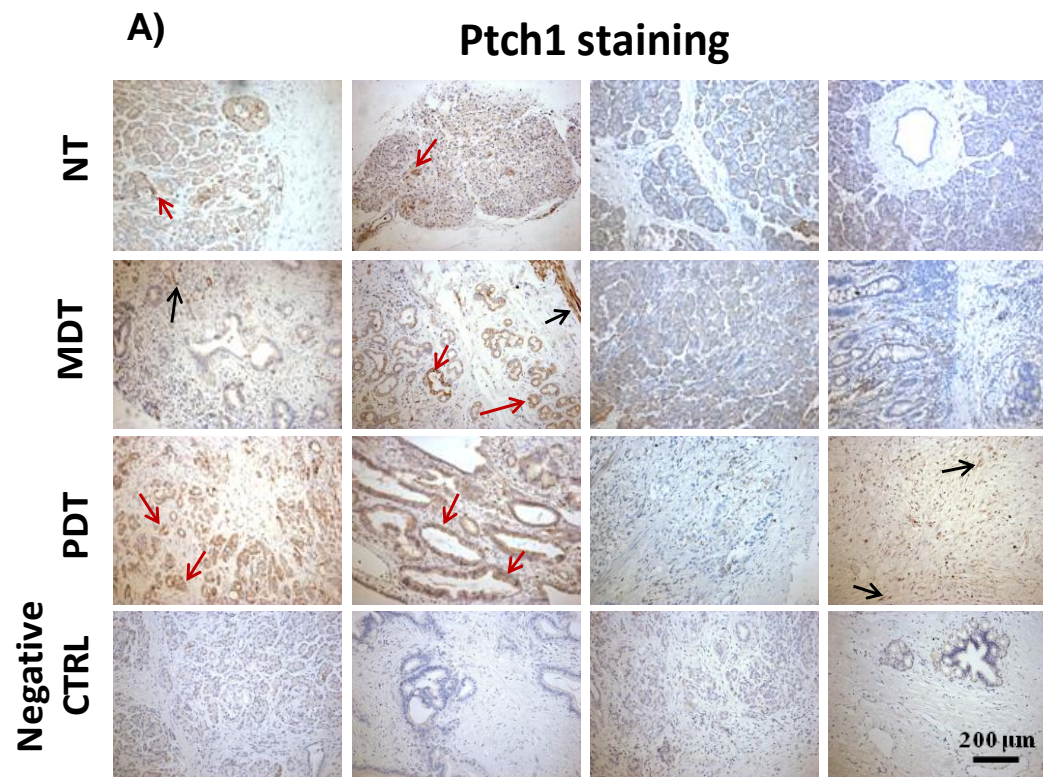


Figure 3.12 Ptch1 protein expression analyses in normal and tumour pancreatic tissues.. A) Example of Ptch1 staining by IHC in different grades of tumour differentiation (PDT and MDT). Red and black arrows indicate Ptch1 expression mainly in epithelial ductal cells, and in stromal cells, respectively. Bottom Row: negative controls in the same tissue sections. B) Comparison between Ptch1 staining intensity in normal NT (blue circles); moderately differentiated tumour MDT (green squares); poorly differentiated tumour PDT (red triangles). The quantification of Ptch1 expression was achieved by H-score. Statistical analysis (Kruskal-Wallis non parametric test) between the NT, MDT and PDT groups of samples did not show any significance.

In order to localise the Ptch1 expression and to investigate if there is a correlation between the Hh pathway activity at the epithelial and stromal levels in pancreatic cancer, Ptch1 staining was also quantified based on percentage of staining, in the epithelial and stromal component of each of the 39 sections included in this study.

In contrast with Shh (figure 3.10), Ptch1 protein expression did not increase in epithelial cells in parallel with increased stromal staining (Figure 3.13 A). Moreover, no significant (Spearman test) correlation between the percentage of staining detected in the stroma and that measured in epithelium (Figure 3.13 B) was observed. In this analysis, as for Shh analyses, only samples with a visible and detectable stromal component were included. Many normal tissues and some MDT were in fact characterised by the absence of a stromal component.

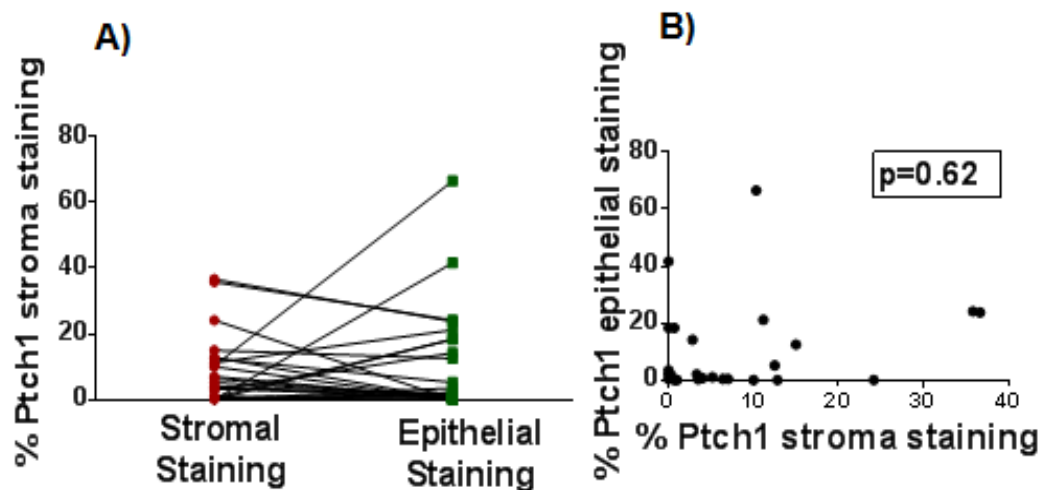


Figure 3.13 Ptch1 expression at the stromal level does not correlate with its expression in the epithelial component.. A) The trend of Ptch1 expression at stroma level was compared with its expression in the epithelial component contained in the same sample. B) Correlation analysis between the percentage of Ptch1 expression in the stroma and in the epithelial component was calculated by Spearman correlation test ($p=0.62$)

Ptch1 percentage expression at the epithelial and stromal levels was then analysed and correlated with the stromal component, quantified by vimentin staining. There was no correlation (Spearman correlation analysis) between Ptch1 epithelial (Figure 3.14 A) and stromal staining (Figure 3.14 B) with the stromal component in contrast to what was observed for Shh protein expression (Figure 3.10). However, statistical analysis between Ptch1 stroma staining and stromal component was on the limit of significance ($P=0.05$).

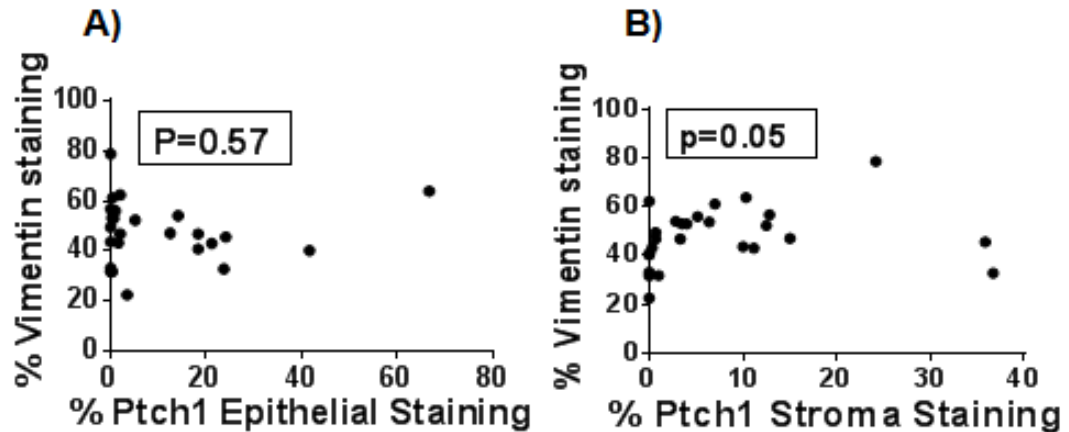


Figure 3.14 Expression of Ptch1 within the epithelial and stroma compartments do not correlate.. A) Percentage Ptch1 staining in the epithelial component of normal and tumour sections was compared with the percentage staining in the stroma component detected by vimentin staining and the correlation analysed by Spearman correlation test ($p=0.57$). B) Trend of variation of Ptch1 in stroma component of pancreatic tissues was compared with the stroma component in the same tissue. As in figure (A) correlation analysis was investigated by using Spearman correlation test. The correlation was on the limit of significance ($p=0.05$).

In order to further investigate if Hh pathway transmission occurs through autocrine signalling at the epithelial level or can be paracrine/autocrine at the stromal level, Ptch1 expression in stromal and epithelial cells was compared. From this analysis Ptch1 was higher, but not significantly (Figure 3.15), in the epithelial component.

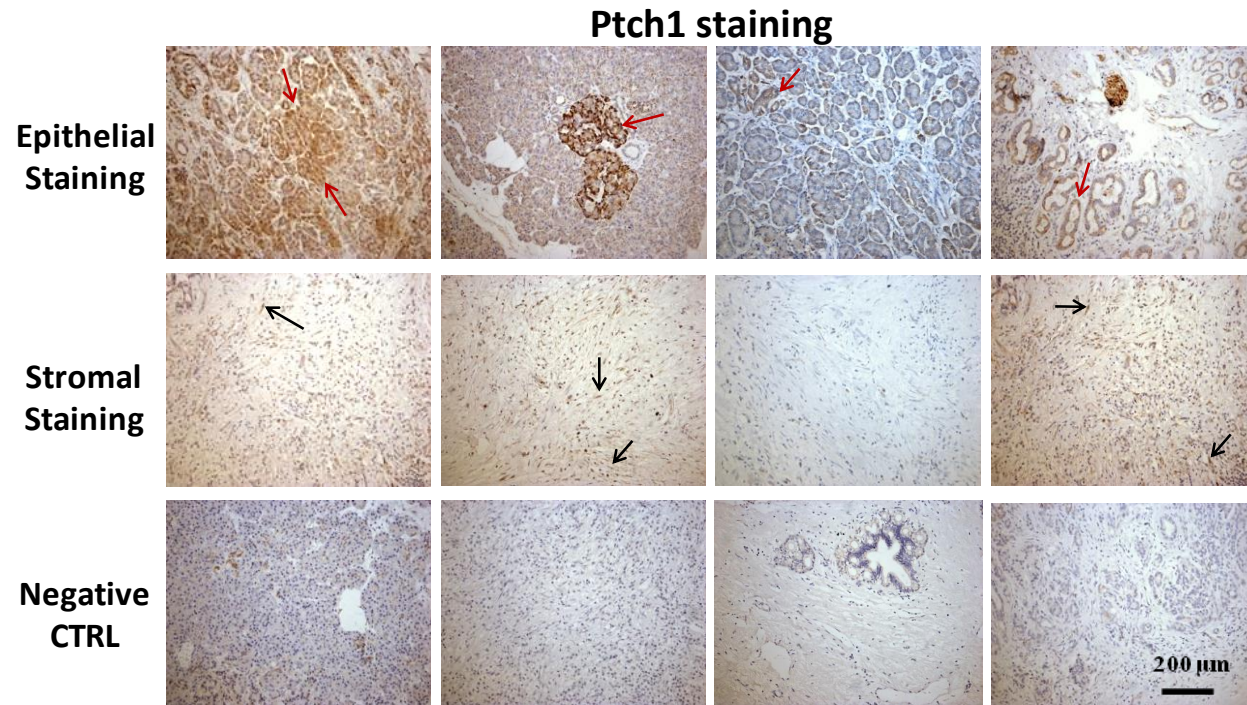


Figure 3.15 Ptch1 is highly expressed in the epithelial component of normal and tumour pancreatic tissues . Examples of Ptch1 staining at epithelial and stromal level. Red arrows: Ptch1 staining in epithelial component. Black arrows: Ptch1 staining in the stromal component. Ptch1 was expressed in both epithelial and stromal components but higher staining intensity was observed in the epithelium. Bottom Row: negative controls of Ptch1 staining in pancreatic samples.

Since Shh and Ptch1 were both expressed at the epithelial and stromal levels, the possibility that Hh pathway activity in the tumour microenvironment was a result either of paracrine activation or of an autocrine signal within stromal cells was suggested.

No significant correlation was observed between Shh protein expression in epithelial cells and Ptch1 protein expression when expressed in epithelial cells (Figure 3.16 A) (reducing the possibility of induction of the Hh pathway at the epithelial level). However, significant correlation was observed between epithelial Shh expression and stromal Ptch1 expression (Figure 3.16 B) (increasing the possibility of paracrine activation of the pathway). Finally, significant correlation was detected between Shh and Ptch1 expression in stromal cells (Figure 3.16 C) (supporting the possibility of an autocrine Hh signal at stromal level).

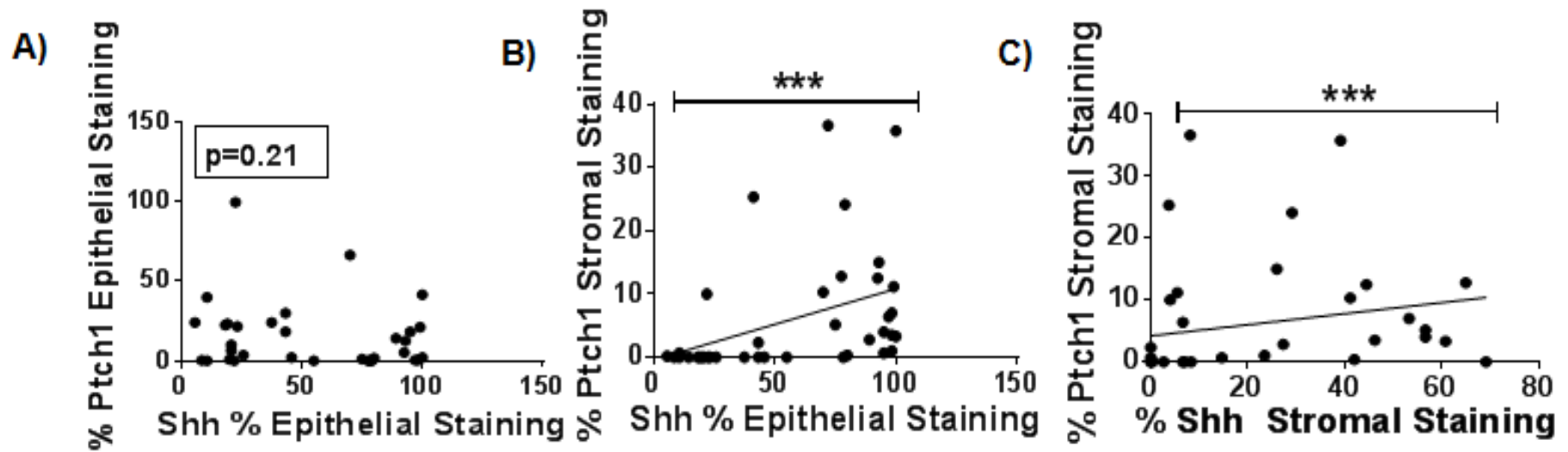


Figure 3.16 Correlation analysis between Shh and Ptch1 protein expressions in pancreatic normal and tumour tissues. A) Spearman correlation analysis between Shh expression at epithelial level and Ptch1 expression in epithelial cells. The analysis was performed to investigate the existence of an Hh autocrine signal in epithelial cells. No significant correlation was observed in this analysis ($p=0.21$) B) Correlation analysis (Spearman correlation test) between Shh epithelial expression and Ptch1 expression at stromal level in order to investigate the paracrine induction of Hh pathway in the tumour microenvironment. Significant correlation was observed in this analysis ($p<0.0001$) C) Correlation analysis (Spearman correlation test) between Shh expression in stromal cells and Ptch1 expression at stromal level in order to investigate the autocrine signalling transmission of the Hh pathway in the stromal cells of pancreatic tissue. Significant correlation was observed in this analysis ($***p<0.001$).

3.4 Summary of results

In this chapter the following results were demonstrated:

- No over-expression of the Hh pathway, based on *SHH* and *GLI1* expression, was detected in lung tumour tissues in comparison to normal samples
- *SHH* and *GLI1* genes were highly expressed in pancreatic tumour samples in comparison to normal samples.
- The analysis of the expression of the other two Hh ligands *IHH* and *DHH* showed no or low expression in normal and tumour samples suggesting *SHH* is the main ligand acting in pancreatic tumour.
- Overall, Shh protein expression was significantly more highly expressed in more aggressive pancreatic tumour (PDT) than in normal samples.
- Shh protein was not just expressed at the epithelial level but at the stromal level too. Moreover, the percentage of Shh epithelial staining increased in parallel with percentage of staining at the stromal level.
- Shh expression in epithelial and stromal cells both correlated with the stromal component evaluated by vimentin staining.

- Ptch1 protein expression did not correlate with tumour aggressiveness and no correlation was observed between its expression at epithelial and stromal level.
- Correlation analysis between Shh protein expression at the epithelial level and Ptch1 protein expression in epithelial cells decreased the probability of an autocrine Hh signalling pathway transmission in epithelial cells. However, correlation between Ptch1 expression in stromal cells and Shh expression at the epithelial and stromal level left open the possibility of both paracrine and autocrine Hh signalling transmission in the stromal component.

Taken together these results show an important role for Shh in pancreatic cancer and its expression in the stroma, suggesting a potential role for this molecule in the stromal compartment. The expression of Ptch1 protein expression both in epithelial and stromal cells and the correlation between Shh and Ptch1 protein expression in the epithelial and stromal cells raises the possibility of both epithelial autocrine and paracrine Hh pathway transmission in the tumour microenvironment with both paracrine and autocrine transmission in the stromal cells.

Chapter 4 - Results:

Characterisation of Hh pathway in epithelial and stromal cells

4.1 Introduction

Overexpression of the Hh pathway in pancreatic cancer has been demonstrated in the literature [Bailey *et al*, 2008; Tian *et al*, 2009] and confirmed in chapter 3 of this thesis. Pancreatic cancer is characterised by having a high stromal component; this, together with the observation of Hh pathway paracrine induction in stromal cells, makes pancreatic cancer a good candidate for investigation of the role of Hh pathway signalling in the formation and maintenance of the stroma and its effect on the epithelial component [Bailey *et al*, 2008; Tian *et al*, 2009]. In particular, few studies have so far included primary CAFs in the exploration of the role of the Hh pathway in tumour progression, making this study a further step in this investigation.

In this chapter a panel of pancreatic fibroblasts and epithelial cells, including fibroblasts derived from primary tumour samples, were profiled for Hh pathway expression at the gene and protein level, providing important information about the presence of components of the Hh pathway in fibroblast cells and guiding the choice of cells to be used in future experiments. Finally, Hh paracrine induction in primary pancreatic CAFs was further investigated by treatment of these cells with NShh molecule or tumour-conditioned media (TCM), and use of 2D direct and trans-well co-cultures with pancreatic epithelial tumour cells. A higher resolution of the IF images showed in this chapter is available in the CD version of the thesis.

4.2 Screening of pancreatic epithelial and fibroblast cells

4.2.1 Hh pathway expression in pancreatic cancer epithelial and primary-derived fibroblasts cells

In order to characterise the pancreatic cancer cells to be used in the *in vitro* investigation of Hh pathway cross-talk between cancer cells and the stromal microenvironment, a panel of pancreatic epithelial cells (PANC1, BXPC3, P308T, PAN1) and CAFs were profiled by qRT-PCR for gene expression of the main components of the Hh pathway (*SHH*, *DHH*, *IHH*, *GLI1*, *SMO*, *PTCH1*, *PTCH2*). The same cells were also investigated for gene markers of epithelial (*CDH1*) and mesenchymal phenotypes (*VIM* and *HGF*) to confirm and characterise their identity in the tumour context. *CDH1*, *VIM* and *HGF* are all genes that encode proteins involved in the EMT process. For this reason they are normally used as identification markers of the loss or acquisition by epithelial cancer cells of a mesenchymal phenotype [Frixen *et al* 1991; Tuxhorn *et al* 2002; Adegboyega *et al* 2002; Zhang *et al* 2012]. *CDH1* (gene of E-cadherin protein) is normally highly expressed in cancer cells with an epithelial phenotype and its down-regulation is correlated with increased invasiveness and mesenchymal phenotype acquisition of cancer cells [Frixen *et al* 1991]. On the other hand, *HGF* and *VIM* have been used in many studies as markers of myofibroblasts or CAFs in the tumour microenvironment and their expression tends to increase when epithelial cells acquire a mesenchymal phenotype [Shaw *et al.* 2009;

Spaeth *et al.* 2009, Dandachi *et al* 2001; Tuxhorn *et al* 2002 ;Zhang *et al* 2012]. Moreover, their expression is an indicator of an activated and aggressive state that seems to support tumour growth and progression [Shaw *et al.* 2009; Tuxhorn *et al* 2002]. Using these markers, the epithelial or mesenchymal phenotype of cancer epithelial cells and CAFs was assessed and correlated with Hh pathway expression in this study.

The two cell-types (epithelial cells and CAFs) were compared for epithelial/mesenchymal and Hh markers in the following graphs: Figure 4.1A in which the expression of epithelial and fibroblast markers are shown and Figure 4.1B in which the main genes of the Hh pathway expression are shown.

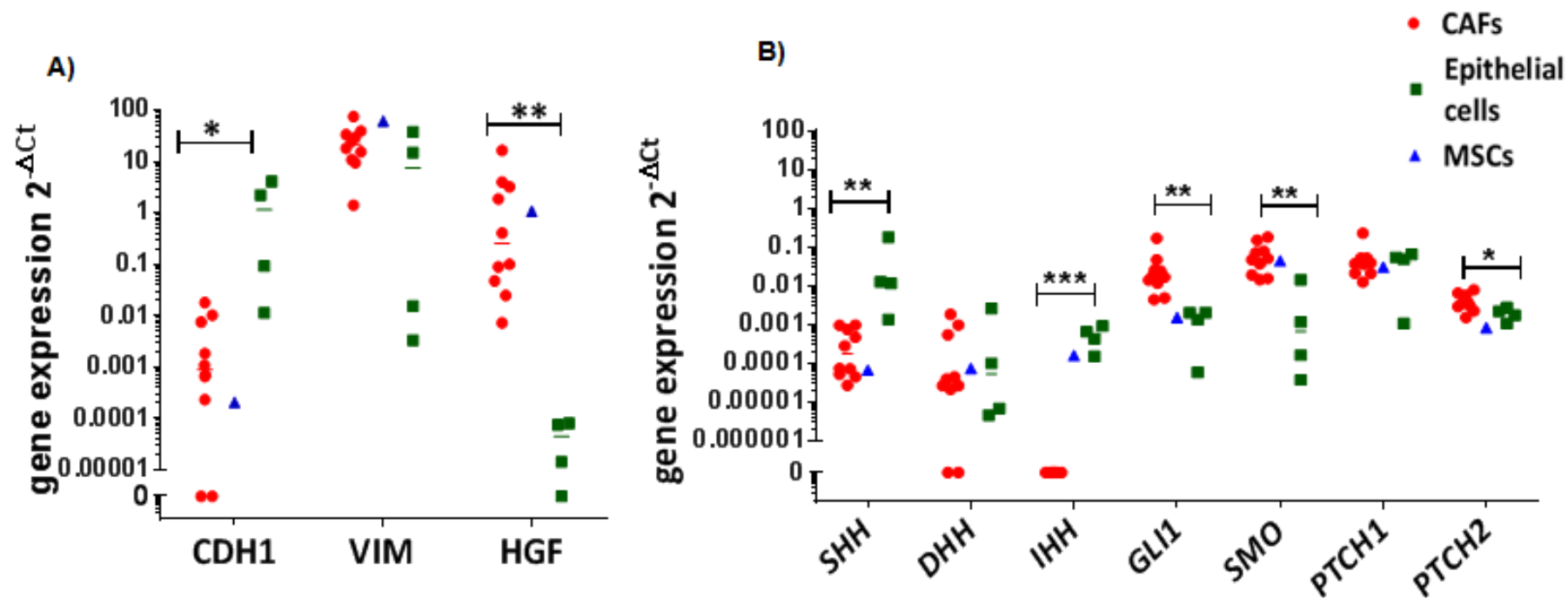


Figure 4.1 Screening of epithelial cells, CAFs and MSCs for the main genes associated with the Hh pathway and epithelial/ myofibroblast markers. A) Screening of 4 pancreatic epithelial cancer cells, 10 pancreatic primary CAFs and 1 MSC line for the expression of an epithelial phenotype marker (*CDH1*) and the expression of mesenchymal phenotype markers (*VIM* and *HGF*). B) Screening of the same cell lines for the main genes involved in the Hh pathway: 3 ligands *SHH*, *DHH* and *IHH* and 4 genes involved in the signalling transmission (*PTCH1*, *PTCH2*, *GLI1*, and *SMO*). *GLI1* and *PTCH1/2* are also gene target of the Hh pathway and so indicators of its activity. Statistics between different cell lines were performed by using non-parametric t Test (* $p < 0.05$), (** $p < 0.01$), (***) $p < 0.001$).

Analysis of myofibroblast and epithelial markers showed higher expression of *CDH1* ($p<0.05$) in epithelial cells in comparison to CAFs and MSCs. Moreover, significantly higher *HGF* expression ($p<0.01$) was observed in CAFs and MSCs in comparison to epithelial cells (Figure 4.1A). Both these observations are consistent with the expected phenotypes of the cell lines analysed [Frixen *et al* 1991; Spaeth *et al* 2009]. However, a high level of *VIM* expression was observed in both cell types (epithelial and CAFs) (Figure 4.1A). The analysis of the expression of the main Hh pathway genes confirmed significantly highest expression ($p<0.05$) of Shh ligand in epithelial pancreatic tumour cells in comparison to CAFs. Moreover, *SHH* was also highly expressed in pancreatic epithelial cells in comparison to *DHH* (non significant difference) and *IHH* ($p<0.05$) (the others two ligands of the Hh pathway)(Figure 4.1B). *DHH* expression was, in fact, generally expressed at a low level both in pancreatic epithelial (except in PANC1s) and fibroblast cells, limiting the importance of this ligand in this type of cancer. *IHH* as well as *DHH* was poorly expressed in epithelial cancer cells when compared with the level of *SHH* expression; however, much higher expression of *IHH* was present in epithelial than fibroblast cells ($p=0.0006$) (Figure 4.1B). Interestingly *SMO* ($p<0.01$), *GLI1* ($p<0.01$), *PTCH2* ($p<0.05$) expression were significantly higher in CAFs than epithelial cells suggesting a higher activity of the downstream Hh pathway signalling in these cells. *PTCH1* expression analysis did not show any significant difference between the pancreatic epithelial and

fibroblast cells suggesting its expression in both types of cell lines (Figure 4.1B). In view of this observation, even if *PTCH1* gene expression is considered a marker of the Hh pathway activity [Hidalgo and Ingham 1990], due to the negative feedback exerted on the pathway [Goodrich *et al* 1999], its gene expression could be partly inhibited and as a consequence it may not always perfectly reflect Hh pathway activity. However, considering the frequent use of *Ptch1* gene and protein expression in different studies [Tian *et al* 2009; Lee *et al* 2013] and the fact that *GLI1* expression (the other gene target of Hh pathway used to analyse its activity) can in some cases be activated by non-canonical pathways, its investigation at the gene and protein levels was included in this study taking into account the potential changes in its gene expression.

Correlation analysis (Spearman test) between Hh pathway and epithelial and mesenchymal markers showed a significant association between *SHH* and *CDH1* expression ($p < 0.01$). Moreover, *CDH1* also correlated with *GLI1* ($p < 0.05$) and *SMO* ($P < 0.001$) expression. These results suggest Hh pathway activity in cells with an epithelial phenotype. However, *SMO* expression was also significantly correlated with *VIM* ($p < 0.05$) and *HGF* ($p < 0.05$), and *PTCH2* was positively associated with *VIM* ($p < 0.05$). These results support the possibility of Hh autocrine signal in cells with epithelial phenotype but also suggest the existence of the pathway activity in mesenchymal-like cells.

4.2.2 Protein expression analysis of Hh ligand expression in cancer epithelial cells

In order to confirm at the protein level the results achieved by gene expression analysis and select the epithelial cells to include in a model to investigate Hh paracrine induction in the tumour microenvironment, some of the epithelial cell lines included in this study were also investigated for Shh and Dhh protein expression by immunofluorescence staining.

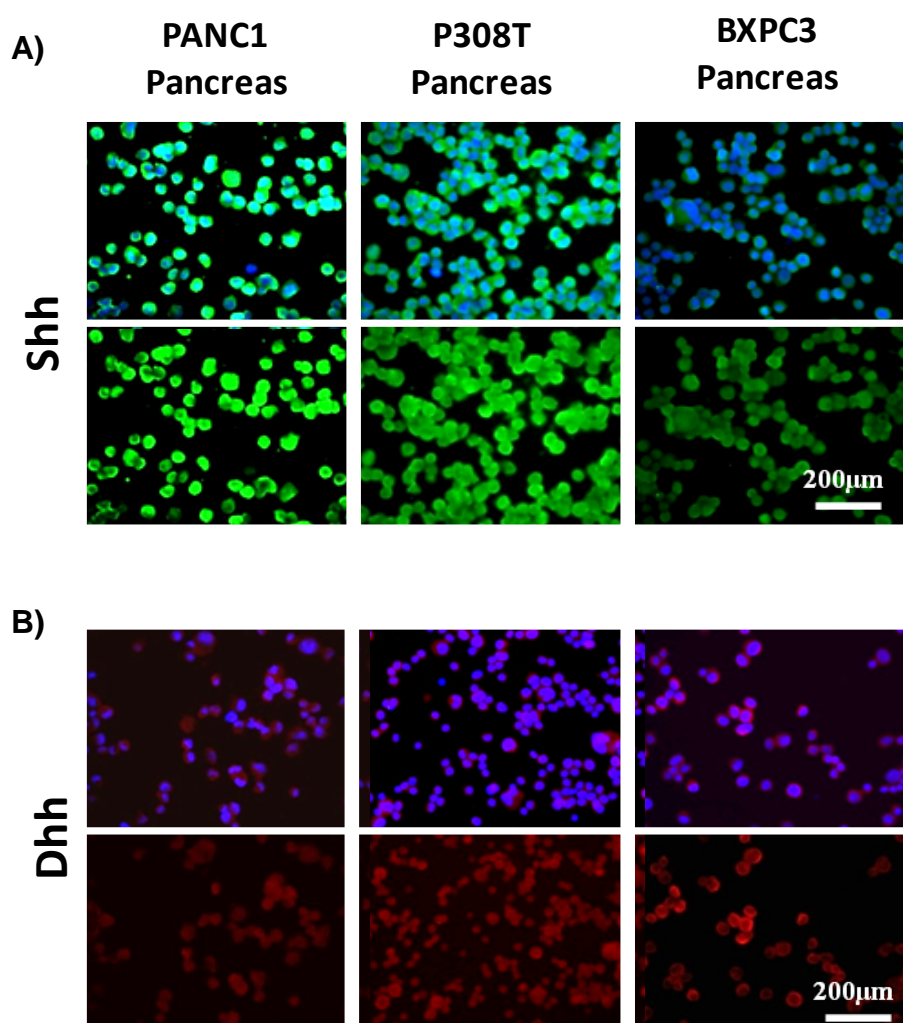


Figure 4.2 Shh and Dhh protein expression analyses by IF in epithelial pancreatic cancer cells. A) Shh protein expression (green staining) in PANC1, P308T and BXPC3 pancreatic cancer cells. Top row: cells with nuclei highlighted (DAPI blue staining). Bottom row: Shh staining without combined nuclear staining. B) Dhh protein expression (red staining) with (top) and without (bottom) DAPI nuclear staining

Shh protein (Figure 4.2 A) was highly expressed in PANC1 cell lines and, although at a lower level, in P308T and BXPC3 lines. Dhh protein expression analysis showed low expression in P308T and BXPC3 and very low levels in PANC1 cell lines. In this and in the previous analysis (Figure 4.1), the comparison between Shh and Dhh protein expression

in the same pancreatic cell lines (PANC1, P308T, and BXPC3) clearly showed highest expression of Shh, supporting the conclusion that it is the main Hh ligand acting in pancreatic cancer.

As in chapter 3, Gli1 expression was investigated as a measure of Hh pathway activity as it is not just a transcription factor involved in the pathway but also, as consequence of positive feedback, a gene target of the pathway. For this reason, Gli1 protein expression was analysed in the same pancreatic epithelial cells lines used for investigation of Shh and Dhh protein.

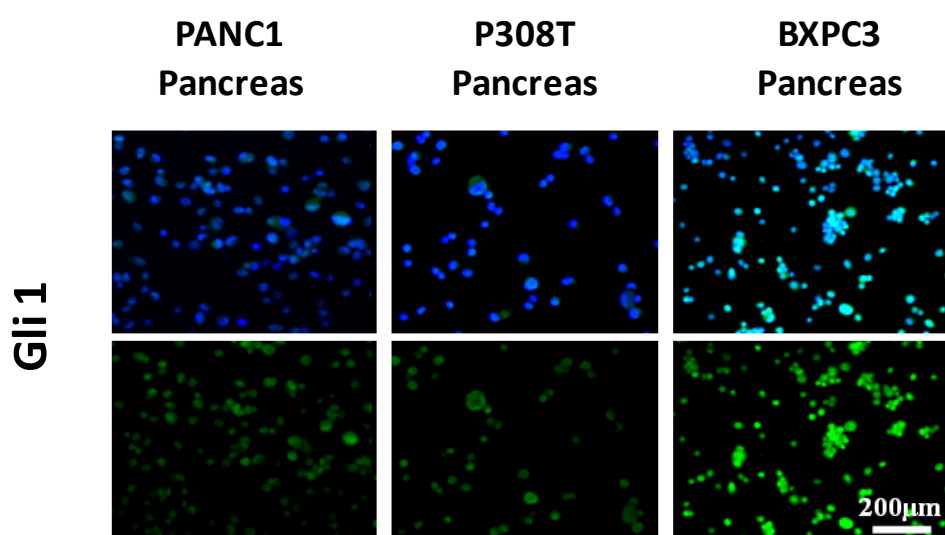


Figure 4.3 Gli1 expression in pancreatic epithelial cancer cells . Gli1 protein expression analysis by IF (green staining) in PANC1, P308T and BXPC3 pancreatic cancer cells. Images on top: cells with nuclei highlighted (DAPI blue staining); images on bottom: Gli1 staining without combined nuclear staining.

Higher Hh signalling pathway activity was observed in BXPC3 and low level activity in PANC1 and P308T epithelial cells indicating that the pathway is not always fully active in cancer epithelial cells but can be expressed at higher (BXPC3 cells) or lower (PANC1, P308T)

background levels in different cell lines. Consistent with these observations, different Hh pathway basal activity levels was previously observed in a panel of pancreatic epithelial cells including PANC1 and BXPC3 [Yauch *et al* 2008].

4.3 Investigation of pancreatic CAF responsiveness to exogenous Hh stimuli

In order to investigate Hh paracrine induction in cancer stromal cells, a panel of pancreatic CAFs (screened for Hh pathway expression in section 4.2), were analysed for their ability to respond to Hh ligand in response to NShh treatment or tumour-conditioned medium and in 2D co-culture assays. Pancreatic epithelial cancer cells (PANC1, BXPC3 and P308T) characterised in this study for Shh gene and protein expression (sections 4.2.1 and 4.2.2) were included in this investigation as examples of cells with different levels of Hh ligand expression with potential to cause paracrine signalling.

4.3.1 Investigation of the mesenchymal-like phenotype in CAFs stroma cells

Evidence from the literature describes myofibroblast cells in the tumour microenvironment as fibroblast cells with high expression of α SMA and vimentin (Shaw *et al* 2009; Spaeth *et al* 2009). The expression of these two markers indicates an activated phenotype that correlates with a more aggressive behaviour able to support tumour growth and progression [Shaw *et al* 2009; De Wever *et al* 2008; Mishra *et al* 2008; Spaeth *et al* 2009; Tuxhorn *et al* 2002]. Cell activation (increased α SMA expression) is believed to be triggered as a result of interplay between tumour stromal cells and epithelial cancer cells. For this reason α SMA expression was monitored to investigate if the level of cell activation

affects the cells' responsiveness, and if activation can be affected by Hh paracrine signalling from tumour cells as shown previously [Bailey *et al* 2008].

Initially, *ACTA2* (α SMA gene) and α SMA protein expression was determined in CAFs cultured over time (Figure 4.4). No changes in gene expression over time were observed in pancreatic CAFs, and protein expression analysis confirmed the expression of this protein in this type of cell suggesting their activation. However, these data do not yet indicate the effect of FBS percentage contained in the media and the level of expression detected (high or low) in comparison with other cell lines, factors that will be further investigated later in this study.

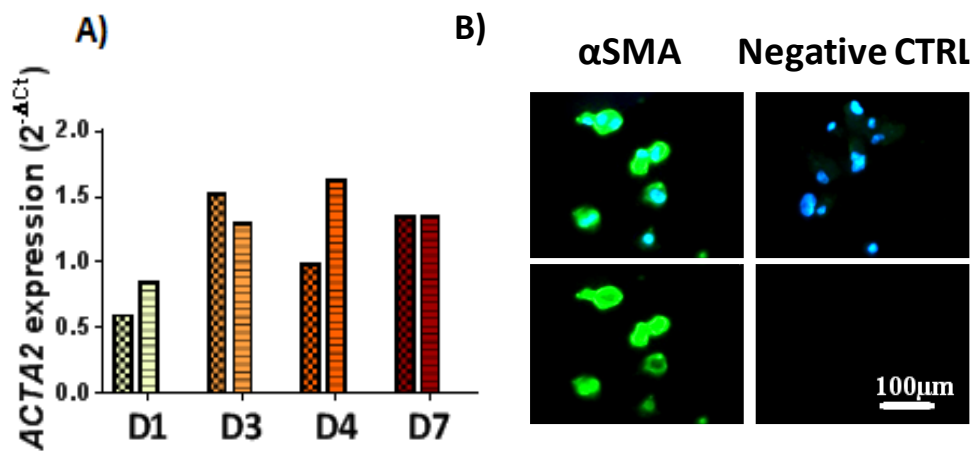


Figure 4.4 CAF cells express α SMA cell activation marker.. A) *ACTA2* gene expression in pancreatic CAFs on day1; 3; 4 and 7 (D1, D2, D3, D7) of cell culture. Two repetition wells were performed for each time point. The bars with the same pattern show the gene expression detected in the same well. B) α SMA protein expression in pancreatic CAFs and negative CTRL (Sample stained by substituting primary antibody with Isotype IgG).

4.3.2 Investigation of responsiveness of CAFs to NShh treatment

Several studies (Taipale *et al* 2000; Chen *et al* 2002; Bailey *et al.* 2008; Zacharias *et al* 2011,) have shown induction of the Hedgehog pathway in myofibroblast cells, detected as increased Gli1 gene and protein expression, following NShh treatment. NShh is a palmitoyl and cholesteryl modified polypeptide, able to trigger the Hh pathway in the targeted cell by binding to the Ptch1 receptor and inhibiting its function. A dose of 5nM and time point of 48h was used to investigate responsiveness (Figures 4.5; 4.6), but in addition higher concentrations (10-20nM), previously used successfully (Taipale *et al* 2000) were also included. In a first experiment the responsiveness of the CAFs (P3T and P5T) to NShh induction was evaluated *via* *GLI1* (gene target of Hh pathway) and *SMO* gene expression analysis. Moreover, the effect of Shh exogenous treatment on *ACTA2* gene expression was also investigated (Figure 4.6). The CAFs used (P5T) did not show an induction of *GLI1* and *SMO* expression after 48h of treatment (Figure 4.5 A and B). Increasing and decreasing but inconsistent effects on *ACTA2* expression were observed in both cell lines (Figure 4.5C).

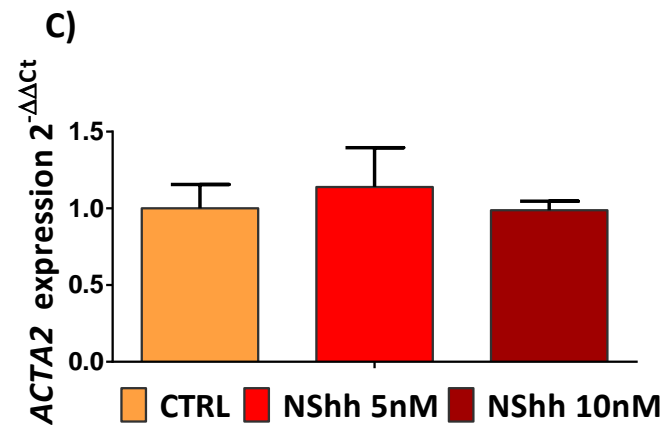
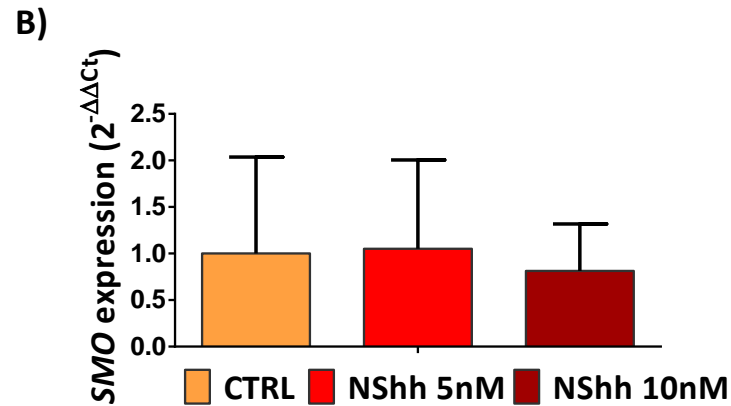
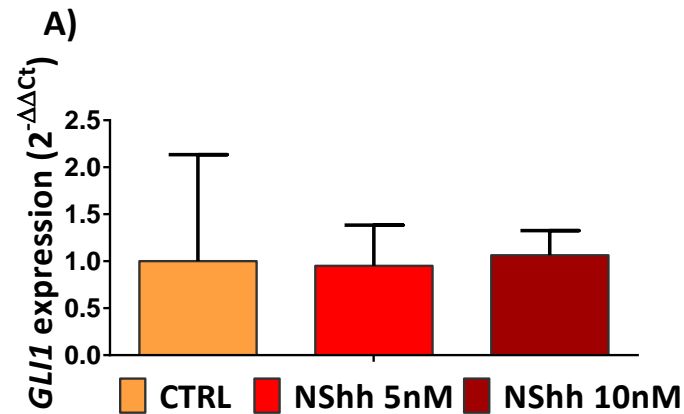


Figure 4.5 Investigation of the responsiveness of CAFs to NShh.. (A) *GLI1*, (B) *SMO* and (C) *ACTA2* gene expression in CAFs after treatment with 5nM and 10nM of NShh. P5T is a primary tumour-derived cell line. Each bar in these graphs shows the result of the average gene expression detected in treated samples from three replicates (two from well replicates performed during the same experiment and one from a different experiment) normalised to that detected in the samples control. Statistical analysis of this experiment was performed by using Krustal-Wallis non parametric test. No significance was observed between the CTRL and the treated samples for any of the genes analysed.

NShh treatment was then repeated to test the responsiveness to Hh stimuli at different time points (3 and 6 days). The rationale of this experiment was not just to test the reproducibility of previous data (Figure 4.5A), but also to analyse the level of cell activation (*ACTA2* expression) with time in culture and determine if it could affect or be affected (as observed in Bailey *et al*, 2008 and Zacharias *et al*, 2011) by response to the Hh pathway.

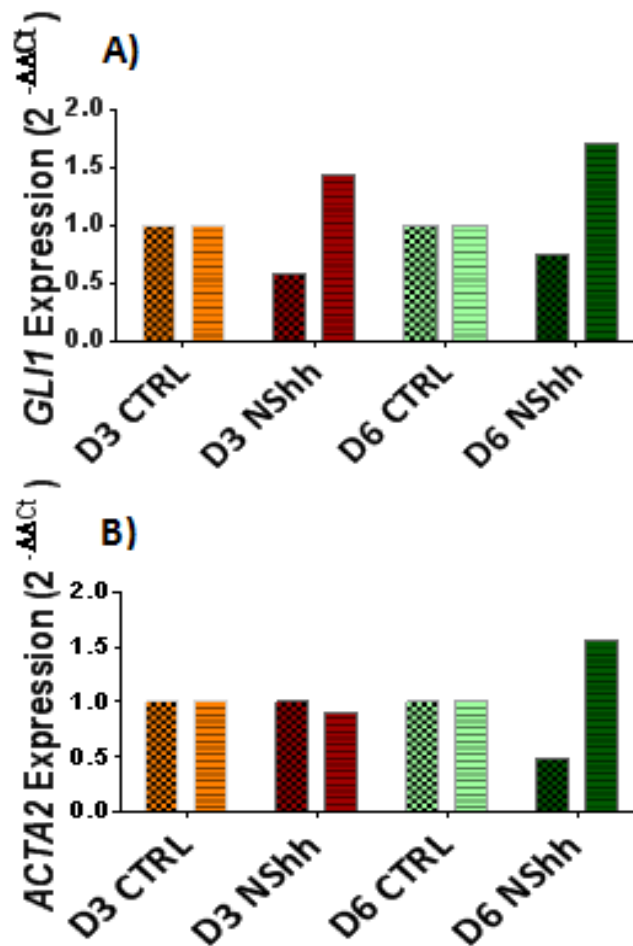


Figure 4.6 *GLI1* and *ACTA2* gene expression induction in pancreatic CAFs treated with NShh..A) *GLI1* and B) *ACTA2* gene expression in pancreatic CAFs (P5T) grown for 6 days in MSCM 5% FBS and treated with 10nM NShh. The gene expressions in treated cells was normalised to the expression observed in control samples. The treatment was renewing every 2 days during culture. The two graphs above compare the results, represented by double bars, of two well replicates performed under the same experimental conditions during the same single experiment.

GLI1 and *ACTA2* gene expression analysis did not show a response to NShh treatment at any of the time points analysed (Figure 4.6). Thus it proved difficult to show an effect of treatment on cell activation.

4.4 Investigation of the CAF responsiveness to paracrine signals in 2D co-culture and using tumour-conditioned medium (TCM)

4.4.1 TCM effect of Hh signalling pathway paracrine induction in CAFs

A TCM assay was used to further test the CAF responsiveness to Hh paracrine signalling from epithelial pancreatic cells. The principle of this assay is that epithelial cancer cells release growth factors, cytokines, and chemokines into the growth medium. This medium can then be used to investigate the effect on fibroblast cells. Evidence from the literature previously showed the validity of this assay in studies focused on the investigation of paracrine interactions between different types of cells [Karnoub *et al*, 2007; Mishra *et al* 2008; Mishra *et al*, 2009; Kurcekova *et al*, 2010]. The effect of TCM on Hh pathway activity in fibroblast cells and the responsiveness of activated cells grown in this media were therefore investigated in this section.

In order to prepare the TCM, a panel of pancreatic tumour epithelial cells expressing Shh ligand (PANC1, P308T, PAN1, BXPC3) were grown in MSCM 5% FBS for 72h, as this media supported growth of the CAF cells better than other media tested. Pancreatic CAFs (P3T and

P5T) were then cultured in those media for 3 and 14 days. Effects on Hh signalling activity was assessed by gene expression analysis of Hh target genes (*GLI1*; *PTCH1*) (Figure 4.7).

The effect on CAF activation was also assessed by measuring *ACTA2* expression. Pancreatic CAFs (P3T and P5T) showed variable Hh pathway induction and decrease (Figure 4.7). Reduced *GLI1* gene expression in P3T cells was observed after 3 days of conditioning (Figure 4.7 A). However, an increase in *GLI1* expression after BXPC3 and P308T TCM exposure was observed on day 14 in P3T cells. The same effect was observed in P5T cells grown in PAN1 TCM, although this was not confirmed by the other TCMs tested on this cell line.

The same decrease or lack of effect of TCMs was observed on *PTCH1* (Figure 4.7B) gene expression on day 3 in both cell lines included in this assay. However, again, some, but not consistent effects on *PTCH1* expression were observed on day 14 both in P3T and in P5T CAFs.

Finally *ACTA2* expression (Figure 4.8C) showed a fairly consistent increase after 14 days of exposure to P308T TCM both in P3T and P5T CAFs. However, the other TCMs tested showed variable small effects in both cell lines at both time-points.

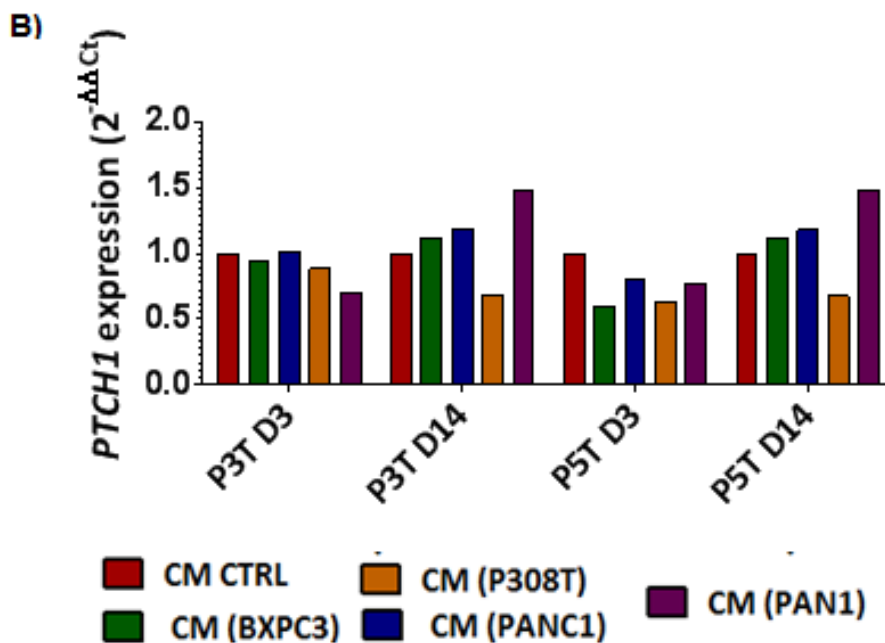
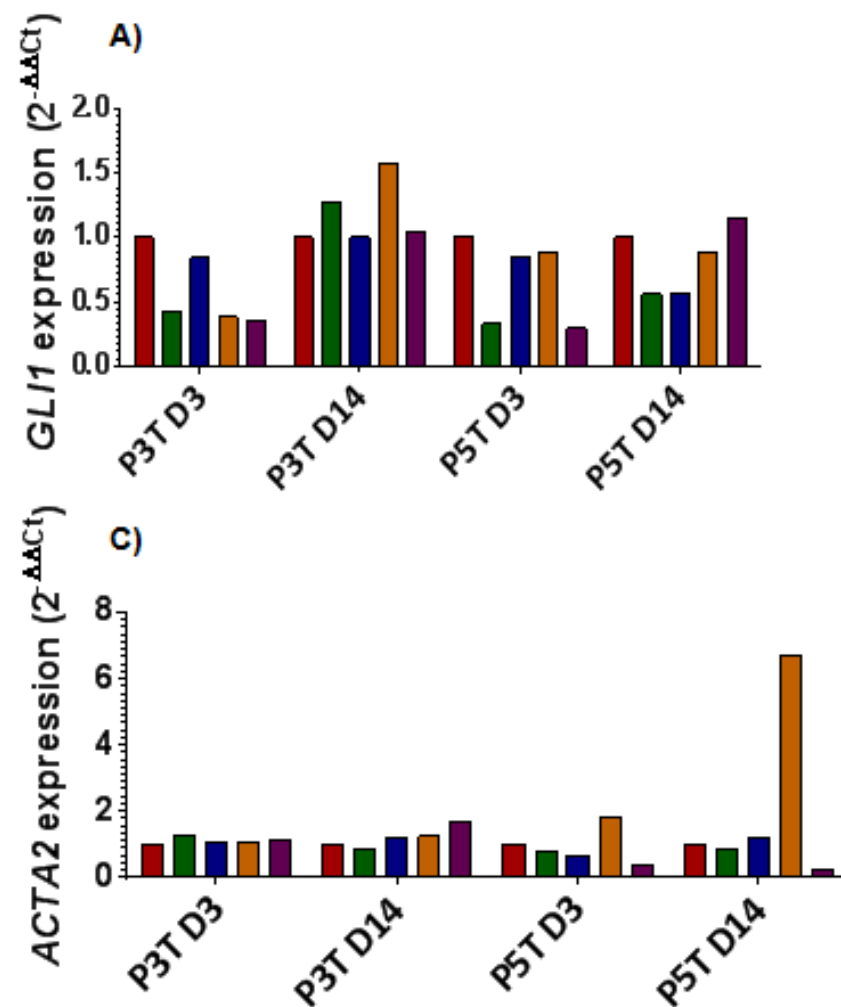


Figure 4.7 Pancreatic TCM effect on Hh pathway expression in CAFs. *GLI1* (A); *PTCH1* (B), and *ACTA2* (C) expression was investigated by PCR-RT in pancreatic CAFs (P3T and P5T) cultured for 7 and 14 days in TCM obtained by growing epithelial cancer cells (BXPC3, PANC1, P308T, PAN1) in MSCM 5% for 72h. Each bar represents the gene expression detected in CAFs grown in CM obtained from tumour cells, normalised to the sample control CM (CTRL). Each bar represents the results of one single experiment.

Summarising these results (Figure 4.7) it seemed that day 14 may be a better time point to test the effect of TCM on gene expression. However, the variability observed between the effect of different TCMs and the general small changes observed, led to use of a further approach (2D *in vitro* co-culture) to investigate Hh pathway paracrine signalling.

4.4.2 Investigation of Hh pathway paracrine induction in stromal-like cells by 2D *in vitro* co-culture assays

Direct and trans-well *in vitro* co-culture assays were chosen and performed in this study for their ability to provide continuous stimulation of the fibroblast cells by the tumour epithelial cells mixed or cultured with them. Several studies in the literature support the ability of 2D co-cultures to demonstrate reciprocal interaction between stroma and cancer cells resulting in effects on the behaviour of both cell lines. (Spaeth *et al* 2009, Kucerova *et al* 2010; Karnoub *et al* 2007)

4.4.2.1 The pancreatic CAFs responsiveness in a trans-well system.

In a first co-culture experiment primary P5T CAFs and P308T primary tumour epithelial cells (chosen for being a primary-derived cell line and so believed to better reproduce the *in vivo* context and for its relatively high expression of Shh protein, Figure 4.2) were grown in a trans-well system in order to investigate paracrine induction of the Hh signalling in CAFs. The modulation of the Hh pathway in fibroblasts after 72h of co-culture with epithelial cells was analysed *via* *GLI1* and *SMO* gene

expression normalised to their expression in control samples (fibroblasts in both compartments). *ACTA2* gene expression was also investigated.

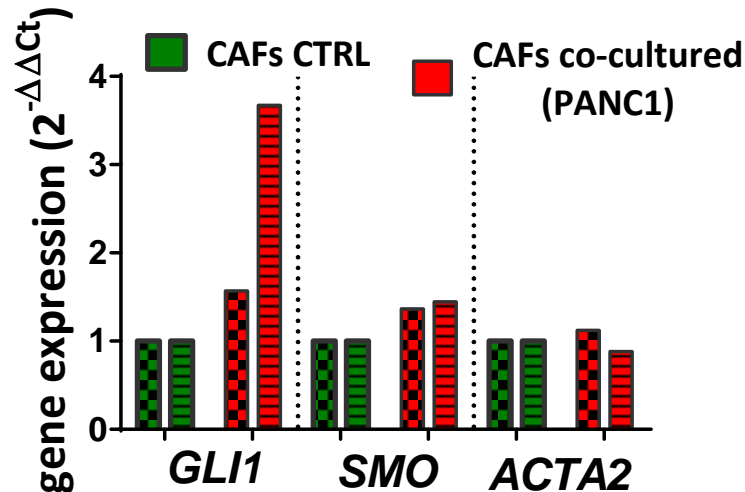


Figure 4.8 Investigation of paracrine interaction between P5T pancreatic fibroblast and P308T primary epithelial cancer cells. *GLI1*, *SMO* and *ACTA2* gene expression in P5T cells co-cultured with P308T epithelial cancer cells for 3 days. Each bar represents the gene expression detected in each of two different well repetitions (bars with same colors but different patterns) performed under each experimental condition. The gene expression detected in co-cultured samples was normalised to the gene expression detected in control samples. .

Small increases in *GLI1* and *SMO* gene expression in the CAFs was observed after trans-well co-culture (Figure 4.8) and no changes in cell activation (*ACTA2* expression) were seen in this assay.

As a next step, a new trans-well assay was performed by co-culturing pancreatic cancer (PANC1) epithelial cells (that showed the highest level of Shh protein expression in comparison to all other cell lines included in this study, Figure 4.2) with P5T pancreatic CAFs, at a range of time points in order to exclude time as a cause of no responsiveness

in the previous assay (Figure 4.8). Finally *PTCH1* Hh target gene was used to further confirm that the results observed was due to canonical Hh pathway activation and not involvement of other pathways. Since the *SMO* gene expression is not a direct target of the pathway, its detection was excluded in this and in the next assays.

Cells were plated in a 12-well trans-well plate and harvested after 2 or 5 days. *GLI1* (Figure 4.9 A), *PTCH1* (Figure 4.9 B), and *ACTA2* (Figure 4.9 C), gene expression were assessed.

Hh pathway gene targets (*GLI1* and *PTCH1*) did not show any induction in CAFs after 2 and 5 days of co-culture with epithelial cells but a decreasing effect on the pathway (*GLI1*; *PTCH1* expression reduction) was observed after 5 days. No changes of *ACTA2* expression was observed in CAFs after 2 or 5 days co-culture

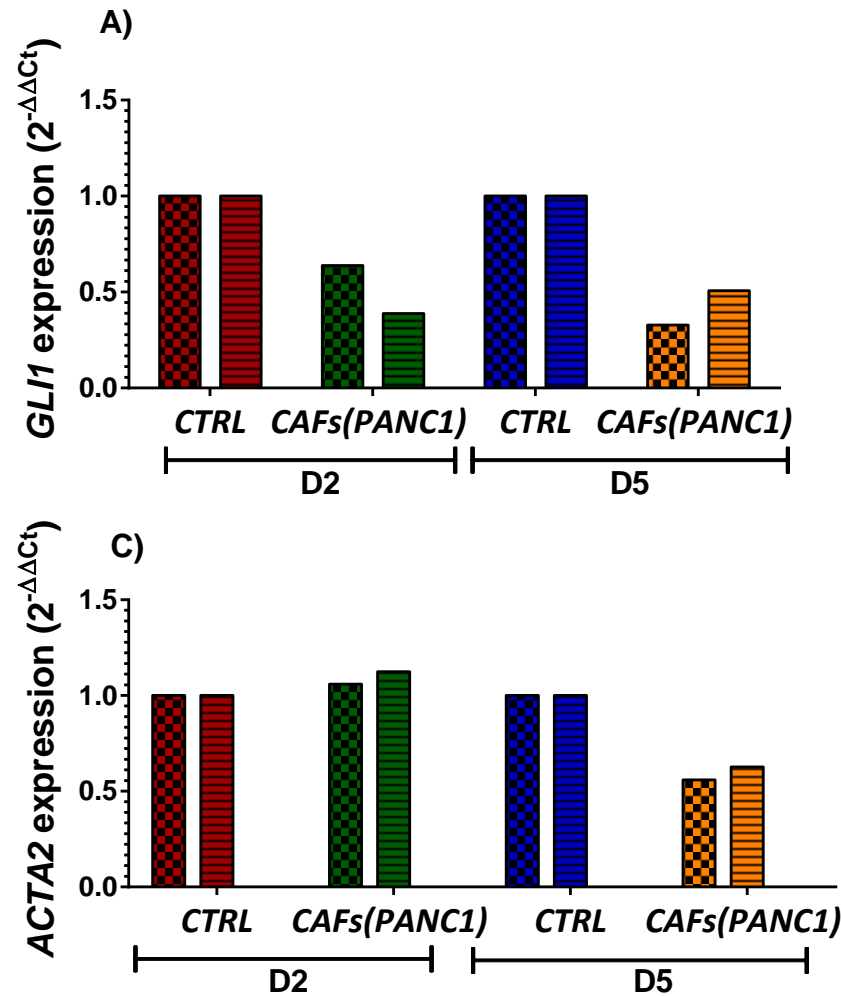


Figure 4.9 Time-course of Hh pathway paracrine induction in pancreatic CAFs. *GLI1*(A) and *PTCH1* (B) Hh signalling pathway gene targets and *ACTA2* (C) marker of cell activation expression in pancreatic CAFs (P5T). CAFs were co-cultured for 2 and 5 days with PANC1 pancreatic cancer cells and the gene expression detected in them was normalised to the gene expression in CAF control samples (CAFs co-cultured with themselves). Each double bar represents the $2^{-\Delta\Delta C_t}$ gene expression of 2 different wells performed under each experimental condition.

A final trans-well experiment (Figure 4.10) was then included to test the effect on the Hh pathway paracrine induction in CAFs of a larger panel of epithelial pancreatic cancer cells (BXPC3, PANC1 and P308T). All these cancer epithelial cells showed different levels of Shh expression at protein level (Figure 4.2), so the rationale of this experiment was to test if a ligand dose-dependent induction was visible in pancreatic CAFs. The experiment was run once by including two well repetitions under each experimental condition tested.

No consistent changes in Hh gene target expression were observed in any of the pancreatic CAFs tested (P3T Figure 4.10A and P5T Figure 4.10B) after trans-well co-culture with pancreatic tumour cells. An increase by 10 times in the *ACTA2* gene expression was observed in one of the two well repetitions after co-culture of P5T cells with BXPC3 cancer cells. However, the difference between the two well repetitions for this experimental condition was quite high (2.6 times), compromising the reliability of these data.

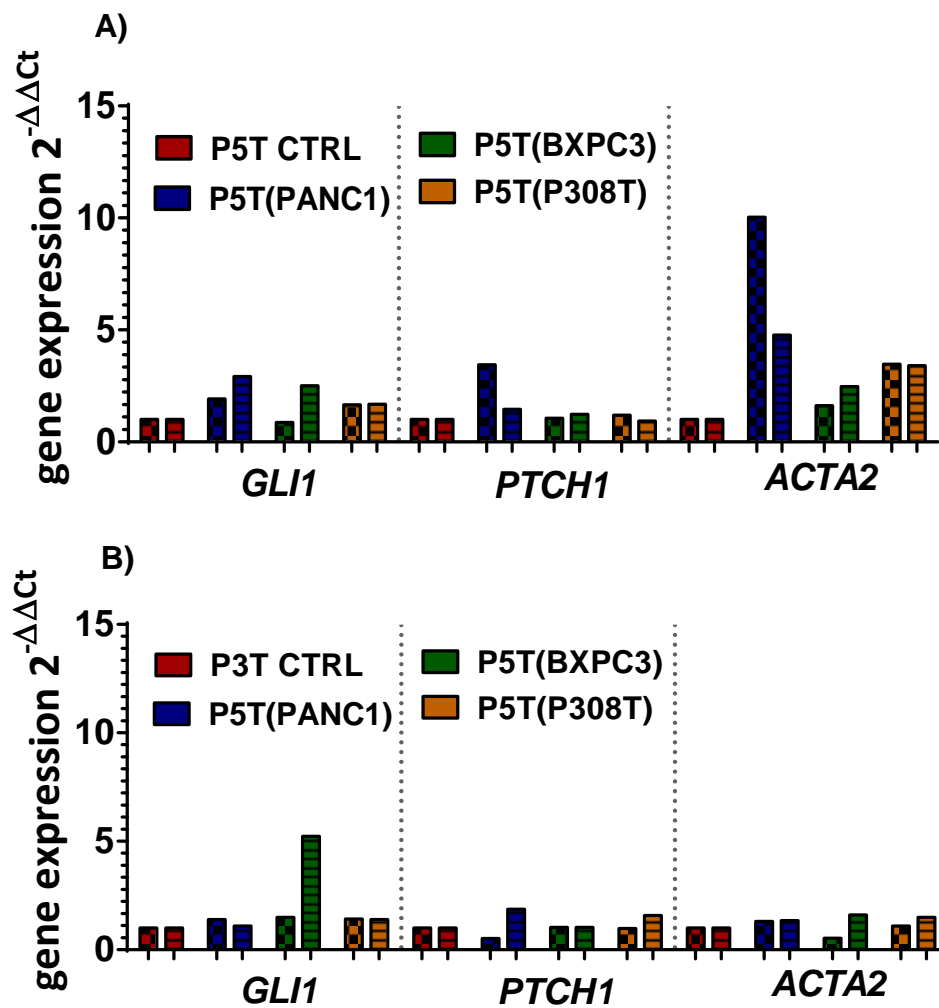


Figure 4.10 Investigation of pancreatic CAFs dose-dependent responsiveness to Hh ligands paracrine induction. *GLI1*, *PTCH1*, *ACTA2* gene expression analysis in P3T (A) and P5T (B) pancreatic CAFs after 2 days of co-culture with a panel of pancreatic cancer cells with different level of ligand expression. The gene expression of all target genes was showed for two different wells (bars with the same colours but different patterns) performed under the same experimental conditions as part of the same single experiment and was normalised to their level of expression detected in samples CTRL (CAFs co-cultured with them-selves).

4.4.2.2 The responsiveness of pancreatic CAFs in a direct co-culture system.

In order to exclude that the variability of *GLI1*, *PTCH1* and *ACTA2* expression observed in CAFs after treatment with TCM or the non-responsiveness after trans-well co-culture was not due to the absence of direct contact between CAFs and cancer epithelial cells, a direct co-culture experiment was carried out with pancreatic CAFs (P5T). After 48h co-culture, the Hh pathway was analysed in CAFs separated from epithelial cells using magnetic beads conjugated with antibodies able to bind specific fibroblast and epithelial markers expressed on the surface membrane of cells (CD90 and EpCam, respectively). *GLI1* and *ACTA2* expression increased after co-culture with BXPC3 cancer epithelial cell. However, neither *GLI1* nor *ACTA2* expression increases were consistent in the two well repetitions performed under the same conditions.

No other changes for *GLI1*, *ACTA2* and *PTCH1* expression in CAFs following co-culture with a panel of pancreatic cancer cells were observed (Figure 4.11).

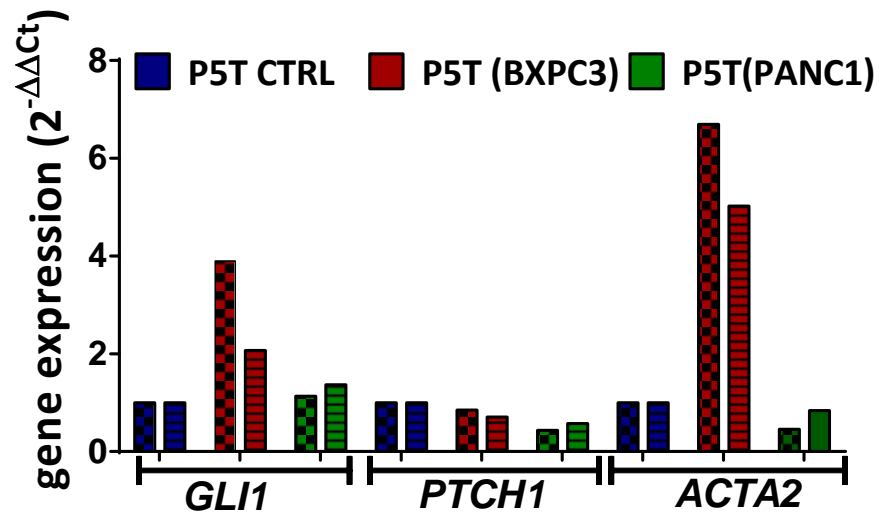


Figure 4.11 Epithelial pancreatic primary fibroblast direct co-cultures. *GLI1*, *PTCH1*, *ACTA2* gene expression analysis in P5T pancreatic CAFs after 48h of direct co-culture with pancreatic cancer cells (BXPC3 and PANC1). The gene expression of all target genes was showed for two different wells (bars with the same colors but different patterns) performed under the same experimental conditions as part of the same single experiment and was normalised to their level of expression detected in samples CTRL.

4.5 Summary of chapter

Summarising the results observed in this chapter:

- Shh gene and protein expression analysis was highly expressed in epithelial cancer cells and correlated with *CDH1* expression suggesting that cancer epithelial cells are able to secrete the Hh ligand.
- *SMO* and *PTCH2* genes and Gli1 gene and protein were highly expressed in CAFs but a background level was also observed in epithelial cancer cells. *GLI1* and *SMO* correlated with E-Cadherin (*CDH1*) but also with Vimentin and *HGF* supporting the possibility of Hh autocrine signal in cells with epithelial phenotype and a background pathway activity in fibroblast cells.
- Hh pathway expression and the cell activation detected in CAFs after NShh treatment, TCM and 2D co-culture was variable and within experimental error leading to the idea that these cells were not able to respond to paracrine stimuli *in vitro*.

This aspect and its reason will be further investigated in the next chapter.

Chapter 5 - Results: The Stem Cell Niche

5.1 Introduction

The paracrine induction of the Hh pathway investigated in CAFs in Chapter 4 showed the inability of these cells to respond to Hh exogenous stimuli. A reason for this result could be that since CAFs are already activated (high expression of α SMA) and differentiated they are not able to respond to Hh stimuli. In agreement with this hypothesis, it has been observed that Shh can promote stromal cell differentiation into myofibroblast-like cells (tested as increase of α SMA at the gene and protein levels) [Bailey *et al.* 2008; Zacharias *et al* 2011] suggesting that the cells able to respond to Hh paracrine stimuli are cells that are not fully activated or, more precisely, cells that are capable of becoming activated.

To test this hypothesis, in the first part of this chapter, the responsiveness to Hh paracrine stimuli was tested in bone-marrow derived MSCs using TCM and 2D transwell assays, since MSCs are still undifferentiated and not activated (low level of α SMA expression). Next, the effect of the medium used to grow stem cells on cell activation was investigated; to then investigate the ability of MSCs to form an *in vitro* model of the mSCN (mesenchymal stem cell niche) (a mixed population comprising MSCs and myofibroblast-like cell). In Quante *et al* 2011 the formation of this mixed population was correlated with an increase in *SHH* expression. The expression of protein Shh at the stromal level observed in Chapter 3 of this study, also suggested the need to investigate Shh as a possible marker of the mSCN in aggressive

pancreatic tumours. Finally, the mSCN as the best context for investigation of the response to Hh exogenous stimuli was examined.

A higher resolution of the IF images showed in this chapter is available in the CD version of the thesis.

5.2 Investigation of the responsiveness of MSCs to Hh paracrine stimuli

5.2.1 NShh treatment of MSCs

In order to investigate the activation of the Hh pathway in bone marrow-derived MSCs by exogenous stimuli, the cells were treated with 10nM NShh for 48h and harvested at different time points (3, 6 and 9 days). As in previous assays (Chapter 4), the Hh pathway activity was detected via *GLI1* gene expression analysis and the effect of this pathway on cell activation was tested via *ACTA2* gene expression variation (Figure 5.1).

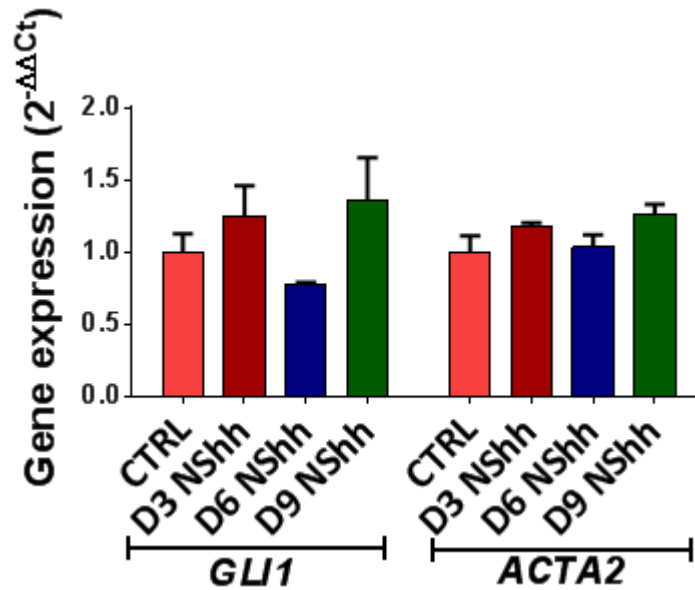


Figure 5.1 MSC responsiveness to NShh treatment.. *GLI1* and *ACTA2* gene expression in MSCs treated with 10nM NShh. Cells were harvested on day 3, 6 and 9 of culture in MSCM 5%. The treatment was refreshed every 2 days. Each bar represents the average between the gene expressions detected in cells grown in two different wells. This value in treated samples was then normalised to the gene expression in CTRL samples. A very similar trend was observed for both genes after NShh treatment.

A similar pattern of gene expression was observed after NShh treatment for both *GLI1* and *ACTA2*. *GLI1* analysis showed a fairly constant level of basal gene expression over time (data not shown) that increased, but not significantly, after NShh treatment, on day 3 and day 9 of the culture (Figure 5.1). *ACTA2* expression was also generally constant at a low level. No effect on *ACTA2* gene expression was as well observed following NShh treatment (Figure 5.1).

In order to further investigate the correlation between *GLI1* and *ACTA2* gene expression, MSCs were cultured for up to 21 days and *ACTA2* and *GLI1* gene expression monitored at different time points. Considering the previous results (Figure 5.1) NShh treatment was not

included on this occasion. This experiment was repeated twice and the average of the results of two experiments is showed in Figure 5.2.

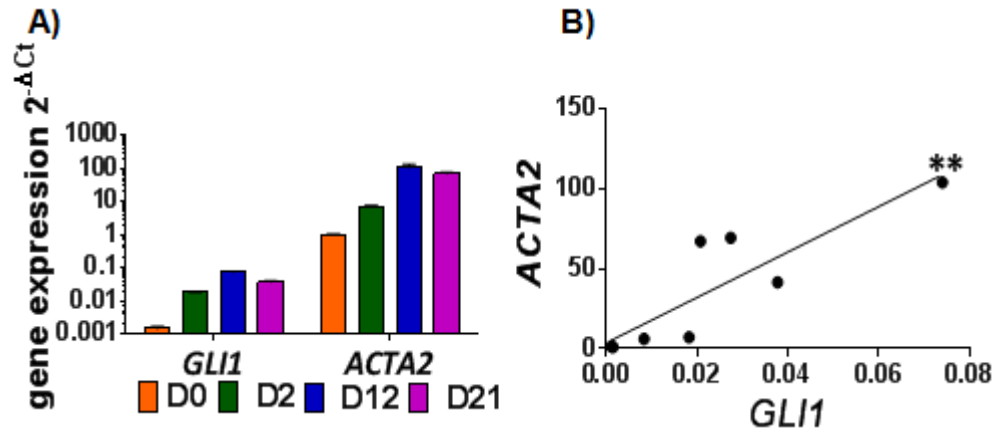


Figure 5.2 *GLI1* expression correlated with *ACTA2* gene expression.

A) *GLI1* and *ACTA2* expression in MSCs cultured for 21 days. Each bar represents the average value between two experiments. No significant differences in *GLI1* and *ACTA2* expression were observed between different time points (1 way ANOVA) B) Significant correlation ($p < 0.01$) (Pearson correlation test) of *GLI1* and *ACTA2* gene expressions over time.

The *GLI1* and *ACTA2* expression measured in this assay (Figure 5.2) showed a similar trend over time and the correlation analysis showed a significant value (Pearson $P < 0.01$), confirming the relationship between these two genes and suggesting a possible interaction between the Hh pathway and cell activation which will be further investigated.

5.2.2 Effect of TCM on Hh paracrine activation in MSCs

Using the same approach used for pancreatic CAFs (chapter 4), the effect of tumour-conditioned medium on Hh pathway paracrine induction was analysed in MSCs to investigate if they are more responsive since they are less activated and differentiated.

TCM was prepared by growing a panel of epithelial cancer pancreatic cells (BXPC3, P308T, PANC1, and PAN1) for 72h in MSCM 5%. In parallel, a conditioned medium (CM) to be used as control (CTRL) was prepared by growing MSCs under the same condition as epithelial cancer cells for 72h. All media were then used to grow MSCs for 3 and 14 days. MSCs with different passage numbers (P5 and P11), which should have different levels of activation, were used. It is in fact believed that MSCs tend to become activated and produce myofibroblast-like cells (increase of α SMA) over the culture. [Quante *et al* 2011]. Hh pathway activity was detected via *GLI1* and *PTCH1* Hh pathway gene expression and changes in cell activation were identified via *ACTA2* gene expression analysis (Figure 5.3).

The analysis of *ACTA2* showed low and no consistent effect of TCM in the induction of cell activation (Figure 5.3 C).

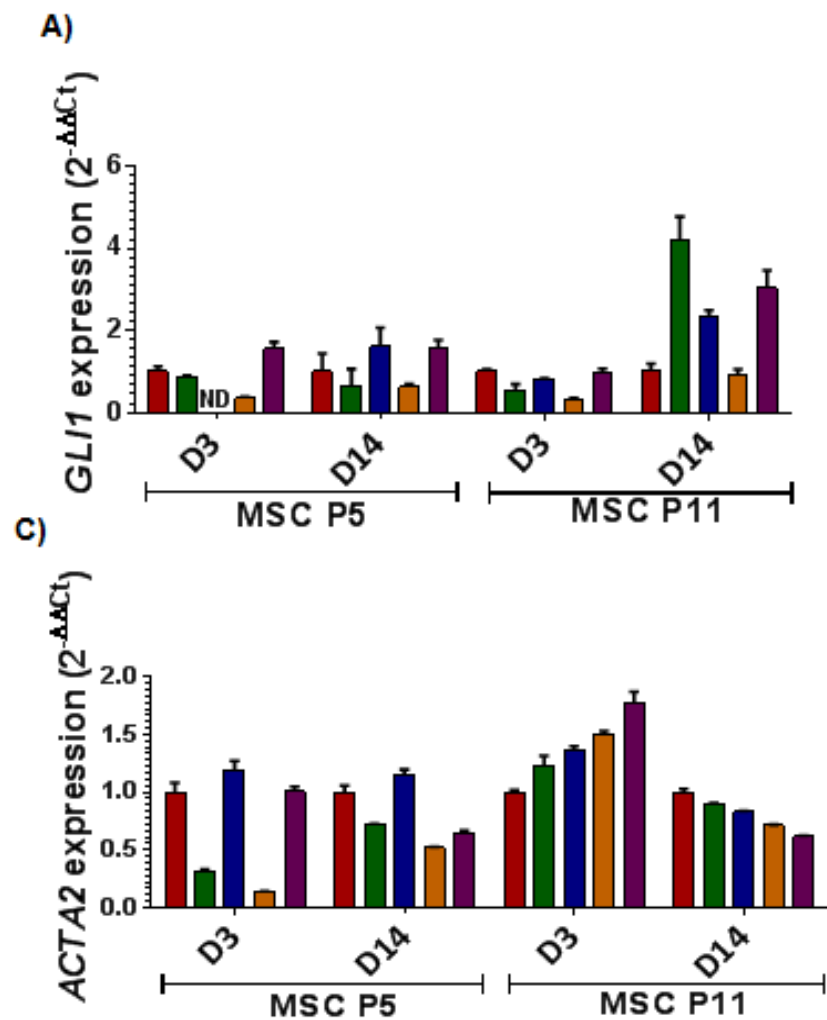


Figure 5.3 Effect of pancreatic tumour conditioned medium (CM) on Hh pathway expression in MSCs. *GLI1* (A), *PTCH1* (B), *ACTA2* (C) gene expression analysis in MSCs grown for 3 and 14 days in TCM prepared from a panel of epithelial pancreatic cancer cells (BXPC3, PANC1, P308T, and PAN1). Each gene expression detected in each sample was normalised to the sample control (MSCs grown in Control TCM). Each bar represents the gene expression detected in one single experiment. ND: not detected value (below detection limit).

GLI1 and *PTCH1* Hh gene expression in MSCs after 3 and 14 days of culture showed low (<2) and inconsistent (increase and decrease) changes in the gene expression in comparison to the sample control (Figure 5.3 A, B) and so it was difficult to consider these changes a consistent result. However, a strong increase in *GLI1* gene expression was observed in MSC P11 after 14 days of tumour (BXPC3, PANC1 and PAN1) conditioning (Figure 5.3 A) suggesting that MSCs are able to respond to paracrine stimuli following long exposure to Hh ligand. The analysis of *ACTA2* showed low and no consistent effect of TCM in the induction of cell activation (Figure 5.3).

From the above, the only MSCs responsive to the stimuli were the late passage MSCs (P11) expected to be the cells with higher *ACTA2* expression. However these two cells lines (earlier and later passages) came from different batches and so their level of *ACTA2* was not directly comparable as MSCs originating from different human patients even if at the same passage number in culture, could have different levels of activation. Actually, whereas CAFs were believed to be completely activated (figure 4.4) and so with maximal *ACTA2* expression, the activation of MSCs could be induced by a number of factors and so may change over time in culture. This aspect means that use of the same MSCs, grown in the same media and harvested at different passages, essential for a direct comparison between the level of cell activation at low and later passages. For this reason, the ability of MSCs to differentiate and increase *ACTA2* over time in culture, a comparison between early and late passages of MSCs from the same

batch of cells was performed and the effect of *ACTA2* expression on cell responsiveness to exogenous signals was taken into consideration. MSCs were grown in this assay (Figure 5.4) for 14 days considering the fact that this was the time point in which an effect on *GLI1* expression was observed previously (Figure 5.3).

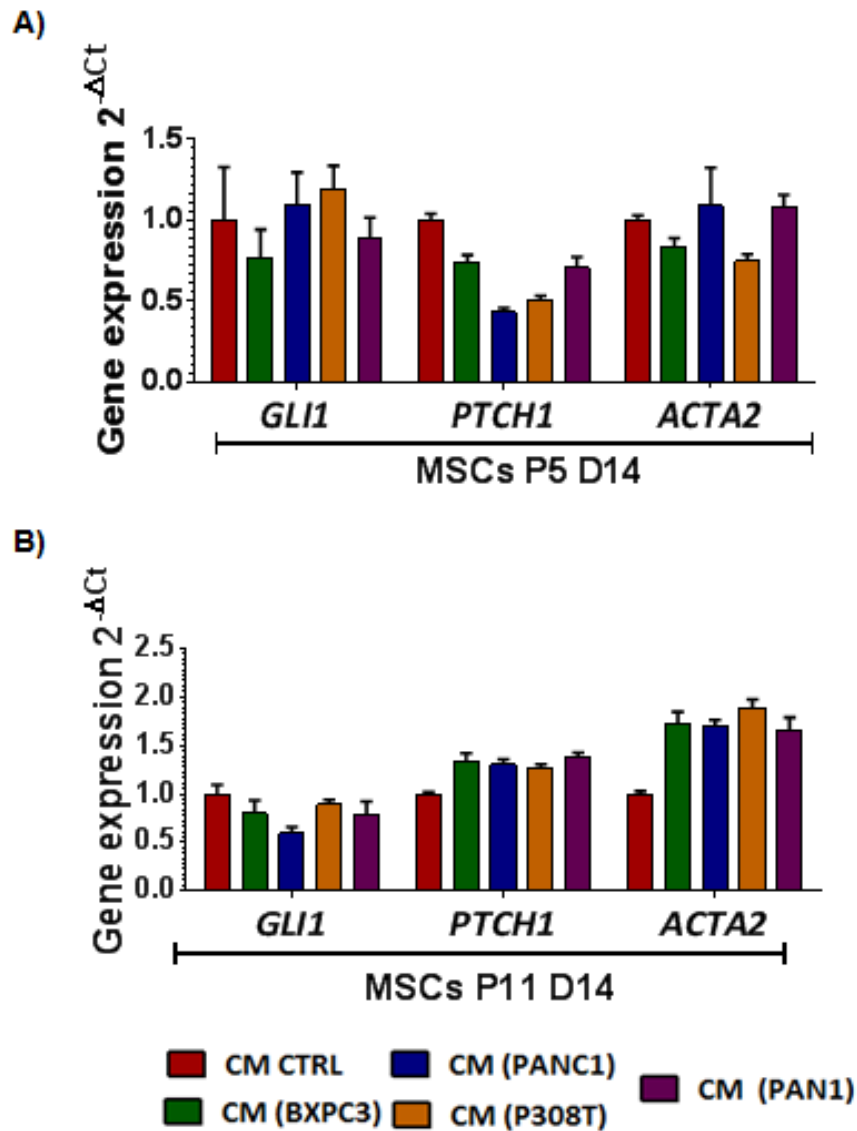


Figure 5.4 MSCs passage effects on Hh pathway paracrine responsiveness to TCM stimuli. *GLI1*, *PTCH1*, *ACTA2* gene expression analysis in MSCs at earlier (P5) (A) and later passages (P11) (B). MSCs were grown in TCM obtained from pancreatic tumour cells (BXPC3, PANC1, P308T, PAN1) for 14 days. Each bar represents the gene expression detected in one single experiment.

The analysis of *PTCH1* gene expression in MSCs of higher passage grown in pancreatic TCM for 14 days seems to suggest some induction of the Hh pathway (Figure 5.4). However, the size of the changes in gene expression observed in this assay is still too low to be considered reliable and moreover, *GLI1* gene expression analysis did not confirm the induction observed in the previous experiment (Figure 5.3), suggesting that these experimental conditions are not suitable for demonstrating paracrine induction in MSCs.

5.2.3 Effect of 2D transwell co-culture on Hh paracrine activation in MSCs

In order to further investigate the responsiveness of MSCs to Shh ligands and to allow a direct comparison with the CAF assays performed in chapter 4, MSCs at earlier and later passages from the same batch were grown in a trans-well co-culture assay with a panel of pancreatic epithelial cancer cells (BXPC3, P308T, PANC1), previously characterised for Shh gene and protein level (Figure 4.2). The data were normalised to the sample control (mesenchymal cells grown in trans-well with other MSCs) (Figure 5.5).

No paracrine induction of Hh pathway gene targets (*GLI1*, *PTCH1*) was observed in most of the cell-lines tested after 3 days (chosen because is the time point when maximum confluence is reached for the cells in the insert) of co-culturing (Figure 5.5) suggesting no responsiveness of these cells in these experimental conditions. *ACTA2* gene expression remained stable in all co-cultures performed (Figure 5.5).

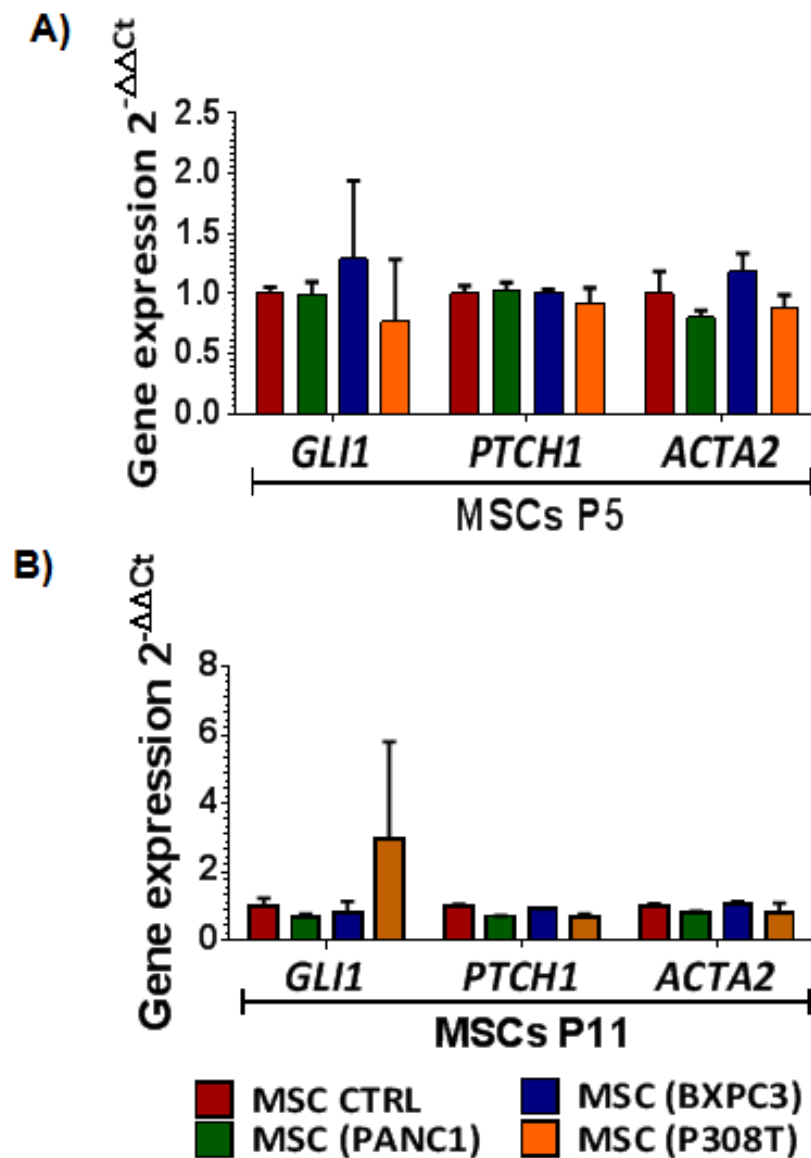


Figure 5.5 MSCs passage effects on paracrine responsiveness to Hh pathway stimuli in 2D co-culture.. *GLI1*, *PTCH1*, *ACTA2* gene expression analysis in MSCs at earlier and later passages, co-cultured in a trans-well system with a panel of pancreatic epithelial cells (PANC1, BXPC3, P308T) with different levels of Shh gene and protein expression. Each bar represents the average between the gene expressions detected in two replicated wells. No significant differences in *GLI1*, *ACTA2* and *PTCH1* expression were observed between co-cultured samples and CTRL sample (Kruskal-Wallis test).

In summary, NShh, TCM and 2D co-culture assays showed some MSC responsiveness, but only after 14 days of stimulation. An explanation of these results could be that the medium used to carry out all these assays, designed to culture stem cells, tends to maintain the MSCs in an inactivated and undifferentiated phenotype, but occasionally at later time points it could happened some level of activation. This could also be the reason for the variability and difficulty to see responsiveness to Hh exogenous stimuli in MSCs even if more responsiveness in general was seen with MSCs compared to CAFs.

5.3 Investigation of the effect of different media on MSC activation and Hh pathway activation

Based on the above results, MSCM 5%, previously used in all assays for the investigation of stromal-like cell responsiveness to Hh ligands, was tested for its ability to prevent cell activation. In order to test this hypothesis a comparison between the α SMA gene and protein expression in MSCs at low passage (and so still able to differentiate) cultured in MSCM 5% and in a new free-differentiation medium was performed. The new medium selected to grow the MSCs in this assay was PCA (DMEM medium with 20% FBS), chosen for its high percentage of FBS, that should encourage the cell activation and differentiation (this is an example of a "free differentiation medium"). α SMA gene and protein expression was then analysed over time in MSCs grown in PCA medium and compared with that in MSCs grown in MSCM and harvested at the start of the experiment (sample control) (Figure 5.6).

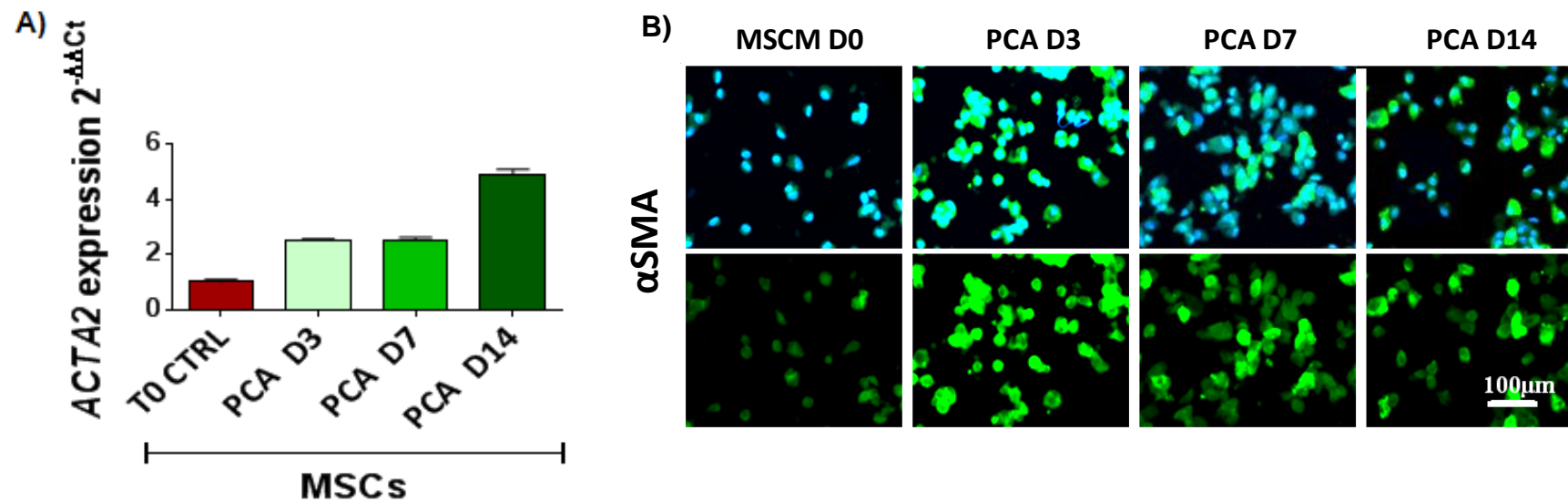


Figure 5.6 Gene and protein expression analysis of α SMA in MSCs cultured in free differentiation medium. . A) *ACTA2* expression analysis in MSCs grown for 3, 7 and 14 days in DMEM 20% FBS (PCA medium), normalised to the gene expression detected in MSCM at the start of the experiment. Each bar represents the gene expression detected in one single experiment. B) Protein expression analysis of α SMA in MSCs grown in MSCM and harvested on day 0 of experiment and after 3, 7 and 14 days in PCA medium. Squares on top: blue staining represent cells nuclei stained with DAPI and green staining represent α SMA expression. Squares on the bottom: α SMA protein expression without combined DAPI staining.

Interestingly, after 3 days *ACTA2* gene expression increased in MSCs grown in the PCA medium 2.5 fold. No further changes were detected after 7 days. After 14 days it increased an additional 2.5 times (total 5 times) (Figure 5.6A) indicating their activation in comparison to the control sample. Protein expression of α SMA (Figure 5.6 B) confirmed the increase of the population of activated cells in PCA media. Moreover, immunofluorescence images on day 3, 7 and 14 suggests that despite a peak of 80% α SMA⁺positive cells (myofibroblast-like population) on day 3, that dropped off at later time points (50% and 40% on day 7 and 14 respectively), the mesenchymal stem cell α SMA negative cells survive over time (day 7, day 14) resulting in a mixed population.

To further investigate the effect of MSCM (preventing differentiation medium) in maintaining MSCs in an undifferentiated or inactivated state, a direct comparison of the effect of different media on α SMA gene and protein expression was carried out with all cells cultured in each media (including the medium control MSCM 5% FBS) for the same number of days.

The cells were harvested at time 0 of the experiment after being grown in MSCM for 3 days and then split and grown in the following media: PCA medium (DMEM 20% FBS); DMEM 0.5% FBS; MSCM 5% FBS and MSCM without GF (thought to induce stem cell self-renewal) but containing 5% FBS (MSCM no GF). Cells were tested for the effect on cell activation after 72h of culture (time point already demonstrated to be able to induce stem cell activation). The media effect on cell

activation was, as previously, tested via α SMA protein and gene expression analysis (Figure 5.7). The aim of this experiment was to test if MSC cells would remain undifferentiated in MSCM, while an increase of α SMA expression in all DMEM media and probably in MSCM with no GF added (all considered free differentiation media) was anticipated.

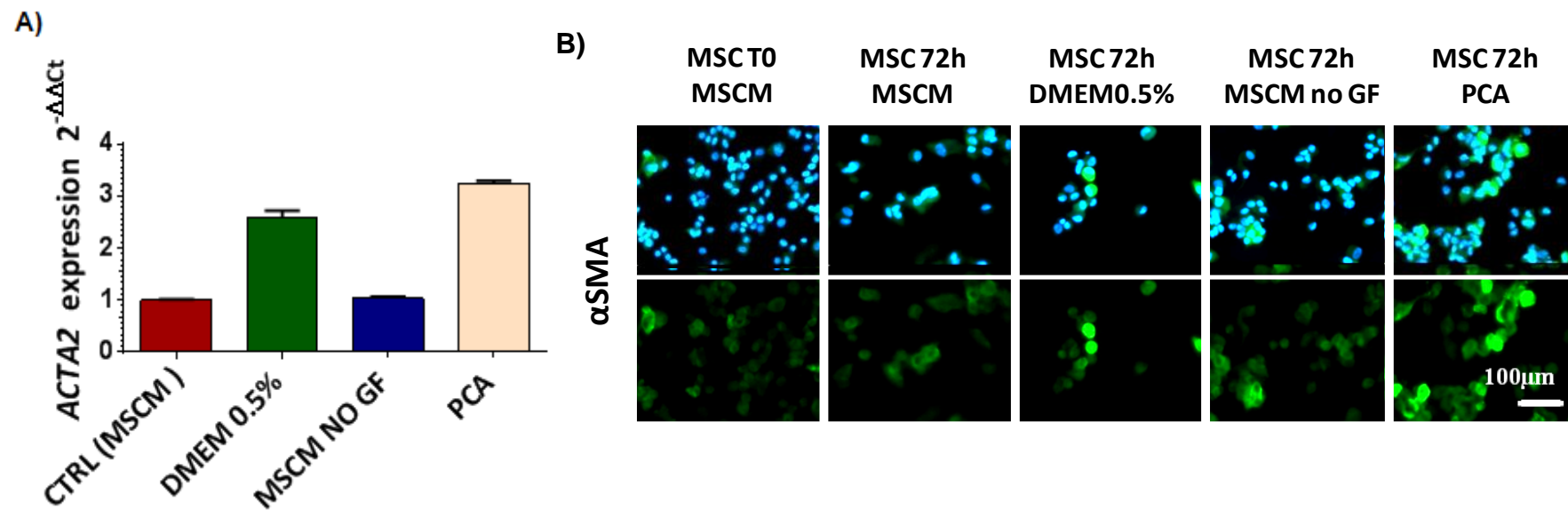


Figure 5.7 MSCM prevented the activation of MSCs over time.. A) *ACTA2* expression in MSCs grown for 72h in different media with different percentage of FBS (MSCM 5% FBS, DMEM 0.5% FBS, MSCM no GF 5% FBS, PCA 20% FBS). Each bar represents the results of one single experiment. B) α SMA protein expression in MSCs grown for 72 h in the same media of Figure (A). Top row: MSCs with nuclei stained with DAPI (blue) and α SMA stained in green. Bottom row: same images without DAPI staining.

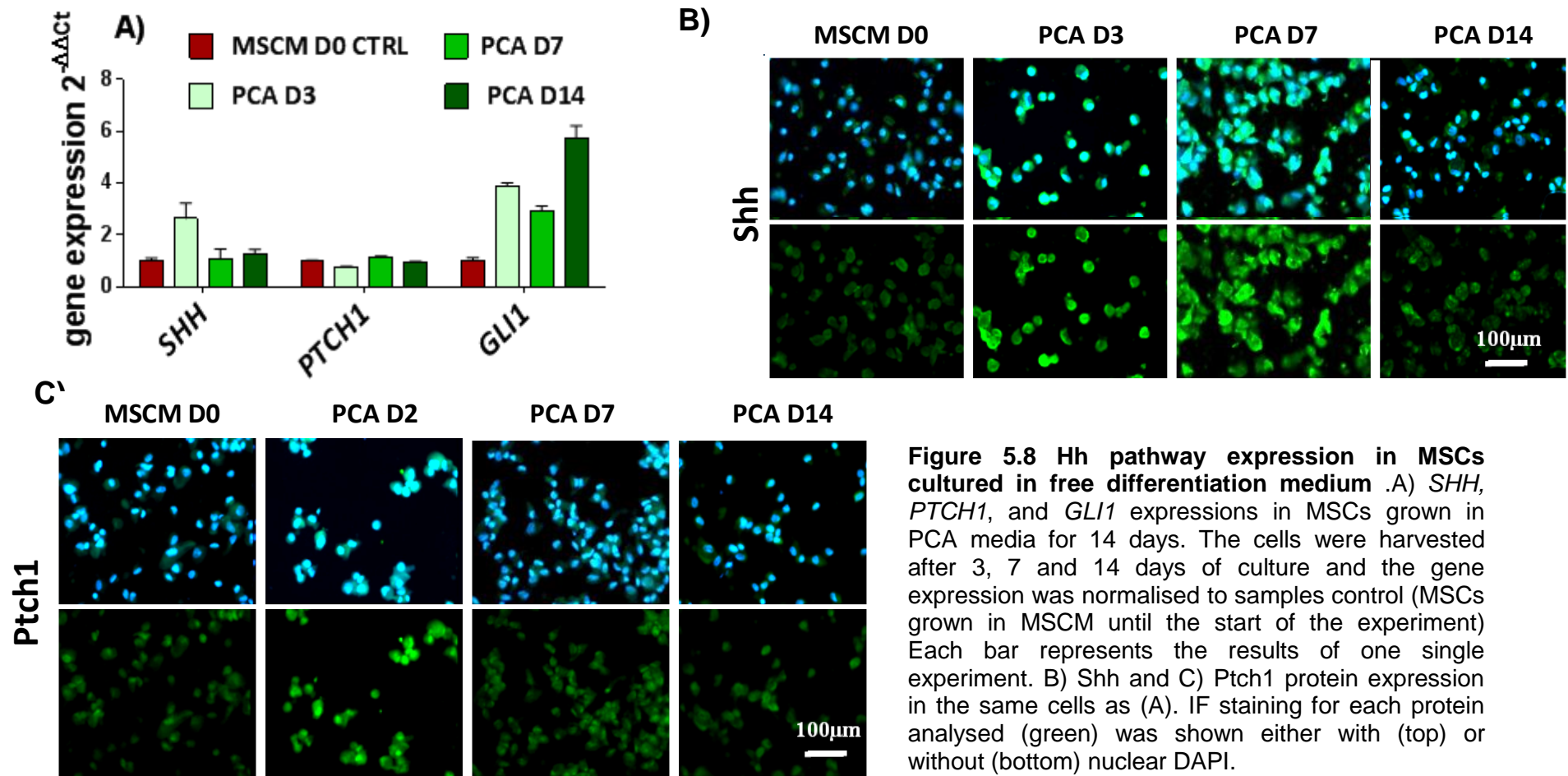
ACTA2 gene and protein expression (Figure 5.7 A and B) increased in all media considered “free differentiation medium” (2.5 times in DMEM 0.5% and 3.2 times in PCA media) in comparison to cells grown in MSCM and MSCM with no GF for 72h. This result seems to suggest no role for the growth factors normally added to MSCM in preventing cell differentiation. Moreover, no increase in α SMA protein expression was observed after 72h of MSCs cultured in MSCM and MSCM with no GF in comparison to MSCs harvested from MSCM at day 0 of culture (Figure 5.7B). These data strongly suggest that MSCM slow down the activation of MSCs that, when free to differentiate, tend to form a mixed population.

5.3.1 *In vitro* investigation of Hh pathway in MSCs cultured in “free differentiation” medium

In order to investigate the role of the Shh ligand expression in the stromal context observed in chapter 3 and to further investigate the relationship between the Shh pathway and cell activation, Shh, Ptch1 and Gli1 expression were investigated in MSCs grown for 14 days in PCA medium. *GLI1* expression increased in PCA medium (Figure 5.8 A), supporting the idea that Hh pathway activation increases in parallel with the increase of myofibroblast-like cell differentiation. Moreover, the *SHH* expression showed an increase of 2.6 times after 3 days of culture in PCA medium in comparison to the level of gene expression detected in cells grown in MSCM (Figure 5.8A). Consistent with gene expression analysis, Shh protein expression increased on day 3 (80% Shh positive

cells) and, as for α SMA protein expression (Figure 5.6B), dropped again after 7 (60% Shh positive cells) and 14 (40% Shh positive cells) days (Figure 5.8B).

In this assay, Ptch1 expression was also investigated at the protein level as further confirmation of the results observed. From this analysis (Figure 5.8C) a similar trend for Ptch1 protein expression to that observed for the Shh protein expression trend was observed (Figure 5.8B). An important aspect of this result is that Ptch1 gene and protein expression do not match. This apparent inconsistency of results could be a consequence of the negative feedback that Ptch1 exerts on the Hh pathway [Goodrich *et al* 1999]. Therefore, in future experiments protein expression rather than gene expression was measured as a more reliable indicator of Hh pathway activity.



The Hh pathway was also studied in the MSCs cultured in free differentiation media (Figure 5.9) previously tested for α SMA expression (Figure 5.7).

Interestingly *SHH* gene expression increased in DMEM 0.5% reinforcing the idea that it was expressed when a myofibroblast-like population was present. However, no increase was observed at the gene level in PCA medium (Figure 5.9A). *GLI1* expression (Figure 5.9B), as confirmation of Hh pathway activation when myofibroblast-like cells were present, increased in free-differentiation media (DMEM 0.5%; PCA) as well as in MSCM no GF confirming the results achieved so far. Moreover, consistent with the gene expression analysis, Shh (Figure 5.9 C) and Ptch1 (figure 5.9D) protein were highly expressed (80% of Shh positive cells) in free differentiation media (DMEM 0.5%; PCA and MSCM no GF) in comparison to MSCM.

In summary, the above data suggest a tendency for MSCs to become myofibroblast-like activated cells (α SMA increase). Moreover, expression of the Shh signalling pathway seems to occur when the myofibroblast-like population forms.

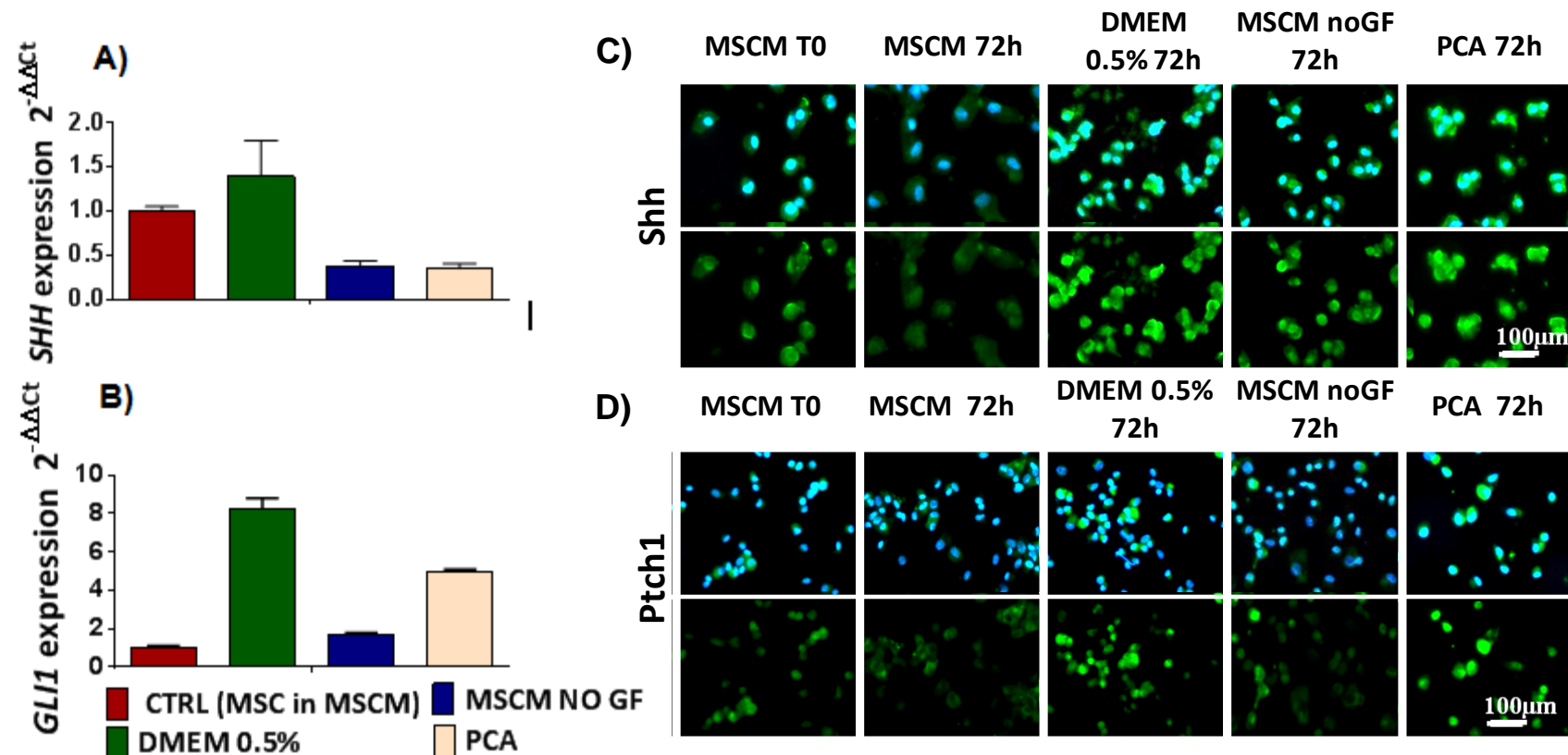


Figure 5.9 Media effect on Shh signalling pathway expression in MSCs.. *SHH* (A) and *GLI1* (B) expression in MSCs grown in DMEM 0.5% FBS, MSCM 5% FBS, MSCM no GF 5%, PCA 20% FBS media for 72h. The gene expression was normalised to samples control (MSCs grown in MSCM for 72h from the start of experiment). Each bar represents the results of one single experiment. Shh (C) and Ptch1 (D) protein expression in MSCs grown in MSCM 5% FBS and harvested at the start of the experiment, and also grown for 72h in MSCM 5% FBS, DMEM 0.5% FBS, MSCM no GF 5% FBS and in PCA medium. IF staining for each protein analysed was shown either with (rows on top) and without (bottom rows) nuclei stained in blue with DAPI.

5.4 Investigation of the effect of TGF- β on the differentiation of MSCs and Hh pathway expression

The role of TGF- β in the acquisition of a myofibroblast-like phenotype either as a result of MSC differentiation or EMT has been shown in the literature demonstrating the importance of this factor in the tumour context and in its progression [Hu *et al* 2003; Bardeesy *et al* 2006].

Therefore, the role of TGF- β function in stimulating MSCs to differentiate into myofibroblasts and the consequent effects on Hh pathway activation was analysed.

5.4.1 TGF- β effect on MSC activation

Initially, MSCs grown in PCA media (DMEM 20%) for 14 days were treated with TGF- β (10 ng/ml), with treatment refreshed every 2 days. As controls, MSCs were grown in PCA medium without any TGF- β treatment. *ACTA2* gene expression detected in treated samples was normalised to the gene expression in samples control (untreated cells). The cells were harvested and analysed for α SMA gene and protein level on day 3, day 7 and day 14 (Figure 5.10).

In this experiment, *ACTA2* expression increased after the treatment suggesting MSC responsiveness to TGF- β treatment (Figure 5.10A). However, α SMA protein expression analysis did not confirm the induction observed at the gene level (Figure 5.10B). This discrepancy could be due to the fact that often changes in gene expression require more time to be visible at the protein level.

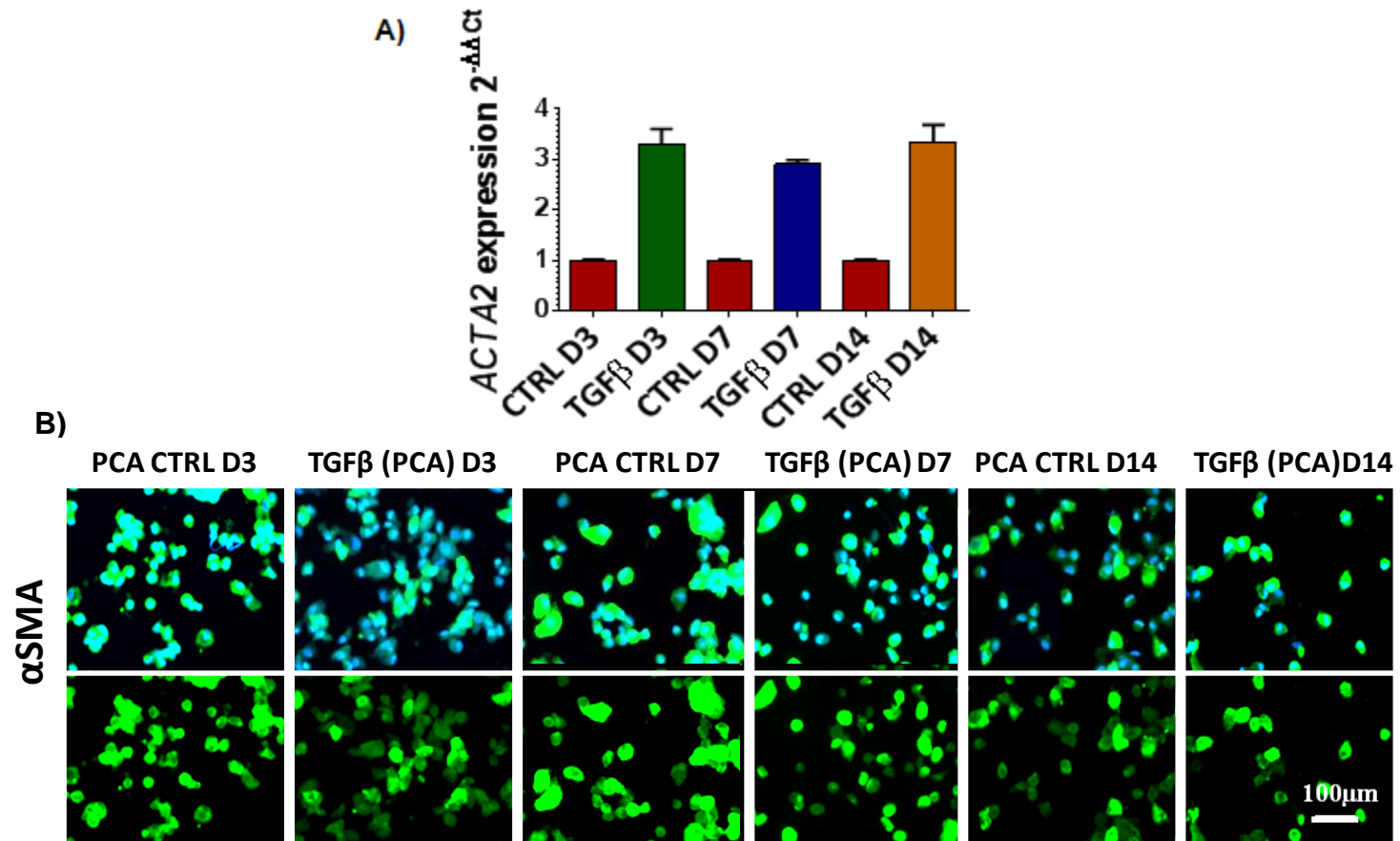


Figure 5.10 Effect of TGF- β on MSCs activation in PCA free differentiation media.. α SMA gene (A) and protein (B) expression in MSCs grown in PCA medium and harvested after 3, 7, 14 days of culture. Gene expression in treated samples were normalised and compared respectively to the samples control (untreated cells harvested on day 3, 7 and 14 of the culture). Each bar represents the results of one single experiment. IF staining was shown with (top row) and without (bottom row) blue nuclei stained with DAPI.

To test the effect of FBS concentration on TGF- β responsiveness, MSCs (same cells used in Figure 5.7) were treated with 10 ng/ml TGF- β in different media with different percentages of FBS (DMEM 0.5%FBS; PCA; MSCM 5% FBS; MSCM 5% FBS with no GF).

Higher α SMA expression both at the gene and protein level was observed in TGF- β treated samples when grown in free differentiation media (DMEM 0.5%; PCA) and in MSCM with no GF, in comparison to control samples (untreated cells grown in the same media), confirming the role of TGF- β in the induction of myofibroblast-like differentiation (Figure 5.11 A and B). Finally, immunofluorescence images suggest a more homogeneous population of α SMA positive cells (80-90% in both FDM) than the population observed in the controls suggesting a role of TGF- β treatment in pushing inactivated cells to an activated state resulting in a single, activated population rather than a mixed population (Figure 5.11B).

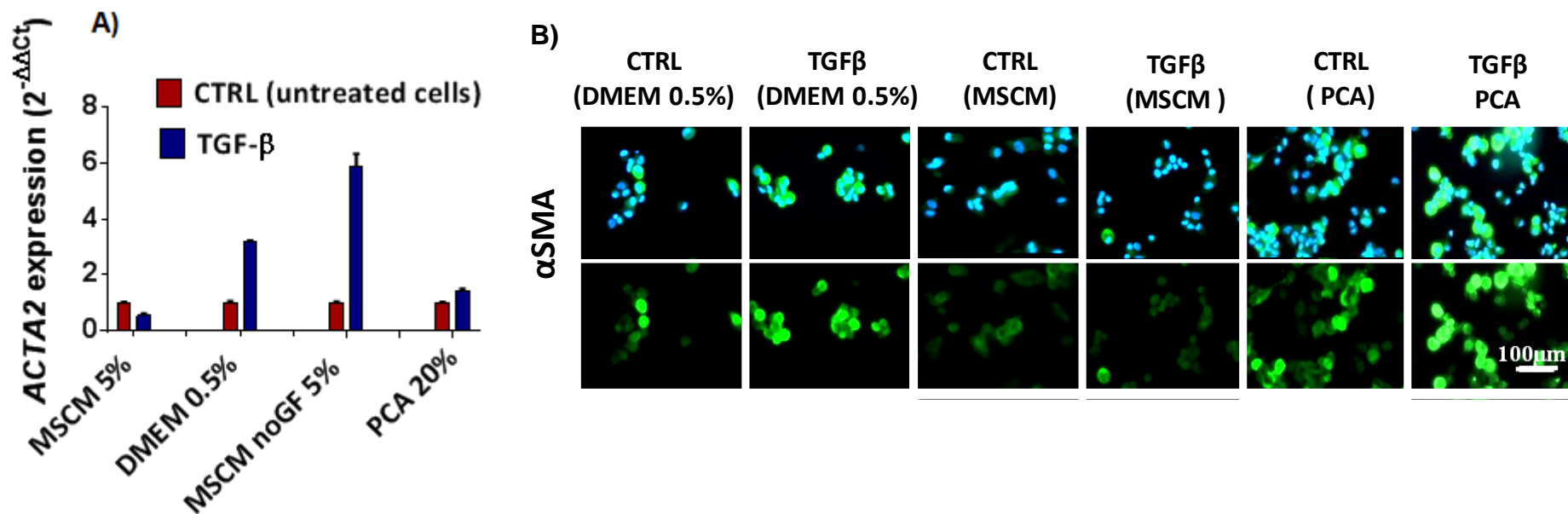


Figure 5.11 Different media effect on TGF-β treatment of MSCs.. αSMA gene (A) and protein expression (B) in MSCs grown for 72h in DMEM 0.5% FBS; PCA; MSCM 5% FBS; MSCM 5% FBS with no GF (only gene expression analysed). In figure (A) treated samples were normalised and compared to the sample controls (untreated cells grown for 72h in all media tested). Each bar shows the results of one single experiment. IF staining was shown with (top row) and without (bottom row) blue nuclei stained with DAPI.

5.4.2 TGF- β Effect on the Hh pathway

In order to investigate the TGF- β effect on the Hh pathway, Shh gene and protein expression and Ptch1 protein expression were investigated in MSCs grown for 3, 7 and 14 days in PCA medium and treated with 10 ng/ml TGF- β , and in MSCs grown in different media with different percentage of FBS (DMEM 0.5% FBS, PCA, MSCM 5% FBS, MSCM with no GF) treated with the same concentration of TGF- β (10ng/ml) as above. The MSCs included in both these assays were the same ones used in sections 5.2 and 5.3.1.

The aim of this analysis was to investigate the role of TGF- β in the promotion of Shh gene and protein expression and its downstream Hh gene pathway activity (*GLI1*, *PTCH1*), and provide information on the correlation between α SMA positive cells and Shh expression under the effect of TGF- β treatment.

SHH gene expression in MSCs grown in PCA medium (Figure 5.12A) showed a small increase after 3 days of culture, but in general, a reduction in expression was observed both for Shh at gene (Figure 5.12 A) and protein (Figure 5.12 C) expression and Ptch1(Figure 5.12 D) at protein expression on day 7 and 14. These results seem to suggest an inhibitory effect of TGF- β on Hh pathway. Interestingly, *GLI1* gene expression (Figure 5.12 B) showed an independent trend very similar to *ACTA2* gene expression (Figure 5.10 A).

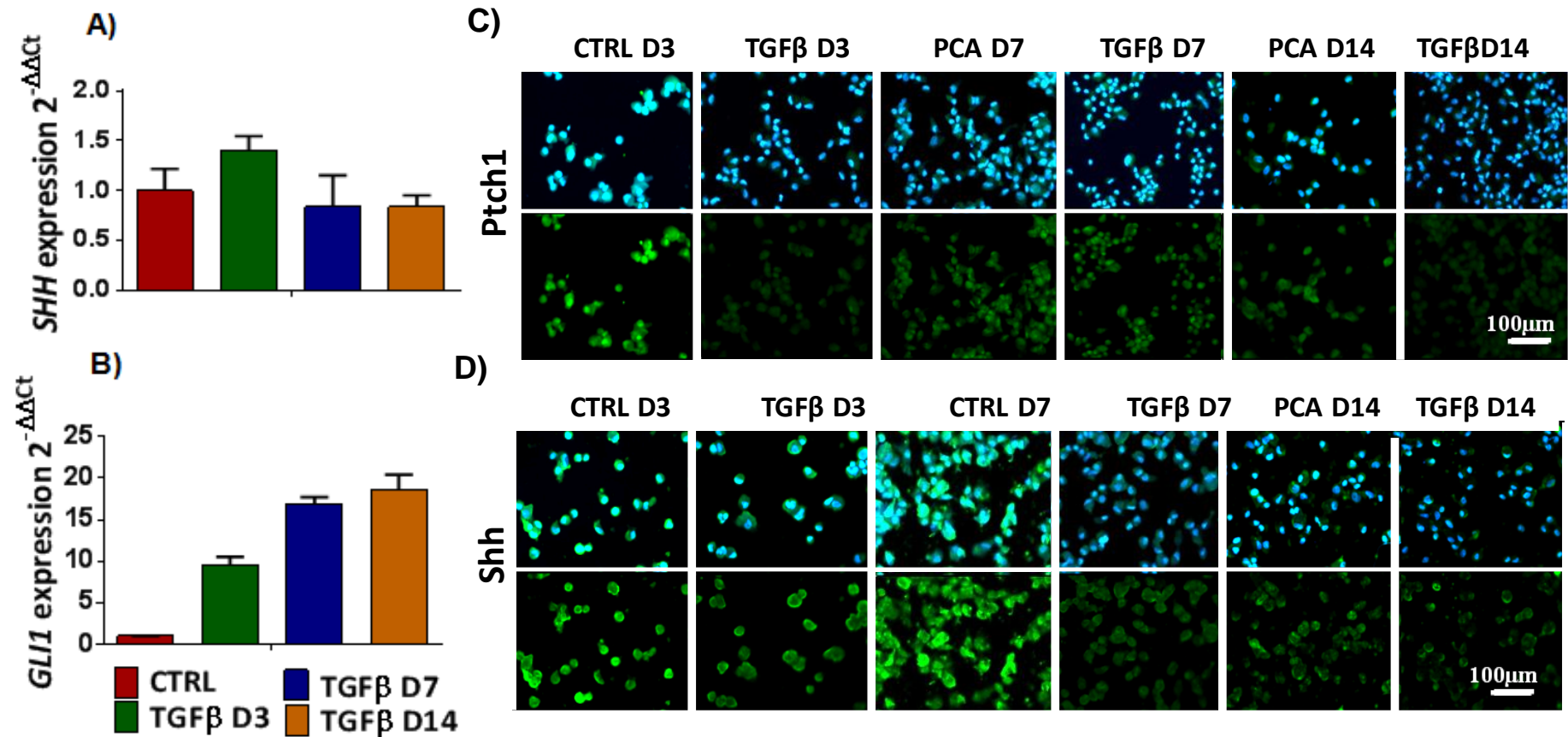


Figure 5.12 Effect of TGF- β treatment on Hh pathway expression in MSCs cultured in PCA free differentiation media.. *SHH* (A), *GLI1* (B) expression in MSCs grown in PCA medium for 3, 7 and 14 days. Gene expression in treated samples was normalised and compared respectively to the samples control (untreated cells harvested on day 3, 7 and 14 of the culture). *Shh* (C) and *Ptch1* (D) protein expression before and after treatment with 10ng/ml TGF- β . IF staining was shown for each protein with (top row) and without (bottom row) blue nuclei stained with DAPI.

In agreement with the results observed in PCA medium (Figure 5.12), *GLI1* gene expression (Figure 5.13 A), unlike other Hh pathway genes tested, increased markedly in MSCs grown in various media after TGF- β treatment with the *GLI1* expression pattern matching that of *ACTA2* (Figure 5.11) as already observed also in section 5.2 where no treatment was included (Figure 5.2). These results seem to indicate that the correlation observed is more a consequence of a TGF β -dependent non-canonical pathway than an effect due to Hh signalling activation. Consistent with what was observed in the previous assay performed in PCA media (Figure 5.12), TGF- β treatment of MSCs cultured in different media (Figure 5.13), resulted in a decrease in Hh pathway gene expression detected as *SHH* (Figure 5.13 B) in all media tested.

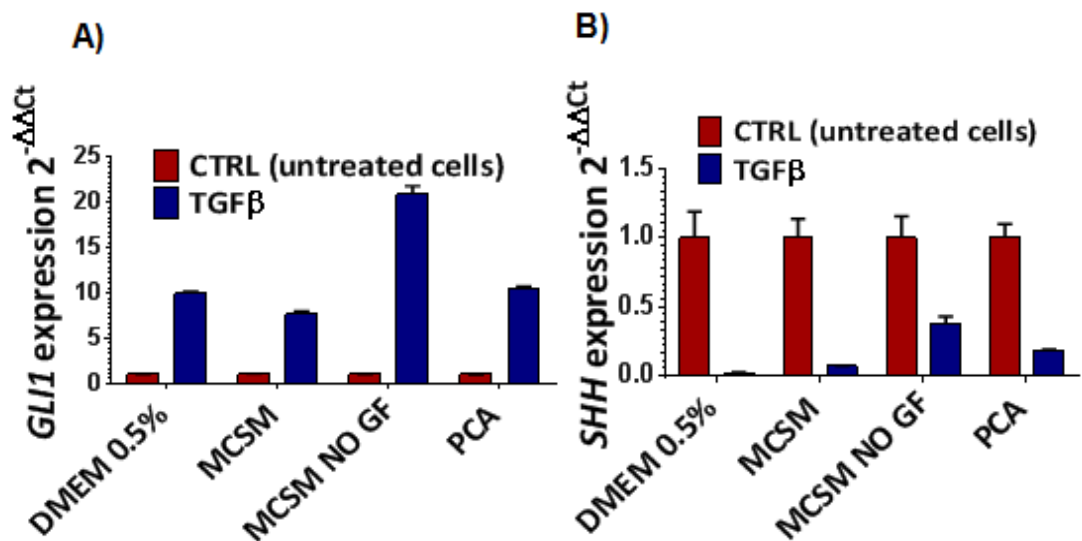


Figure 5.13 TGF- β treatment effect on Hh pathway gene expression in MSCs grown in different media.. *GLI1* (A) and *SHH* (B) expression +/- TGF- β treatment for 72h in MSCs cultured in DMEM 0.5%FBS, MSCM 5% FBS, MSCM no GF 5% FBS, PCA 20% FBS medium. Each bar represents the results of one single experiment.

Nevertheless, Shh and Ptch1 protein expression analysis did not show the same effect (Figure 5.14), but an increase in expression especially in medium with lower amounts of FBS. It seems probable that the high level of FBS in the PCA medium could have hidden the effect of TGF β treatment. The discrepancy between gene and protein expression may be due to a cross-reaction between the Gli1 non canonical activation from TGF- β pathway and the Gli1 regulation from the Hh pathway.

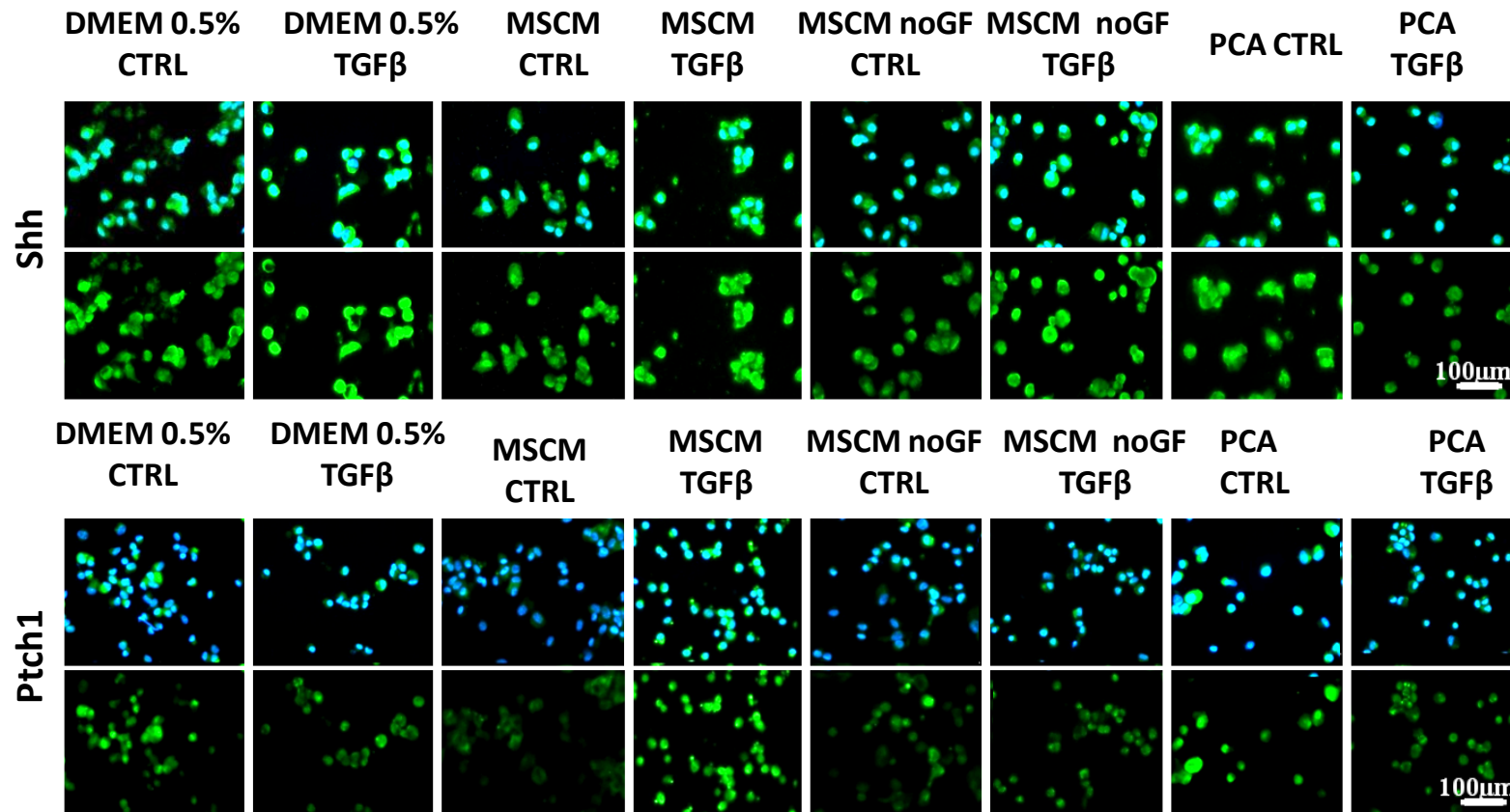


Figure 5.14 Effect of TGF-β treatment on Hh pathway expression in MSCs grown in different media.. Shh and Ptch1 protein expression in MSCs +/- TGF-β treatment performed in DMEM 0.5%FBS, MSCM 5% FBS, MSCM no GF 5% FBS, PCA 20% FBS medium. IF staining for each protein analysed, was shown either with (rows on top) and without (bottom rows) nuclei stained in blue with DAPI.

.Correlation analysis of *ACTA2* and *GLI1* expression after TGF β treatment (Figure 5.15) supported the hypothesis of *ACTA2* and *GLI1* correlation under TGF β treatment showing a significant relationship between these two genes.

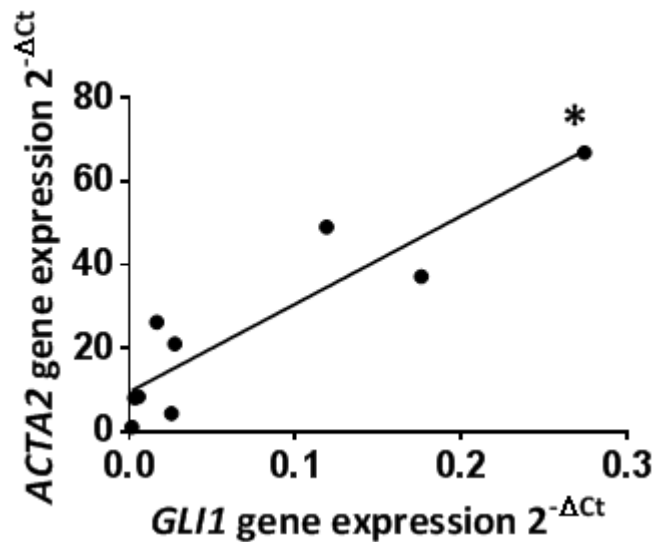


Figure 5.15 Correlation analyses between *GLI1* and *ACTA2* gene expression after TGF- β treatment.. Pearson correlation analysis (* $P < 0.05$) of *ACTA2* and *GLI1* expression after 10ng/ml TGF- β treatment of MSCs cultured in different media.

This raises questions about the relationship between Shh and α SMA expression that will be further investigated in the next section of this chapter.

5.5 The mesenchymal stem cell niche and the establishment of an *in vitro* model

In previous sections, the expression of Shh gene and protein expression increased, especially after 3 days of culture, when MSCs cultured in free differentiation medium became activated. A study has previously suggested the ability of MSCs to form a mSCN by differentiating into myofibroblast-like cells, with *SHH* gene expression only found in a mixed population formed by mixing bone marrow MSCs and myofibroblast cells but not in either population alone (Quante *et al* 2011). Moreover, the role of the Hh pathway in the stem cell niche was hypothesised and supported by the literature [Yeung *et al* 2011; Quante *et al* 2011; Alison *et al* 2012].

Considering the results in this chapter so far, the *in vitro* formation of the mSCN was analysed by artificially mixing MSCs and myofibroblast-like cells or primary pancreatic CAFs, in order to further investigate the role of Shh in this context and to understand if it can be considered a marker of the mSCN; this could be important in understanding the role of the Hh pathway in pancreatic cancer.

The constitution of the mSCN model was analysed by investigating not just Shh but also expression of α SMA (to examine the formation of myofibroblast cells in this context) and the expression of two new markers, Nestin (a marker of mesenchymal stem cells) and Periostin (a marker of myofibroblast cells that is highly expressed when these cells

are part of the mesenchymal stem cell niche) [Mendez-Ferrer *et al* 2010; Quante *et al*, 2011; Malanchi *et al* 2012].

5.5.1 Investigation of Shh as marker of the stem cell niche

In order to investigate the Shh gene and protein expression in the stem cell niche context, an *in vitro* model of the mSCN model was established by mixing MSCs, treated with TGF β for one week in MSCM with no GF added (medium that showed the highest induction of *ACTA2* expression after TGF β treatment (Figure 5.11 A)), with MSCs at low passage (P4 PD3) and cultured in MSCM until the moment of mixing in order to keep them undifferentiated. The mixed population was then cultured for 12 days and analysed on day 0, day 2 and day 12. The DMEM 10% FBS was chosen as the media to be used in this and the following experiments. 10% of FBS concentration was chosen as being high enough to keep the cells healthy for 12 days of culture (higher than 0.5% FBS previously used for cell cultures not longer than 3 days), but not high enough to push the activation process too far (as the PCA medium in figure 5.14). The effect of the mSCN model on *SHH* gene expression was investigated by calculating the difference between the level of expression detected in the mSCN compared with the level of expression attained as a result of calculating the average between the expression values detected in the original single populations (MSCs and myofibroblast like cells (MF-like)) i.e. $[(\text{MSCs } 2^{-\Delta\text{Ct}})/2 + (\text{MFs } 2^{-\Delta\text{Ct}})/2]$. The *SHH* expression increased by 25 times in the mixed population after 2 days of culture (Figure 5.15A). However, this effect

did not persist over time, and by day 12 no difference was observed (Figure 5.16A).

Shh protein expression (Figure 5.16B) analysis confirmed the high expression in the mixed population, but only after 12 days rather than after 2 days, as expected from the gene expression, perhaps due to the fact that the increase in protein expression requires more time to become visible. Shh gene and protein expression (Figure 5.16B and C) also increased in MSCs on day 2 and day 12 in comparison to day 0. The same analysis in the MF-like population showed instead a much lower level of Shh gene and protein expression, reinforcing the idea of Shh being expressed less in highly differentiated populations.

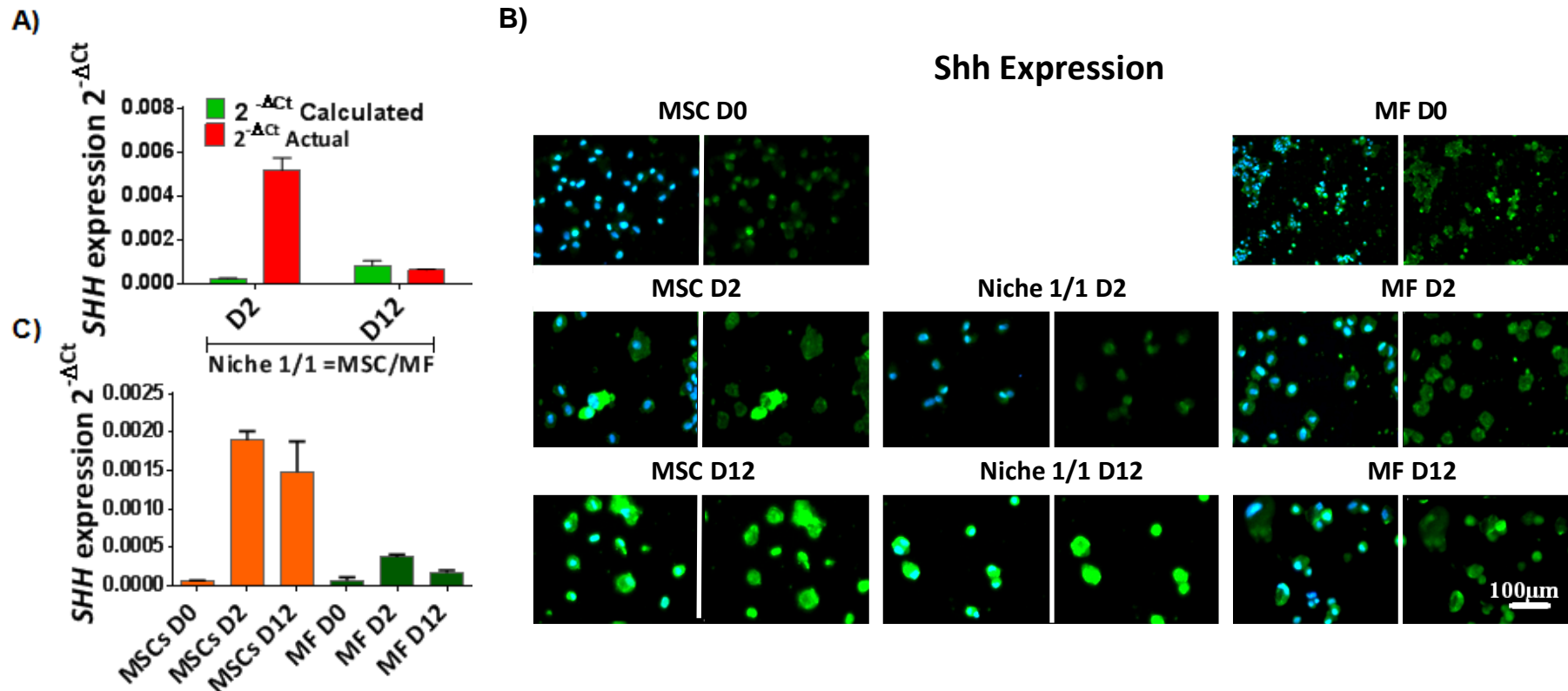


Figure 5.16 Investigation of *SHH* gene expression in a stem cell niche *in vitro* model.. A) Comparison between the *SHH* expression calculated by using the formula $[(MSCs\ 2^{-\Delta Ct})/2 + (MFs\ 2^{-\Delta Ct})/2]$ and the actual *SHH* expression measured by qPCR-RT in the 1/1 Niche= MSCs/MF. Each bar represents one single experiment. B) Protein expression in MSCs, myofibroblast-like cells, and mixed population (1/1 ratio of MSCs and MF-like cells) All cell populations included were cultured for 12 days in DMEM 10% FBS. IF images show cells with (first, third and fifth column) and without (second, fourth and sixth columns) the nuclei stained with blue (DAPI). C) *SHH* gene expression in single populations: MSCs and MF-like cells.

The same samples were also investigated for α SMA gene and protein expressions and *POSTN* and *NES* gene expressions to better characterise their stem cell niche properties. The basal expression of *POSTN* (5.17A) is believed to increase in MF-like cells when they are part of a mixed population in comparison to single population. Therefore, higher expression of *POSTN* was expected in the mSCN model (the actual value higher than the calculated value) in comparison to the single populations (MSCs and MF-like population) that constitute the *in vitro* mSCN. However, no differences were observed in this comparison (Figure 5.17A).

ACTA2 (Figure 5.17B) and *NES* (Figure 5.17C) gene expressions were used, as explained, to assess the presence of MF-like and MSC populations respectively over time. Both *ACTA2* and *NES*, being markers of single populations, were expected not to show any difference between the actual and the calculated values in the *in vitro* mSCN model. The *ACTA2* expression analysis did confirm this expectation, both after 2 and 12 days of culture. The *NES* gene expression, like the *ACTA2* expression, did not show differences between the actual and calculated value in the mSCN model after 2 days of culture. However, a small change (2 times) was observed after 12 days of culture.

Interestingly, *POSTN* and *ACTA2* in the mSCN model (Niche 1/1) (Figure 5.17A and B) and in MSCs (Figure 5.17D and E) increased over time, indicating the generation of MF-like cells in these two populations (as already observed in a previous section (5.3) of this chapter, and in

agreement with Quante *et al* 2011). This result confirmed the ability of unmixed MSCs to be activated and to form a myofibroblast-like cell population when grown in a free differentiation medium. MF-like cells showed a variable but high level of *POSTN* (Figure 5.17D) and *ACTA2* (Figure 5.17E) gene expressions consistent with the cells being activated. The decrease in these two genes on day 2 in the MF-like cells may be due to stopping TGF β treatment and seems to suggest a reversibility of cell activation when no stimuli are present. *NES* gene expression (Figure 5.17 C and F) was fairly constant over time in all the populations tested, suggesting that Nestin is not a good marker for detecting changes in the stem cell population in the mSCN model. However, it will be further investigated in other mSCN models analysed later in this chapter.

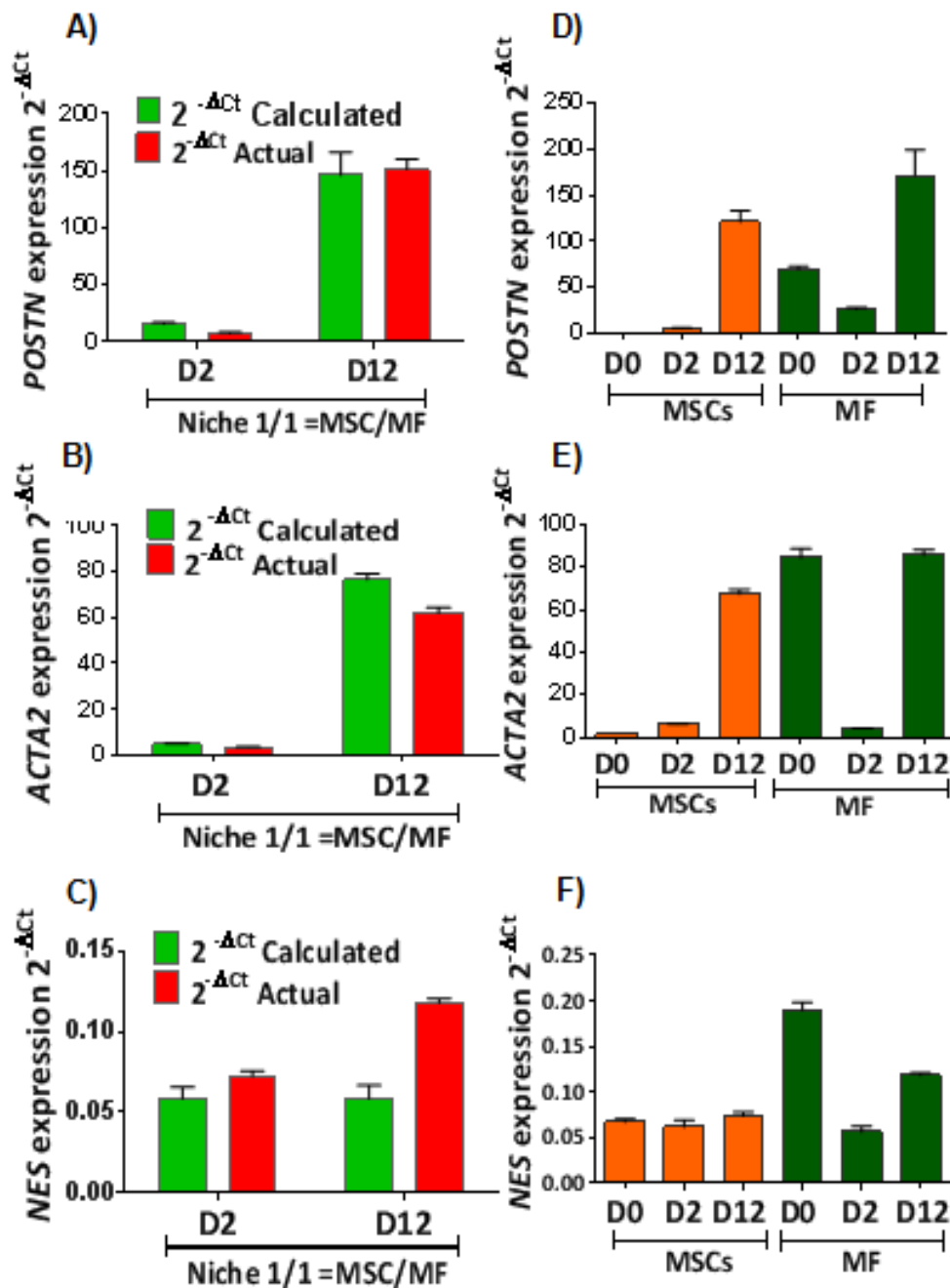


Figure 5.17 Investigation of stem cell niche marker gene expression in a stem cell niche *in vitro* model. Comparison between *POSTN* (A), *ACTA2* (B) and *NES* (C) gene expression calculated by using the formula: $[(\text{MSCs } 2^{-\Delta Ct})/2 + (\text{MFs } 2^{-\Delta Ct})/2]$ and their actual expression measured by qPCR-RT in the 1/1 Niche= MSCs/MF. *POSTN* (D), *ACTA2* (E), *NES* (F) gene expression in MSCs and myofibroblast-like cells (MF). All cell populations were cultured for 12 days in DMEM 10% FBS. The cells were harvested on day 0, 2 and 12 of the culture. Each bar is the result of one single experiment

α SMA protein expression analysis (Figure 5.18) as well as the gene expression (5.17 B and E) increased over time in the mSCN model and in MSCs. Moreover α SMA protein expression also increased overtime in the MF-like cells.

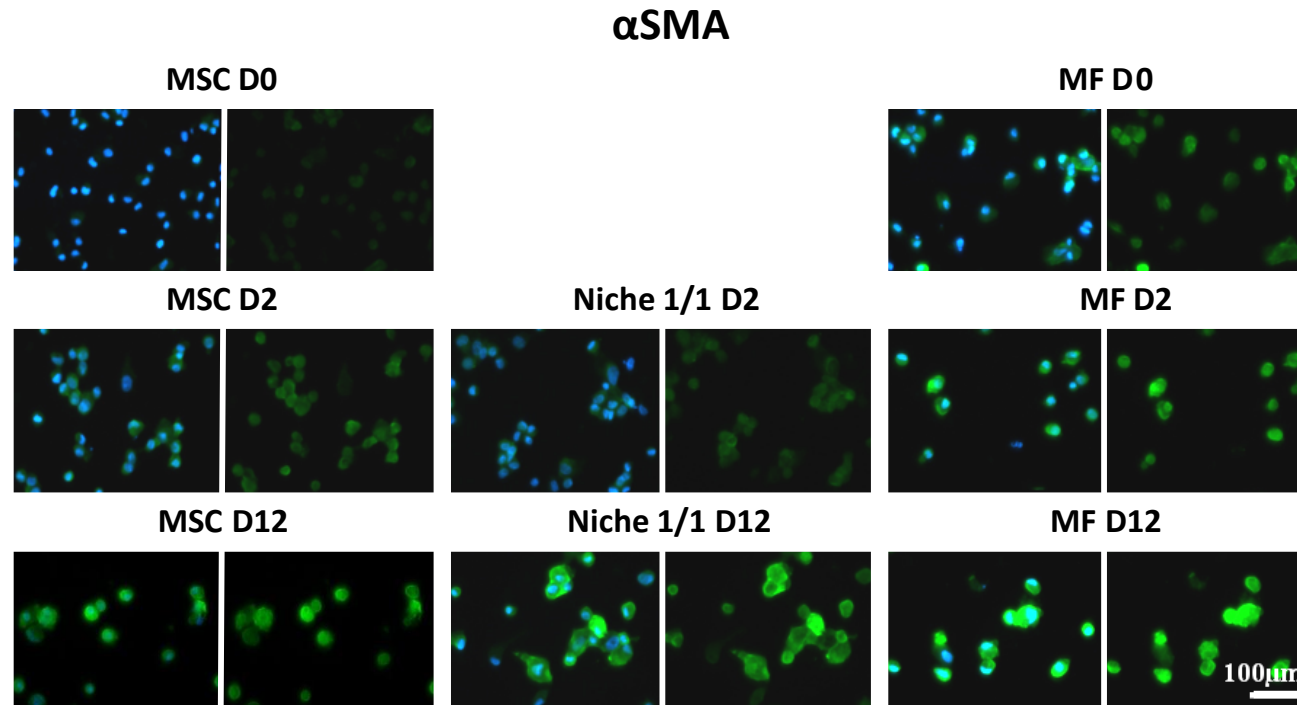


Figure 5.18 Investigation of α SMA protein expression in a stem cell niche *in vitro* model.. α SMA protein expression in MSCs, mSCN model (Niche 1/1) and myofibroblast-like cells (MF) cultured for 12 days in DMEM 10% FBS. The cells were harvested on day 0, 2 and 12 of the culture. IF images shows cells with (first, third and fifth column) and without (second, fourth and sixth column) nuclei stained with DAPI (blue).

Considering the results observed in the previous assay, the *SHH* expression was also tested using different ratios of MSCs and MF-like cells (again obtained by treating MSCs with TGF β for one week) and was compared to MSCs and MF-like cell single populations. As previously, a direct comparison between the data for Niche 3/1 $[(3*(MSCs\ 2^{-\Delta Ct}) + (MFs\ 2^{-\Delta Ct}))/4]$ and Niche 1/3 $[(3*(MFs\ 2^{-\Delta Ct}) + (MSCs\ 2^{-\Delta Ct}))/4]$ and the calculated values (used as representative values of the contribution of the single populations to the gene expression in the niche models) was performed. The assay was run for a longer time (21 days) in order to further investigate the effect of Shh over time, and harvested on days 0, 2, 12, and 21. Interestingly, the greatest up-regulation of *SHH* gene expression in the mSCN model (Figure 5.19) was observed exclusively in the Niche 1/3 model. In fact, the comparison between the *SHH* gene expression value in Niche 1/3 model calculated as $[(3*(MFs\ 2^{-\Delta Ct}) + (MSCs\ 2^{-\Delta Ct}))/4]$ and the actual values on day 2, day 12 and day 21 were increased 1.3, 2.1 and 2.8 times respectively. The same comparison between Niche 3/1 model calculated as $[(3*(MSCs\ 2^{-\Delta Ct}) + (MFs\ 2^{-\Delta Ct}))/4]$ and the actual value did not show a *SHH* expression increase either on day 2 or day 12 or day 21. Moreover, the *SHH* gene expression level in this experiment remained high on day 21 both in the Niche 3/1 and in the Niche 1/3 samples, without any decrease as observed in the previous assay (Figure 5.19 A).

Even if the *SHH* expression increase observed in the mSCN model 1/3 ratio was not as high as that observed in the previous experiment

(Figure 5.17) in this later experiment a time point's dependent increase was shown, reinforcing the reliability of this evidence.

The analysis of *SHH* expression in the single populations (MSCs and MF-like cells) showed, consistent with the previous experiment, (Figure 5.16) an increase in MSCs of 2.15 times on day 2 that drops down on day 12 and day 21 (Figure 5.19B). *SHH* expression in MF-like cells even if increased in comparison to day 0 (4 and 5.7 times respectively on day 12 and day 21), maintained a lower level of expression in comparison to the other cell populations (MSCs and Niche 3/1) (Figure 5.19B).

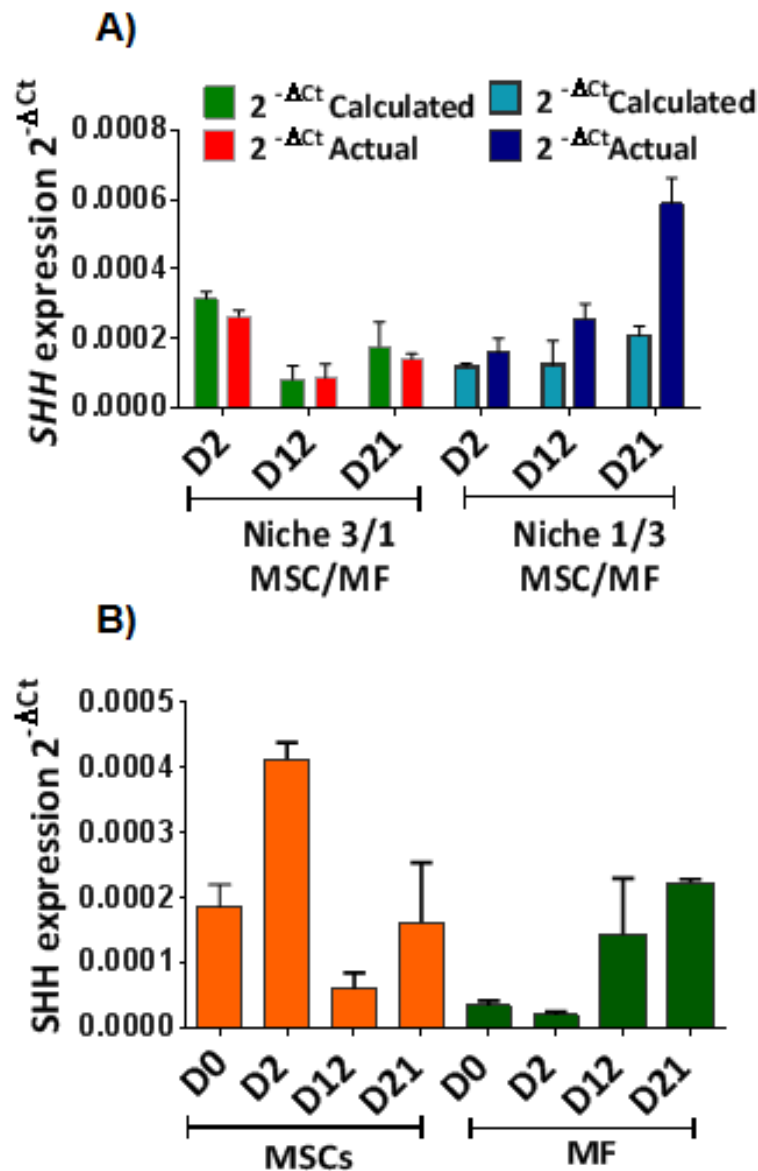


Figure 5.19 Investigation of *SHH* gene expression in different ratios of MSCs and MF-like cells in the mSCN *in vitro* model.. A) Comparison between *SHH* expression detected in Niche 1/3 model and the calculated value $[(3 \times (\text{MFs } 2^{-\Delta Ct}) + (\text{MSCs } 2^{-\Delta Ct})) / 4]$ and between *SHH* expression in Niche 3/1 model and the calculated value $[(3 \times (\text{MSCs } 2^{-\Delta Ct}) + (\text{MFs } 2^{-\Delta Ct})) / 4]$ on day 2, 12 and 21. B) *SHH* expression in MSCs and myofibroblast-like cells (MF) single populations cultured for 2, 12, 21 days in DMEM 10% FBS. Each bar represents one single experiment.

Consistent with the results on the *SHH* gene expression analysis (Figure 5.18A), *POSTN* expression (Figure 5.20 A) slightly increased exclusively in the 1/3 Niche model on day 12 (i.e *POSTN* expression increased 1.4 times in the Niche 1/3 model in comparison to the single populations as shown from the comparison between the calculated $:[(3*(MFs \ 2^{-\Delta Ct}) + (MSCs \ 2^{-\Delta Ct}))/4]$ and the actual value). However, this increase was quite low, it was not present on day 2 and it dropped down on day 21. The comparison between the calculated and actual values for *ACTA2* (Figure 5.20 B) and *NES* (Figure 5.20 C) expressions in the Niche 1/3 and in the 3/1 models did not show any difference confirming the hypothesis. *ACTA2* and *POSTN* gene expressions in the single populations (MSCs and MF-like cells) (Figure 5.20 D and E) showed a significant increase in MF-like cells (*ACTA2*, *POSTN* positive cells) over time. The *NES* gene expression (Figure 5.20 F) showed a constant expression over time in all cell populations tested.

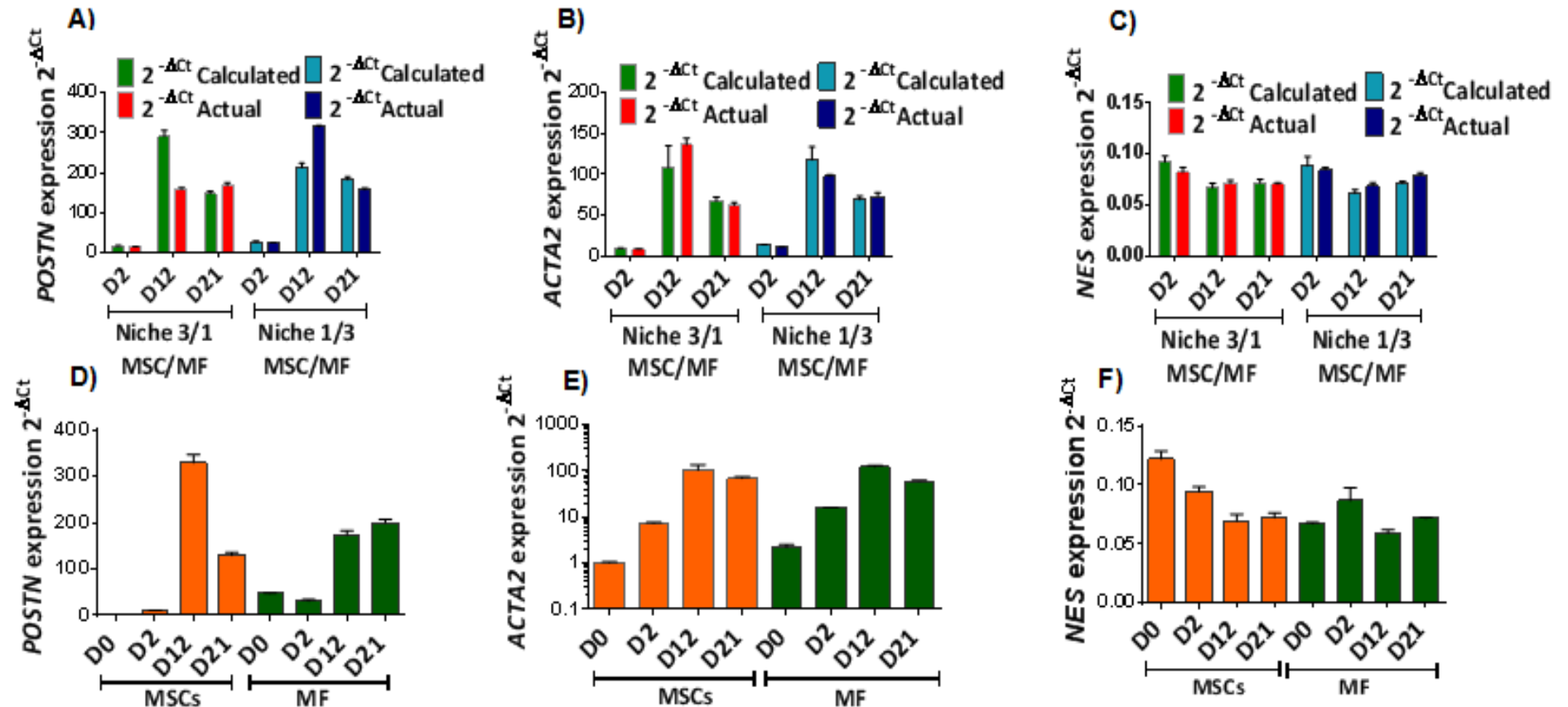


Figure 5.20 Investigation of mSCN marker gene expression in different mSCN model co-culture ratios.. Comparison of the *POSTN* (A) *ACTA2*, (B), *NES* (C) expression between the actual and calculated values in 2 mixed population (3/1 and 1/3 ratio of MSCs and MF like cells) cultured for up to 21 days in DMEM 10% FBS. The cells were harvested on days 0, 2, 12, and 21 of the culture. *POSTN* (D), *ACTA2* (E), *NES* (F) expression in MSCs, myofibroblast-like (MF) cells cultured for 21 days in DMEM 10% and harvested on day 2, 12 and 21. Each bar represents one single experiment.

Finally, the effect of mixing in 1/1 ratio [that previously showed an increase of *SHH* gene expression (figure 5.16)] MSCs and primary pancreatic CAFs on Shh gene and protein expression was tested over 21 days in culture (Figure 5.21 A). As previously, cells were harvested on day 2, 12 and 21 and the effect of cell mixing was analysed as the difference between the calculated $[(\text{MSCs } 2^{-\Delta\text{Ct}})/2 + (\text{CAF}s 2^{-\Delta\text{Ct}})/2]$ and the actual *SHH* gene expression (Figure 5.21 A). In this experiment Shh gene (Figure 5.21 A) and protein expression (Figure 5.21 C) increased in the mixed population in comparison to both single populations after 2 days of culturing (Figure 5.20 A and B). However, the level of *SHH* gene expression in the Niche (MSCs + CAFs) 1/1 model on day 2 was around 4 times and 64 times lower than in the previous experiment (Figure 5.19 A) and in the first experiment (Figure 5.16 A) respectively, suggesting a less strong effect of CAFs on the mSCN model than MF-like cells. As for one of the experiments with MF-like cells (Figure 5.16), the increasing effect on *SHH* gene expression in the mSCN model was not observed on day 12 and 21 (Figure 5.21 A). The *SHH* expression in single populations (MSCs and MF-like cells) strongly increased, as in the previous experiments (figure 5.16A and 5.19A), in the MSCs after 2 days and moreover the increase was maintained over time.

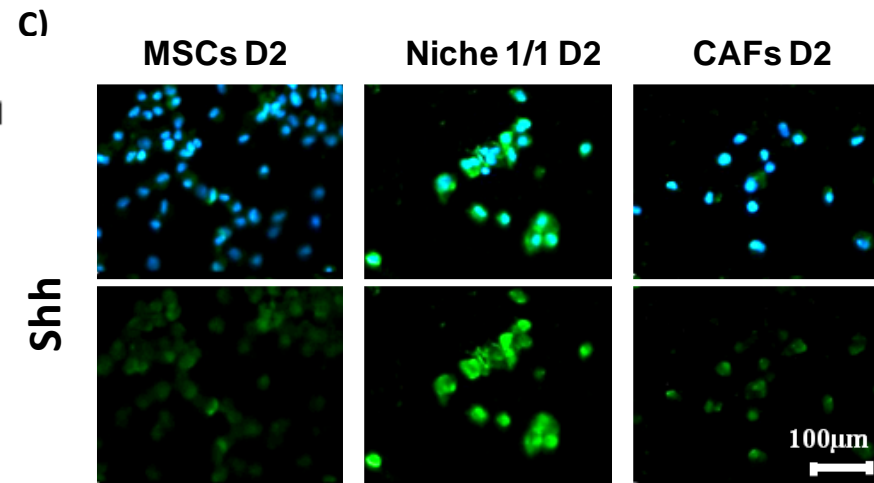
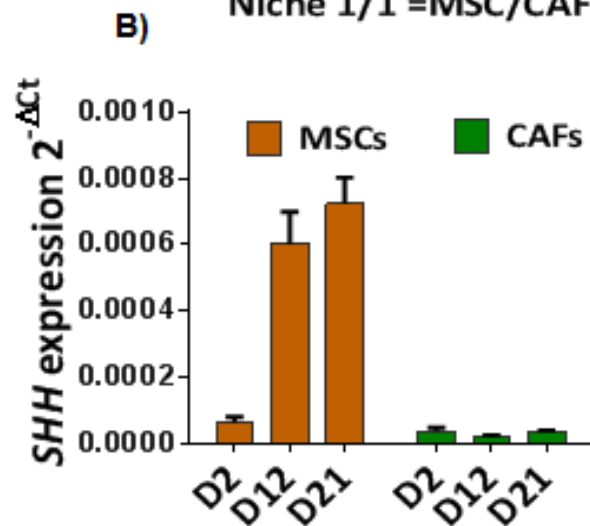
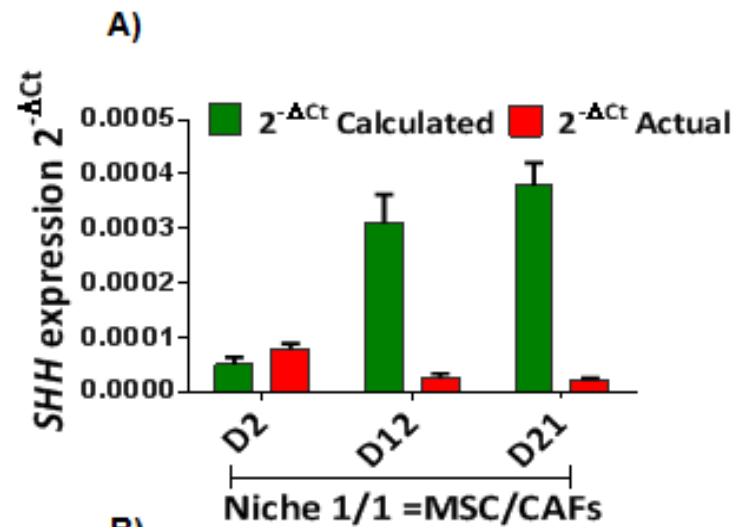


Figure 5.21 Investigation of the effect of CAFs on mSCN *in vitro* model and *SHH* gene and protein expression. A) Comparison between *SHH* actual gene expression value and the calculated one in the mixed population Niche 1/1 (1/1 proportion of MSCs and CAFs) after 2, 12 and 21 days of culture in DMEM 10% media. B) *SHH* gene expression in MSCs and pancreatic tumour-derived CAFs grown for 2, 12, 21 days in DMEM 10% FBS. Each bar represents one single experiment. C) Comparison between Shh protein expression on day 2 in co-cultured MSCs and CAFs cells (Niche 1/1) with MSC and CAF single populations harvested at the same time point. All cell populations were grown in DMEM 10% free differentiation medium. IF images shows cells with (top row) and without (bottom row) nuclei stained with DAPI (blue).

Interestingly, *POSTN* expression analysis (Figure 5.22 A) showed a 15.8 and 4 times higher actual value than the calculated one after 12 and 21 days respectively. The same analysis performed for *ACTA2* (Figure 5.22 B) and *NES* (Figure 5.22 C) expressions, as expected, did not show relevant differences between the calculated and the actual values (Figure 5.22 B and C). *POSTN* (Figure 5.22 A and D) and *ACTA2* (5.22 B and E) gene expressions generally increased over time in all cell populations tested (MSCs, mSCN model, CAFs) confirming earlier observations. Interestingly, *POSTN* gene expression in CAFs (Figure 5.22 D) showed a lower level of expression in comparison to the other populations, confirming the hypothesis that it increases its expression in fibroblasts when part of a mSCN. Consistently, a much higher *POSTN* expression was observed in the mSCN model in comparison to single populations at all time points tested (18.6 and 90.2 times on day 2; 69.3 and 9.5 times on day 12; 2.2 and 16.5 times on day 21 in comparison to MSCs and CAFs respectively) (Figure 5.22 A and D).

The *NES* gene expression (Figure 5.20 C) did not change in any population tested and the fact that it is also expressed in CAFs demonstrates that it is not suitable as a marker of stem cells in the mSCN niche model and for this reason it was no longer used.

The *Postn* (Figure 5.23) and α SMA (Figure 5.24) protein expression increased over time in all population including an unexpected increase in CAF cells (believed to be cells already fully activated).

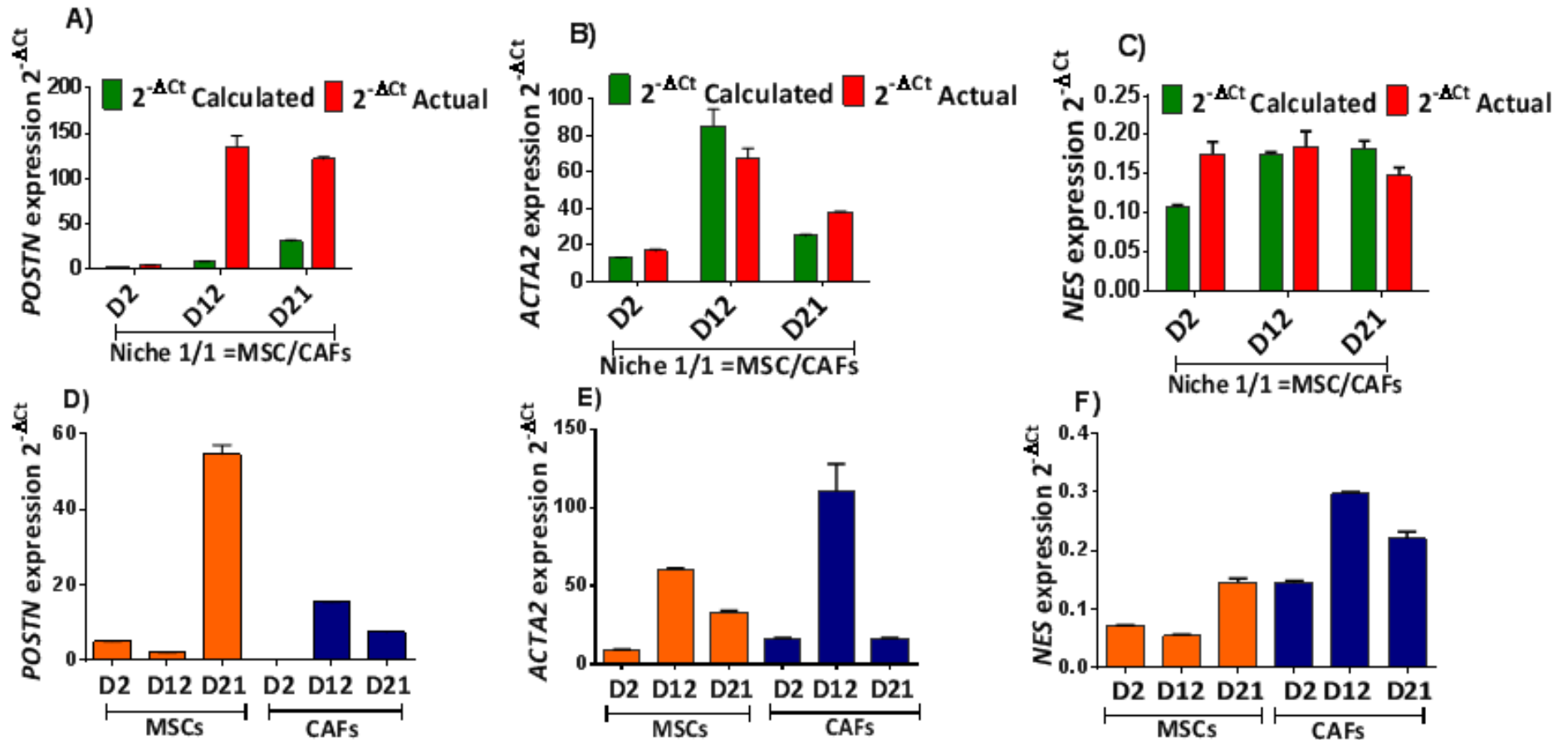


Figure 5.22 Investigation of the effect of CAFs on mSCN marker expression in an *in vitro* model.. Comparison between the actual and calculated value of the *POSTN* (A), *ACTA2* (B), *NES* (C) gene expression in a mSCN model (1/1 MSCs/CAFs) after 2, 12 and 21 days of culture in DMEM 10%. *POSTN* (D), *ACTA2* (E) and *NES* (F) gene expressions in MSCs and pancreatic CAFs grown for 2, 12, 21 days in DMEM 10% FBS. Each bar represents one single experiment.

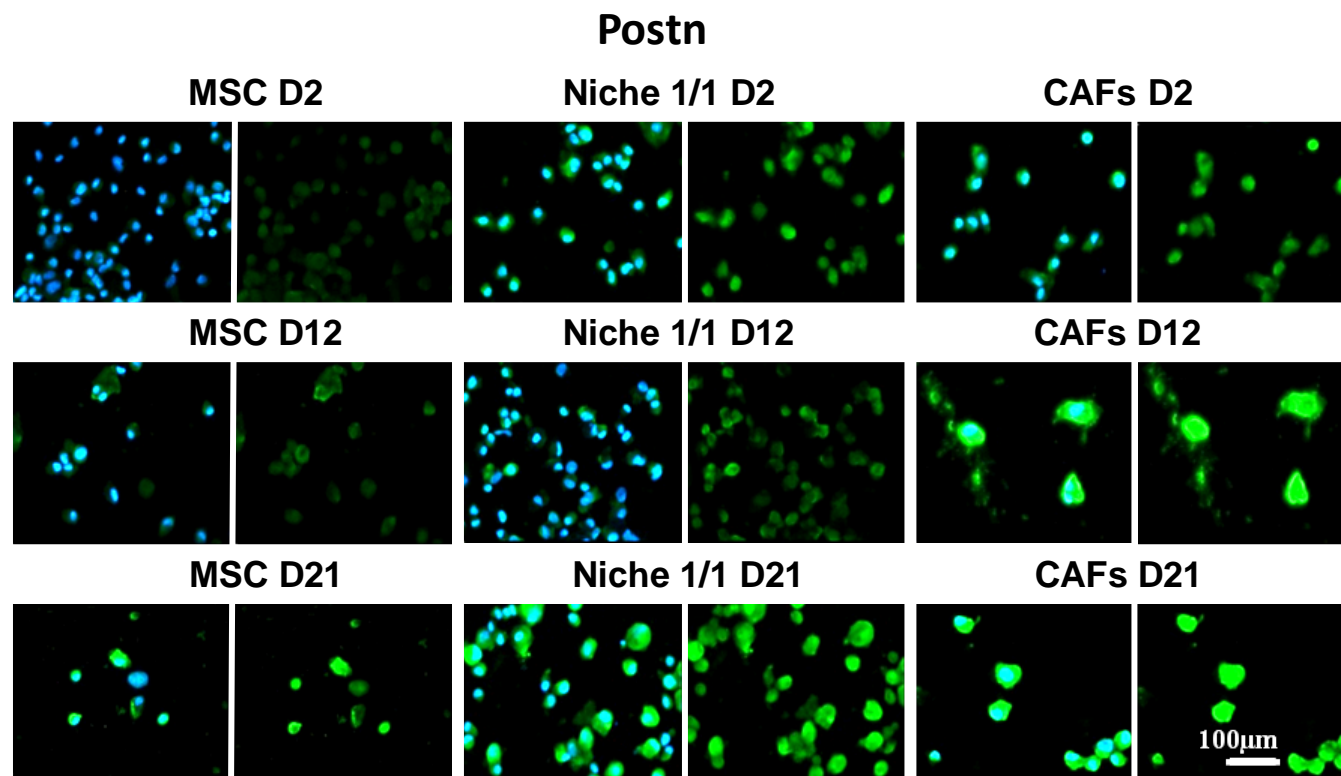


Figure 5.23 Investigation of the effect of CAFs on Postn protein expression in a mSCN *in vitro* model .Postn protein expression in MSCs, pancreatic CAFs and mixed population Niche 1/1 (1/1 proportion of MSCs and CAFs) grown for 2, 12, 21 days in DMEM 10% FBS. IF images shows cells with (first, third and fifth column) and without (second, fourth and sixth column) nuclei stained with DAPI (blue).

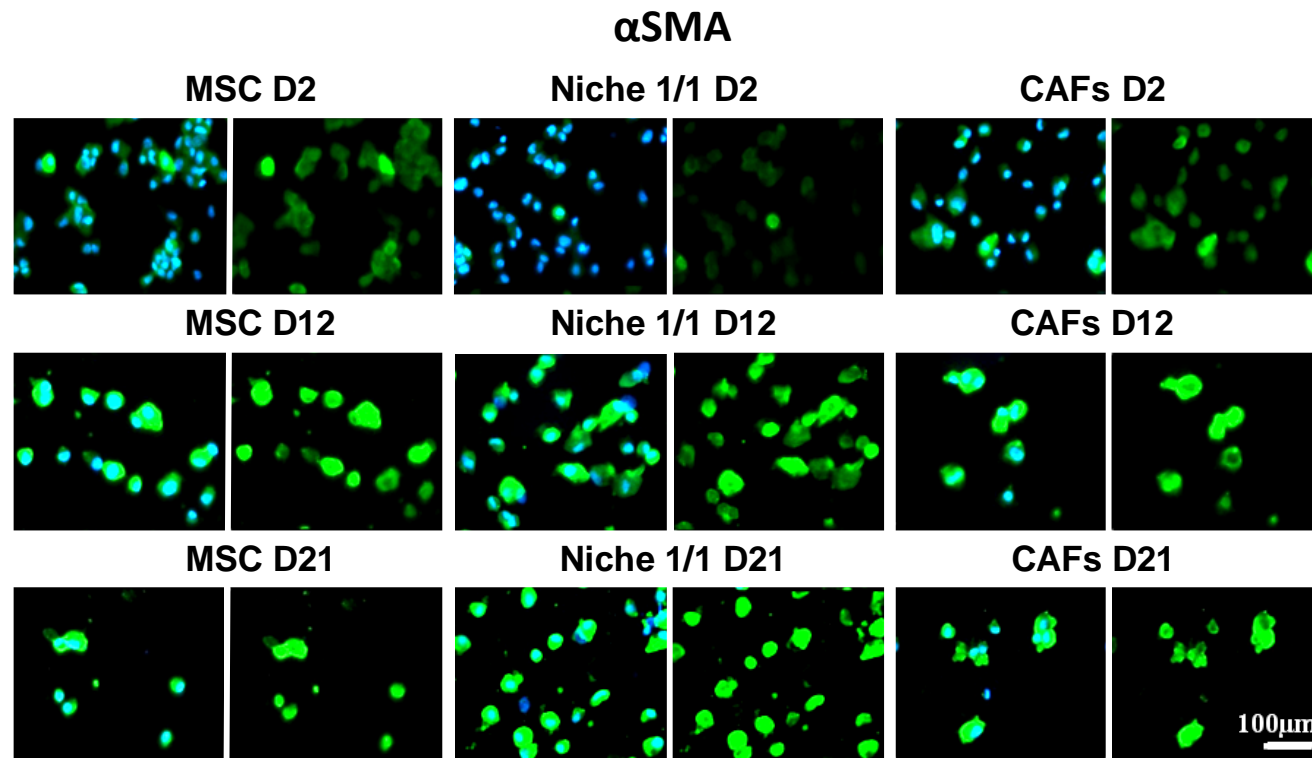


Figure 5.24 Investigation of the effect of CAFs on the α SMA protein expression in a mSCN *in vitro* model. α SMA protein expression in MSCs, pancreatic CAFs and mixed population Niche 1/1 (1/1 proportion of MSCs and CAFs) grown for 2, 12, 21 days in DMEM 10% FBS. IF images shows cells with (first, third and fifth column) and without (second, fourth and sixth column) nuclei stained with DAPI (blue).

Summarising the results in this section:

- Shh gene and protein expression increased in a mSCN *in vitro* model obtained by mixing MSCs and MF-like in different ratios. An increase in Shh was also observed in MSCs alone over time, together with an increase in α SMA and Postn suggesting that MSCs alone when cultured in FDM are able to form a mixed population that is maintained over time. This may explain why at times the mixed population does not appear to maintain increased Shh gene and protein expression in comparison to component populations.
- MF-like cells showed an increase in Shh expression, albeit at a low level, that suggests this cell population is an impure single population consisting of a low proportion of MSCs and a high proportion of MF-like cells.
- *POSTN* expression seems to be good markers of MF-like cells population and it is expressed at higher level when MF-like cells/CAFs are mixed with MSCs (mSCN *in vitro* models).
- The increase of the α SMA and Postn expression in CAF cells over time revealed that on day 0 of the cell culture they cannot be considered fully activated cells. It also suggests that α SMA and Postn are markers of cell activation rather than differentiation and shows how their expression depends on external signals such as growth factors in free differentiation media, presumably also present in the tumour microenvironment.

5.5.2 Investigation of Shh expression in the mesenchymal stem cell niche

The previous data do not assess if Shh is expressed from MF-like cells that expand over time in a culture of MSCs grown in free differentiation medium or is exclusively expressed, probably from MF-like cells, in mixed and not single populations. A direct comparison between the mSCN model with CAFs (activated cells) and MSC single populations over time had not been carried out since the previous experiments were all performed in free-differentiation media in which MSCs can become a mixed population over time. Even the MF-like cells used in this study, (originated from MSCs treated with TGF β), as said, could be considered a mixed population with a high number of MF-like activated cells.

For this reason, in this section, the stem cell niche markers (Shh, α SMA and Postn), used so far, were analysed on day 2, 12 and 21 in MSCs cultured in MSCM throughout their culture (named MSC single population, MSC S.P.), in a mSCN model obtained by growing MSCs in free differentiation medium (DMEM 10 %) and in CAFs grown in DMEM 10% demonstrated to be an activated population when cultured in this medium. The comparison between the mSCN model and the 2 single populations analysed in this assay showed the gene (Figure 5.25 A) and protein (Figure 5.25 B) expression of Shh exclusively in the mixed population and confirmed the ability of MSCs alone to form a mSCN *in vitro* model when grown in FDM. Very low Shh gene and protein expression was observed on day 2 in all cell populations, but increased Shh expression was detected on day 14 and day 21 in MSCs grown in

free differentiation medium (mSCN model) (Figure 5.25 A and B).

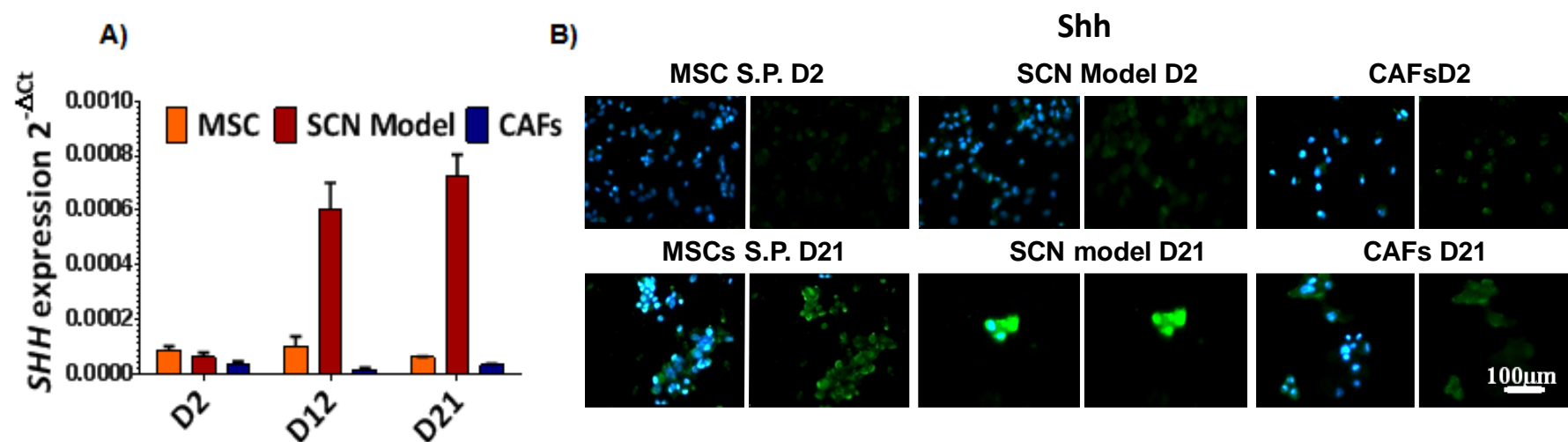


Figure 5.25 Investigation of Shh as marker of stem cell niche.. Shh gene (A) and protein expression (B) in MSCs single population (S.P.), mSCN *in vitro* model and CAFs differentiated cells. Each bar represents one single experiment. IF images show cells with (first, third and fifth column) and without (second, fourth and sixth column) nuclei stained with DAPI (blue).

Further analysis of these samples showed that there was an increase in activated Postn-positive cells (Figure 5.26 A and B) in the mSCN model and in the CAFs cells and a very low increase of these markers in MSC S.P. *POSTN* expression strongly increases in the mSCN model on day 21 showing a higher expression than in the single populations, consistently with its definition as a marker of MF-like activated cells that increases when they are part of a mixed population. The increase of expression of Postn in CAFs is steady with their activation over time in a free-differentiation medium but at lower level than in the mSCN model. α SMA gene and protein expression (Figure 5.27 A and B), such as Postn, increased mainly in the mSCN model and in the CAFs cells and at lower level in MSCs. These results were in agreement with the previous results and so with the experimental expectations.

Interestingly, no expression of Shh was observed in the MSC single population and no expression of Shh was observed in CAFs at any of the time points (Figure 5.25) although an increase in α SMA and Postn positive cells was observed over time (Figure 5.26 and 5.25), dissociating these two markers from the expression of Shh.

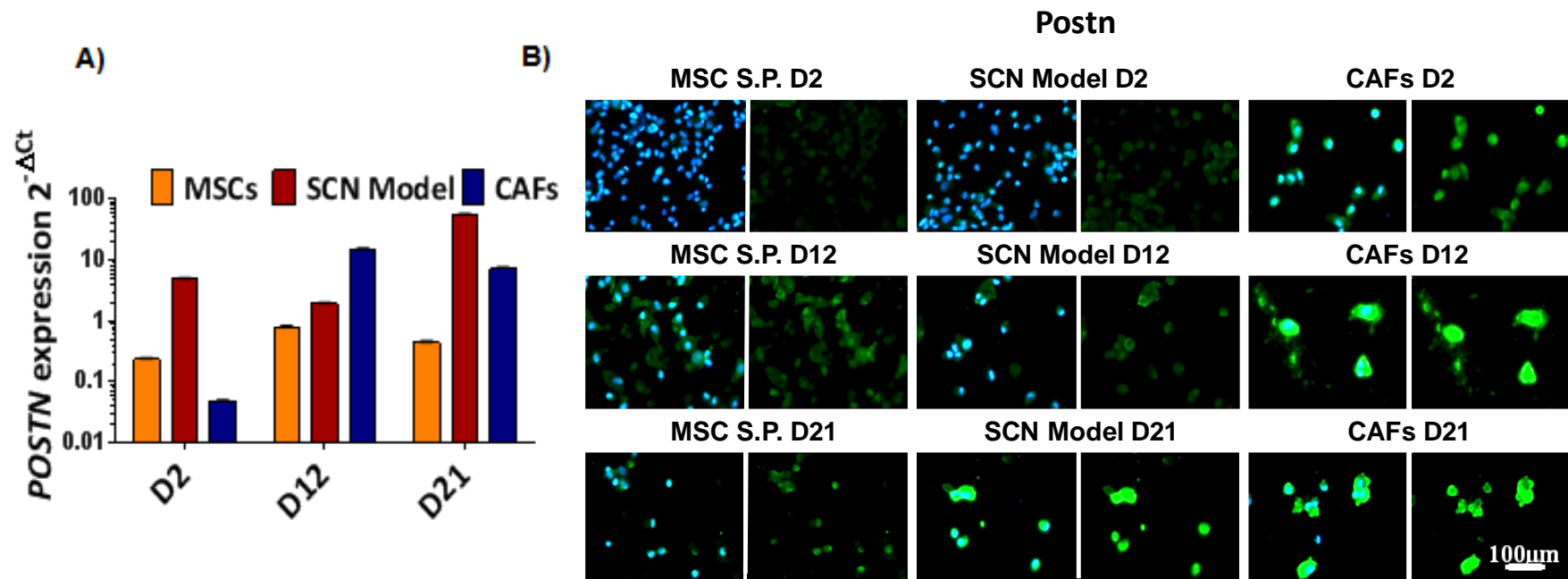


Figure 5.26 Comparison between Postn marker in the mSCN model and single populations .Postn gene (A) and protein (B) expression in MSCs single population (S.P), mSCN *in vitro* model and CAFs. Each bar represents one single experiment. IF images show cells with (First, third and fifth column) and without (second, fourth and sixth column) nuclei stained with DAPI (blue).

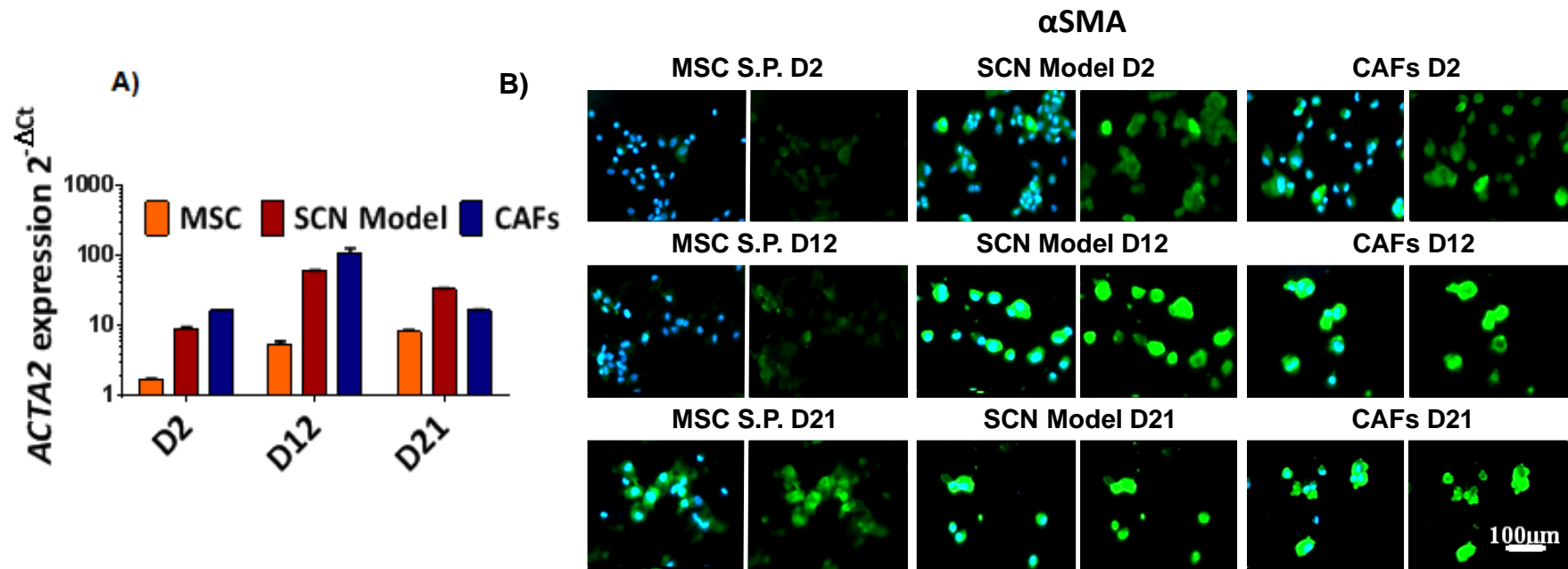


Figure 5.27 Comparison between α SMA marker in the mSCN model and single populations . α SMA gene (A) and protein (B) expression in MSCs single population (S.P), mSCN *in vitro* model and CAFs. Each bar represents one single experiment. IF images show cells with (First, third and fifth column) and without (second, fourth and sixth column) nuclei stained with DAPI (blue).

5.6 Investigation of paracrine responsiveness to Hh pathway stimuli in the stem cell niche model

Based on the above data, MSC (section 5.2) and CAF (Chapter 4) single populations are not able to respond to Hh paracrine stimuli from pancreatic cancer epithelial cells and do not express Shh at the gene and protein level (section 5.4). Shh seems to be exclusively expressed in the mSCN model and for this reason can be considered a marker of the mSCN. Moreover, Shh has been shown to be expressed in advanced stages of PDAC at the stromal level (Chapter 3). Therefore, we hypothesised that the mesenchymal stem cell niche is formed and increased in advanced stages of pancreatic cancer and that this could be the best context in which a response to Hh paracrine stimuli from cancer cells can be detected.

In order to investigate this, the mSCN *in vitro* model was tested for its responsiveness to Hh paracrine stimuli (evaluated *via* *GLI1* and *Ptch1* expression). Various mSCN *in vitro* models were also included in this investigation to further characterise and compare them.

5.6.1 Investigation of the effect of pancreatic TCM and NShh on Hh pathway activation in the mSCN *in vitro* model

Initially, MSCs cultured in PCA free differentiation medium were used as a mSCN model to test for Hh paracrine induction. The cells were grown in TCM from PANC1 and P308T pancreatic epithelial cell lines.

The effect of Hh pathway induction was investigated via analysis of the Hh gene target *GLI1*.

GLI1 gene expression was detected after 3, 7 and 14 days of culture in TCM obtained by culturing pancreatic epithelial cancer cells (PANC1 and P308T) in PCA medium for 72h and their values were normalised to MSCs cultured for the same time points in control conditioned medium (CM CTRL).

Some induction of *GLI1* was observed in this assay (Figure 5.28) after 14 days of treatment with PANC1 TCM. Over time (with formation of the mSCN model) there was an increase in sensitivity to Hh paracrine stimuli.

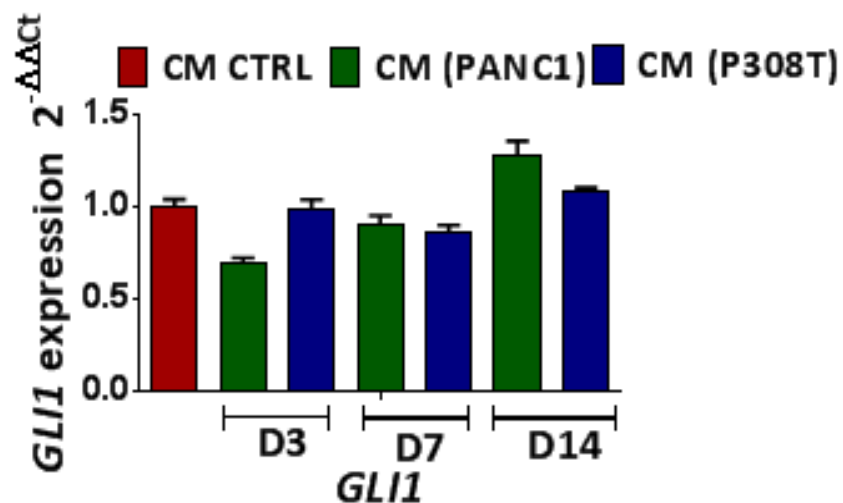


Figure 5.28 TCM effect on mSCN *in vitro* model. *GLI1* expression in MSCs cultured in PCA TCM from pancreatic epithelial cells (PANC1, P308T) for 3, 7, and 14 days. Gene expression detected in samples grown in TCM was normalised to control samples (CM CTRL). Each bar is the results of one single experiment.

On day 3 and 7, *GLI1* expression slightly decreased after TCM treatment suggesting no Hh pathway induction by pancreatic cancer cells under this experimental condition. An explanation could be that the

very high percentage of serum in PCA medium (20% of FBS) hides the effect of ligand released in the conditioned media.

To further investigate Hh pathway paracrine induction, MSCs cultured in PCA media or in DMEM with 5% FBS were treated for 48h with 1µg/ml NShh. The NShh concentration used was based on Bailey *et al* 2008, in which, stromal cells from pancreatic tumours significantly increased Gli1 and αSMA gene and protein expression after treatment and was 100 times higher than that used previously (chapter 4 and 5).

Since, as shown previously, *GLI1* gene expression may be affected by cross-reaction with a non-canonical pathway, the effect of NShh treatment was assessed not just via *GLI1* gene expression but also via Ptch1 protein expression analysis.

GLI1 expression also increased in PCA medium after NShh treatment; however, the degree of change was very low making it difficult to draw firm conclusions (Figure 5.29 A). On the other hand, protein expression analysis of Ptch1 showed a clear increase after treatment in both media tested (Figure 5.29 C and D) suggesting responsiveness of MSCs to Hh stimuli under these conditions.

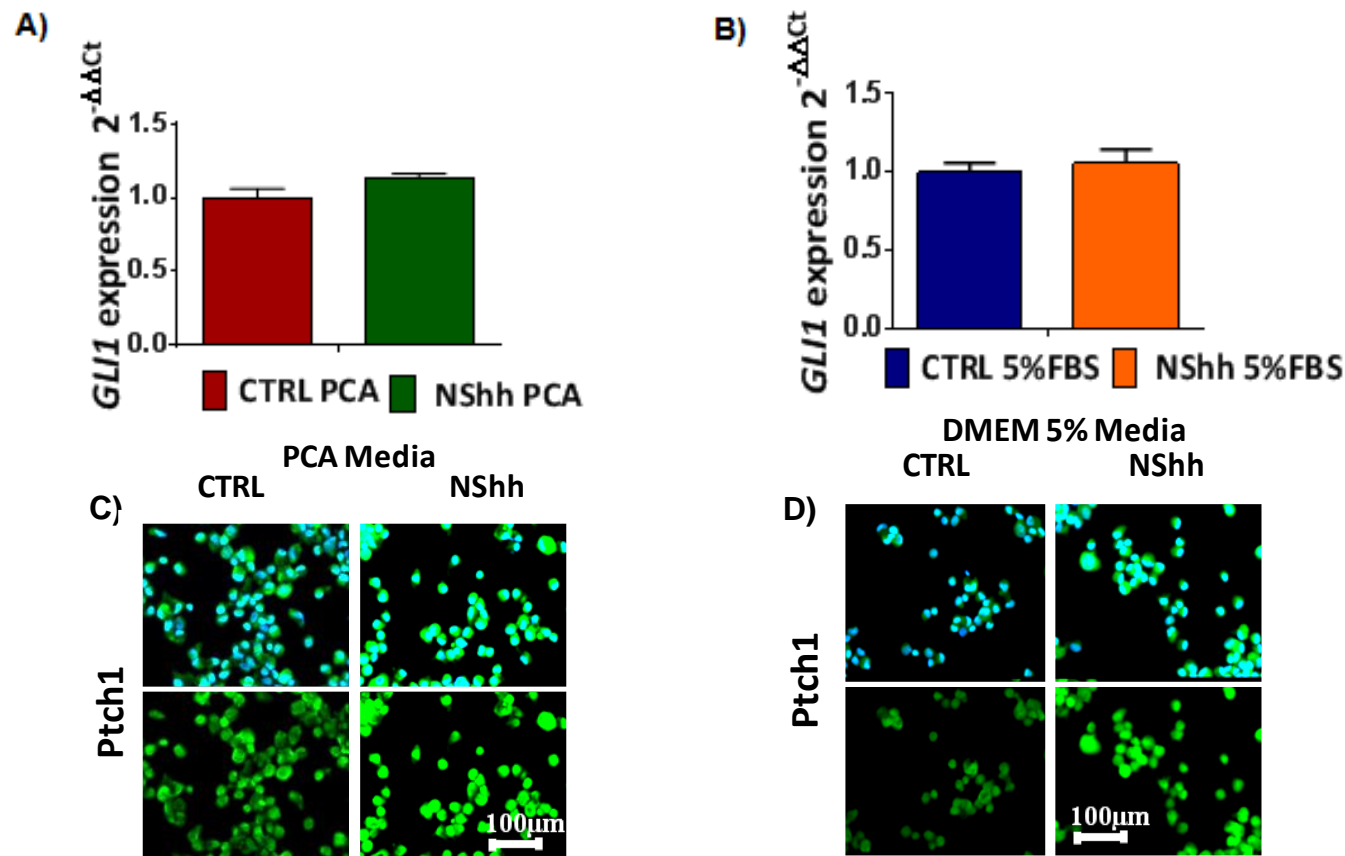


Figure 5.29 Effect of NShh and FBS concentration on the paracrine responsiveness of the Hh pathway in a mSCN *in vitro* model.. *GLI1* gene expression in MSCs grown for 72h in PCA (A) and DMEM 5% (B) +/- NShh treatment for 48h. Each bar was the results of one single experiment. C) and D) Ptch1 protein expression in MSCs cultured in PCA medium and DMEM 5% FBS. IF images show cells with (top row) and without (bottom row) nuclei stained with DAPI (blue).

These data support the hypothesis of the mixed population as a responsive context for paracrine stimuli; however, to further investigate this, a direct comparison of the responsiveness of MSCs between single populations and the stem cell niche model needed to be performed.

5.6.2 Comparison between the responsiveness of MSC single population and mSCN model to Hh paracrine stimuli

To ascertain if cells in the mSCN context respond better to Hh paracrine stimuli than single populations, a trans-well (TW) 2D system was used in which epithelial pancreatic cancer cells (PANC1) were co-cultured with MSCs for 3 days in DMEM 10% free differentiation medium (mSCN model) or in MSCM (single population). Higher expression of the Hh pathway gene and protein targets (Gli1; Ptch1) was expected in the mSCN model than the single population. In the same experiment MSCs treated with TGF- β were also included and the treatment was maintained throughout the co-culture (Figure 5.30). The rationale for maintaining the TGF- β treatment was to allow investigation of the response of a myofibroblast-like single population to paracrine stimuli, since TGF- β was shown (figure 5.10 and 5.11) to promote MSCs differentiation into myofibroblast cells. In parallel, treatment with NShh (1 μ g/ml) was used to further investigate paracrine induction specifically via this ligand (Figure 5.31 A, B and C).

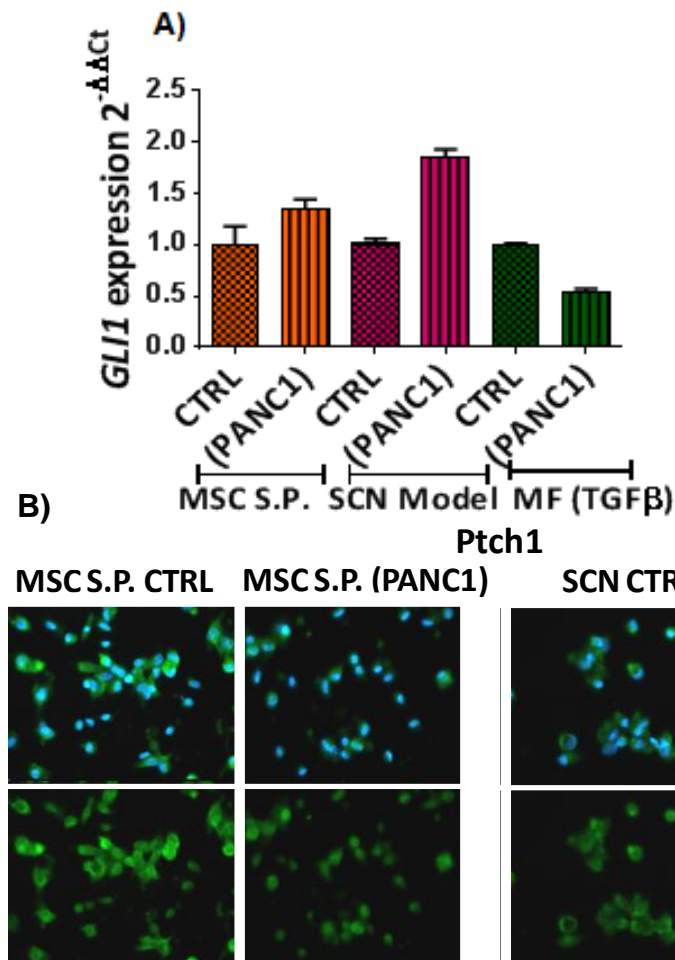
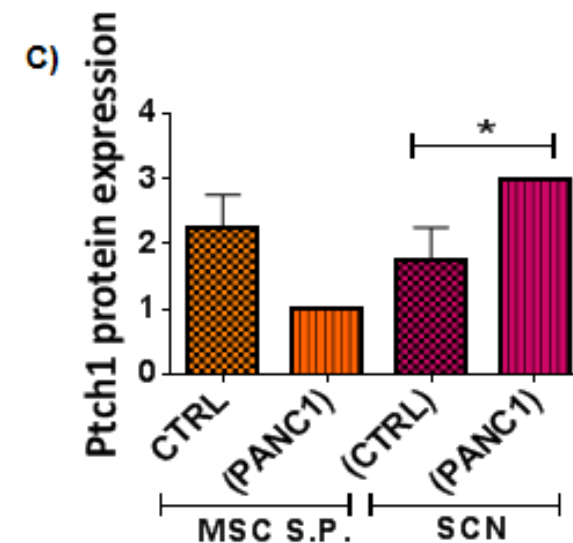


Figure 5.30 Comparison between MSC single population and mSCN model responsiveness to Hh paracrine stimuli in a transwell (TW) system .A) *GLI1* gene expression in MSC single population (S.P.), mSCN model and MF-like cells co-cultured with PANC1 pancreatic cancer cells in a trans-well (TW) system for 72h. Each bar was the results of a single experiment. B) *Ptch1* protein staining by IF in MSC S.P. and mSCN model co-cultured with PANC1 cells (same condition as Figure A) IF images show cells with (top row) and without (bottom row) nuclei stained with DAPI (blue) C) *Ptch1* protein expression quantification in MSC S.P. and mSCN model co-cultured with PANC1 cells in a transwell system for 72h.



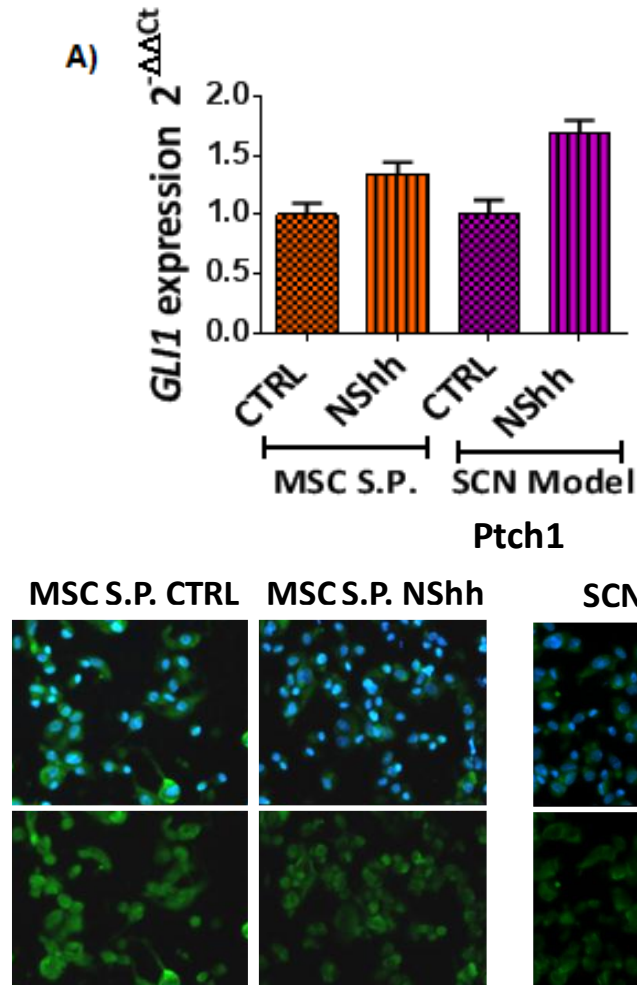
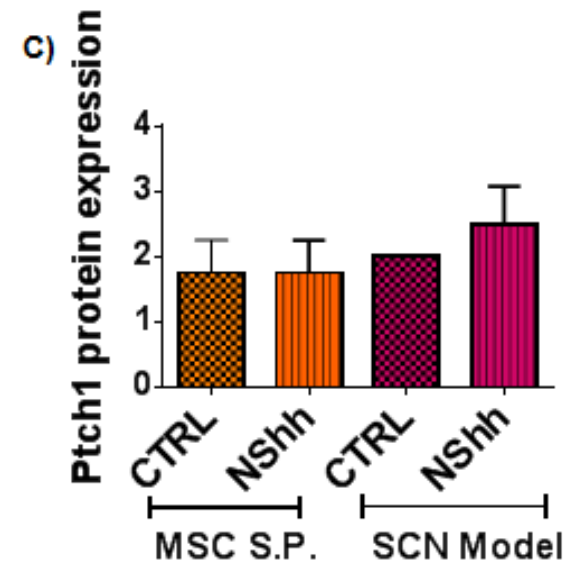


Figure 5.31 Comparison between MSC single population and mSCN model responsiveness to NShh stimuli .A) *GLI1* gene expression in MSC S.P. and mSCN model+/- NShh. Each bar is the results of one single experiment. B) *Ptch1* protein staining by IF in MSC S.P. and mSCN model+/- NShh treatment. IF images show cells with (top row) and without (bottom row) nuclei stained with DAPI (blue) C) *Ptch1* protein expression quantification in MSC S.P. and mSCN model+/- NShh.



GLI1 expression showed a greater increase in the mSCN model than in the MSC single population (S.P.) both after co-culture with PANC1 (Figure 5.30 A) and NShh treatment (Figure 5.31 A) in comparison to control samples. Moreover, in accordance with the niche theory, trans-well co-culture as well as NShh treatment induced a *Ptch1* protein expression increase only in the mSCN *in vitro* model as indicated by the IF images (Figure 5.30 B and 5.31B) and from the quantification analysis (Figure 5.30C and 5.31C). However, only the increase of *Ptch1* expression observed in the SCN model co-cultured with PANC1 epithelial cell line showed significance in comparison to the control sample (SCN model co-cultured with SCN model) ($P<0.05$) (Figure 5.30 C). Finally, TGF- β treated cells (MF-like cells) did not show any responsiveness to paracrine stimuli from pancreatic epithelial cells in the 2D trans-well system as measured by *GLI1* gene expression (Figure 5.30 A). These results confirmed that the completely activated single cell population is not able to respond to Hh exogenous stimuli.

Summarising the results described in this section, the mSCN *in vitro* model seems to be the best context in comparison to MSC and CAF single populations for a response to Hh paracrine stimuli.

5.6.3 Comparison between responsiveness of different mSCN models to Hh paracrine stimuli

The observation of Shh higher expression in co-cultured MSCs with MF-like cells (Figure 5.16) suggests the need to also test the responsiveness of this and other stem cell niche models to Hh

paracrine stimuli, in order to further characterise them and understand the best way to reproduce the mSCN *in vitro*. The responsiveness of all mSCN *in vitro* models to Hh paracrine stimuli was tested using a trans-well system with PANC1 pancreatic epithelial cells. MSC S.P. obtained by culturing low passage MSCs for as few days as possible in MSCM (in order to keep them undifferentiated) was also included as a negative control.

The mSCN models tested in this experiment are the following:

- 1) MSCs cultured in DMEM 10% for 1 week (mSCN model 1)
- 2) MSCs S.P. mixed in 1/1 proportion with MF-like cells (obtained by treating MSCs with TGF- β for 1 week). This co-culture was performed in MSCM (mSCN Model 2)
- 3) MSCs S.P. mixed in 1/1 proportion with MF-like cells (obtained by treating MSCs with TGF- β for 1 week). This co-culture was performed in DMEM 10% medium (mSCN Model 3)
- 4) MSCs cultured for 1 week in DMEM 10% (considered in this context as source of MF-like cells) and mixed with MSC S.P. This co-culture was performed in MSCM in order to “fix” the stage of cell differentiation (mSCN model 4)
- 5) MSCs cultured for 1 week in DMEM 10% (considered in this context as source of MF-like cells) and mixed with MSC S.P. This co-culture was performed in DMEM 10% (mSCN Model 5)

The Hh paracrine induction in these models was analysed *via GLI1* gene expression and Ptch1 protein expression.

GLI1 gene expression (Figure 5.31) and Ptch1 protein expression (Figure 5.33) showed an increase in all models (mSCN model 3 and 5) performed in free differentiation media (DMEM 10%) but no changes were observed neither in *GLI1* gene expression nor in Ptch1 protein expression in mSCN Model1 [MSC cultured in free differentiation media (DMEM10%) for 1 week]. An unexpected result was the increase of the Hh pathway activity in the negative control (MSC S.P.) after co-culture with pancreatic epithelial cells. However, all other models performed in MSCM did not show any stimulation of the pathway. mSCN model 5 [MSC cultured for 1 week in DMEM 10% (considered in this context as source of MF-like cells) mixed with MSC S.P. showed the highest Hh paracrine induction by epithelial cancer cells.

Thus, the ratio between the two populations (MF-like cells and MSCs) is crucial in the constitution of a mSCN *in vitro* model and can affect the responsiveness to paracrine stimuli.

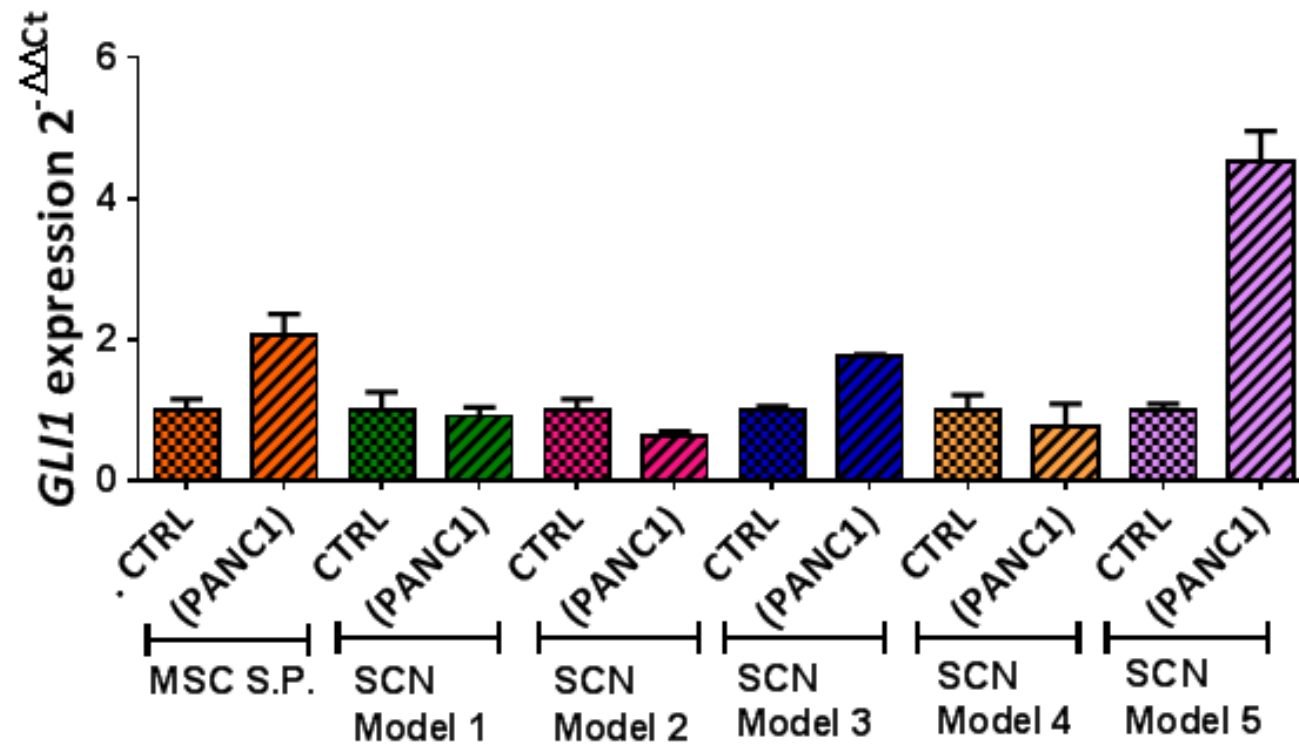


Figure 5.32 Comparison between different mSCN models in their responsiveness to Hh paracrine signalling: *GLI1* gene expression analysis in 5 different mSCN *in vitro* model co-cultured in a TW system with pancreatic cancer cells (Panc1) known to highly express Shh ligand. In general only the models performed in free differentiation media were responsive and the mSCN model 5 showed the highest induction.

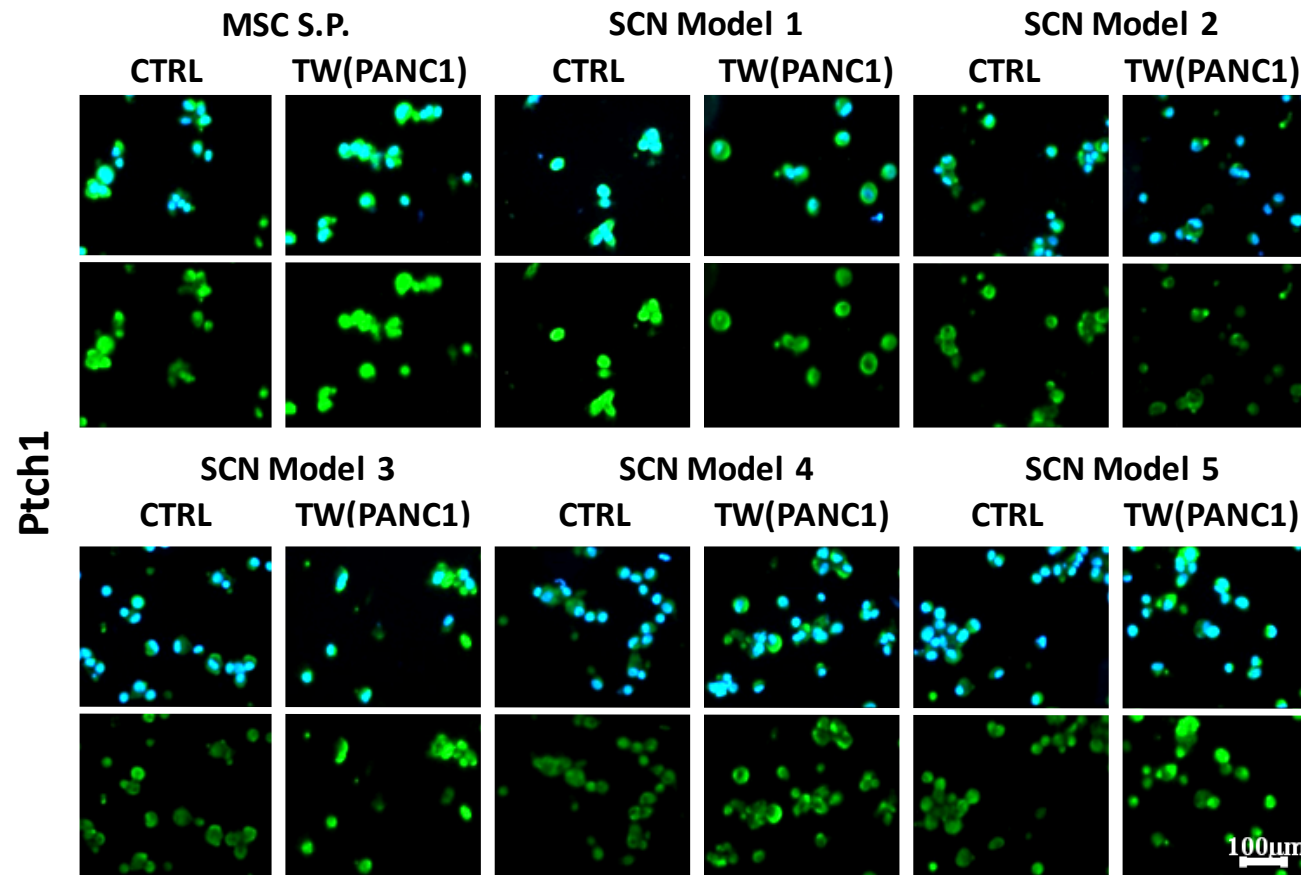


Figure 5.33 Ptch1 protein expression induction by Hh paracrine signalling in different mSCN models: Ptch1 protein expression was used as markers of responsiveness of 5 different mSCN *in vitro* model to Hh paracrine stimuli. In general only the models performed in free differentiation media were responsive and the mSCN model 5 showed the highest induction.

5.7 Summary of results

Summarising the results described in this chapter:

- MSCs showed some responsiveness to Hh paracrine induction only after 14 days of paracrine stimulation by TCM. However in general NShh, TCM and 2D co-culture did not induce any consistent effect on Hh pathway expression. The explanation of these results is probably the tendency of the medium used to carry out all these assays, to keep MSCs in an inactivated and undifferentiated state.
- The effect of MSCM in keeping MSCs inactivated was confirmed by experiments in free differentiation media (PCA, DMEM 0.5 %). In these media, MSCs tend to differentiate into myofibroblast-like cells as indicated by the increase of α SMA gene and protein expression.
- The expression of the Shh signalling pathway seems to occur when the myofibroblast-like population forms.
- The investigation of TGF β treatment on MSCs activation seems to suggest an effect of this growth factor in promoting this process.
- Investigation of the effect of TGF β on the Hh pathway seems to suggest a decreasing effect. However, incongruence between gene and protein expression lead to the necessity of further investigation.

- *GLI1* and *ACTA2* gene expression correlated after treatment with TGF β suggesting an involvement of a non-canonical pathway in the regulation of *GLI1* expression.
- Shh gene and protein expression significantly increased in a mSCN *in vitro* model obtained by mixing MSCs and MF-like or CAF cells in different ratios. An increase in Shh was also observed in single populations of MSCs over time together with an increase in α SMA and Postn.
- CAFs removed from an *in vivo* context are not fully activated cells and their activation can be induced by growth factors present in the FBS in free differentiation medium.
- Shh gene and protein were highly expressed in mixed populations in comparison to the two single populations of CAFs (fully activated) and MSCs (undifferentiated), suggesting Shh is a marker of the mixed populations.
- The mSCN *in vitro* model seems to be the best context in comparison to MSC and CAF single populations for a response to Hh paracrine stimuli. However, different mSCN models respond differently to paracrine stimuli indicating a key role of the ratio between the two populations in this response.

Chapter 6 - Discussion

6.1 Results overview

The investigation of Hh signalling pathway in PDAC performed in this study resulted in a number of novel outcomes. The most important of them was the demonstration of Shh ligand expression not just at the epithelial level but at the stromal level too. This aspect could open up a new chemotherapeutic approach in the fight against this type of cancer that still has a poor prognosis and weak therapeutic strategies [Hidalgo *et al* 2010]. The evidence of Shh expression at the stromal level is supported by a number of reports in the literature [Becher *et al* 2008; Quante *et al* 2011; Siu Wai Tsang *et al* 2013] but its role in this context is still not clear.

In this study, Shh was observed to be expressed at the gene and protein level by a mixed population comprising MSCs from bone marrow and MF-like cells (activated αSMA^{+ve} cells) representative of an *in vitro* mSCN (mesenchymal stem cell niche) model. This result is in agreement with the Quante *et al* work in gastric cancer that showed the same increased expression of *SHH* in a mixed population. Moreover, in this study, the role of Shh in the mSCN was further investigated demonstrating Shh expression by MF-like cells but only in a mSCN context. This observation suggests that Shh may be a marker of the mSCN within the tumour microenvironment. Furthermore, stromal expression was high in poorly differentiated tumour (PDT) co-locating the mesenchymal stem cell niche in the late stage of PDAC and

highlighting Shh as an interesting target, particularly at this stage of pancreatic tumour progression.

In the literature, the role of the Hh pathway in PDAC suggests paracrine transmission between epithelial cells and stromal-like cells [Yauch *et al* 2008, Tian *et al* 2009]. In order to further investigate this signalling transmission CAFs and MSCs (both known to be components of the tumour microenvironment) were tested for their responsiveness to Hh paracrine signalling using a panel of pancreatic cancer cells. Interestingly both CAFs and MSCs showed a variable and small degree of paracrine induction of Hh pathway, which suggests the inability of these cells to individually respond to Hh paracrine stimuli. Based on this evidence and taking into account the expression of Shh in the stromal context and its role as a marker of the mSCN, the response to Hh paracrine signalling within mSCN was then investigated. Different *in vitro* models of the mSCN were able to respond to tumour paracrine stimuli as measured by triggering downstream of Hh pathway components to a greater degree than single populations such as CAFs, MF-like cells or MSCs alone.

In this chapter these results will be further discussed as well as their utility from a point of view of developing novel chemotherapeutic approaches.

6.2 Shh is over-expressed in primary tumour pancreatic tissues at the epithelial and stromal level

The expression of the Hh pathway in different types of cancer has been described in many papers [Tao *et al* 2011; Bian *et al* 2007 ;Chen *et al* 2009, Yuan *et al* 2007; Feldman *et al* 2008; Xu *et al* 2009]. Hh signalling was investigated in particular in pancreatic cancer and contrasting data supported both autocrine [Thayer *et al* 2003] and paracrine transmission [Yauch *et al* 2008; Tian *et al* 2009] of this pathway in this tumour. Moreover, the involvement of the pathway in different stages of pancreatic tumour progression has been demonstrated [Thayer *et al* 2003; Morton *et al* 2007; Bailey *et al* 2008]. Considering the fact that the role of the Hh pathway in cancer in general and in particular in PDAC still needs clarification, this study was focused on investigating the Hh pathway mechanism of action in pancreatic cancer.

6.2.1 SHH ligand is over express in pancreatic primary tissue in comparison to lung tissues

SHH gene expression was investigated in this study in 14 paired normal and tumour human pancreatic tissues (28 in totals) and in 12 normal and 35 tumour human lung tissues. This analysis showed an over-expression of the Hh ligand in pancreatic tumours, in comparison to the normal samples, with few exceptions (only 2 patients) in which normal samples showed a higher expression than in tumour samples

(Figure 3.1). The overexpression of *SHH* at gene level in tumour was confirmed by investigation of Shh at the protein level (Figure 3.6 and 3.7). Moreover, investigation of the Hh pathway activity (*GLI1* expression) confirmed this result (Figure 3.3). In pancreatic tissues, *SHH* expression was also compared with the expression of the other two Hh ligands (*DHH* and *IHH*). *IHH* was over-expressed in tumour samples but the level of expression was much lower than that of *SHH*. Also, neither *DHH* nor *IHH* was expressed in several tumour tissues leading to the idea that *SHH* is the main Hh ligand which acts in pancreatic cancer (Figure 3.1). In agreement with this hypothesis, almost all the literature existing on the role of the Hh pathway in pancreatic cancer exclusively focuses on the analysis of Shh ligand expression at the gene and protein level with Shh shown to be over-expressed in pancreatic cancer [Thayer *et al* 2003; Bailey *et al* 2008; Singh *et al* 2012]. For these reasons, this study focused on Shh and Dhh/Ihh was not further investigated.

In this study, Hh pathway expression was also investigated in lung tumours. Higher expression of *SHH* was observed in normal samples than in tumours. Moreover, the low *SHH* level of expression in lung tumour samples suggested the lack of an important role for this pathway in this type of tumour. Finally, the analysis of the Hh pathway activity (*GLI1* gene expression) in the same human lung normal and tumour samples confirmed this conclusion. The expression of *SHH* and *GLI1* was also analysed specifically in two different type of lung tumours: SCLC (13 samples) and NSCLC (17 samples) (data not shown). This

investigation confirmed no overexpression of the Hh pathway in either tumour type. However, the number of tumour samples included in this analysis was quite low so perhaps a further analysis with more primary samples could better clarify the role of the Hh pathway in this type of tumour. In agreement with the results shown in this study, a recent study in NSCLC showed very low expression of Shh at the gene and protein level and no correlation with the clinical outcome [Savani *et al* 2012]. On the other hand, other studies were in contrast with this conclusion and showed over-expression of Shh at the gene and protein level in SCLC and NSCLC tumours at the epithelial level [Watkins *et al* 2003; Gialmanidis *et al* 2009, Yuan *et al* 2007]. Thus, the role of the Hh pathway in lung tumours is still not clear and a further investigation on it could be interesting to clarify the discrepancy found in the literature.

6.2.2 Shh is over-expressed in pancreatic cancer not only at the epithelial level but also at the stromal level.

The over-expression of *SHH* at the gene level in pancreatic tumours led to the investigation of its expression at the protein level in primary human normal and tumour pancreatic tissues .

19 paired normal and tumour samples plus 1 unpaired tumour samples (39 samples in total) were investigated for Shh protein expression, initially considering its overall expression in the entire tissues. Then, Shh expression specifically at the stromal level and at the epithelial level was also analysed to further understand the role of the Hh pathway not just at the epithelial but also at the stromal level and to

correlate it with tumour aggressiveness. Tumour aggressiveness was evaluated as level of histological differentiation within tumour samples and classified as normal tissues (NT), moderately differentiated tissue (MDT), or poorly differentiated tissues (PDT). The Shh and, as discussed later, the Ptch1 proteins expression at the stromal and epithelial level were quantified by eye and expressed as percentage. This method has some limitations due to the fact that is a consequence of a subjective valuation and not of computer software, and for this reason has to be considered a semi-quantitative system. This approach was, however, chosen based on the fact that a quantification of the protein investigated in two distinct compartments (stromal and epithelial) of the same tumour sample it would have required manual selection of the areas to quantify and so it would have been affected by variability and loss of accuracy related to a subjective valuation. Generally, the IHC quantification of a protein should take into account the relationship between the number of cells expressing the protein (stained) with the total number of cells (stained and unstained cells). In a context such as that of pancreatic cancer with a very high stromal content, a high percentage of extracellular matrix between the cells is present. Considering this aspect, another and more important reason for use of the semi-quantitative approach, is that computer software would have not been able to correctly calculate the total stromal area based on the number of total stained and unstained stroma cells but it would have erroneously included the ECM component, misleading the final calculation of the percentage protein expression.

To improve the reliability of the data obtained each section was divided into 6 squares and the average of the quantification obtained in each square calculated. Moreover, the quantification was confirmed by a second blinded observer. However, a semi-quantitative approach, by its nature, should not be expressed as a percentage and a ranking system might be more appropriate in this context.

This study showed up-regulation of Shh (H-score) in poorly differentiated pancreatic tumours highlighting a role of the Hh pathway in the advanced stages of PDAC (Figure 3.6 and 3.7). However, this result does not necessarily imply that the expression of Shh occurs exclusively at the late stage of tumour progression. Statistical analysis performed in this study did not show any difference between Shh protein expression in NT and MDT. However, normal samples included in this study are obtained from patients affected by tumours, and taken at the resection margin. For this reason, in some cases, NT samples may have unexpected expression of Shh because the sample taken contained some tumour cells. This could slightly affect the statistical comparison of NT and MDT samples, leaving open the possibility of an increased expression of Shh also in less aggressive tumours. Evidence from the literature has shown absence of Shh expression in normal tissues and its expression in the precursor lesion PanIN of pancreatic tumour, as well as in advanced stage primary tumours and metastasis [Thayer *et al* 2003].

The highest overall expression of Shh in PDT samples could be explained by increasing percentage of stromal Shh expression in more

aggressive tumours observed in this study (Figure 3.11). In MDT samples the expression of Shh was mainly at the epithelial level (Figure 3.11 A) whereas PDT showed a much higher stromal Shh expression. The Shh over-expression in pancreatic PDT samples could be a consequence of expression of Shh at the stromal level exclusively in advanced tumours or an outcome of an increasing stromal component with pancreatic tumour progression. In line with this last theory, Shh expression at the stromal level correlated in this study with vimentin staining (used to quantify the stromal component) (Figure 3.9 B), indicating that Shh is expressed at the stromal level and its expression in PDTs increases as a consequence of the stromal component increasing at this stage of pancreatic tumour progression. Considering this result, a significant increase of stromal component (vimentin staining) along with tumour progression was expected. However, statistical analysis of vimentin quantification in NT, MDT and PDT (performed with accurate computer programs as average of 6 different sections for each sample) did not confirm a significant difference. Nevertheless, the analysis by eye of 6 images for each section in the three groups considered, strongly suggested a gradual increase of stromal component starting from NT, through MDT, to PDT (Figure 3.8 A). The criteria chosen to distinguish stromal component from epithelial component was focused on the cell shape, and the different cell organisation. The discrepancies between instrumental quantification and observation by eye regarding the vimentin expression are hard to explain but could be a consequence of the relatively small number of

samples analysed. A number of studies have confirmed the strong increase in the desmoplastic effect in pancreatic tumour that often starts with pancreatitis and then degenerates further to PDAC [Chu *et al* 2007; Korc *et al* 2007; Feig *et al* 2012; Merika *et al* 2012]. This change is a consequence of the interplay between epithelial cancer cells and pancreatic stellate cells that in normal tissues are in a quiescent state. The progression of cancer triggers different signalling pathways (including Hh pathway) which activate PCS (inducing their proliferation) and elicit the proliferation of other resident fibroblasts and the recruitment of MSCs from bone marrow, leading to an overall increase of the tumour stromal component characterised from a gene expression signature specific of the tumour profile [Crnogorac-Jurcevic *et al* 2001; Chu *et al* 2007; Korc *et al* 2007; Bailey *et al* 2008; Feig *et al* 2012].

The observation of Shh expression at the stromal level in different types of cancer has only been previously observed in a small number of studies [Quante *et al* 2011; Becher *et al* 2008]. In particular, the detection of Shh in pancreatic cancer stroma was only recently observed in work focused on the inhibition of the PSC proliferation by treating them with 10 μ M of Rhein (a Natural Anthraquinone Derivative). This treatment resulted in decreased Shh, Gli1, α SMA and TGF β expression in these cells [Siu Wai Tsang *et al* 2013] and confirmed the expression of the Hh ligand in the tumour stroma observed in this study. However, no further investigation has been done yet on Hh autocrine signalling at the stromal level.

The funding of Shh expression at the stromal level may have important implications for cancer therapy. In fact, Shh could be a new target to reduce the stromal component, which is known to have important role in sustaining tumour progression and also in affecting drug delivery [Olive *et al* 2009; Kucerova *et al* 2010; Brentnall *et al* 2012].

The investigation of Shh at the epithelial level was also performed in this study to clarify Shh epithelial expression and its impact on the stromal component and on the Shh expression at the stromal level. An interesting correlation was observed in NT, MDT and PDT pancreatic tissues between Shh expression in the two components (epithelial and stromal) analysed, indicating an increase in Shh stromal staining with increased Shh epithelial expression (Figure 3.10). This evidence together with the correlation between Shh epithelial expression and vimentin staining (stromal component quantification) (Figure 3.9A) highlighted a possible role of Shh at the epithelial level in promoting the desmoplastic effect typical of PDAC. This observation is supported by studies in which *in vitro* and *in vivo* experiments showed the induction of pancreatic stromal proliferation and activation by a paracrine effect triggered by Shh expressed in cancer epithelial cells [Bailey *et al* 2008; Jung *et al* 2011]. Moreover, the Hh paracrine reactivation in the stromal component was also observed to correlate with development of fibrosis in kidney and non-alcoholic steatohepatitis [Syn *et al* 2011; Fabian *et al* 2012].

All these results taken together led to further investigating the mechanism of the Hh pathway transmission in PDAC and the role of Shh expression in the stromal component.

6.2.3 Hh downstream pathway expression suggests the existence of both paracrine and stromal autocrine signal in PDAC.

In order to clarify the mechanism of the Hh pathway transmission in PDAC, Ptch1 (Hh pathway gene target expression) at the gene and protein level was investigated in this study as an indicator of the Hh pathway activity.

The overall expression analysis of Ptch1 at the gene and protein (H-score) level did not show a difference between NT, MDT and PDT tissues (Figure 3.12), in contrast with what was observed for Shh gene (Figure 3.2) and protein (Figure 3.7) expression and for *GLI1* (Figure 3.3) gene expression which were over-expressed in tumour samples. However, higher expression of Ptch1 was observed both in the stromal and in the epithelial component of tumour samples in comparison to normal samples (Figure 3.15), although the difference was not significant. The non significance of statistical analysis could be explained, as for Shh analysis, in the origin of normal tissues that showed the same tumour-like zones that could have altered the outcome.

In agreement with these observations, evidence from the literature showed the over-expression of Ptch1 both in epithelial pancreatic cancer cells and in the pancreatic cancer stromal component

[Nakamura *et al* 2007; Tian *et al* 2009]. In fact, the inhibition of Ptch1 expression in two different cancer epithelial pancreatic cells (PANC1 and SUIT2), by using a specific antibody, reduced the Hh pathway expression (detected as *GLI1* and *PTCH1* gene expression) in these cells as well as their proliferation [Nakamura *et al* 2007]. On the other hand, transgenic mouse models were responsive to the constitutively expression of the oncogene allele SmoM2 (a mutation in the exon 2 of the Smo gene sequence) only when it was expressed in the mesenchymal compartment of the pancreas but not in the epithelium [Tian *et al* 2009].

As for Shh, correlation analysis between Ptch1 protein expression in the two tissue compartments (stromal and epithelial) and the amount of stroma (vimentin staining) (Figure 3.14) was made in this study. The goal of this analysis was to investigate the effect of Hh pathway expression at the epithelial level on the desmoplasia (typical of PDAC progression) and the investigation of increased Hh pathway activity at the stromal level with an increased stromal component, as observed for Shh protein. However, this analysis did not show any correlation. The fact that Ptch1 at the epithelial level did not correlate with the amount of stroma in MDT and PDT samples was not surprising and in agreement with the literature. Bailey *et al* 2008 showed that desmoplasia in PDAC progression is a consequence of a paracrine and not autocrine Hh signalling transmission. However, the lack of correlation between Ptch1 at the stromal level and the stroma amount was in contrast with the hypothesis of an increase of Hh pathway activity in the stroma over the

desmoplastic effect. In order to clarify this discrepancy and better understand the type (autocrine/paracrine) of Hh signalling in the PDAC context, correlation analysis between Shh and Ptch1 at the epithelial and stromal level in all possible combinations (Figure 3.16) was carried out. This showed a significant association between Shh expression at the epithelial and stromal level with Ptch1 expression in the stromal component. These results seems to exclude an autocrine Hh transmission signalling in the cancer epithelial cells and support paracrine signalling between cancer cells and the tumour microenvironment but also a possible autocrine signalling in the stromal cells. A number of studies strongly support the hypothesis of Hh paracrine transmission in PDAC [Yauch *et al* 2008; Tian *et al* 2009; Bailey *et al* 2008; Nakamura *et al* 2010]; in contrast, the possibility of autocrine Hh signalling transmission in the stromal component has not previously been demonstrated, highlighting the novelty of these results and the need for further investigation of this aspect.

6.3 Hh pathway expression in epithelial and stromal pancreatic tumour cells

Based on the Hh pathway analysis in primary pancreatic tissues, a need to further understand the mechanism of transmission of the Hh pathway in PDAC emerged. A panel of epithelial cancer cells (PANC1, BXPC3, P308T and PAN1) and cancer associated fibroblast (CAFs) from pancreatic tumours was analysed for basal expression of the Hh pathway (Figure 4.1). *SHH* gene expression was higher in epithelial pancreatic cells in comparison to pancreatic CAFs (Figure 4.1) and protein expression analysis confirmed its expression in epithelial cells especially in the PANC1 pancreatic tumour cell line (Figure 4.2).

These results confirmed the observations in the literature of over-expression of the Hh pathway in tumour cells and suggested epithelial pancreatic cells as a source of Shh ligand expression [Berman *et al* 2003; Thayer *et al* 2003; Morton *et al* 2007; Yang *et al* 2013].

Moreover, as observed in primary tissues *SHH* was much more highly expressed than the other two Hh ligands: *DHH* and *IHH* (Figure 4.1). *IHH* was, however, significantly more highly expressed in epithelial cancer cells than CAFs. Considering also its higher gene expression in primary PDAC in comparison to NT (Figure 3.1) a role of this ligand in pancreatic cancer cannot be excluded and could be interesting to further investigate to look for a possible synergistic effect between the two Hh ligands in the PDAC context. In agreement with this observation, in the literature, the *Ihh* ligand was observed to be reactivated and to be

simultaneously over-expressed with Shh in pancreatic cancer [Berman *et al* 2003; Kaye *et al* 2004]. The analysis of the same pancreatic cells for *SMO* and *GLI1* expression showed a significantly higher expression of both genes in pancreatic CAFs in comparison to epithelial cancer cells.

The above gene expression analysis of the Hh pathway in epithelial cancer cells and in CAFs seems to suggest a role of epithelial cells in secreting the Hh ligands and the ability of stromal cells to respond. However, correlation analysis between the main genes of the Hh pathway and the markers of epithelial (*CDH1*) and of mesenchymal (*VIM* and *HGF*) phenotype, performed in this study, left open the possibility of downstream pathway expression in epithelial cancer cells. In fact, *GLI1* and *SMO* expression correlated with *CDH1*, an indicator of an epithelial phenotype, indicating that autocrine Hh pathway transmission signalling could be possible in epithelial pancreatic cancer cells. As expected, *SHH* also correlated with *CDH1*, again associating the ligand secretion to the epithelial cell type. On the other hand the *SMO* and *PTCH2* expression correlation with the expression of the markers of mesenchymal cells chosen in this study (*VIM* and *HGF*) kept open the role of the CAFs as the cells in which the Hh pathway can be triggered and that are able to express its gene targets. These results, taken together, seem in contrast with the autocrine signal at the stromal level suggested by the analysis of the Hh gene and protein expression in primary tissues. This discrepancy could be explained by the fact that in the *in vitro* stromal context, CAFs do not have the same properties as

in the *in vivo* context. Consistent with this hypothesis is in fact the observation, investigated in this study, that CAFs *in vitro* are not fully activated and can further increase α SMA and Postn expression at the gene and protein level when stimulated by growth factors such as those contained in culture medium (Figure 5.22; .23; 5.24). This aspect will be further discussed later on in this chapter.

The existence of different types of the Hh transmission is in keeping with observations in the literature on PDAC, which demonstrate autocrine signalling at the epithelial level [Thayer *et al* 2003; Xu *et al* 2009] as well as paracrine transmission between cancer cells and tumour microenvironment [Yauch *et al* 2008, Bailey *et al* 2008; Tian *et al* 2009]. Since the evidence supporting both mechanisms of transmission are strong it seems possible that both occur. However, many questions arise from this possibility, such as if there is a correlation between tumour stage and type of the Hh transmission, if different experimental approaches can influence the type of signalling observed, whether different tumours show different types of transmission, or if only specific cell types are able to receive the Hh stimuli and trigger its downstream signalling activating the expression of its gene targets. In this study this last aspect was further investigated.

6.3.1 Pancreatic CAF or MSCs alone are not able to respond to Hh paracrine stimuli in 2D *in vitro* assays.

To further characterise the ability of cells to respond to paracrine induction of the Hh signalling by epithelial pancreatic tumour cells,

MSCs and CAFs were included in this study and investigated for their paracrine responsiveness taking into account their different levels of activation. This analysis originated from the idea that different levels of activation could affect a cell's ability to respond to Hh ectopic stimuli and also to support tumour growth and progression.

Studies on Hh pathway paracrine transmission have been carried out both *in vivo* and *in vitro*. Stromal origin cells from xenograft mice or human tumours were shown able to respond to Hh paracrine stimuli by triggering Hh pathway downstream signalling and expression of its gene targets [Yauch *et al* 2008; Tian *et al* 2009; Bailey *et al* 2008]. However, correlation studies between responsiveness to Hh paracrine stimuli and the level of cell activation have provided contrasting results.

Shh was observed to promote stromal cell activation into myofibroblast-like cells (detected as increase of α SMA), with their proliferation resulting in increased desmoplasia in pancreatic cancer and increased fibrosis in renal interstitial fibrogenesis [Bailey *et al* 2008; Ding *et al* 2012]. These observations suggest two important aspects: cell activation measured by α SMA expression can be induced by the Hh pathway and cells not completely differentiated and activated are the ones responsive to Hh paracrine stimuli. In agreement with this last statement, in normal prostate development Shh triggers the Hh pathway in mesenchymal multipotent cells by paracrine induction [Lamm *et al* 2002] and also in normal adult gut, by the same mechanism, seems to affect the localisation and formation of myofibroblast cells

(characterised by a reduction of desmin expression and a parallel increase in α SMA expression) [Zacharias *et al* 2011].

In contrast, in prostate cancer only tumour with an already-activated myofibroblast (expressing α SMA and vimentin) component, defined as reactive tumour, had the relevant phenotype (defined with a nine gene target signature) to respond to Hh paracrine induction from epithelial tumour cells. This could suggest that cells need to be completely differentiated and activated to be responsive to Hh stimuli [Shaw *et al* 2009]. Moreover, in line with this last observation, a comparison between CAFs (considered fully activated and differentiated cells) and NAFs (Normal Associated Fibroblasts) from pancreatic tumour showed a significantly higher expression of SMO in α SMA and vimentin positive CAF cells (myofibroblast signature), and increased Gli1 expression after N-Shh stimulation was observed [Walter *et al* 2010].

Taken together this raises the question of a possible correlation between the level of cell activation, required for the acquisition of a myofibroblast-like phenotype, and the ability of stromal cells to respond to paracrine induction.

In order to then further investigate the role of cell activation on the responsiveness to paracrine MSCs (undifferentiated cells) and CAFs cells (fully differentiated cells) were included in this study.

MSCs came from human bone marrow and, as said, were chosen for their property of being able to be activated (acquisition of α SMA expression vimentin, desmin, Collagen Type 1) [De Wever *et al* 2008] and for their ability to support tumour progression and express, in

response to the interplay with tumour cells, a panel of genes correlated with an aggressive and invasive phenotype [thrombospondin-1 (Tsp-1) and tenascin-C (Tn-C)] [Tuxhorn *et al* 2002; Spaeth *et al* 2009]. On the other hand, CAFs, which in the literature are described as highly expressing α SMA were considered fully differentiated fibroblast cells expressing FSP and FAP [Spaeth *et al* 2009].

In order to investigate the correlation between cell activation and paracrine responsiveness, the experimental design included NShh treatment in 2D assays as well as direct and transwell co-culture and treatment with TCM.

NShh treatment of pancreatic CAFs was performed 3 times on the same cell lines (P5T). In a first analysis, two similar experiments (one experiment performed including 2 wells repetition and one with no repetitions, 3 replicates in total) were performed in the same conditions and showed identical results (Figure 4.5): NShh treatment on P5T CAFs did not induce Hh pathway paracrine signalling (detected as *GLI1* and *SMO* expression) or cell activation (detected as *ACTA2* gene expression) in P5T cells (Figure 4.5). Finally, a third experiment was performed by using the same NShh doses used in all previous experiments but also testing additional time points (D0; D3; D6). This experiment was a single assay and the results were shown for two wells replicates. Again no induction in P5T CAFs of the Hh pathway and cell activation was observed after this treatment at any of the time points tested (Figure 4.6). In this experiment, the analysis of only two wells replicates for one experiment did not allow a proper statistical analysis.

However, figure 4.5 represents the results of 3 replicates under each experimental condition where the statistical analysis for the comparison of treated and control sample did not show any significance. Summarising, the first overall view of the three experiments suggested that the NShh treatment did not have a consistent effect in pancreatic CAFs.

A similar experiment to investigate NShh effects on MSCs at different time points (Day 3, 6 and 9) did not show any Hh induction or cell activation (Figure 5.1) resulting in the same conclusion as for CAFs being reached for these cells. This experiment was performed as single assay by including 2 well repetitions.

The effect of TCM on CAFs and MSCs was analysed in this study by growing both types of cells for 3 and 14 days in conditioned media obtained from a panel of pancreatic cancer epithelial cells (PANC1, BXPC3, PAN1, P308T) that showed different levels of Shh expression at the gene and protein level. As a great number of cells was needed to perform these experiments, only one well/flask was plated. 2 CAF cell lines showed variable changes (decrease and increase) in the Hh target gene expression (*GLI1* and *PTCH1*) and in cell activation (*ACTA2* expression) (Figure 4.7). The same experiment was carried out using MSCs with different passages (lower and higher) and showed a slightly more consistent induction of the Hh pathway and cell activation after 14 days of cell culture, but still low and variable (Figure 5.3 and 5.4). These results led to trying different experimental approaches that allows

exposure of the mesenchymal cells to constant secretion of the Hh ligand in the 2D transwell and direct co-culture assays.

Three different trans-well co-culture experiments were performed using the same CAFs included in all assays performed in this study (P5T and P3T) (Figure 4.8; 4.9; 4.10). These experiments were carried out once by carrying out 2 well repetitions under each experimental condition. The sequence of these experiments was characterised by a progressive analysis that included the use of different pancreatic epithelial cancer cells, use of additional time points and analysis of more Hh gene targets. No responsiveness of CAFs to Hh paracrine induction from epithelial cells and no effect of the Hh pathway on cell activation or, *vice versa*, no effect of cell activation on the responsiveness to Hh paracrine stimuli was observed. The same transwell co-cultures were tested using MSCs at different passages (and so with different levels of activation). These cells also did not show responsiveness to Hh paracrine induction (Figure 5.5). Finally, direct co-culture between epithelial cancer cells and CAFs excluded the need for cell contact as a reason for lack of observation of responsiveness to Hh stimuli (Figure 4.11). The conclusions of all these experiments highlighted the fact that both CAFs and MSCs in the condition used in this study were not able to respond to Hh paracrine stimuli and moreover cell activation did not seem a factor that affected this ability. Thus, no further experiments investigating modulation of the Hh pathway were performed using CAFs or MSCs. An exception to these observations was found in *ACTA2* expression after transwell co-culture, as well as in *GLI1* and *ACTA2*

expression after direct co-culture in CAFs (P5T) with BXPC3 cancer cells (Figure 4.10B and 4.11) However, neither *GLI1* nor *ACTA2* expression increases for this condition were consistent in the two well repetitions performed in each experiment in these co-culture assays. This fact influenced the reliability of these results and would have affected the significance of a statistical analysis for the comparison of the control (CAF's co-cultured with themselves) and the co-cultured samples.

As explained, in all these assays the results of each experiment was derived from the average of results for 2 wells plated in parallel during the same experiment. In case of TCM assay only one well/flask was plated. This could have affected the reliability of the results in which the changes observed in the Hh pathway gene expression could have reached significance, although very low. It was in fact not possible to test the significance of the conclusion reached in these assays, due to the low statistical power of the experimental design. Ideally, the data would be the result of multiple independent experiments. However, it is important to note that, as shown above, the experimental plan used in this study followed a strict line of progression in which each experiment was repeated, but focusing on those conditions which appeared to influence the experimental outcome (time, dose of treatments or cell type). The goal of this plan was to move forward the investigation of the hypothesis and maximise the experimental conditions tested.

The above results seem in contrast with studies that support the idea of paracrine induction of the Hh pathway in stromal cancer cells in PDAC

(constituted by both CAFs and MSCs) [Yauch *et al* 2008, Bailey *et al* 2008]. The treatment of CAFs or MSCs with recombinant rShh has been observed to induce the increase of *GLI1* and *PTCH1* gene expression [Chan *et al* 2012; Li *et al* 2008; De Wever *et al* 2008]. Transwell co-cultures were also used in other studies focused on the characterisation of the cancer stromal cells ability to respond to Hh pathway paracrine signal. Both MSCs and CAFs populations were shown to increase Gli1 and Ptch1 expression when co-cultured with cells over-expressing Shh [Li *et al* 2008; Domenech *et al* 2012, Chan *et al* 2012]

The reason for these discrepancies may be explained by the experimental conditions in which NShh treatment and the co-cultures were performed. In this study, all *in vitro* experiments with CAFs and MSCs were performed in MSCM with 5% of FBS, demonstrated to be able to keep the cells in an inactivated (no α SMA expression) state. In the literature, the induction of the Hh pathway in myofibroblast or MSC cells was instead observed only in assays performed in media like DMEM 10% of FBS or RPMI 5% FBS [Li *et al* 2008; De Wever *et al* 2008; Domenech *et al* 2012, Chan *et al* 2012], classified in this project, as free differentiation media. These observations, opened the possibility that stromal cells, in order to be responsive to Hh paracrine, needed to be free to become activated and, moreover, suggested the necessity of investigating the effect of MSCM on cell activation as will be explained in the next section of this chapter.

6.4 A myofibroblast-like cell population originates from MSCs and expresses Shh ligand

Evidence from the literature showed that when quiescent hepatic stellate cells Q-HSC (a type of multipotent cell normally present in liver and considered very similar to pancreatic stellate cells) are grown in DMEM 10% they acquire a mesenchymal phenotype (M-HSC) and become activated cells, expressing α SMA, collagen and mesenchyme-associated transcription factors Lhx2 and Msx2. This activation process was demonstrated to be Hh pathway dependent [Choi *et al* 2009].

MSCM (the media used in all *in vitro* assays performed in this study) was a medium designed to grow mesenchymal stem cells. This medium contained 5% of FBS and mesenchymal stem cell growth supplement, which contains growth factors, hormones, and proteins necessary for the culture of normal human pre-adipocytes. A hypothesis formulated in this study was that the growth factors added as supplement in this media were able to keep the cells inactivated and undifferentiated.

In order to investigate this and look for the effect of other media on the activation of MSCs, these cells were grown in PCA medium (DMEM with 20% FBS) but also in DMEM 0.5% and MSCM 5% with no growth factor added (MSCM no GF). These media were chosen for their known ability to support the growth of primary cells (PCA) and in order to test the effect of low percentage of serum (DMEM 0.5%) as well as the role of the GF added during the preparation of the MSCM (MSCM no GF) on MSC activation. Different time points were tested in these experiments

and the effect on cell activation of the different media was analysed as α SMA gene and protein expression and compared with α SMA expression in MSCs grown in MSCM 5% (the media used in all previous experiments). In agreement with the literature, MSCs grown in DMEM at both percentages of FBS (Figure 5.7) showed increased α SMA expression after 3 days of culture. However, MSCs grown in MSCM no GF showed a level of α SMA expression comparable to cells grown in MSCM with GF added and significantly lower than the other two media (DMEM 0.5% and PCA). These results suggested that the GF were not the reason for MSCM's ability to keep cells inactivated. Based on these results DMEM media used in this study were considered and named "free-differentiation media" (FDM) to be distinguished from MSCM and MSCM no GF considered instead: "preventing differentiation media (PDM)".

The investigation of the α SMA trend over time in MSCs cultured for 14 days in PCA media showed an initial rapid differentiation of these cells into α SMA^{+ve} cells, and then development into a mixed population in which α SMA^{+ve} and α SMA^{-ve} cells are both present. These observations confirmed findings in the literature [Quante *et al* 2011].

The role of the Hh pathway in the induction of cell activation in Q-HSC [Choi *et al* 2009], the observation of Shh expression during liver fibrosis in a mesenchymal stem cell niche (mSCN) constitute from MSCs and MF-like cells [Lin *et al* 2008] and the strong increase of *SHH* gene expression in the mixed population in comparison to the single populations (α SMA^{-ve} and α SMA^{+ve}) [Quante *et al* 2011], led to further

investigation of Hh pathway expression in FDM. MSCs grown in DMEM 0.5% and PCA free-differentiation media showed an increase in Shh and Ptch1 protein expression. Some discrepancies between *SHH* gene and Shh protein expression was observed in these assays (Figure 5.8). The explanation could reside in the generally low expression of SHH at the gene level that made detection of its expression difficult at times. On the other hand, each q-RT-PCR performed for *SHH* was repeated twice at very high concentration of cDNA in order to reduce as much as possible the error in its detection.

The same was not true for Ptch1 that quite often showed inconsistency between the gene and protein levels (Figure 5.8). The reason for this discrepancy could be the negative feedback exerted by Ptch1 on Hh gene targets including *PTCH1* and *GLI1* (a fundamental mechanism that prevents Hh overexpression) [Goodrich *et al* 1999]. It is possible in fact that the increase of Ptch1 protein due to the increase of the Hh pathway in activated cells triggers the inhibition of the Hh gene targets (*GLI1* and *PTCH1*) and that this change took longer to be reflected at the protein level. However, in this case, *GLI1* gene expression should also have reduced, but regulation of Gli1 expression via the non-canonical pathway could hide this decrease [Nolan-Stevaux *et al* 2008]. To complicate this aspect further, there is also evidence that the inhibition of the Hh gene targets by Ptch1 can be triggered by a non-canonical mechanism that does not involve Hh pathway molecules like SUFU and SMO [Rahnama *et al* 2006]. Finally, It is possible that post-translational regulation of gene expression due to different binding of

regulatory factors to the 5'- and 3'-UTR of *Ptch1* mRNA could affect and enhance the rates of translation resulting in higher protein expression [Wilkie *et al* 2003].

In this study, due to this divergence, protein expression of *Ptch1* was considered the reliable result to be used for evaluation of Hh pathway activity. The match between Shh and *Ptch1* protein expression in the assays focused on the Hh pathway expression in activated MSCs (Figure 5.9) strongly supported the results obtained and the reliability of protein expression analysis for both these Hh molecules (Shh and *Ptch1*).

The culture of MSCs in PCA media for 14 days resulted in higher expression of the Hh pathway (Shh and *Ptch1* protein expression) after 3 days and a reduction of both on day 7 and day 14 (Figure 5.8). Considering also the peak of expression of α SMA observed after 3 days in PCA media, it seemed that Shh could be expressed by α SMA^{+ve} cells. However, correlation analysis between *SHH* and *ACTA2* gene expression did not showed significance (data not shown).

On the other hand, in the assays performed by growing MSCs in different media and in PCA media for 14 days, *GLI1* expression showed a different trend from Shh and *Ptch1* and a very similar trend was found instead between *GLI1* and *ACTA2* gene expression. This result could be interpreted as regulation of *GLI1* by a non-canonical pathway that interacts with the Hh pathway in the regulation of cell activation.

Summarising, the results discussed so far suggest the tendency of MSCM to maintain cells in an undifferentiated state and the expression of Shh and Ptch1 seem to be affected by this condition. A possible expression of the Hh pathway in αSMA^{+ve} cells was further investigated in this study as well as the correlation between *GLI1* and *ACTA2* and the possible pathway that could interact with the Hh pathway in the regulation of Gli1.

6.4.1 TGF- β treatment of MSCs triggers an increase in αSMA expression and is likely to be responsible for GLI1 gene expression regulation

The role of TGF β in the increase of αSMA expression as a consequence of cell activation and EMT has been demonstrated. TGF β was observed to be expressed by epithelial cancer cells but also at the stromal level [Hu *et al* 2003; Bardeesy *et al* 2006]. Moreover, heterogeneity in TGF β expression in stromal cells seems to affect tumour progression [Franco *et al* 2011].

Cross-reaction between TGF β and Hh signalling has also been demonstrated and seems to act at different levels. TGF β is able to induce the expression of the Hh ligand in NSCLC and in alcoholic liver disease [Jung *et al* 2008; Maitah *et al* 2011]. Moreover TGF β was observed to be able to regulate Gli1 and Gli2 expression [Dennler *et al* 2007; Nolan-Stevaux *et al* 2008]. It has also been demonstrated that Shh is able to mediate αSMA induction by TGF β in PSC directly linking these pathways [Siu Wai Tsang *et al* 2013]. Interestingly it has also

been observed that TGF β treatment of MSCs enhances the responsiveness to Shh paracrine signalling but only in the presence of epithelial cancer cells [Domenech *et al* 2012]. In contrast with this interdependence between TGF β signalling and the Hh pathway, SMAD3 (a cytoplasmic protein that act in the TGF β signalling) is able to trigger, by a non-canonical Hh-independent pathway, the Gli2 transcription factor, which in turn induced expression of Gli1 [Dennler *et al* 2007].

Considering then that the literature shows the ability of TGF β to induce expression of α SMA and Gli1 [Hu *et al* 2003; Bardeesy *et al* 2006; Dennler *et al* 2007; Nolan-Stevaux *et al* 2008], the correlation between these two molecules may be driven by TGF β . In order to confirm this hypothesis, the effect of TGF β on MSCs activation was investigated in a range of different media after 3 days of treatment and, additionally, in PCA media after 14 days of culture.

Consistent with the tendency for MSCM to keep cells in an inactivated state, TGF β treatment of MSCs induced an increase in cell activation, based on gene and protein expression, only in free-differentiation media (DMEM 0.5% and PCA media) (Figure 5.11). Culture and treatment of MSCs in PCA media for 14 days confirmed at the gene level the same induction of *ACTA2* gene expression after 3 -7 and 14 days. However, it took more time (14 days) to be able to observe the same α SMA induction at the protein level (Figure 5.10). The IF staining of α SMA in TGF β treated samples, grown in FDM, showed a more homogeneous α SMA^{+ve} population than in untreated samples, suggesting that the role

of this growth factor was to push the activation of MSCs into a single activated MF-like population (Figure 5.10).

Once the effect of TGF β on cell activation had been shown, its interaction with the Hh pathway was investigated. Again, this interaction was investigated in MSCs under the same culture conditions (cells grown and treated for 3 days in different media and in PCA media for 14 days). Considering the evidence from the literature an increasing effect of TGF β on Shh and, as a consequence, on Ptch1 was expected [Jung *et al* 2008; Maitah *et al* 2011]. Surprisingly, in both assays TGF β treatment induced a decrease in *SHH* and *PTCH1* gene expression (Figure 5.12 and 5.13). Protein expression analysis in MSCs grown in PCA media for 3, 7 and 14 days confirmed this observation. However, protein expression analysis of Shh in different media indicated an increase in Shh after treatment in media with lower concentrations of FBS (DMEM 0.5%; MSCM 5% and MSCM no GF 5%). It could then be possible that percentage of FBS, if too high, could hide (as in PCA media) the effect of the treatment. The mismatch between gene and protein expression, as explained, could be due to differences in timing of expression at the protein and gene levels. However, these observations need further investigation to reach a conclusion.

A more consistent observation was that there were often parallel changes in *GLI1* and *ACTA2* gene expression, and correlation analysis between these two molecules after TGF- β treatment was significant. This aspect strongly supports the hypothesis of regulation of GLI1 by

the TGF β non-canonical pathway as demonstrated in the literature [Nolan-Stevaux *et al* 2008].

Gli1 expression at the stromal level, then, should not be considered exclusively the result of the Hh pathway paracrine induction but also a result of a non-canonical pathway and a possible marker of acquisition of a myofibroblast (MF)-like cell phenotype.

6.5 The mesenchymal stem cell niche

The role of a mesenchymal stem cell niche made up of MSCs and MF cells (niche cells) has recently been investigated in a number of studies in order to understand the nature and composition of the tumour stromal components and better clarify their role in tumour progression and metastasis [Lin *et al* 2008; Quante *et al* 2011; Malanchi *et al* 2012; Lonardo *et al* 2012]. It has been demonstrated that MSCs are recruited from the cancer cells into the tumour microenvironment where they differentiate into MF-like cells [Ishii *et al* 2003; Spaeth *et al* 2009, Paunescu *et al* 2011]. However, investigation of the formation of the mesenchymal stem cell niche in contexts such as the desmoplastic reaction may provide a better understanding of these processes Based on the mesenchymal stem cell niche concept, MF cells (also called niche cells) derive from the differentiation of MSCs. The role of these cells is to maintain the survival and induce the proliferation of MSCs and vice versa [Lin *et al* 2008; Quante *et al* 2011]. MF-like cells derived from MSCs were demonstrated to be more aggressive than the other tumour stromal cells having a stronger impact on the promotion of tumour growth and progression [Quante *et al* 2011].

Hence, in view of evidence from the literature [Choi *et al* 2009; Siu Wai Tsang *et al* 2013] and the results observed so far, the expression of Shh ligand and probably also of the downstream Hh pathway could be a property of αSMA^{+ve} myofibroblast-like cells. However, the expression of Shh was demonstrated to increase strongly only in a mixed

population consisting of MSCs and MF-like cells [Quante *et al* 2011]. In agreement with this observation, in this study Shh and α SMA expression in MF-like cells or CAFs was not correlated suggesting that Shh expression even if expressed by MF-like cells is a consequence of the presence of a mixed population (stem cell niche) in pancreatic tumour stroma.

6.5.1 A mesenchymal stem cell niche (mSCN) model can be reproduced *in vitro* and results in up regulation of the Shh ligand

In order to investigate the role of Shh in the mesenchymal stem cell niche and its eventual expression only in a mixed population, different *in vitro* models of the mesenchymal stem cell niche were tested in this study.

MSCs were shown in the literature [Ishii *et al* 2003; Direkze *et al* 2004; Spaeth *et al* 2009; Quante *et al* 2011; Barcellos-de-Souza *et al* 2013], and confirmed in this study, to be able to differentiate into MFs/CAF, and TGF β was identified as a growth factor able to stimulate this activation [Hu *et al* 2003; Bardeesy *et al* 2006; Domenech *et al* 2012].

In this study, treatment of MSCs for one week with TGF β (10ng/ml in MSCM no GF) resulted in maximal up-regulation of ACTA2 in comparison to the untreated cells (Figure 5.11 A). For this reason, this condition was used to obtain an MF-like cell population. MSCs at low passage were grown in MSCM (demonstrated in this study to maintain cells in an inactivated state) in order to ensure the use of more stem-like undifferentiated cells. The mSCN *in vitro* models initially tested

used these two populations of cells at a number of ratios (1/1; 3/1 and 1/3).

The mixed and the unmixed populations were characterised for their expression of 4 genes (*SHH*, *ACTA2*, *POSTN*, *NES*) and, additionally in some experiments, for their expression of 3 proteins (α SMA, Shh and Postn) chosen as mSCN markers. The choice of α SMA and Nestin as markers of MF cells and MSCs is supported by the literature [Ishii *et al* 2003; Direkze *et al* 2004; Becker *et al.* 2008 Spaeth *et al* 2009, Mendez-Ferrer *et al* 2010 Paunescu *et al* 2011; Quante *et al* 2011;Barcellos-de-Souza *et al* 2013]. α SMA expression is in fact a well known indicator of MSC differentiation into CAFs [Shaw *et al* 2009; Gravina *et al* 2013] Moreover, MSC *in vitro* culture showed the expression of nestin as well as a PDGFR α ⁺-CD51⁺ subpopulation of MSC in the bone marrow stem cell niche [Moradi *et al* 2011; Pinho *et al* 2013]. Finally, the role of Shh and Postn expression as markers of a MSC and MF-like cell mixed population have recently been described [Lin *et al* 2008; Quante *et al* 2011; Malanchi *et al* 2012].

In order to investigate the effect of MSCs and MF-like cell mixing on the 4 mSCN markers, the actual gene expression values (*POSTN*, *NES*, *SHH*, *ACTA2*), obtained from the analysis of the q-RT-PCR results, were compared to the calculated values. These latter were mathematically calculated taking into account the contribution (respecting the cell proportions used) of the mSCN marker expression in the single populations that constitute the mSCN models (i.e in the 1 MSCs/1 MF-like cells model the calculated value was the average of

the $2^{-\Delta Ct}$ gene expression measures in the two single niche populations). Moreover, the trend of the mSCN markers was investigated over time in all cell populations. This analysis was used to understand the behaviour of the mSCN in culture and to compare the trend over time of the mSCN markers between the unmixed single populations and the *in vitro* mSCN models.

The graphs representing the comparison between the actual and calculated values and the mSCN markers' expression in the single populations (Figures 5.16; 5.17; 5.19; 5.20; 5.21; 5.22) were the result of one experiment. However, as explained before, the same hypothesis was tested several times (3 times in this type of experiment) but slightly varying at every step those conditions which did not show interesting changes in the gene or protein expression of the mSCN markers chosen. So, for example, in a first experiment 1/1 MSCs/MF-like mSCN-model was compared for the actual value of Shh, Postn, Nestin and α SMA at 0, 3 and 12 days of culture in FDM (DMEM 10%) to the calculated values as well as the over time trend of the mixed population was compared to that in the unmixed cells (Figure 5.16; 5.17). In a second experiment the same evaluation was performed for 0, 3, 12 and 21 days using 3/1 and 1/3 ratios (Figure 5.19; 5.20). In a third experiment the mSCN-model was obtained by mixing MSCs with primary pancreatic CAFs instead of MF-like cells at 1/1 ratios at 2, 12 or 21 days of culture in FDM (Figure 5.21; 5.22). This experimental design was carried out to guarantee at the same time the repetition of the hypothesis tested by adding new steps of investigation every time.

However, a limit of this experimental design is that it makes statistical analysis difficult.

In these experiments, the actual *SHH* expression value detected in the mSCN *in vitro* models was higher in comparison to the calculated value. This result was observed in all three assays tested (Figure 5.16; 5.19; 5.21) and it supports the idea that the mixing of two niche populations affects the Hh ligand expression and, moreover, suggests its role as marker of the mSCN. Interestingly the *SHH* gene expression increased after the 1 MSC: 1 MFs (Figure 5.16) and 1 MSC:3 MF cell mixing (Figure 5.19), but not in the 3 MSC:1 MF (Figure 5.19) model indicating that different ratios of MSCs and MF-like cells can affect the mSCN *in vitro* models and the expression of the Hh ligand. In comparison to the models obtained by mixing MSCs and MF-like cells (TGF β treated MSCs) the mSCN model obtained by mixing 1 CAF: 1 MSC showed a lower increase in *SHH* expression and only after 2 days of culture. This result can be explained by the fact that MF-like cells were directly derived from MSCs. Since CAFs or MF that originate from bone marrow MSCs are more aggressive cells, they are able to better sustain tumour growth in comparison to CAFs with other origins [Mishra *et al* 2008; Spaeth *et al* 2009; Quante *et al* 2011]. Moreover, they probably better mimic the *in vivo* mSCN that is formed in the bone marrow as a consequence of the MSC activation in response to infections or tumour progression [Lin *et al* 2008; Quante *et al* 2011]. The Shh protein expression analysis confirmed the conclusion described for the *SHH* gene expression analysis in these experiments. In general, a good

match was observed but in the 1 MSC: 1 MF-like cell model the effect of mixing took a longer time (on day 12) to be visible at the protein level.

Considering these results, the expression of *Shh* at the stromal level in primary pancreatic tumours observed in Chapter 3 could indicate the presence of a bone-marrow derived stem cell niche and suggest a new role of Hh pathway in determining the composition of pancreatic cancer stroma.

The observation that in these experiments *Shh* gene and protein expression in the mSCN-models analysed was not maintained at higher levels compared to MSCs alone at all time points (Figure 5.16; 5.19; 5.21) is interesting. An explanation of this result could be found in the analysis of the MF-like population (α SMA gene and protein expression) in the same experiments. The analysis of α SMA gene and protein expression showed a quite consistent increase in this cell population not just in the mixed population but also in MSCs alone and in MF-like cells supposed to be already fully activated (Figure 5.17; 5.18; 5.20; 5.22; 5.24). The increase in α SMA^{+ve} cells in MSCs is consistent with their property of being able to become an MF-like population when grown in FDM. Therefore, probably only the results for MSCs in the first three experiments at 2 days of culture are relevant. At this time point, the number of α SMA^{+ve} cells was probably still low enough for them to be considered a single population and a relevant control. In agreement with this conclusion, increased *SHH* gene expression in the mixed population was observed in comparison to this control (Figure 5.16; 5.19; 5.21).

Taking this argument further, MSCs grown in DMEM 10% for a longer time than 2 days could be considered as another possible *in vitro* mSCN model. This is in agreement with published data showing that MSCs in culture are able to differentiate into MF-like cells (identified by expression of a red fluorescence protein RFP under the control of the α SMA promoter), producing a mixed population [Quante *et al* 2011]. Moreover, this mixed population could survive for 80 passages or more in comparison to single FACS-sorted MF cells that became senescent after a few passages (Figure 6.1).

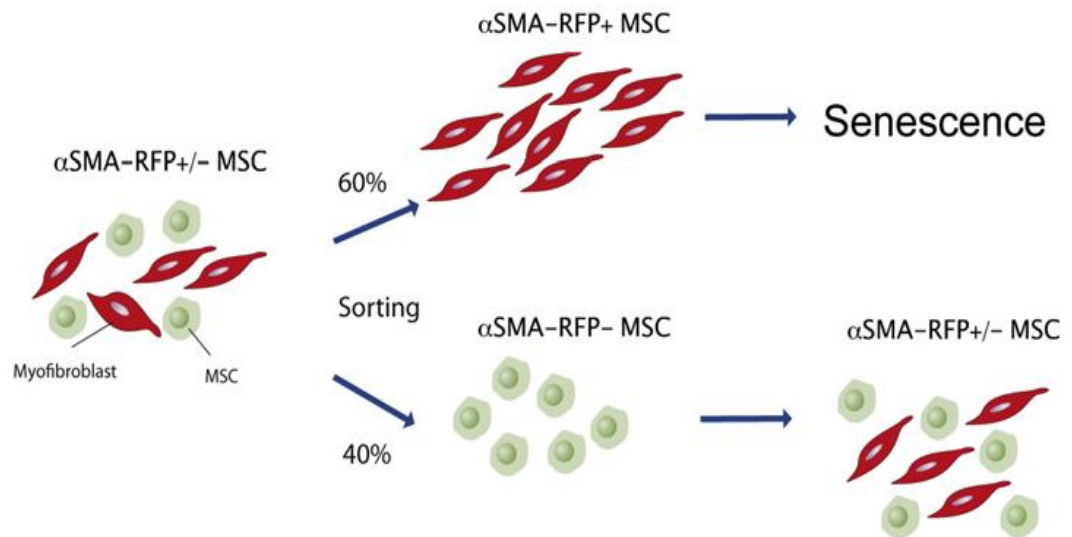


Figure 6.1 MSCs in culture are able to differentiate into MF-like cells. Picture taken from Quante, M, *et al.* *Cancer cell* 19, 257–272, February 15, 2011. Copyright licence obtained from Elsevier.

Another aspect to consider is that the expression of α SMA in MF-like cells was observed in these experiments to increase over time, suggesting that the activation obtained after TGF β treatment was not maintained (as shown from the drop down on day 2 of figure 5.16) when the treatment were interrupted at the start of each assay. This observation suggested a new view of cell activation as a transient stage

that can be reversed *in vitro* and that needs constant growth factor induction to be maintained. In agreement with this aspect, in work focused on the analysis of MSC responsiveness to Hh paracrine signalling, it has been shown that the TGF β -induced α SMA expression persists *in vitro* no longer than 72h from the suspension of the treatment [Domenech *et al* 2012].

The variability of α SMA in MF-like cells led to use of CAF primary cells, believed to be fully activated cells, in the third experiment (Figure 5.19; 5.20. Surprisingly the level of α SMA at the gene and protein level also increased in these cells over time, suggesting the reversibility of cell activation and opening a new view of CAF *in vitro* cells as not fully activated cells. Since α SMA expression is considered to be, an indicator of cell aggressiveness [Speath *et al* 2009], based on the results in this study, *in vitro* CAFs, probably lose their activation and their aggressiveness, becoming phenotypically similar to normal associated fibroblasts NAF.

Postn gene and protein is believed to be expressed in MF-like cells [Erkan *et al.* 2007] especially when part of a niche with stem cells [Malanchi *et al* 2012]. So in this study an increase in Postn was expected in a mixed population and a lower but detectable level of expression in MF-like cells or CAFs cells single population. The *POSTN* expression in the mSCN models constituted from MSCs and MF-like cells was not affected by the cell mixing (comparison actual vs calculated values) either in the 1MSC:1MF model (Figure 5.17) or in the 3MSC:1MF (Figure 5.20) models. An interesting POSTN expression

increase was instead observed after the mixing in the 1 MSC: 3 MF model (Figure 5.20) suggesting an impact of the cell ratio on its expression, as well as on *Shh* expression. However, the difference between *POSTN* expression in these mSCN models and in the MF-like cells was not large (Figure 5.17 A and D; Figure 5.20 A and D) suggesting a similar expression of this marker in single and in mixed populations. At a first glance, these results seem in contrast with the starting assumption of increased expression of *Postn* in MF-like cells when part of a mesenchymal stem cell niche. This aspect can be explained by the experimental conditions used in these assays. The MF-like cells used cannot be considered a single population due to the interruption of the TGF β treatment. This would also explain the absence of a difference in the *POSTN* expression between actual and calculated values in the mSCN models obtained by mixing MSCs and MF-like cells. In these models, the calculated value was in fact the result of the combination of *POSTN* expression in already impure single populations and for this reason probably higher than in hypothetical single populations.

In agreement with these considerations, *POSTN* expression in the mSCN model, obtained by 1/1 mixing CAFs (single population) and MSCs, markedly increased after 12 and 21 days in the actual gene expression in comparison to the calculated expression value suggesting a clear effect of the cell mixing on its expression (Figure 5.22). Moreover, its expression was much higher in this mSCN model than in CAFs alone (Figure 5.22 A and D) supporting the idea of *POSTN* as

marker of MF-like cells in the niche context. The analysis of Postn protein expression increased over time in all population tested (MSCs, CAFs, MF-like cells and mSCN models). These results, in addition to the very similar trend observed between α SMA and Postn gene and protein expression, suggest that Postn is mainly a marker of cell activation that reflects the proportion of activated cells but is expressed at highest levels in a mSCN context. In agreement, induction of α SMA by Postn expression via positive feed-back has been observed in the tumour microenvironment context [Erkan *et al.* 2007].

Finally Nestin expression remained constant in all cell populations tested, although it has been described as a marker of MSCs [Mendez-Ferrer *et al* 2010; Moradi *et al* 2011; Quante *et al* 2011; Pinho *et al* 2013]; this suggests Nestin is a poor marker for detection of MSCs in the context analysed in this study.

In summary, a number of *in vitro* mSCN models were tested; the comparison to a single population was most reliable during the first days of culture (day 0 and day 2) when MSCs could still be considered as undifferentiated. The variability of *SHH* expression depending on the ratio of MSCs to MF-like cells in the mSCN models strongly reinforced the hypothesis of its expression being dependent on the presence of a mixed population, and demonstrates the need to strictly follow the same experimental protocol when using these mSCN *in vitro* models. α SMA and Postn had been demonstrated to be good markers of activated cells (MF-like population). In particular Postn expression seems to increase in the mixed population.

In contrast with the conclusion of Shh as marker of a mixed population, evidence from literature showed and supported the expression of Shh in MSCs and MF like cells single populations. The investigation of Hh signalling in liver fibrosis demonstrated in fact the existence of a bone marrow stem cell niche constituted from bone marrow MSCs and hepatic stellate cells HSC (an activated stroma cell type expressing α SMA similar to MF-like cells) in which both type of cells endogenously express Shh ligand. Moreover, *in vitro* culture of MSCs showed the expression of Shh ligand and its knock-down by using an shRNA affected the IFN γ -induced proliferation in MSCs [Lin *et al* 2008; Donnelly *et al* 2013]. Such evidence strongly supports the existence of the stem cell niche in inflammatory condition like desmoplasia, fibrosis and cancer but also contrast the idea of Shh expression exclusively in the mixed population. However, interestingly, these results were achieved by growing the MSCs in DMEM 10%, a condition that was here demonstrated to induce the differentiation of MSCs into MF-like cells. The expression of Shh observed in these contexts could be then associated with a mixed population suggesting the reliability of the results found in this study. On the other hand, as explained above, Shh expression was observed in hepatic and pancreatic stellate (activated cells expressing α SMA) single populations [Lin *et al* 2008; Siu Wai Tsang *et al* 2013] .

All these aspects taken together reveal the necessity for further investigation to confirm the conclusion of Shh as exclusive marker of a mixed population. A possible approach could be the stable transfection

of MSC cells with GFP (green fluorescence protein) or RFP (red fluorescent protein) whose expression should be linked to the activity of α SMA promoter, as done by Quante *et al*, in order to isolate the MF-like cell population. At the same time, identification of a marker that would allow MSCs to be isolated in the same way is required. By then mixing these populations, the effect on Shh expression could be ascertained and, in addition, using different ratios, the importance of each population in the induction of Shh expression could be evaluated.

However, this experimental design also has some limitations. Firstly, finding a cell-surface marker for MSCs is still a challenge. If such a marker were available, the stress to which cell lines are exposed during the transfection (e.g. due to cytotoxicity of the transfection reagents) can alter the expression of certain genes [Jacobsen *et al* 2009]. Moreover, the cell sorting process requires good recovery of the cells and the purity of the sorted cells after a single sorting cannot be guaranteed (<http://www.facs.ethz.ch/docs/lit>). Lastly, sorting of cells to obtain a pure population may result in loss of subpopulations of cells which are poorly transfected.

For this reason, an alternative method able to maintain the cells in the best culture conditions and so to better mimic the *in vivo* conditions was used. The new assay was based on: 1) the fact that in the previous experiments, as explained, the single populations (MSC and MF-like cell) used were impure and 2) on the following assumptions:

- MSCs grown in FDM could be considered a mSCN model

- MSCs, to be maintained as single population, need to be kept in MSCM over time: MSC S.P. (mesenchymal stem cells single population)
- CAFs, to be fully activated, need to be grown in FDM that contains growth factors able to induce and maintain their activation mimicking their real *in vivo* phenotype

Shh, α SMA and Postn expression in the mSCN *in vitro* model (MSCs grown in DMEM) was compared after 2, 14 and 21 days of culture to the single populations (MSCs grown in MSCM and CAFs grown in FDM). Shh at the gene and protein level in the mSCN model (MSC grown in FDM) used in this assay was much higher after 14 and 21 days of culture than that in the MSC S.P. (MSCs grown in MSCM) or the CAF single population (Figure 5.25). Moreover, consistent with this observation, the increase in α SMA and Postn at the gene and protein level over time observed in CAFs, did not match with Shh, which remained low and constant (Figure 5.25 ; 5.26; 5.27). Furthermore, only a small increase in α SMA and Postn was observed in MSC S.P. over time confirming their stem cell phenotype and the preservation of this phenotype in MSCM over time (Figure 5.26 and 5.27).

This strongly supports the role of Shh as a marker of the stem cell niche as previously suggested [Quante *et al* 2011].

6.5.2 The mSCN is the best tumour stromal context able to respond to Hh paracrine stimuli

Another important hypothesis formulated in this study arose from the failure of MSCs and CAFs, grown in MSCM, to respond to Hh paracrine stimuli as observed in chapter 4 and 5. It was in fact postulated that this failure was a consequence of the inability of MSCs to differentiate and to form a mixed population (mSCN model). Based on this idea, the mSCN should be the best context in the pancreatic tumour microenvironment able to respond to Hh paracrine stimuli. The confirmation of this idea would provide a new view of Hh signalling in pancreatic cancer which would have important consequences for pancreatic cancer therapy.

MSCs grown in FDM were shown to provide a model of the mSCN (sections 6.5.1; 6.5.2). The increase in MF-like cells over time was demonstrated, as well as an increase in Shh gene and protein expression as a mixed population formed. Furthermore, the trend in α SMA gene and protein expression by 21 days showed not only the formation of a new MF-like population, but also that the behaviour of these cells was comparable to that observed in the literature in a very similar *in vitro* model (rapid increase of the MF-like cells after 3 days of culture and then stabilisation of a mixed population) [Quante *et al* 2011]. Co-culture of this mSCN model with epithelial pancreatic cancer cells or treatment with NShh in media with different percentages of FBS showed induction of the Hh pathway (tested as *GLI1* gene and Ptch1 protein expression), which was higher in the mSCN model than in MSC

S.P. (figure 5.30; 5.31). The analysis of Ptch1 protein expression, in both these assays, by IF quantification (Figure 5.30C and 31C) showed significance ($p < 0.05$) for the increase of Ptch1 expression in the SCN model co-cultured with PANC1 pancreatic cancer cells in comparison to the control (SCN model co-cultured with SCN model). This result confirmed the changes observed at gene level (*GLI1* expression) and those showed by IF images (Ptch1 protein staining) (Figure 5.30 B).

The IF quantification was performed by using a semi-quantitative ranking system. This choice was dictated by the detection limitations when working with fluorescent labelled cells. Computer-aided image analysis can only measure and analyse those features, in this case cells that have been optically labelled (membrane and cytoplasm) and thus made visible to the camera. Unstained cell cytoplasm and nuclei or negatives cannot be identified for measurement. In all cases, cell nuclei are counterstained with DAPI and are visible, which makes all the cells present accurately countable. It is not however possible to use a computer-aided image analysis to measure the areas of all these cells. Any attempt to do so would skew the data in favour of positive staining cells, no matter their proportion, in relation to unstained cells. The decision to carry out manual quantification improved the accuracy and reproducibility, by taking into account the total number of cells present on the basis of nuclear counterstaining.

This approach, however, as it is the result of a subjective evaluation does not give perfectly reproducible quantitative information and can be affected by analysis variability. For this reason it has been defined as

semi-quantitative. In order to reinforce the reliability of this quantification, the study was performed blinded under the conditions investigated.

In contrast with the Hh pathway induction (*GLI1* gene and Ptch1 protein expression) observed in the SCN model after co-culture with pancreatic epithelial cancer cells (PANC1) and after NShh treatment described above (Figure 5.3 and 5.31), an increase in *GLI1* gene expression, although to a smaller degree in MSC S.P. (cells grown in MSCM), was observed under the same experimental conditions. This could be due to the fact that even if MSCM keeps the cells in an inactivated state, a certain level of differentiation does occur.

An important aspect to analyse in this investigation was therefore the stability of the MSCs grown in FDM as mSCN model or, in other words, the characterisation of these cells as a source of MF-like single population or as a reliable mSCN model. The ability of MF-like cells (CAFs expressing α SMA) to respond to Shh paracrine induction from cancer cells has been described [Chan *et al* 2012; Hwang *et al* 2012; Wilkinson *et al* 2013], suggesting the need to compare the responsiveness to Shh paracrine induction of MF-like cells with a mSCN model. CAFs grown in MSCM (i.e. inactivated cells) were unable to respond to Hh ectopic stimuli (chapter 4). However, it is still necessary to investigate whether fully activated CAFs (i.e. grown in FDM: MF-like cells) are able to better respond to Shh paracrine induction and compare this capability with the responsiveness of a mSCN *in vitro* model. In order to test these options different mSCN

models and CAFs grown in FDM (data not showed) were compared for their responsiveness to Hh paracrine stimuli.

6.5.2.1 *Shh* paracrine responsiveness comparison between different mesenchymal mSCN in vitro models

The paracrine induction of the Hh pathway in five mesenchymal mSCN models was compared with the MSCs S.P. All models previously used in the study were included (MSC S.P. mixed with MF-like cells obtained by treating them with TGF β for 1 week; MSCs simply grown in FDM) with a new model that considered MSCs as a source of MF-like cells (MSCs were in FDM for 1 week and mixed them with MSC S.P. grown at low passages in MSCM). Responsiveness to Hh paracrine stimuli was assessed using co-culture with pancreatic cancer cells carried out either in FDM or in MSCM. The highest induction of the Hh pathway was observed in the assays performed in FDM and in the mSCN model obtained by mixing MSCs grown for 1 week in FDM and mixed 1/1 with MSC S.P. This confirms the previous observation that different ratios of MF-like cells and MSCs affect *SHH* expression (Figure 5.19): the proportion of MF-like cells is fundamental for the constitution of the mSCN *in vitro* model and for the responsiveness to paracrine stimuli, with higher ratios of this cell type proportionally increasing the responsiveness. Finally CAF activated cells (grown in FDM and expressing α SMA) were tested for their responsiveness to different concentrations of NShh by analysing *GLI1* gene expression. No induction was observed in any of the conditions tested (data not

showed). Moreover MSCs, constantly treated with TGF β , which results in differentiation into an MF-like single population, confirmed the inability of fully activated cells to undergo paracrine induction, via co-culture with pancreatic epithelial cells or NShh treatment. However, Hh pathway activation was tested in these experiments only at the gene level, and for this reason further investigation will be required to confirm these observations at the protein level.

These results further support the idea that cells in the mSCN are better able to respond to Hh paracrine signalling than single populations (MSCs and activated CAFs) and they represent a finding that suggests the mSCN as an important component of the tumour microenvironment. However, further investigations are necessary to definitely ascertain this conclusion.

6.5.2.2 Next step in the paracrine induction of Hh signalling in a *in vitro* mSCN model

In order to definitely ascertain the mSCN as the context able to respond to Shh paracrine induction there is again a need for two pure single populations (MFs and MSCs) that can be mixed at different ratios to test the influence of the MF population on responsiveness to paracrine induction. Paracrine induction could be assessed using the assays already described in this thesis (Chapter 4 and 5) but in addition it will be important to extend the work to 3D *in vitro* assays that better mimic the *in vivo* interaction between epithelial and stromal-like cells. Moreover, a further step that would need to be performed is the

modulation of the Hh pathway (Shh silencing in epithelial cancer cells) to definitely address the induction observed in the mSCN models as a consequence of the Hh pathway paracrine stimuli and not of other non-canonical pathways.

6.6 Applicability of the data presented in this thesis for development of novel therapeutic approaches

A number of studies have been carried out to investigate the effect of the Hh pathway inhibition on cancer [Taipale *et al.* 2000; Chen *et al.* 2002; Williams *et al.* 2003; Feldmann *et al.* 2008; Lipinsky *et al.* 2008; Lo Russo *et al.* 2011] So far there are over 50 compounds that are able to inhibit Hh signalling acting at different levels of the pathway. [Yang *et al.* 2010]. More than one has shown an effect on xenograft tumour reduction and decreased proliferation of tumour cells *in vitro* confirming the validity of the Hh pathway inhibition as a chemo-preventive method in prostate cancer [Lauth^{article 2} *et al.* 2007].

Based on the data in this thesis and recent literature regarding the paracrine transmission of the Hh signalling in cancer, further inhibitors need to be tested in order to check their efficiency in tumour types with paracrine Hh signalling. In fact, in the presence of this kind of transmission there is the need for an inhibitor able to block the pathway at the stromal level. This inhibition should then reduce the amount of drug necessary to block tumour growth and therefore toxicity associated with chemotherapeutic treatment. In agreement with this last theory, treatment with IPI-296, that is known to inhibit SMO, was found to be able to reduce the stromal component in PDA (Pancreatic Ductal Adenocarcinoma) mouse models and to allow a more efficient gemcitabine drug effect with an overall effect on tumour mass reduction [Olive *et al.* 2009]. In this study, Shh expression at the stromal

level was observed in the advanced tumour stage (PDT) of pancreatic cancer and was suggested as a marker of the presence of a mesenchymal stem cell niche in the cancer stroma. Targeting Shh in the stromal context could affect not just the survival of the myofibroblast-like cell population but also the equilibrium of the mesenchymal stem cell niche (constituted from MF-like cell and MSCs) that makes an important contribution to tumour growth and survival (Quante *et al* 2011). Moreover, once the function of Shh in the pancreatic tumour microenvironment has been confirmed it will provide a valuable therapeutic target whether it is a marker of the mSCN or expressed by MF cells. Another issue to consider is the presence of a cancer stem cell niche (to be distinguished from the mesenchymal stem cell niche). In this context, the use of inhibitors of Shh downstream targets as a chemotherapeutic approach may not be successful. It is in fact known that cancer stem cells are able to resist to chemotherapeutic agents making the treatment with drug ineffective. To overcome the cancer stem cell resistance to chemotherapeutic treatment a triple drug treatment has been suggested [Lonardo *et al* 2012]. In this study the Hh pathway was shown to be expressed by pancreatic stellate cells which in turn, through the nodal/activin pathway promote the survival of cancer stem cells (CSC). By targeting the PSC (using CUR199691 Hh pathway inhibitor), the interplay between CSC and PSC (using the nodal/activin inhibitor SB431542) and the tumour cells (using gemcitabine), a reduction in the stromal component of pancreatic cancer was observed [Lonardo *et al* 2012]. It is important not to confuse

the mesenchymal stem cell niche (MF-like cells and MSCs) with the cancer stem cell niche that consists of cancer stem cells and myofibroblast-like cells. However, a common cell population between these two niches is the MF-like cells. Interestingly, this population is known to be important for the survival of both niches [Quante *et al* 2011; Lonardo *et al* 2012]. For this reason, another interesting hypothesis is that targeting Shh and causing the disruption of the stem cell niche, and so the MF-like population, could indirectly affect the cancer stem cell niche balance.

Treatment of orthotopically transfected mice with 5E1 (a Shh antibody) showed the depletion of the stromal component in PDAC [Bailey *et al* 2008]. This result was interpreted as a consequence of Shh inhibition at the epithelial level; however, this does not exclude the possibility that it could be a consequence of its inhibition in the stromal component in agreement with the theory outlined above. Shh could then become a very interesting target that could enable a much more powerful chemotherapeutic approach especially in the late stage of tumour development.

In order to investigate this aspect, different *in vivo* mouse models could be used. Transgenic mice expressing fluorescent stromal cells could be used. Targeting these mice with Shh inhibitors (e.g. 5E1 or robtokinine) it would be possible to use luminescent images to assess its effect on depletion of the stromal component. The combination between gemcitabine and Shh inhibitors treatment would also be tested to assess its effect on tumour size.

Genetically engineered mouse models could also be used for this purpose. In particular KPC mice seem to reproduce a PDAC model very similar to the human one. These mice, obtained by constitutive expression of mutant KRas and P53, seems to reproduce the desmoplastic reaction typical of pancreatic tumours [Olive *et al* 2009]. Using this model, having ascertained the expression of Shh at the stromal level by IHC, the effect of Shh could be investigated. The combination of Shh inhibitors and gemcitabine would also be tested in these mice. The effect of double treatment in comparison to gemcitabine alone would be firstly investigated, then, the effect of Shh inhibition on the survival of the mesenchymal and cancer stem cell niches would be investigated. For this purpose the engineered mice will be sacrificed and analysed for the presence of the stromal component in the pancreatic tumour and for the presence of mSCN markers (α SMA, Postn, Shh) and CSC markers by IHC. Treated mice would be compared to the untreated ones.

6.7 Conclusions

- Shh, a ligand of the Hh signalling pathway is expressed at the stromal and epithelial level in human PDAC.
- The expression of Shh at the stromal level appears mainly in more aggressive tumours (PDT).
- There is a role for Shh as a marker of the mesenchymal stem cell niche consisting of both human bone marrow MSCs and MF-like stromal cells that are hypothesised to co-exist in the stroma of advanced pancreatic cancer.
- Shh gene and protein expression depends on the ratio of the two populations used to establish each mSCN model.
- α SMA and Postn are good markers of MF-like cells and initial data on Shh expression in the mSCN models tested, suggest that the population able to express this ligand is the MF-like cells.
- MSCs and CAFs when grown alone in medium able to prevent their activation (MSCM) are unable to respond to Hh paracrine stimuli from epithelial pancreatic cancer cells but are responsive in the context of the mSCN.

The following diagram summarise the conclusions of this study, the new hypothesis generated and ideas for future investigations.

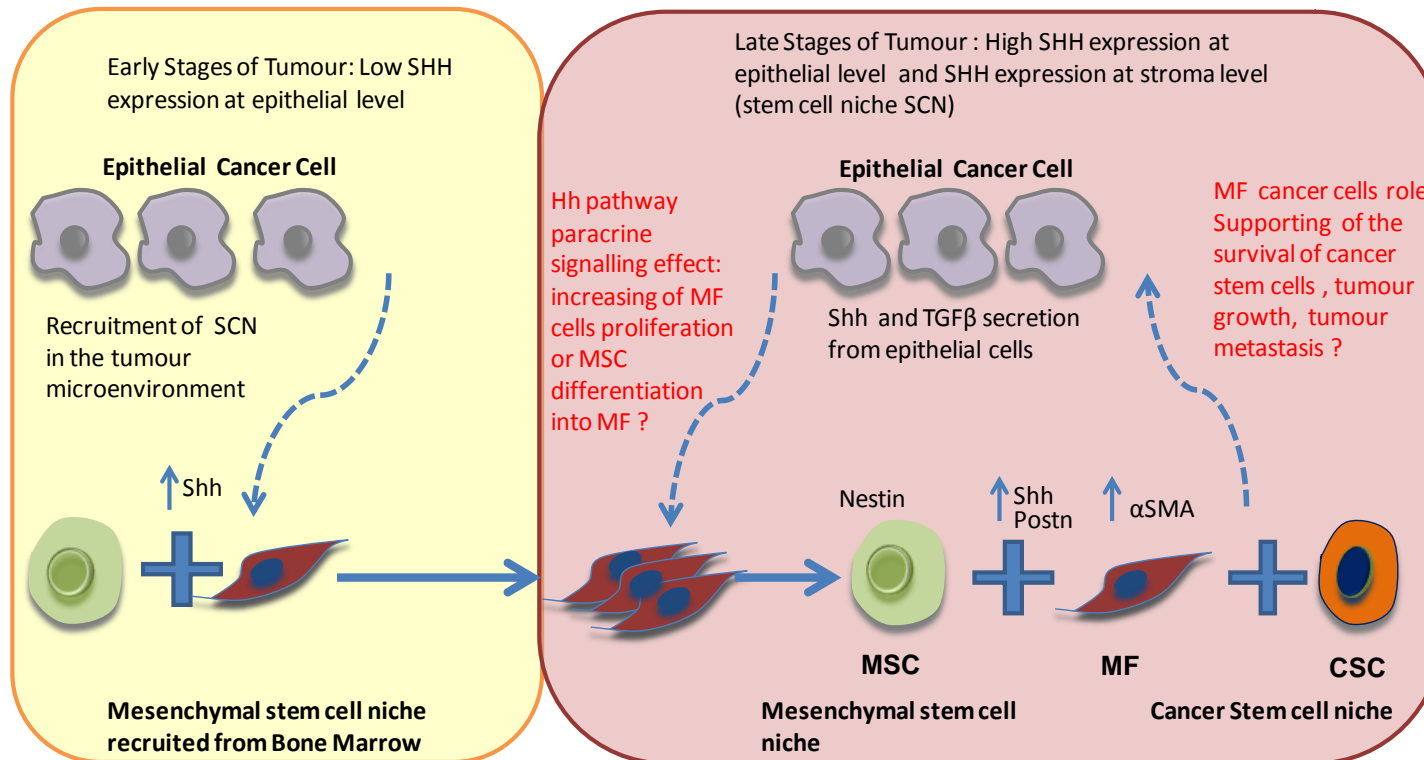


Figure 6.2 Schematic diagram that depicts the conclusions, hypothesis and future aims (red writing) defined in this project.. Shh expression increases in the late stage of pancreatic tumour (PDAC) progression in the tumour cells. Epithelial cancer cells also produce TGFβ which in turn induce the expansion of niche cells recruited from the bone marrow (BM). The mesenchymal stem cell niche express Shh which expression is then visible at stroma level in the late stage of PDAC. -mSCN is able to respond to Hh paracrine signalling from epithelial cancer cells. It is not clear yet the effect of Hh pathway activation in the mSCN: MF cells proliferation or MSCs differentiation into MF cells?. MF cells in the mesenchymal niche context are strongly activated and so they express αSMA and Postn. The mSCN help the survival and proliferation of MF cells which in turn sustain the survival of cancer stem cells (CSC), as well present in the tumour microenvironment, forming the cancer stem cell niche. MF cells also sustain the tumour growth and the tumour metastasis. Targeting Shh expression in the-mSCN in the tumour microenvironment should destabilised the activation and the survival of MF like cells and as consequence blocking the tumour growth and progression.

6.8 Future work

This work provides a first analysis of a possible new paradigm underlying the development of stroma in pancreatic cancer and suggests a possible new role for the Hh pathway in PDAC. The conclusions reached in this study suggest a new therapeutic approach but need further confirmation.

The further steps required to move the project forwards are as follows:

- The presence of stem cell niche in the stromal context was hypothesised and suggested by the detection of Shh protein expression (believed to be a marker of mSCN). However, confirmation of the existence of a mSCN in the tumour stroma of patients and of the role of Shh as a marker of the mSCN is still necessary. IHC co-staining for markers of MSCs and MF-like cells (α SMA or Postn) could be used to demonstrate their co-existence in the cancer stroma. Moreover, comparison between normal tissues and tissues taken at different stages in tumour progression will also help to confirm the presence of stem cell niche in the advanced phase of pancreatic cancer. Co-staining of Shh and α SMA could also confirm its expression in the stem cell niche and which of the two populations is able to express it.
- Shh was observed to be expressed in the stem cell niche but it is still not clear if it can be considered a marker of the niche or is simply expressed by MF-like cells. In both cases the discovery of

its expression in cancer stromal-like cells is novel and the data suggest it is a mSCN marker.

To further confirm this aspect *in vitro*, the isolation of the two niche populations (MSCs and MF-like cells) will clarify this aspect. To perform this isolation an RFP- α SMA or Postn targeted cell population (as used by Quante *et al* 2011) could help to isolate the MF-like population by fluorescent activated cell sorting (FACS) and assess if these cells are able to express Shh. The unsorted cells should be MSCs that, to confirm their nature, should be characterised for their expression of mesenchymal stem cell markers and their ability to differentiate into adipocytes, chondrocytes and osteocytes. Mixing the two isolated populations at different ratios and comparing them for Shh expression to single populations, will clarify the exclusivity of Shh expression in mixed populations as well as the relative importance of the two niche populations on Shh expression.

Another way to investigate the role of Shh as a marker of stem cell niche and to discover which cell type in the niche is able to express it could be to mix the two niche populations (obtained by growing MSC in MSCM for as few passages as possible and by treating MSCs with TGF β in FDM) followed by co-staining them for Shh and α SMA/Postn expression. The Shh expression in these mSCN models would be compared to single populations in order to definitely ascertain the correlation of Shh with mixed

population as indicated in this work and in the literature [Lin *et al* 2008; Quante *et al* 2011].

- The role of Shh in the mSCN is another aspect that needs to be clarified. A way to investigate it could be by silencing its expression (by using the already optimised siRNA) in cells demonstrated to express it and then plating the two niche populations in two different compartments of a 2D transwell system. In this way it would be possible to investigate the effect of Shh knock-down on cell survival, proliferation (Ki67 gene and protein expression) and differentiation (gene and protein expression of α SMA) in both cell populations. The effect of Shh silencing on the survival of the mSCN could also be investigated by co-culturing the MSCs and MF-like cells in a 3D model, in order to better mimic the *in vivo* interaction between these two populations. Moreover, the investigation of the effect of Shh inhibitors (like robtokinin or 5E1 antibody) on the mSCN survival would add further to understanding of its role in this mixed population and the applicability of its inhibition as chemotherapeutic approach.
- Another area of investigation is the role of Shh expression in the *in vivo* stromal context. More precisely, the investigation of the Shh knock-down on *in vivo* tumour cell survival and tumour growth. A new technique that seems very approachable and efficient to investigate this aspect is the hollow-fibre assay. [Mi *et*

al 2009]. This method consists of the insertion of luminescent labelled human cell populations in a sealed hollow fibre tube under the mouse skin. Each hollow fibre has pores that allow the passage of protein and molecules but not of cells. The advantage of this method in comparison to xenograft and transgenic mice, is the necessity of a much lower number of animals, considering that more than one hollow fibre can be implanted in the same mouse. In this way the experimental variability of data will be also reduced and the human mesenchymal cells would be preserved and not replaced by mouse stromal cells as commonly happens in xenograft mice. Moreover, lower costs and shorter study times will be achieved using this method [Mi *et al* 2009].

As a first step, the investigation of the mSCN on tumour growth would be performed by inserting in each hollow fibre the best mSCN *in vitro* model, obtained in this study, mixed with luminescent pancreatic cancer cells. In this way the effect of the mSCN on tumour cell proliferation and tumour growth will be clarified by bioluminescence images of the hollow-fibre. Epithelial cancer cell mSCN co-cultures would be compared with epithelial cells cultured alone and co-transplanted in the same mouse. Then a co-culture model using mSCN cells transfected with a shRNA targeting Shh would be used. The comparison between the effect of transfected and un-transfected mSCN cells on

cancer cell growth would help to understand the effect of Shh stromal expression on tumour growth.

By using the same type of analysis the effect of Shh inhibitors on the depletion of the stroma component could also be investigated. In order to achieve this goal, the luminescent mSCN model would be co-inserted in the hollow-fibre with epithelial cancer cells stably transfected with shRNA targeting Shh. In the same mouse two other hollow fibres would be transplanted: containing epithelial shRNA negative cancer cell-mSCN co-cultures (with no target: shNeg) or un-transfected cancer cell-mSCN co-cultures. By treating the mouse with 5E1 or robotnikinin (Shh inhibitors) it would be possible to assess by using bioluminescence images if the expected mSCN depletion in the stroma is a consequence of the inhibition of Shh in cancer cells that block the mesenchymal mSCN recruitment (as showed in Bailey *et al* 2008) or a consequence of Shh inhibition at the stromal level. This latter option would be confirmed if the 3 hollow fibres with transfected, un-transfected or shNeg transfected cancer cells show the same depletion of the mSCN population after the treatment with the Shh inhibitor.

- Further investigations also need to be performed on stem cell niche responsiveness to Hh paracrine signal from epithelial cancer cells. To investigate this aspect, siShh transfected and un-transfected epithelial pancreatic cancer cells would be co-

cultured in 2D and 3D assay with the mSCN *in vitro* model. The effect of Shh silencing on Hh pathway expression (Gli1 and Ptch1 gene and protein expression) in the niche cells would be analysed.

Moreover, considering that Hh pathway canonical activation requires localisation of the SMO and Gli transcription factors in the cilium [Zeng *et al* 2010 Qin *et al* 2011], the mSCN model should be analysed for the presence of the cilium by investigating the protein expression of two known cilium markers: γ -tubulin and α -acetylated tubulin (Grzelak *et al* 2014). This analysis would also determine if the observed Gli1 paracrine activation in the mSCN is a consequence of an Hh canonical pathway activation. Both cell populations of the mSCN model would then be treated with NShh and/or co-cultured with pancreatic cancer cells. At the end of the treatment/co-culture the mSCN cells would be analysed by IF for the expression of γ -tubulin and α -acetylated tubulin that constitute the basal components of the axoneme and of the cilium respectively (Grzelak *et al* 2014). Moreover, analysis of gene and protein expression of IFT122 and PKA in the mSCN would further confirm whether the machinery implicated in the Hh signalling transduction via SMO and in the localisation of Gli2 and Gli3 transcription factors is activated [Zeng *et al* 2010; Qin *et al* 2011]. The comparison between treated/ co-cultured mSCN models and

untreated / normal cultured mSCN models for these proteins would further confirm the niche model as a context able to respond to Hh paracrine signalling. Co-staining of the cilium markers and the MF-like cell marker α SMA could also address which cell type in the mSCN model directly responds to the paracrine stimuli. Furthermore, the comparison between single MSC and MF-like populations and the mSCN model in the same experimental design could assess if the mSCN is a better context for responsiveness to Hh paracrine signal.

- The interaction between the Shh and TGF β pathways in the mSCN context, observed in this study, also needs further clarification. *In vitro* treatment of the mSCN with TGF β would be repeated and the effect on Shh, Gli1 and Ptch1 further investigated not just in 2D but in 3D assays as well in order to better mimic the *in vivo* interaction between the cells. Moreover, in order to investigate if the activation of Gli1 from TGF β is a consequence of canonical activation of Hh or a non-canonical pathway the presence of the cilium and the SMO localisation would be investigated by IF analysis as described above, before and after the TGF β treatment. Further investigation could be also done by checking the expression of TGF β in the mSCN and the effect of its knock-down by siRNA on cell differentiation and Shh expression.

- Another final important aspect to evaluate is the effect of Hh paracrine induction on mSCN proliferation. Treated and untreated NShh mSCN models would be compared for their viability and their level of proliferation using an MTT assay (a colorimetric assay that allows measurement of cell proliferation and survival of viable cells) [Mosmann *et al* 1983] or for their expression of Ki67 (a proliferation marker).

6.9 Final Conclusions

Hh pathway is overexpressed in pancreatic tumours. The desmoplastic effect, typical of this cancer, is characterised by the recruitment into the stromal component of a mesenchymal stem cell niche from the bone marrow. The recruitment probably happens in the advanced stages of tumour progression. The mSCN is known to support pancreatic tumour growth and could be the stromal context capable of responding to Hh paracrine stimuli from epithelial cancer cells. Shh seems to be a marker of this niche and its inhibition could result depletion of the stromal mass and, as consequence, to an increase in the effectiveness of chemotherapeutic agents (such as gemcitabine) in reducing tumour volume and progression.

Chapter 7 - References

Adegboyega, P. A., R. C. Mifflin, *et al.* (2002). "Immunohistochemical study of myofibroblasts in normal colonic mucosa, hyperplastic polyps, and adenomatous colorectal polyps." Archives of Pathology & Laboratory Medicine **126**(7): 829-836.

Al-Hajj, M., M. S. Wicha, *et al.* (2003). "Prospective identification of tumorigenic breast cancer cells." Proceedings of the National Academy of Sciences of the United States of America **100**(7): 3983-3988.

Alison, M. R., W.-R. Lin, *et al.* (2012). "Cancer stem cells: In the line of fire." Cancer Treatment Reviews **38**(6): 589-598.

Almoguera, C., D. Shibata, *et al.* (1988). "MOST HUMAN CARCINOMAS OF THE EXOCRINE PANCREAS CONTAIN MUTANT C-K-RAS GENES." Cell **53**(4): 549-554.

Amakye, D., Z. Jagani, *et al.* (2013). "Unraveling the therapeutic potential of the Hedgehog pathway in cancer." Nature Medicine **19**(11): 1410-1422.

Anand, P., A. B. Kunnumakara, *et al.* (2008). "Cancer is a Preventable Disease that Requires Major Lifestyle Changes." Pharmaceutical Research **25**(9): 2097-2116.

Anderberg, C. and K. Pietras (2009). "On the origin of cancer-associated fibroblasts." Cell Cycle **8**(10): 1461-1462.

Atwood, S. X., A. L. S. Chang, *et al.* (2012). "Hedgehog pathway inhibition and the race against tumor evolution." Journal of Cell Biology **199**(2): 193-197.

Ayers, K. L., A. Gallet, *et al.* (2010). "The Long-Range Activity of Hedgehog Is Regulated in the Apical Extracellular Space by the Glypican Dally and the Hydrolase Notum." Developmental Cell **18**(4): 605-620.

Aza-Blanc, P., H. Y. Lin, *et al.* (2000). "Expression of the vertebrate Gli proteins in Drosophila reveals a distribution of activator and repressor activities." Development **127**(19): 4293-4301.

Bai, C. B., D. Stephen, *et al.* (2004). "All mouse ventral spinal cord patterning by hedgehog is Gli dependent and involves an activator function of Gli3." Developmental Cell **6**(1): 103-115.

Bailey, J. M. and M. A. Hollingsworth (2009). "Sonic hedgehog paracrine signaling regulates metastasis and angiogenesis in pancreatic cancer." Proceedings of the American Association for Cancer Research Annual Meeting **50**: 1149.

Bailey, J. M., B. J. Swanson, *et al.* (2008). "Sonic Hedgehog Promotes Desmoplasia in Pancreatic Cancer." Clinical Cancer Research **14**(19): 5995-6004.

Bajestan, S. N., F. Umehara, *et al.* (2006). "Desert hedgehog-patched 2 expression in peripheral nerves during Wallerian degeneration and regeneration." Journal of Neurobiology **66**(3): 243-255.

Barcellos-de-Souza, P., V. Gori, *et al.* (2013). "Tumor microenvironment: Bone marrow-mesenchymal stem cells as key players." Biochimica Et Biophysica Acta-Reviews on Cancer **1836**(2): 321-335.

Bardeesy, N., K.-h. Cheng, *et al.* (2006). "Smad4 is dispensable for normal pancreas development yet critical in progression and tumor biology of pancreas cancer." Genes & Development **20**(22): 3130-3146.

Barone, C., A. Cassano, *et al.* (2003). "Weekly gemcitabine and 24-hour infusional 5-fluorouracil in advanced pancreatic cancer: A phase I-II study." Oncology **64**(2): 139-145.

Becher, O. J., D. Hambardzumyan, *et al.* (2008). "Gli activity correlates with tumor grade in platelet-derived growth factor-induced gliomas." Cancer Research **68**(7): 2241-2249.

Berman, D. M., S. S. Karhadkar, *et al.* (2003). "Widespread requirement for Hedgehog ligand stimulation in growth of digestive tract tumours." Nature **425**(6960): 846-851.

Bhattacharya, R., J. Kwon, *et al.* (2008). "Role of Hedgehog Signaling in Ovarian Cancer." Clinical Cancer Research **14**(23): 7659-7666.

P

Bian, Y.-H., S.-H. Huang, *et al.* (2007). "Sonic hedgehog-Gli1 pathway in colorectal adenocarcinomas." World Journal of Gastroenterology **13**(11): 1659-1665.

Bigelow, R. L. H., N. S. Chari, *et al.* (2004). "Transcriptional regulation of bcl-2 mediated by the sonic hedgehog signaling pathway through gli-1." Journal of Biological Chemistry **279**(2): 1197-1205.

Brentnall, T. A., L. A. Lai, *et al.* (2012). "Arousal of Cancer-Associated Stroma: Overexpression of Palladin Activates Fibroblasts to Promote Tumor Invasion." Plos One **7**(1).

Buttitta, L., R. Mo, *et al.* (2003). "Interplays of Gli2 and Gli3 and their requirement in mediating Shh-dependent sclerotome induction." Development **130**(25): 6233-6243.

Catenacci, D.V.T. *et al.* (2013) Final analysis of a phase IB/randomized phase II study of gemcitabine (G) plus placebo (P) or vismodegib (V), a hedgehog (Hh) pathway inhibitor, in patients (pts) with metastatic pancreatic cancer (PC): A University of Chicago phase II consortium study. Journal of Clinical Oncology **31**, abstr 4012 .

Carpenter, D., D. M. Stone, *et al.* (1998). "Characterization of two patched receptors for the vertebrate hedgehog protein family." Proceedings of the National Academy of Sciences of the United States of America **95**(23): 13630-13634.

Chan, I. S., C. D. Guy, *et al.* (2012). "Paracrine Hedgehog Signaling Drives Metabolic Changes in Hepatocellular Carcinoma." Cancer Research **72**(24): 6344-6350.

Chen, J. K., J. Taipale, *et al.* (2002). "Inhibition of Hedgehog signaling by direct binding of cyclopamine to Smoothened." Genes & Development **16**(21): 2743-2748.

Chen, M., M. Tanner, *et al.* (2009). "Androgenic regulation of hedgehog signaling pathway components in prostate cancer cells." Cell Cycle **8**(1): 149-157.

Choi, S. S., A. Omenetti, *et al.* (2009). "Hedgehog pathway activation and epithelial-to-mesenchymal transitions during myofibroblastic transformation of rat hepatic cells in culture and cirrhosis." American Journal of Physiology-Gastrointestinal and Liver Physiology **297**(6): G1093-G1106.

Chu, G. C., A. C. Kimmelman, *et al.* (2007). "Stromal biology of pancreatic cancer." Journal of Cellular Biochemistry **101**(4): 887-907.

Clement, V., P. Sanchez, *et al.* (2007). "HEDGEHOG-GLI1 signaling regulates human glioma growth, cancer stem cell self-renewal, and tumorigenicity." Current Biology **17**(2): 165-172.

Corbit, K. C., P. Aanstad, *et al.* (2005). "Vertebrate Smoothened functions at the primary cilium." Nature **437**(7061): 1018-1021.

Coultas, L., E. Nieuwenhuis, *et al.* (2010). "Hedgehog regulates distinct vascular patterning events through VEGF-dependent and -independent mechanisms." Blood **116**(4): 653-660.

Crnogorac-Jurcevic, T., E. Efthimiou, *et al.* (2001). "Gene expression profiles of pancreatic cancer and stromal desmoplasia." Oncogene **20**(50): 7437-7446.

Curran, T. and J. M. Y. Ng (2008). "Cancer - Hedgehog's other great trick." *Nature* 455(7211): 293-294.

Dai, P., H. Akimaru, *et al.* (1999). "Sonic hedgehog-induced activation of the Gli1 promoter is mediated by GLI3." *Journal of Biological Chemistry* **274**(12): 8143-8152.

Dandachi, N., C. Hauser-Kronberger, *et al.* (2001). "Co-expression of tenascin-C and vimentin in human breast cancer cells indicates phenotypic transdifferentiation during tumour progression: correlation with histopathological parameters, hormone receptors, and oncoproteins." *Journal of Pathology* **193**(2): 181-189.

Daniel, V. C., L. Marchionni, *et al.* (2009). "A Primary Xenograft Model of Small-Cell Lung Cancer Reveals Irreversible Changes in Gene Expression Imposed by Culture In vitro." *Cancer Research* **69**(8): 3364-3373.

De Wever, O., P. Demetter, *et al.* (2008). "Stromal myofibroblasts are drivers of invasive cancer growth." *International Journal of Cancer* **123**(10): 2229-2238.

De Wever, O., Q. D. Nguyen, *et al.* (2004). "Tenascin-C and SF/HGF produced by myofibroblasts in vitro provide convergent proinvasive signals to human colon cancer cells through RhoA and Rac." *Faseb Journal* **18**(6): 1016-+.

Dennler, S., J. Andre, *et al.* (2007). "Induction of sonic hedgehog mediators by transforming growth factor-beta: Smad3-dependent activation of Gli2 and Gli1 expression in vitro and in vivo." *Cancer Research* **67**(14): 6981-6986.

Ding, H., D. Zhou, *et al.* (2012). "Sonic Hedgehog Signaling Mediates Epithelial-Mesenchymal Communication and Promotes Renal Fibrosis." *Journal of the American Society of Nephrology* **23**(5): 801-813.

Ding, Q., J. Motoyama, *et al.* (1998). "Diminished Sonic hedgehog signaling and lack of floor plate differentiation in Gli2 mutant mice." *Development* **125**(14): 2533-2543.

Direkze, N. C., K. Hodivala-Dilke, *et al.* (2004). "Bone marrow contribution to tumor-associated myofibroblasts and fibroblasts." *Cancer Research* **64**(23): 8492-8495.

Domenech, M., R. Bjerregaard, *et al.* (2012). "Hedgehog signaling in myofibroblasts directly promotes prostate tumor cell growth." *Integrative Biology* **4**(2): 142-152.

Dominici, M., K. Le Blanc, *et al.* (2006). "Minimal criteria for defining multipotent mesenchymal stromal cells. The International Society for Cellular Therapy position statement." Cytotherapy **8**(4): 315-317.

Donnelly, J. M., A. Chawla, *et al.* (2013). "Sonic Hedgehog Mediates the Proliferation and Recruitment of Transformed Mesenchymal Stem Cells to the Stomach." Plos One **8**(9).

Duman-Scheel, M., L. Weng, *et al.* (2002). "Hedgehog regulates cell growth and proliferation by inducing cyclin D and cyclin E." Nature **417**(6886): 299-304.

E. E.Merika, K. N. S., 1 andM.W. Saif2 (2012). "Desmoplasia in Pancreatic Cancer. CanWe Fight It?" Gastroenterology Research and Practice **2012**.

El-Zaatari, M., A. Tobias, *et al.* (2007). "De-regulation of the sonic hedgehog pathway in the InsGas mouse model of gastric carcinogenesis." Br J Cancer **96**(12): 1855-1861.

Elliott, C. G., J. Wang, *et al.* (2012). "Periostin modulates myofibroblast differentiation during full-thickness cutaneous wound repair." J Cell Sci **125**(1): 121-132.

Erkan, M., J. Kleeff, *et al.* (2007). "Periostin creates a tumor-supportive microenvironment in the pancreas by sustaining fibrogenic stellate cell activity." Gastroenterology **132**(4): 1447-1464.

Fabian, S. L., R. R. Penchev, *et al.* (2012). "Hedgehog-Gli Pathway Activation during Kidney Fibrosis." American Journal of Pathology **180**(4): 1441-1453.

Feig, C., A. Gopinathan, *et al.* (2012). "The Pancreas Cancer Microenvironment." Clinical Cancer Research **18**(16): 4266-4276.

Feldmann, G., R. Beaty, *et al.* (2007). "Molecular genetics of pancreatic intraepithelial neoplasia." J Hepatobiliary Pancreat Surg **14**(3): 224-232.

Feldmann, G., V. Fendrich, *et al.* (2008). "An orally bioavailable small-molecule inhibitor of Hedgehog signaling inhibits tumor initiation and metastasis in pancreatic cancer." Mol Cancer Ther **7**(9): 2725-2735.

Franco OE, J. M., Strand DW, Peacock J, Fernandez S, Jackson RS 2nd, Revelo MP, Bhowmick NA, Hayward SW. (2011). "Altered TGF- β signaling in a subpopulation of human stromal cells promotes prostatic carcinogenesis." Cancer Res. **71**(4): 1272-1281.

Frixen, U. H., J. Behrens, *et al.* (1991). "E-CADHERIN-MEDIATED CELL CELL-ADHESION PREVENTS INVASIVENESS OF HUMAN CARCINOMA-CELLS." Journal of Cell Biology **113**(1): 173-185.

Fu, X. Y., F. Guadagni, *et al.* (1992). "A METASTATIC NUDE-MOUSE MODEL OF HUMAN PANCREATIC-CANCER CONSTRUCTED ORTHOTOPICALLY WITH HISTOLOGICALLY INTACT PATIENT SPECIMENS." Proceedings of the National Academy of Sciences of the United States of America **89**(12): 5645-5649.

Gialmanidis, I. P., V. Bravou, *et al.* (2009). "Overexpression of hedgehog pathway molecules and FOXM1 in non-small cell lung carcinomas." Lung Cancer **66**(1): 64-74.

Goodrich, L. V., D. Jung, *et al.* (1999). "Overexpression of ptc1 inhibits induction of Shh target genes and prevents normal patterning in the neural tube." Developmental Biology **211**(2): 323-334.

Goodrich, L. V., L. Milenkovic, *et al.* (1997). "Altered neural cell fates and medulloblastoma in mouse patched mutants." Science **277**(5329): 1109-1113.

Gravina, G. L., A. Mancini, *et al.* (2013). "Phenotypic characterization of human prostatic stromal cells in primary cultures derived from human tissue samples." Int J Oncol **42**(6): 2116-2122.

Grover, V. K., J. G. Valadez, *et al.* (2011). "Lipid Modifications of Sonic Hedgehog Ligand Dictate Cellular Reception and Signal Response." Plos One **6**(7).

Grzelak, C. A., L. G. Martelotto, *et al.* (2014). "The intrahepatic signalling niche of hedgehog is defined by primary cilia positive cells during chronic liver injury." J Hepatol **60**(1): 143-151.

Haber, P. S., G. W. Keogh, *et al.* (1999). "Activation of pancreatic stellate cells in human and experimental pancreatic fibrosis." American Journal of Pathology **155**(4): 1087-1095.

Han, F., C.-Y. Wang, *et al.* (2012). "Contribution of murine bone marrow mesenchymal stem cells to pancreas regeneration after partial pancreatectomy in mice." Cell Biology International **36**(9): 823-831.

Hanahan, D. and R. A. Weinberg (2011). "Hallmarks of Cancer: The Next Generation." Cell **144**(5): 646-674.

Haycraft, C. J., B. Banizs, *et al.* (2005). "Gli2 and Gli3 localize to cilia and require the intra-flagellar transport protein polaris for processing and function." Plos Genetics **1**(4): 480-488.

Hidalgo, A. and P. Ingham (1990). "CELL PATTERNING IN THE DROSOPHILA SEGMENT - SPATIAL REGULATION OF THE SEGMENT POLARITY GENE PATCHED." Development **110**(1): 291-301.

Hidalgo, M. (2010). "Pancreatic cancer." N Engl J Med **362**(17): 1605-1617.

Hinterseher, U., A. Wunderlich, et al. (2014). "Expression of hedgehog signalling pathway in anaplastic thyroid cancer." Endocrine **45**(3): 439-447.

Hruban, R. H., N. V. Adsay, et al. (2001). "Pancreatic intraepithelial neoplasia - A new nomenclature and classification system for pancreatic duct lesions." American Journal of Surgical Pathology **25**(5): 579-586.

Hsu, Y.-C. and E. Fuchs (2012). "A family business: stem cell progeny join the niche to regulate homeostasis." Nature Reviews Molecular Cell Biology **13**(2): 103-114.

Hu, B., Z. Wu, et al. (2003). "Smad3 mediates transforming growth factor-beta-induced alpha-smooth muscle actin expression." American Journal of Respiratory Cell and Molecular Biology **29**(3): 397-404.

Hwang, R. F., T. T. Moore, et al. (2012). "Inhibition of the Hedgehog Pathway Targets the Tumor-Associated Stroma in Pancreatic Cancer." Molecular Cancer Research **10**(9): 1147-1157.

Ingham, P. W. (2008). "Hedgehog signalling." Current Biology **18**(6): R238-R241.

Ingham, P. W. and A. P. McMahon (2001). "Hedgehog signaling in animal development: paradigms and principles." Genes & Development **15**(23): 3059-3087.

Ischenko, I., H. Seeliger, et al. (2010). "Pancreatic cancer stem cells: new understanding of tumorigenesis, clinical implications." Langenbecks Archives of Surgery **395**(1): 1-10.

Ishii, G., T. Sangai, et al. (2003). "Bone-marrow-derived myofibroblasts contribute to the cancer-induced stromal reaction." Biochem Biophys Res Commun **309**(1): 232-240.

Jacobsen, L. B., S. A. Calvin, et al. (2009). "Transcriptional effects of transfection: the potential for misinterpretation of gene expression data

generated from transiently transfected cells." Biotechniques **47**(1): 617-+.

Jimeno, A., G. Feldmann, *et al.* (2009). "A direct pancreatic cancer xenograft model as a platform for cancer stem cell therapeutic development." Mol Cancer Ther **8**(2): 310-314.

Jones, S., X. Zhang, *et al.* (2008). "Core signaling pathways in human pancreatic cancers revealed by global genomic analyses." Science **321**(5897): 1801-1806.

Jung, I. H., D. E. Jung, *et al.* (2011). "Aberrant Hedgehog Ligands Induce Progressive Pancreatic Fibrosis by Paracrine Activation of Myofibroblasts and Ductular Cells in Transgenic Zebrafish." Plos One **6**(12).

Jung, Y., K. D. Brown, *et al.* (2008). "Accumulation of hedgehog-responsive progenitors parallels alcoholic liver disease severity in mice and humans." Gastroenterology **134**(5): 1532-1543.

Karnoub, A. E., A. B. Dash, *et al.* (2007). "Mesenchymal stem cells within tumour stroma promote breast cancer metastasis." Nature **449**(7162): 557-U554.

Kasper, M., H. Schnidar, *et al.* (2006). "Selective modulation of hedgehog/GLI target gene expression by epidermal growth factor signaling in human keratinocytes." Molecular and Cellular Biology **26**(16): 6283-6298.

Kato, Y. and M. Kato (2006). "Hedgehog signaling pathway and gastrointestinal stem cell signaling network (Review)." International Journal of Molecular Medicine **18**(6): 1019-1023.

Kawakami, T., T. Kawcak, *et al.* (2002). "Mouse dispatched mutants fail to distribute hedgehog proteins and are defective in hedgehog signaling." Development **129**(24): 5753-5765.

Kayed, H., J. Kleeff, *et al.* (2004). "Indian hedgehog signaling pathway: Expression and regulation in pancreatic cancer." International Journal of Cancer **110**(5): 668-676.

Kim and Rudin (2014) in: <http://am.asco.org/hedgehog-signaling-pathway-therapeutic-abrogation-fundamental-developmental-molecular-pathway>

Kopetz, S., R. Lemos, *et al.* (2012). "The Promise of Patient-Derived Xenografts: The Best Laid Plans of Mice and Men." Clinical Cancer Research **18**(19): 5160-5162.

Korc, M. (2007). "Pancreatic cancer-associated stroma production." American Journal of Surgery **194**(4A): S84-S86.

Kucerova, L., M. Matuskova, *et al.* (2010). "Tumor cell behaviour modulation by mesenchymal stromal cells." Molecular Cancer **9**.

Kuhn, N. Z. and R. S. Tuan (2010). "Regulation of Stemness and Stem Cell Niche of Mesenchymal Stem Cells: Implications in Tumorigenesis and Metastasis." Journal of Cellular Physiology **222**(2): 268-277.

Lam, C. W., J. W. Xie, *et al.* (1999). "A frequent activated smoothened mutation in sporadic basal cell carcinomas." Oncogene **18**(3): 833-836.

Lamm, M. L. G., W. S. Catbagan, *et al.* (2002). "Sonic hedgehog activates mesenchymal Gli1 expression during prostate ductal bud formation." Developmental Biology **249**(2): 349-366.

Lapidot, T., C. Sirard, *et al.* (1994). "A CELL INITIATING HUMAN ACUTE MYELOID-LEUKEMIA AFTER TRANSPLANTATION INTO SCID MICE." Nature **367**(6464): 645-648.

Lauth ^{article 2}, M., A. Bergstrom, *et al.* (2007). "Inhibition of GLI-mediated transcription and tumor cell growth by small-molecule antagonists." Proceedings of the National Academy of Sciences of the United States of America **104**(20): 8455-8460.

Lauth, M. and R. Toftgard (2007). "Non-canonical activation of GLI transcription factors - Implications for targeted anti-cancer therapy." Cell Cycle **6**(20): 2458-2463.

Lee, J., K. A. Platt, *et al.* (1997). "Gli1 is a target of Sonic hedgehog that induces ventral neural tube development." Development **124**(13): 2537-2552.

Lee SJ, D. I., Lee J, Kim KM, Jang J, Sohn I, Kang WK. (2013). "Gastric cancer (GC) patients with hedgehog pathway activation: PTCH1 and GLI2 as independent prognostic factors." Targeted Oncology.

Lee, Y., R. Kawagoe, *et al.* (2007). "Loss of suppressor-of-fused function promotes tumorigenesis." Oncogene **26**(44): 6442-6447.

Li, C., D. G. Heidt, *et al.* (2007). "Identification of pancreatic cancer stem cells." Cancer Research **67**(3): 1030-1037.

Li, X., W. Deng, *et al.* (2006). "Snail induction is an early response to Gli1 that determines the efficiency of epithelial transformation." Oncogene **25**(4): 609-621.

Liao, X., M. K. Y. Siu, *et al.* (2009). "Aberrant activation of hedgehog signaling pathway in ovarian cancers: effect on prognosis, cell invasion and differentiation." Carcinogenesis **30**(1): 131-140.

Lin, N., Z. Tang, *et al.* (2008). "Hedgehog-mediated paracrine interaction between hepatic stellate cells and marrow-derived mesenchymal stem cells." Biochem Biophys Res Commun **372**(1): 260-265.

Lipinski, R. J., P. R. Hutson, *et al.* (2008). "Dose- and route-dependent teratogenicity, toxicity, and pharmacokinetic profiles of the Hedgehog signaling antagonist cyclopamine in the mouse." Toxicological Sciences **104**(1): 189-197.

Liu, S. L., G. Dontu, *et al.* (2006). "Hedgehog signaling and Bmi-1 regulate self-renewal of normal and malignant human mammary stem cells." Cancer Research **66**(12): 6063-6071.

Lonardo, E., J. Frias-Aldeguer, *et al.* (2012). "Pancreatic stellate cells form a niche for cancer stem cells and promote their self-renewal and invasiveness." Cell Cycle **11**(7): 1282-1290.

LoRusso, P. M., C. M. Rudin, *et al.* (2011). "Phase I Trial of Hedgehog Pathway Inhibitor Vismodegib (GDC-0449) in Patients with Refractory, Locally Advanced or Metastatic Solid Tumors." Clinical Cancer Research **17**(8): 2502-2511.

Maitah, M. Y., S. Ali, *et al.* (2011). "Up-regulation of sonic hedgehog contributes to TGF-beta1-induced epithelial to mesenchymal transition in NSCLC cells." PLoS One **6**(1): e16068.

Madden, J.I.in:<http://www.businesswire.com/news/home/20120618005411/en/Infinity-Stops-Phase-2-Trials-Saridegib-Chondrosarcoma>.

Maitra, A. and R. H. Hruban (2008). "Pancreatic cancer." Annu Rev Pathol **3**: 157-188.

Malanchi, I., A. Santamaria-Martinez, *et al.* (2012). "Interactions between cancer stem cells and their niche govern metastatic colonization." Nature **481**(7379): 85-U95.

Mattie, M., A. Christensen, *et al.* (2013). "Molecular Characterization of Patient-Derived Human Pancreatic Tumor Xenograft Models for Preclinical and Translational Development of Cancer Therapeutics." Neoplasia **15**(10): 1124-1136.

- Mendez-Ferrer, S., T. V. Michurina, *et al.* (2010). "Mesenchymal and haematopoietic stem cells form a unique bone marrow niche." Nature **466**(7308): 829-U859.
- Merika, E. E., K. N. Syrigos, *et al.* (2012). "Desmoplasia in Pancreatic Cancer. Can We Fight It?" Gastroenterology Research and Practice.
- Mi, Q., J. M. Pezzuto, *et al.* (2009). "Use of the in Vivo Hollow Fiber Assay in Natural Products Anticancer Drug Discovery." Journal of Natural Products **72**(3): 573-580.
- Mishra, P. J., P. J. Mishra, *et al.* (2008). "Carcinoma-associated fibroblast-like differentiation of human mesenchymal stem cells." Cancer Research **68**(11): 4331-4339.
- Mishra, P. J., P. J. Mishra, *et al.* (2009). "Mesenchymal Stem Cells: Flip Side of the Coin." Cancer Research **69**(4): 1255-1258.
- Moradi, F., M. H. G. Kashani, *et al.* (2012). "Spontaneous Expression of Neurotrophic Factors and TH, Nurr1, Nestin Genes in Long-term Culture of Bone Marrow Mesenchymal Stem Cells." Cell Journal **13**(4): 243-250.
- Morris, J. P., S. C. Wang, *et al.* (2010). "KRAS, Hedgehog, Wnt and the twisted developmental biology of pancreatic ductal adenocarcinoma." Nature Reviews Cancer **10**(10): 683-695.
- Morton, J. P., M. E. Mongeau, *et al.* (2007). "Sonic hedgehog acts at multiple stages during pancreatic tumorigenesis." Proceedings of the National Academy of Sciences of the United States of America **104**(12): 5103-5108.
- Mosmann, T. (1983). "RAPID COLORIMETRIC ASSAY FOR CELLULAR GROWTH AND SURVIVAL - APPLICATION TO PROLIFERATION AND CYTO-TOXICITY ASSAYS." Journal of Immunological Methods **65**(1-2): 55-63.
- Mucci, L. A., S. Wedren, *et al.* (2001). "The role of gene-environment interaction in the aetiology of human cancer: examples from cancers of the large bowel, lung and breast." Journal of Internal Medicine **249**(6): 477-493.
- Mukherjee, S., N. Frolova, *et al.* (2006). "Hedgehog signaling and response to cyclopamine differ in epithelial and stromal cells in benign breast and breast cancer." Cancer Biology & Therapy **5**(6): 674-683.

- Nakamura, K., J. Sasajima, *et al.* (2010). "Hedgehog Promotes Neovascularization in Pancreatic Cancers by Regulating Ang-1 and IGF-1 Expression in Bone-Marrow Derived Pro-Angiogenic Cells." Plos One **5**(1).
- Nakamura, M., M. Kubo, *et al.* (2007). "Anti-patched-1 antibodies suppress hedgehog signaling pathway and pancreatic cancer proliferation." Anticancer Research **27**(6A): 3743-3747.
- Nguyen, V., A. L. Chokas, *et al.* (2005). "Cooperative requirement of the Gli proteins in neurogenesis." Development **132**(14): 3267-3279.
- Nolan-Stevaux, O., J. Lau, *et al.* (2009). "GLI1 is regulated through Smoothed-independent mechanisms in neoplastic pancreatic ducts and mediates PDAC cell survival and transformation." Genes & Development **23**(1): 24-36.
- O'Toole, S. A., D. A. Machalek, *et al.* (2011). "Hedgehog Overexpression Is Associated with Stromal Interactions and Predicts for Poor Outcome in Breast Cancer." Cancer Research **71**(11): 4002-4014.
- Oliani, C., M. Padovani, *et al.* (2004). "Gemcitabine and continuous infusion of 5-fluorouracil in locally advanced and metastatic pancreatic cancer: A phase I-II study." Anticancer Research **24**(3B): 2107-2112.
- Olive, K. P., M. A. Jacobetz, *et al.* (2009). "Inhibition of Hedgehog Signaling Enhances Delivery of Chemotherapy in a Mouse Model of Pancreatic Cancer." Science **324**(5933): 1457-1461.
- Omary, M. B., A. Lugea, *et al.* (2007). "The pancreatic stellate cell: a star on the rise in pancreatic diseases." Journal of Clinical Investigation **117**(1): 50-59.
- Parekkadan, B., D. van Poll, *et al.* (2007). "Immunomodulation of activated hepatic stellate cells by mesenchymal stem cells." Biochem Biophys Res Commun **363**(2): 247-252.
- Park, H. L., C. Bai, *et al.* (2000). "Mouse Gli1 mutants are viable but have defects in SHH signaling in combination with a Gli2 mutation." Development **127**(8): 1593-1605.
- Pasca di Magliano, M., S. Sekine, *et al.* (2006). "Hedgehog/Ras interactions regulate early stages of pancreatic cancer." Genes & Development **20**(22): 3161-3173.
- Paunescu, V., F. M. Bojin, *et al.* (2011). "Tumour-associated fibroblasts and mesenchymal stem cells: more similarities than differences." Journal of Cellular and Molecular Medicine **15**(3): 635-646.

Peacock, C. D., Q. Wang, *et al.* (2007). "Hedgehog signaling maintains a tumor stem cell compartment in multiple myeloma." Proceedings of the National Academy of Sciences of the United States of America **104**(10): 4048-4053.

Peng ^{article 2}, L., J. Hu, *et al.* (2013). "Aberrant methylation of the PTCH1 gene promoter region in aberrant crypt foci." International Journal of Cancer **132**(2): E18-E25.

Peng, Y., Z. Li, *et al.* (2013). "GRP78 secreted by tumor cells stimulates differentiation of bone marrow mesenchymal stem cells to cancer-associated fibroblasts." Biochem Biophys Res Commun(0).

Pepinsky, R. B., C. H. Zeng, *et al.* (1998). "Identification of a palmitic acid-modified form of human Sonic hedgehog." Journal of Biological Chemistry **273**(22): 14037-14045.

Pevsner-Fischer, M., S. Levin, *et al.* (2011). "The Origins of Mesenchymal Stromal Cell Heterogeneity." Stem Cell Reviews and Reports **7**(3): 560-568.

Pinho S, L. J., Hanoun M, Mizoguchi T, Bruns I, Kunisaki Y, Frenette PS. (2013). "PDGFR α and CD51 mark human nestin+ sphere-forming mesenchymal stem cells capable of hematopoietic progenitor cell expansion." J Exp Med. **210**(7): 1351-1367.

Pittenger, M. F., A. M. Mackay, *et al.* (1999). "Multilineage potential of adult human mesenchymal stem cells." Science **284**(5411): 143-147.

Ponchel, F., C. Toomes, *et al.* (2003). "Real-time PCR based on SYBR-Green I fluorescence: An alternative to the TaqMan assay for a relative quantification of gene rearrangements, gene amplifications and micro gene deletions." BMC Biotechnology **3** (18)

Porter, J. A. (1996). "Cholesterol modification of hedgehog signaling proteins in animal development (vol 274, pg 255, 1996)." Science **274**(5293): 1597-1597.

Price, M. A. and D. Kalderon (2002). "Proteolysis of the Hedgehog signaling effector Cubitus interruptus requires phosphorylation by glycogen synthase kinase 3 and casein kinase 1." Cell **108**(6): 823-835.

Qin, J., Y. Lin, *et al.* (2011). "Intraflagellar transport protein 122 antagonizes Sonic Hedgehog signaling and controls ciliary localization of pathway components." Proceedings of the National Academy of Sciences of the United States of America **108**(4): 1456-1461.

Qualtrough, D., A. Buda, *et al.* (2004). "Hedgehog signalling in colorectal tumour cells: Induction of apoptosis with cyclopamine treatment." International Journal of Cancer **110**(6): 831-837.

Quante, M., S. P. Tu, *et al.* (2011). "Bone Marrow-Derived Myofibroblasts Contribute to the Mesenchymal Stem Cell Niche and Promote Tumor Growth." Cancer cell **19**(2): 257-272.

Rahnama, F., T. Shimokawa, *et al.* (2006). "Inhibition of GLI1 gene activation by patched1." Biochemical Journal **394**: 19-26.

Rahnama, F., R. Toftgard, *et al.* (2004). "Distinct roles of PTCH2 splice variants in Hedgehog signalling." Biochemical Journal **378**: 325-334.

Rajan, P. and R. Srinivasan (2008). "Targeting cancer stem cells in cancer prevention and therapy." Stem Cell Reviews **4**(3): 211-216.

Real-Time PCR: from theory to practice" (2008) PDF Retrieved from <http://core.cgrb.oregonstate.edu/sites/default/files/Real%20Time%20PCR.From%20Theory%20to%20Practice.pdf>

"Real Time PCR Handbook" n.d. PDF Retrieved from <http://www.gene-quantification.de/real-time-pcr-handbook-life-technologies-update-flr.pdf>

Reifenberger, J., M. Wolter, *et al.* (1998). "Missense mutations in SMOH in sporadic basal cell carcinomas of the skin and primitive neuroectodermal tumors of the central nervous system." Cancer Research **58**(9): 1798-1803.

Rhim, A. D., P. E. Oberstein, *et al.* (2014). "Stromal Elements Act to Restrain, Rather Than Support, Pancreatic Ductal Adenocarcinoma." Cancer cell **25**(6): 735-747

Rohatgi, R., L. Milenkovic, *et al.* (2009). "Hedgehog signal transduction by Smoothed: Pharmacologic evidence for a 2-step activation process." Proceedings of the National Academy of Sciences of the United States of America **106**(9): 3196-3201.

Ruiz i Altaba, A. (2008). "Therapeutic inhibition of Hedgehog-Gli signaling in cancer: epithelial, stromal, or stem cell targets?" Cancer cell **14**(4): 281-283.

Ruiz i Altaba, A., C. Mas, *et al.* (2007). "The Gli code: an information nexus regulating cell fate, stemness and cancer." Trends in Cell Biology **17**(9): 438-447.

Sanchez, P., A. M. Hernandez, *et al.* (2004). "Inhibition of prostate cancer proliferation by interference with SONICEDGEHOG-GLI1 signaling." Proceedings of the National Academy of Sciences of the United States of America **101**(34): 12561-12566.

Sasaki, H., Y. Nishizaki, *et al.* (1999). "Regulation of Gli2 and Gli3 activities by an amino-terminal repression domain: implication of Gli2 and Gli3 as primary mediators of Shh signaling." Development **126**(17): 3915-3924.

Savani, M., Y. Guo, *et al.* (2012). "Sonic hedgehog pathway expression in non-small cell lung cancer." Therapeutic advances in medical oncology **4**(5): 225-233.

Scales, S. J. and F. J. de Sauvage (2009). "Mechanisms of Hedgehog pathway activation in cancer and implications for therapy." Trends Pharmacol Sci **30**(6): 303-312.

Scarlett, C. J., E. K. Colvin, *et al.* (2011). "Recruitment and Activation of Pancreatic Stellate Cells from the Bone Marrow in Pancreatic Cancer: A Model of Tumor-Host Interaction." Plos One **6**(10).

Schofield, R. (1978). "The relationship between the spleen colony-forming cell and the haemopoietic stem cell." Blood Cells **4**(1-2): 7-25

Schutte, M., R. H. Hruban, *et al.* (1997). "Abrogation of the Rb/p16 tumor-suppressive pathway in virtually all pancreatic carcinomas." Cancer Research **57**(15): 3126-3130.

Shaw, A., J. Gipp, *et al.* (2009). "The Sonic Hedgehog pathway stimulates prostate tumor growth by paracrine signaling and recapitulates embryonic gene expression in tumor myofibroblasts." Oncogene **28**(50): 4480-4490.

Siegel, R., D. Naishadham, *et al.* (2012). "Cancer Statistics, 2012." Ca-a Cancer Journal for Clinicians **62**(1): 10-29.

Singh, A. P., S. Arora, *et al.* (2012). "CXCL12/CXCR4 Protein Signaling Axis Induces Sonic Hedgehog Expression in Pancreatic Cancer Cells via Extracellular Regulated Kinase- and Akt Kinase-mediated Activation of Nuclear Factor kappa B IMPLICATIONS FOR BIDIRECTIONAL TUMOR-STROMAL INTERACTIONS." Journal of Biological Chemistry **287**(46): 39115-39124.

Singh, S., Z. Wang, *et al.* (2011). "Hedgehog-Producing Cancer Cells Respond to and Require Autocrine Hedgehog Activity." Cancer Research **71**(13): 4454-4463.

Siolas, D. and G. J. Hannon (2013). "Patient-Derived Tumor Xenografts: Transforming Clinical Samples into Mouse Models." Cancer Research **73**(17): 5315-5319.

Siu Wai Tsang, H. Z., Chengyuan Lin, Haitao Xiao, Michael Wong, Hongcai Shang, Zhi-Jun Yang, Aiping Lu, Ken Kin-Lam Yung, and Zhaoxiang Bian (2013). "Rhein, a Natural Anthraquinone Derivative, Attenuates the Activation of Pancreatic Stellate Cells and Ameliorates Pancreatic Fibrosis in Mice with Experimental Chronic Pancreatitis." PLoS One **8**(12).

Spaeth, E. L., J. L. Dembinski, *et al.* (2009). "Mesenchymal Stem Cell Transition to Tumor-Associated Fibroblasts Contributes to Fibrovascular Network Expansion and Tumor Progression." Plos One **4**(4).

Stecca, B., C. Mas, *et al.* (2007). "Melanomas require HEDGEHOG-GLI signaling regulated by interactions between GLI1 and the RAS-MEK/AKT pathways." Proceedings of the National Academy of Sciences of the United States of America **104**(14): 5895-5900.

Stecca, B. and A. Ruiz i Altaba (2010). "Context-dependent Regulation of the GLI Code in Cancer by HEDGEHOG and Non-HEDGEHOG Signals." Journal of Molecular Cell Biology **2**(2): 84-95.

Strand, M. F., S. R. Wilson, *et al.* (2011). "A Novel Synthetic Smoothened Antagonist Transiently Inhibits Pancreatic Adenocarcinoma Xenografts in a Mouse Model." Plos One **6**(6).

Straussman, R., T. Morikawa, *et al.* (2012). "Tumour micro-environment elicits innate resistance to RAF inhibitors through HGF secretion." Nature **487**(7408): 500-U118.

Suetsugu, A., M. Katz, *et al.* (2012). "Imageable Fluorescent Metastasis Resulting in Transgenic GFP Mice Orthotopically Implanted with Human-patient Primary Pancreatic Cancer Specimens." Anticancer Research **32**(4): 1175-1180.

Suetsugu ^{article 2}, A., M. Katz, *et al.* (2012). "Multi-color Palette of Fluorescent Proteins for Imaging the Tumor Microenvironment of Orthotopic Tumorgraft Mouse Models of Clinical Pancreatic Cancer Specimens." Journal of Cellular Biochemistry **113**(7): 2290-2295.

Sun, Y., J. Campisi, *et al.* (2012). "Treatment-induced damage to the tumor microenvironment promotes prostate cancer therapy resistance through WNT16B." Nature Medicine **18**(9): 1359-+.

Syn, W.-K., S. S. Choi, *et al.* (2011). "Osteopontin is Induced by Hedgehog Pathway Activation and Promotes Fibrosis Progression in Nonalcoholic Steatohepatitis." Hepatology **53**(1): 106-115.

Taipale, J., J. K. Chen, *et al.* (2000). "Effects of oncogenic mutations in Smoothened and Patched can be reversed by cyclopamine." Nature **406**(6799): 1005-1009.

Tao, Y., J. Mao, *et al.* (2011). "Overexpression of Hedgehog signaling molecules and its involvement in triple-negative breast cancer." Oncology Letters **2**(5): 995-1001.

Thayer, S. P., M. P. di Magliano, *et al.* (2003). "Hedgehog is an early and late mediator of pancreatic cancer tumorigenesis." Nature **425**(6960): 851-856.

Therond, P. P. (2012). "Release and transportation of Hedgehog molecules." Current Opinion in Cell Biology **24**(2): 173-180.

Tian, H., C. A. Callahan, *et al.* (2009). "Hedgehog signaling is restricted to the stromal compartment during pancreatic carcinogenesis." Proceedings of the National Academy of Sciences of the United States of America **106**(11): 4254-4259.

Tostar, U., C. J. Malm, *et al.* (2006). "Deregulation of the hedgehog signalling pathway: a possible role for the PTCH and SUFU genes in human rhabdomyoma and rhabdomyosarcoma development." Journal of Pathology **208**(1): 17-25.

Tuveson, D. A., A. T. Shaw, *et al.* (2004). "Endogenous oncogenic K-ras(G12D) stimulates proliferation and widespread neoplastic and developmental defects." Cancer cell **5**(4): 375-387.

Tuxhorn, J. A., G. E. Ayala, *et al.* (2002). "Reactive stroma in human prostate cancer: Induction of myofibroblast phenotype and extracellular matrix remodeling." Clinical Cancer Research **8**(9): 2912-2923.

Tysnes, B. B. and R. Bjerkvig (2007). "Cancer initiation and progression: Involvement of stem cells and the micro environment." Biochimica Et Biophysica Acta-Reviews on Cancer **1775**(2): 283-297.

Unden, A. B., E. Holmberg, *et al.* (1996). "Mutations in the human homologue of Drosophila patched (PTCH) in basal cell carcinomas and the Gorlin syndrome: Different in vivo mechanisms of PTCH inactivation." Cancer Research **56**(20): 4562-4565.

Vyas, N., D. Goswami, *et al.* (2008). "Nanoscale organization of Hedgehog is essential for long-range signaling." Cell **133**(7): 1214-1227.

Walter, K., N. Omura, et al. (2010). "Overexpression of Smoothed Activates the Sonic Hedgehog Signaling Pathway in Pancreatic Cancer-Associated Fibroblasts." Clinical Cancer Research **16**(6): 1781-1789.

Walters, D. M., J. M. Lindberg, et al. (2013). "Inhibition of the Growth of Patient-Derived Pancreatic Cancer Xenografts with the MEK Inhibitor Trametinib Is Augmented by Combined Treatment with the Epidermal Growth Factor Receptor/HER2 Inhibitor Lapatinib." Neoplasia **15**(2): 143-U207.

Wang, G. L., B. Wang, et al. (1999). "Protein kinase A antagonizes Hedgehog signaling by regulating both the activator and repressor forms of Cubitus interruptus." Genes & Development **13**(21): 2828-2837.

Watkins, D. N., D. M. Berman, et al. (2003). "Hedgehog signalling within airway epithelial progenitors and in small-cell lung cancer." Nature **422**(6929): 313-317.

Wilkie, G. S., K. S. Dickson, et al. (2003). "Regulation of mRNA translation by 5' - and 3' -UTR-binding factors." Trends in Biochemical Sciences **28**(4): 182-188.

Wilkinson, S. E., L. Furic, et al. (2013). "Hedgehog Signaling Is Active in Human Prostate Cancer Stroma and Regulates Proliferation and Differentiation of Adjacent Epithelium." Prostate **73**(16): 1810-1823.

Williams, J. A., C. M. Guicherit, et al. (2003). "Identification of a small molecule inhibitor of the hedgehog signaling pathway: Effects on basal cell carcinoma-like lesions (vol 100, pg 4616, 2003)." Proceedings of the National Academy of Sciences of the United States of America **100**(14): 8607-8607.

Wilson, T. R., J. Fridlyand, et al. (2012). "Widespread potential for growth-factor-driven resistance to anticancer kinase inhibitors." Nature **487**(7408): 505-U1652.

Xie, J. W., M. Murone, et al. (1998). "Activating Smoothed mutations in sporadic basal-cell carcinoma." Nature **391**(6662): 90-92.

Xu, X.-F., C.-Y. Guo, et al. (2009). "Gli1 maintains cell survival by up-regulating IGFBP6 and Bcl-2 through promoter regions in parallel manner in pancreatic cancer cells." Journal of carcinogenesis **8**: 13-13.

Xu, Z., A. Vonlaufen, et al. (2010). "Role of Pancreatic Stellate Cells in Pancreatic Cancer Metastasis." American Journal of Pathology **177**(5): 2585-2596.

Yan, R., X. Peng, *et al.* (2013). "Suppression of growth and migration by blocking the hedgehog signaling pathway in gastric cancer cells." Cell Oncol (Dordr).

Yang, L., G. Xie, *et al.* (2010). "Activation of the hedgehog-signaling pathway in human cancer and the clinical implications." Oncogene **29**(4): 469-481.

Yang, S. H., T. Andl, *et al.* (2008). "Pathological responses to oncogenic Hedgehog signaling in skin are dependent on canonical Wnt/beta-catenin signaling." Nat Genet **40**(9): 1130-1135.

Yang SH, H. C., Lee JC, Tien YW, Kuo SH, Cheng AL. (2013). "Nuclear expression of glioma-associated oncogene homolog 1 and nuclear factor- κ B is associated with a poor prognosis of pancreatic cancer." Oncology **85**(2): 86-94.

Yauch, R. L., G. J. P. Dijkgraaf, *et al.* (2009). "Smoothed Mutation Confers Resistance to a Hedgehog Pathway Inhibitor in Medulloblastoma." Science **326**(5952): 572-574.

Yauch, R. L., S. E. Gould, *et al.* (2008). "A paracrine requirement for hedgehog signalling in cancer." Nature **455**(7211): 406-U461.

Yeung, T. M., L. A. Chia, *et al.* (2011). "Regulation of self-renewal and differentiation by the intestinal stem cell niche." Cellular and Molecular Life Sciences **68**(15): 2513-2523.

Yoo, Y. A., M. H. Kang, *et al.* (2011). "Sonic Hedgehog Pathway Promotes Metastasis and Lymphangiogenesis via Activation of Akt, EMT, and MMP-9 Pathway in Gastric Cancer." Cancer Research **71**(22): 7061-7070.

Yuan, Z., J. A. Goetz, *et al.* (2007). "Frequent requirement of hedgehog signaling in non-small cell lung carcinoma." Oncogene **26**(7): 1046-1055.

Zacharias, W. J., B. B. Madison, *et al.* (2011). "Hedgehog signaling controls homeostasis of adult intestinal smooth muscle." Developmental Biology **355**(1): 152-162.

Zeng, H., J. Jia, *et al.* (2010). "Coordinated Translocation of Mammalian Gli Proteins and Suppressor of Fused to the Primary Cilium." Plos One **5**(12).

Zhang, W., M. C. Mendoza, *et al.* (2012). "Down-regulation of CMTM8 Induces Epithelial-to-Mesenchymal Transition-like Changes via c-

MET/Extracellular Signal-regulated Kinase (ERK) Signaling." Journal of Biological Chemistry **287**(15): 11850-11858.

Zhao, C., A. Chen, *et al.* (2009). "Hedgehog signalling is essential for maintenance of cancer stem cells in myeloid leukaemia." Nature **458**(7239): 776-U117.

Zhou, J.-x., L.-w. Jia, *et al.* (2006). "Role of sonic hedgehog in maintaining a pool of proliferating stem cells in the human fetal epidermis." Human Reproduction **21**(7): 1698-1704.

Appendix: Software Programmes

QWin Standard V3 (Leica microsystems, UK)

H Score macro

Configure (Image Store 2560 x 1920, Grey Images 24, Binaries 8)

Display (Colour0 (on), frames (on,off), planes (off,off,off,off,off,off), lut
0, x 0, y 0, z 1, Reduction off)

Image Setup DC Twain [PAUSE] (Camera 1, AutoExposure Off, Gain
0.00, ExposureTime 75.81 msec, Brightness 0, Lamp 45.00)

Acquire (into Colour0)

Detection

PauseText ("Detect high levels of staining.")

Colour Detect [PAUSE] (RGB: 58-153, 32-102, 0-64, from Colour0
into Binary1)

PauseText ("Detect medium levels of staining.")

Colour Detect [PAUSE] (RGB: 124-171, 84-118, 58-120, from Colour0
into Binary2)

PauseText ("Detect low levels of staining.")

Colour Detect [PAUSE] (HSI: 0-26, 0-89, 0-192, from Colour0 into
Binary3)

PauseText ("A Colour Detection is used to detect total staining.")

Colour Detect [PAUSE] (HSI+: 7-178, 4-237, 33-202, from Colour0
into Binary0)

Binary Edit [PAUSE] (Erase from Binary0 to Binary0, nib Rect, width
1)

351

Measure high area

MFLDIMAGE = 1

Measure field (plane MFLDIMAGE, into FLDRESULTS(1), statistic
into not found)

Selected parameters: Area

HIGH.AREA = FLDRESULTS(1)

Measure total area

MFLDIMAGE = 0

Measure field (plane MFLDIMAGE, into FLDRESULTS(1), statistics
into not found)

Selected parameters: Area

TOTAL.AREA = FLDRESULTS(1)

Measure medium area

MFLDIMAGE = 2

Measure field (plane MFLDIMAGE, into FLDRESULTS(1), statistics
into not found)

Selected parameters: Area

MEDIUM.AREA = FLDRESULTS(1)

Measure low area

MFLDIMAGE = 3

Measure field (plane MFLDIMAGE, into FLDRESULTS(1), statistics
into not found)

Selected parameters: Area

LOW.AREA = FLDRESULTS(1)

Report final results

Results layout = %high staining area, %moderate staining area, %low staining area, h-score

Setup Output Window ("Percentage area measurements and H-Score", Move to x 36, y 783, w 683, h 161)

Display ($100 * (\text{HIGH.AREA} / \text{TOTAL.AREA})$, 1 digit after '.', tab follows)

Display ($100 * (\text{MEDIUM.AREA} / \text{TOTAL.AREA})$, 1 digit after '.', tab follows)

Display ($100 * (\text{LOW.AREA} / \text{TOTAL.AREA})$, 2 digits after '.', tab follows)

Display

($((100 * (\text{HIGH.AREA} / \text{TOTAL.AREA})) * 3) + ((100 * (\text{MEDIUM.AREA} / \text{TOTAL.AREA})) * 2) + (100 * (\text{LOW.AREA} / \text{TOTAL.AREA}))$, 2 digits after '.', tab follows)

Display Line

Pause (No dialog)

DAB count macro

Configure (Image Store 2560 x 1920, Grey Images 24, Binaries 8)

Display (Colour0 (on), frames (on,off), planes (off,off,off,off,off,off), lut
0, x 0, y 0, z 1, Reduction off)

Image Setup DC Twain [PAUSE] (Camera 1, AutoExposure Off, Gain
0.00, ExposureTime 61.16 msec, Brightness 0, Lamp 45.00)

Acquire (into Colour1)

Grey LUT (Normal from Colour1 to Colour1)

PauseText ("A Colour Detection is used to detect positive staining.")

Colour Detect [PAUSE] (HSI: 0-255, 0-255, 0-115, from Colour1 into
Binary1)

Binary Edit [PAUSE] (Erase from Binary1 to Binary1, nib Fill, width 1)

PauseText ("detect total area stained")

Colour Detect (RGB: 0-188, 0-188, 0-191, from Colour1 into Binary0)

Colour Detect [PAUSE] (RGB: 0-164, 0-164, 0-164, from Colour1 into
Binary0)

Binary Edit [PAUSE] (Erase from Binary0 to Binary0, nib Fill, width 1)

Binary Identify (BinMode from Binary0 to Binary0)

MFLDIMAGE = 1

Measure field (plane MFLDIMAGE, into FLDRESULTS(1), statistics
into not found)

Selected parameters: Area

POS.AREA = FLDRESULTS(1)

Measure total area

MFLDIMAGE = 0

Measure field (plane MFLDIMAGE, into FLDRESULTS(1), statistics into not found)

Selected parameters: Area

TOTAL.AREA = FLDRESULTS(1)

Measure degree of positivity by taking integrated optical density of the intensity component where the positive stain is detected

This IOD is later normalized to the total tissue area detected

Grey Calibrate (Optical Density)

MGREYIMAGE = 1

MGREYMASK = 1

Measure Grey (plane MGREYIMAGE, mask MGREYMASK, histogram into GREYHIST(256), stats into GREYSTATS(5))

Selected parameters: Sum Blu, Mean Blu, StdD Blu, Med Blu, Mode

Blu Display Grey Results

Field Data Window (51, 526, 921, 153)

Histogram Results Window (51, 548, 409, 192)

Histogram Window (460, 548, 460, 192)

Setup Results Window (Close Grey Field Data)

Setup Results Window (Close Grey Histogram Data)

Setup Results Window (Move Grey Histogram to x 1002, y 670, w 238, h 286)

Report final results

Setup Output Window ("Immunochemistry Measurement Results",

Move to x 30, y 789, w 527, h 161)

Display (TOTAL.AREA, 1 digit after '.', tab follows)

Display (POS.AREA, 1 digit after '.', tab follows)

Display ($100 * (POS.AREA / TOTAL.AREA)$, 2 digits after '.', tab follows)

Display (GREYSTATS(1) / TOTAL.AREA, 2 digits after '.', tab follows)

Display Line

PauseText ("The final results are calculated and reported.")

Pause (No dialog).

